Investigation of New Classes of Amide and Non-amide Kinetic Hydrate Inhibitors

by

Qian Zhang

Thesis submitted in fulfilment of
the requirements for the degree of
PHILOSOPHIAE DOCTOR
(PhD)

Faculty of Science and Technology
Department of Chemistry, Life Sciences and Environmental Technology
2020

University of Stavanger
NO-4036 Stavanger
NORWAY
www.uis.no

©2020 Qian Zhang

ISBN: 978-82-7644-945-7
ISSN: 1890-1387
PhD: Thesis UiS No. 538

Acknowledgements

I would like to express my sincere gratitude to those people who have helped and supported me during the three years study period at the University of Stavanger, Norway. The last three years have been full of challenges and inspiration. This experience will be the cherished memory in my life.

My supervisor, Professor Malcolm A. Kelland, is the one that I would like to thank firstly. Thank you for giving me the opportunity to work and study in your research group at UiS. Thank you for your guidance and support with the research work, as well as the kind help and caring in daily life. Your valuable insights in the KHI research field and firm scientific attitude helped me to learn a lot.

Secondly, I would like to thank the rest members of our research group, Mohamed F. Mady and Eirin L. Abrahamsen for the training on the high-pressure rocker rigs and general help in the laboratory, Lilian S. Ree and Erik G. Dirdal for support, discussions and co-operation.

To my colleagues at the department of IKBM, thank you for your help and support whenever needed. I have appreciated the friendly environment and good company during the lunch breaks.

To all my friends, thank you for your encouragement and support. Thank you, my new friends, in Norway for being there with me, and my old friends in China for understanding my situation and not forgetting me.

Last but not least, I would like to thank my parents Huagen Zhang and Yumei Guo, my young brother Yang Zhang, and the Li family. I could not have done this without all your support, encouragement, and love. Also, I would like to thank my dearest husband Haohan Li. Although we have endured being apart by the long-distance of 1136 kilometres from Norway to Belgium for the last three years, your understanding and

support let me feel that our hearts are very close. Thank you for your love, patience, and encouragement.

Stavanger, May 15th, 2020

Abbreviations

KHI	Kinetic hydrate inhibitor
PVCap	Poly (*N*-vinyl caprolactam)
PNIPMAM	Poly (*N*-isopropyl methacrylamide)
T_{eq}	Equilibrium temperature
ΔT	Sub-cooling degree
LDHI	Low dosage hydrate inhibitor
THI	Thermodynamic hydrate inhibitor
AA	Anti-agglomerant
sI	Structure I
sII	Structure II
sH	Structure H
MDS	Molecular dynamics simulation
NMR	Nuclear magnetic resonance
$\mathrm{r_{crit}}$	Critical size
$\Delta \mathrm{G_{tot}}$	Total Gibbs free energy
GO	Graphene oxide
L	Lateral size

LCH	Labile cluster hypothesis
LSH	Local structuring hypothesis
RDS	Rate-determining step
CAPEX	Capital expense
OPEX	Operating expense
MEG	Monoethylene glycol
PVP	Poly (*N*-vinyl pyrrolidone)
PAPYD	Polyacryloylpyrrolidine
BET	Brunauer-Emmett-Teller
SNG	Synthetic natural gas
SCC	Slow constant cooling
CGI	Crystal growth inhibition
THF	Tetrahydrofuran
CP	Cyclopentane
MW	Molecular weight
PIPAM	Poly (*N*-isopropylacrylamide)
PDMHMAM	Poly (*N*, *N*-dimethylhydrazidomethacrylamide)
PDMHAM	Poly (*N*, *N*-dimethylhydrazidoacrylamide)

T_{Cl}	Cloud points
VP	*N*-vinyl pyrrolidone
VCap	*N*-vinyl caprolactam
VOH	Vinyl alcohol
VIMA	*N*-Vinyl-*N*-methylacetamide
PNnPAM	Poly (*N*-*n*-propylacrylamide)
PAA	Poly (acrylic acid)
VSAM	*N*-Alkyl-*S*-vinylsulphonamide
IPA	Isopropanol
wt.%	Weight percent
RC5	Rocking cell 5
T_o	Hydrate onset temperature
T_a	Rapid hydrate growth temperature
$\mathrm{t_i}$	Hydrate induction time
$\mathrm{t_a}$	Hydrate rapid formation time
AFP	Anti-freeze protein
AFGP	Anti-freeze glycoprotein
MA-Pep	Poly (glycine-*L*-methylated valine)

EA-Pep	Poly (glycine-*L*-ethylated valine)
PA-Pep	Poly (glycine-*L*-*n*-propylated valine)
EtA-Pep	Poly (glycine-*L*-ethanolated valine)
NVF	*N*-Vinylformamide
nBuNVF	*N*-*n*-Butyl-*N*-vinylformamide
iBuNVF	*N*-*iso*-Butyl-*N*-vinylformamide
MNVA	*N*-Methyl-*N*-vinylacetamide
nPrNVF	*N*-*n*-Propyl-*N*-vinylformamide
iPrNVF	*N*-isopropyl-*N*-vinylformamide
AIBN	a, a’-Azobisisobutyronitrile
SEC	Size exclusion chromatography
DMF	Dimethylformamide
ppm	Parts per million
2-EE	2-Ethoxyethanol
nBGE	Mono-*n*-butyl glycol ether
iBGE	Mono-*iso*-butyl glycol ether
concn.	Concentration
3M2P	3-Methylene-2-pyrrolidone

3M2Pip	3-Methylene-2-piperidone
Me-3M2P	*N*-Methyl-3-methylene-2-pyrrolidone
Et-3M2P	*N*-Ethyl-3-methylene-2-pyrrolidone
nPr-3M2P	*N*-*n*-Propyl-3-methylene-2-pyrrolidone
BuMAAm	*N*-*n*-Butyl methacrylamide
CTA	Chain transfer agent
PMAA	Poly (methacrylic acid)
PMA	Poly (methyl acrylate)
TBD	Triazabicyclodecene
PAPPD	Polyacryloylpiperidine
DIW	Deionized water
NIPAM	*N*-isopropylacrylamide
APYD	Acryloylpyrrolidine
EtVSAM	*N*-Ethylvinylsulphonamide
nPrVSAM	*N*-*n*-Propylvinylsulphonamide
iBuVSAM	*N*-*iso*-Butylvinylsulphonamide
nPrMAM	*n*-Propylmethacrylamide
nPrMA	*n*-Propylmethacrylate

TBAO	Tri (*n*-butyl) amine oxide
TPAO	Tri (*n*-pentyl) amine oxide
TEPA	Tetraethylenepentamine
AO	Amine oxide
HPEI	Hyperbranched polyethyleneimine
PPO	Poly (propylene oxide)
PDEGAO	Poly (*N*, *N*-diethyl glycidyl amine *N*-oxide)
PPiGAO	Poly (piperidine glycidyl amine *N*-oxide)
PGAO	Poly (glycidyl amine *N*-oxide)
GA	Glycidyl amine
PDEGA	Poly (*N*, *N*-diethyl glycidyl amine)
PPiGA	Poly (piperidine glycidyl amine)
b	Block
PEO	Polyethylene oxide
t-test	Statistical hypothesis test
p-value	Probability value
T_{dp}	Peposition point
PSBMA	Zwitterionic poly (sulfobetaine methacrylate)

η	Intrinsic viscosity (dL/g)
M_n	Number average molecular weight (g/mol)
M_w	Weight average molecular weight (g/mol)
Đ	Dispersity
RAFT	Reversible addition-fragmentation chain transfer polymerization
PVAm	Polyvinylamine

Summary

The formation of gas hydrates can cause pipeline blockage during the transportation of gas and oil products, which is one of the main challenges for flow assurance in the petroleum industry. It is uneasy to remove gas hydrates once they have formed in gas and oil transportation pipelines, so the primary method of managing the blockage risk of gas hydrates is to prevent gas hydrates from forming. Compared to other gas hydrates inhibition methods, such as water removal, thermodynamic inhibition, hydraulic and thermal methods, injection of kinetic hydrate inhibitors (KHIs) can be an efficacious and more economical method for some fields.

Most reported KHIs are amide-containing polymers that are soluble in water, e.g., poly (*N*-vinyl caprolactam) (PVCap) and poly (*N*-isopropyl methacrylamide) (PNIPMAM). However, the cloud points of many amide-containing KHI polymers are relatively low, making injection difficult, and they will lose their inhibition effect if the hydrate sub-cooling is above about 10-12 ^{o}C for long periods. These two aforementioned weaknesses limit the application range of current amide-based KHIs. Therefore, there is a need to develop KHIs with improved inhibition performance as well as high cloud point. In addition, the kinetic hydrate inhibition mechanism is still not fully understood. Addressing these issues has been the motivation for the research presented in this thesis.

My PhD studies involved two main projects. (i) Improving the inhibition performance of traditional amide-containing KHI polymers; (ii) Investigating novel classes of polymers with alternative hydrophilic groups to the amide group to determine if they can give superior performance and/or compatibility. The inhibition performance tests of KHI polymers were mainly carried out in high-pressure rocking cells using synthetic natural gas mixture. The slow constant cooling method

was deployed as the standard screening method for KHI performance ranking.

My thesis consists of ten publications. Eight of the papers are published in the journal of Energy & Fuels, and two of the papers are published in the journal of Chemical Engineering Science.

In summary, the inhibition performance of several series of amide-containing KHI polymers, including *N*-alkyl-*N*-vinylamide, 3-methylene-2-pyrrolidone, *N*-vinyl caprolactam, and acrylamide polymers, were improved by using treatments like *N*-alkylation, ring expansion, end-capping modification, copolymerization, and combination of synergist solvents. Tailor-made polypeptides as well as several classes of non-amide polymers, including polyvinylsulphonamides, amine oxide polymers, zwitterionic poly (sulfobetaine methacrylate)s, and polyvinylaminals, have been shown to give excellent inhibition performance. Most of these novel KHIs gave promising high cloud points. In addition, the inhibition mechanisms were discussed with respect to the inhibition performance results of KHIs and their various structures.

Table of Contents

Acknowledgements iii

Abbreviations v

Summary xii

Table of Contents xiv

List of Journal Publications xxi

1 Introduction 1

2 Theoretical Background 4

- 2.1 Gas Hydrate Structures 4
  - 2.1.1 Structure I Hydrates 6
  - 2.1.2 Structure II Hydrates 7
  - 2.1.3 Structure H Hydrates 7
  - 2.1.4 Coexistence of Hydrate Structures 8
- 2.2 Gas Hydrate Formation 9
  - 2.2.1 Hydrate Nucleation 11
  - 2.2.2 Hydrate Crystal Growth 14
- 2.3 Gas Hydrate Control 16
- 2.4 Chemical Inhibition 18
  - 2.4.1 Thermodynamic Hydrate Inhibitors 18
  - 2.4.2 Anti-Agglomerants 19
  - 2.4.3 Kinetic Hydrate Inhibitors 21
- 2.5 Mechanisms for Kinetic Hydrate Inhibition 23
  - 2.5.1 Hypothesized Kinetic Hydrate Inhibition Mechanisms 23
  - 2.5.2 Factors Affecting Kinetic Hydrate Inhibition Performance 27

3 Objectives 36

4 Experimental Methods 37

- 4.1 Syntheses 37
  - 4.1.1 Tailor-made Peptoids 37
  - 4.1.2 N-alkyl-N-vinylamide Copolymers 38
  - 4.1.3 3-Methylene-2-pyrrolidone and 3-Methylene-2-piperidone Polymers 39

4.1.4 Poly (N-vinyl caprolactam) and Poly (N-isopropyl methacrylamide) with Varying End Caps ... 39
4.1.5 Direct Synthesis of Acrylamide-based Polymers from Poly (acrylic acid) ... 40
4.1.6 N-alkyl-S-vinylsulphonamide Polymers ... 41
4.1.7 Amine Oxide Polymers ... 42
4.1.8 Zwitterionic Poly (sulfobetaine methacrylate)s ... 42
4.1.9 Polyvinylaminals. ... 43
4.2 Cloud Point (T_{Cl}) Measurement ... 43
4.3 Kinetic Hydrate Inhibition Performance Testing ... 44
4.3.1 High-pressure Kinetic Hydrate Inhibition Performance Testing ... 44
4.3.2 Tetrahydrofuran (THF) Hydrate Crystal Growth Rate Testing ... 49
5 Completed Studies - Results and Discussion ... 52
5.1 Paper I: Kinetic Hydrate Inhibition of Glycyl-valine-based Alternating Peptoids with Tailor-made N-substituents[188] ... 52
5.2 Paper II: Optimizing the Kinetic Hydrate Inhibition Performance of N-alkyl-N-vinylamide Copolymers[190] ... 55
5.3 Paper III: Improving the Kinetic Hydrate Inhibition Performance of 3-Methylene-2-pyrrolidone Polymers by N-alkylation, Ring Expansion and Copolymerization[193] ... 62
5.4 Paper IV: Study of the Kinetic Hydrate Inhibitor Performance of Poly (N-vinyl caprolactam) and Poly (N-isopropyl methacrylamide) with Varying End Caps[198] ... 67
5.5 Paper V: A Simple and Direct Route to High Performance Acrylamide-based Kinetic Gas Hydrate Inhibitors from Poly (acrylic acid)[205] ... 73
5.6 Paper VI: Polyvinylsulphonamides as Kinetic Hydrate Inhibitors[200] ... 78
5.7 Paper VII: Kinetic Inhibition Performance of Alkylated Polyamine Oxides on Structure I Methane Hydrate[202] ... 83
5.8 Paper VIII: Amine N-oxide Kinetic Hydrate Inhibitor Polymers for High Salinity Applications[239] ... 91
5.9 Paper IX: Zwitterionic Poly (sulfobetaine methacrylate)s as Kinetic Hydrate Inhibitors ... 96
5.10 Paper X: High Cloud Point Polyvinylaminals as Non-amide Based Kinetic Gas Hydrate Inhibitors ... 101
6 Conclusions and Future Work ... 106
6.1 Main Conclusions ... 106

6.2 Future Work 107

7 References 109

Appendices 133

Paper I 134

Paper II 141

Paper III 149

Paper IV 158

Paper V 168

Paper VI 178

Paper VII 187

Paper VIII 200

Paper IX 209

Paper X 231

List of Figures

Figure 1. 1 Example of pressure-temperature graph for gas hydrate formation.[8] 2

Figure 2. 1 Example of cage-like water molecules trapping gas molecules.[13] 4

Figure 2. 2 Typical structures of gas hydrates.[6] 5

Figure 2. 3 Typical faces formed by water molecules through hydrogen bonds in hydrate cavities.[14] 6

Figure 2. 4 Structural interconversion between sI, sII, and sH via abnormal cavities.[28] 9

Figure 2. 5 (a) Relationship between free energy barrier and critical nucleus size of hydrate nucleation; (b) Critical nucleus size affected by temperature.[31] 10

Figure 2. 6 General process of gas hydrate formation. 11

Figure 2. 7 Nucleation pathways from gas and water molecules to the crystalline clathrate. 13

Figure 2. 8 Typical gas consumption versus time curve of gas hydrate formation in a laboratory-scale stirring reactor.[53] 15

Figure 2. 9 Schematic of how THIs, heating and depressurization affect hydrate formation. 17

Figure 2. 10 Structures of butylated quaternary ammonium pipeline AAs. R = long alkyl chain and X = counterion. 20
Figure 2. 11 Structure of polyetherdiamine gas-well AA.[104] 21
Figure 2. 12 Structures of PVP, PVCap, PNIPMAM and poly (*N*-alkylglycines). 22
Figure 2. 13 Structures of hyperbranched polyethyleneimine-alkyl-amine oxide (Left), polyisopropenyloxazoline (Middle), and poly (dialkyl vinylphosphonate) (Right). 22
Figure 2. 14 Gas hydrate formation and inhibition mechanisms.[120] 23
Figure 2. 15 Schematic illustration of KHIs adsorb on the hydrate crystal surface.[122] 24
Figure 2. 16 KHI molecules gradually change the hydrate surface from flat to concave. The blue area is hydrate phase, red spheres represents KHI molecules.[129] 25
Figure 2. 17 Cage-like water-structures from around PVCap molecule. 32

Figure 4. 1 Synthesis of glycine *N*-substituted poly (glycine-valine)s. R = alkyl group containing 1-3 carbons or hydroxyl group. 37
Figure 4. 2 copolymerization of *N*-vinylformamide and *N*-*n*-butyl-*N*-vinylformamide. 38
Figure 4. 3 Synthesis of poly (*N*-vinyl caprolactam) with varying mercaptocarboxylic acid end caps. R = carboxylic acid group. 40
Figure 4. 4 Two-stage synthesis of PNIPAM from PAA. 41
Figure 4. 5 Copolymerization of *N*-alkyl-*S*-vinylsulphonamide and *N*-vinyl-*N*-methylacetamide. R = alkyl group containing 2-4 carbons. ... 42
Figure 4. 6 Synthesis of polyvinylaminal from polyvinlyamine and aldehyde. R = chain or cyclic alkyl group. 43
Figure 4. 7 A photo of the RC5 equipment. 45
Figure 4. 8 T_o and T_a values determined from the graphs obtained from a SCC experiment. 47
Figure 4. 9 t_i and t_a values determined from the graphs obtained from an isothermal experiment. 49
Figure 4. 10 THF hydrate crystals grown on the tip of the hollow glass tube. 51

Figure 5. 1 Structures of the alternating peptides with different *N*- substituents. MA-Pep (up left), EA-Pep (up right), PA-Pep (down left) and EtA-Pep (down right). 53
Figure 5. 2 KHI performance of PA-Pep at different concentrations. 55
Figure 5. 3 Structures of NVA:nBuNVF copolymer (top left), NVA:iBuNVF copolymer (top right), MNVA:nPrNVF copolymer (bottom left) and MNVA:iPrNVF copolymer (bottom right). 56
Figure 5. 4 KHI performance of RK2-034 at varying concentrations. 60
Figure 5. 5 KHI performance of RK2-035 at varying concentrations. 60
Figure 5. 6 Structure of PVP (left) and 3M2P polymer (right). 63
Figure 5. 7 Three methods to improve the KHI performance of 3M2P polymer. R = alkyl groups containing 1-3 carbon atoms. 64
Figure 5. 8 Average T_o values of 3M2P:VCap, 3M2P:BuMAAm and VP:VCap copolymers versus concentration. 67
Figure 5. 9 Summary of the average T_o values for KHI polymers at 2500 ppm both in methane + water and in SNG + water systems. 71
Figure 5. 10 The KHI performance of PVCapSCH(COOH)CH_2COOH at varying concentrations in SNG + water system. 72
Figure 5. 11 Summary KHI performance results for the end groups modified polymers at 2500 ppm in SNG + water + decane system. 73
Figure 5. 12 From left to right: poly (*N*-isopropylacrylamide) (PNIPAM), poly (*N*-*n*-propylacrylamide) (PNnPAM), polyacryloylpyrrolidine (PAPYD) and polyacryloylpiperidine (PAPPD) 75
Figure 5. 13 KHI performance of PNIPAM1 at different concentrations. 78
Figure 5. 14 Structures of modified KHIs by different functional groups. From left to right: VCap: vinyl alcohol copolymer, VCap: vinyl phosphoric acid copolymer, and carboxyl-terminated PVCap. 79
Figure 5. 15 T_o values of the co(nPrVSAM:VIMA) 1:12 synthesized in IPA at different concentrations in water. 83
Figure 5. 16 Structure of HPEI-alkyl-AO. R = alkyl groups containing 2 to 6 carbons. 85
Figure 5. 17 Structures of PPO-*b*-PDEGAO (left), PPO-*b*-PPiGAO (middle) and PPiGAO (right). 92
Figure 5. 18 Results of KHI performance tests for $PPiGAO_{24}$ at different concentrations. 95

Figure 5. 19 Structures of zwitterionic 3-((2-methacryloyloxyethyl)(methyl)(*n*-alkyl)ammonio)propane-1-sulfonate homopolymers with *n*-butyl, *n*-pentyl and *n*-hexyl groups. 97
Figure 5. 20 The KHI performance of P6-1, P6-3 and PCO-1 at different concentrations. 101
Figure 5. 21 Structures of polyvinylaminals (left) and protonated polyvinylaminals in acidic solution. R = chain or cyclic alkyl group. 102

List of Tables

Table 4. 1 Composition of SNG mixture. 44
Table 5. 1 Results of SCC tests for KHI polymers at 2500 ppm. Average of 10 tests. The deviations were calculated by using the formula of STDEV.S in Excel. 54
Table 5. 2 Analytical data of *N*-alkyl-*N*-vinylamide copolymers.[a] 57
Table 5. 3 Cloud point and average KHI performance of *N*-alkyl-*N*-vinylamide copolymers at 2500 ppm. Average of 10 tests. The deviations were calculated by using the formula of STDEV.S in Excel. 59
Table 5. 4 Summary of average KHI performance of *N*-alkyl-*N*-vinylamide copolymers with varying synergists. Average of 10 tests. The deviations were calculated by using the formula of STDEV.S in Excel.. 61
Table 5. 5 Analytical data of the synthesized polymers in this study. 64
Table 5. 6 Summary of the KHI performance of the polymers at 5000 ppm and cloud points. Average of 10 tests. The deviations were calculated by using the formula of STDEV.S in Excel. 66
Table 5. 7 Summary of mercaptocarboxylic acids modified polymers and molecular weight results. 68
Table 5. 8 Summary KHI performance results for the end group-modified polymers at 2500 ppm both in methane + water and in SNG + water systems. Average of 10 tests. 70
Table 5. 9 The KHI performance of the acrylamide-based polymers at 2500 ppm and their cloud points and corresponding original main materials. Average of 10 tests unless otherwise stated. The

deviations were calculated by using the formula of STDEV.S in Excel... 76
Table 5. 10 Analytic results of the synthesized polymers as well as their cloud points (T_{Cl}) and deposition point (T_{dp}) at 2500 ppm. 80
Table 5. 11 Summary results from the SCC tests for KHI polymers at 2500 ppm. Average of 10 tests. The deviations were calculated by using the formula of STDEV.S in Excel. 82
Table 5. 12 Summary of the synthesized oligomers and polymers, as well as their active concentrations in the solvent carriers. 85
Table 5. 13 Summary results of the oligomers and polymers in IPA solvent from SCC tests at 1500 ppm and 2500 ppm in water. Average of 10 tests unless otherwise stated.. 87
Table 5. 14 Summary results of the oligomer and polymers from isothermal tests at 2500 ppm in water. Average of at least 5 tests........... 90
Table 5. 15 Analytical results of PPO-*b*-PDEGA, PPO-*b*-PPiGA and PPiGA as well as the corresponding amine oxide polymers (PGAO). ... 92
Table 5. 16 Summary of the KHI performance results of each amine *N*-oxide polymer at 2500 ppm from SCC tests. Average of 10 tests. The deviations were calculated by using the formula of STDEV.S in Excel... 94
Table 5. 17 Summary of characterization results of zwitterionic polymers. .. 97
Table 5. 18 Summary of KHI performance results from SCC tests of polymers at 2500 ppm, as well as their cloud points (T_{Cl}). Average of 10 tests. The deviations were calculated by using the formula of STDEV.S in Excel. 99
Table 5. 19 Summary results of THF hydrate crystal growth tests. All polyvinylaminals made from the polyvinylamine with *Mw* = 10000 g/mole.. 103
Table 5. 20 Summary results from SCC tests. Average of 6 tests unless otherwise stated. All polyvinylaminals made from the polyvinylamine with *Mw* = 10000 g/mole. 104

List of Journal Publications

I. Zhang, Q.; Koyama, Y.; Ihsan, A. B.; Kelland, M. A., Kinetic Hydrate Inhibition of Glycyl-valine-based Alternating Peptoids with Tailor-made *N*-substituents. *Energy & Fuels* **2020**, 34 (4), 4849-4854.

II. Zhang, Q.; Kawatani, R.; Ajiro, H.; Kelland, M. A., Optimizing the Kinetic Hydrate Inhibition Performance of *N*-Alkyl-*N*-vinylamide Copolymers. *Energy & Fuels* **2018**, 32 (4), 4925-4931.

III. Zhang, Q.; Heyns, I. M.; Pfukwa, R.; Klumperman, B.; Kelland, M. A., Improving the Kinetic Hydrate Inhibition Performance of 3-Methylene-2-pyrrolidone Polymers by *N*-Alkylation, Ring Expansion, and Copolymerization. *Energy & Fuels* **2018**, 32 (12), 12337-12344.

IV. Zhang, Q.; Kelland, M. A., Study of the Kinetic Hydrate Inhibitor Performance of Poly (*N*-vinyl caprolactam) and poly (*N*-isopropyl methacrylamide) with Varying End Caps. *Energy & Fuels* **2018**, 32 (9), 9211-9219.

V. Zhang, Q.; Ree, L. S.; Kelland, M. A., A Simple and Direct Route to High Performance Acrylamide-based Kinetic Gas Hydrate Inhibitors from Poly (acrylic acid). *Energy & Fuels* **2020**, 34 (5), 6279-6287.

VI. Zhang, Q.; Kelland, M. A.; Ajiro, H., Polyvinylsulfonamides as Kinetic Hydrate Inhibitors. *Energy & Fuels* **2020**, 34 (2), 2230-2237.

VII. Zhang, Q.; Kelland, M. A., Kinetic Inhibition Performance of Alkylated Polyamine Oxides on Structure I Methane Hydrate. *Chemical Engineering Science* **2020**, 220 (2020), 115652.

VIII. Zhang, Q.; Kelland, M. A.; Frey, H.; Blankenburg, J.; Limmer, L., Amine *N*-Oxide Kinetic Hydrate Inhibitor Polymers for High-Salinity Applications. *Energy & Fuels* **2020**, 34 (5), 6298-6305.

IX. Zhang, Q.; Kelland, M. A.; Lewoczko, E. M.; Bohannon, C. A.; Zhao, B., Zwitterionic Poly (sulfobetaine methacrylate)s as Kinetic Hydrate Inhibitors. *Chemical Engineering Science* **2020**, 229 (2021), 116031.

X. Kelland, M. A.; Dirdal, E. G.; Zhang, Q., High Cloud Point Polyvinylaminals as Non-amide Based Kinetic Gas Hydrate Inhibitors. *Energy & Fuels* **2020**, 34 (7), 8301-8307.

1 Introduction

Gas hydrates are crystalline solids consisted of water and gas molecules. Gas hydrates form at the conditions of low temperature and high pressure, which are common conditions of gas and oil transportation pipelines in deepwater and cold climate areas.[1] In 1934 Hammerschmidt firstly reported the pipeline blockage caused by the formation of gas hydrates at temperatures above the ice point.[2]

Gas hydrate formation is one of the main problems that must be avoided in the production flow lines of the upstream oil and gas industry. Once gas hydrate plug occurs in flow lines, it usually causes severe safety issues and huge economic losses. In addition, the removal of the gas hydrate plug often comes with the risks of severe damage to equipment and personnel.[3-5]

For gas hydrate to form, the conditions of water contacted with gas, such as nitrogen gas, carbon dioxide, hydrogen sulphide, and lightweight hydrocarbon, at ambient temperature and elevated pressure are required.[6] Figure 1.1 shows an example of the temperature and pressure equilibrium curve of gas hydrate formation. On the right-side region of the gas hydrate equilibrium curve, no gas hydrate is present, while the left side region of the equilibrium curve is where gas hydrates can form. The sub-cooling degree (ΔT) equals to the equilibrium temperature (T_{eq}) minus the operating temperature, at a given pressure. Usually, the sub-cooling degree is considered as the driving force for gas hydrate formation,[7] as the degree of sub-cooling indicates how far the operating temperature is into the hydrate stability zone.

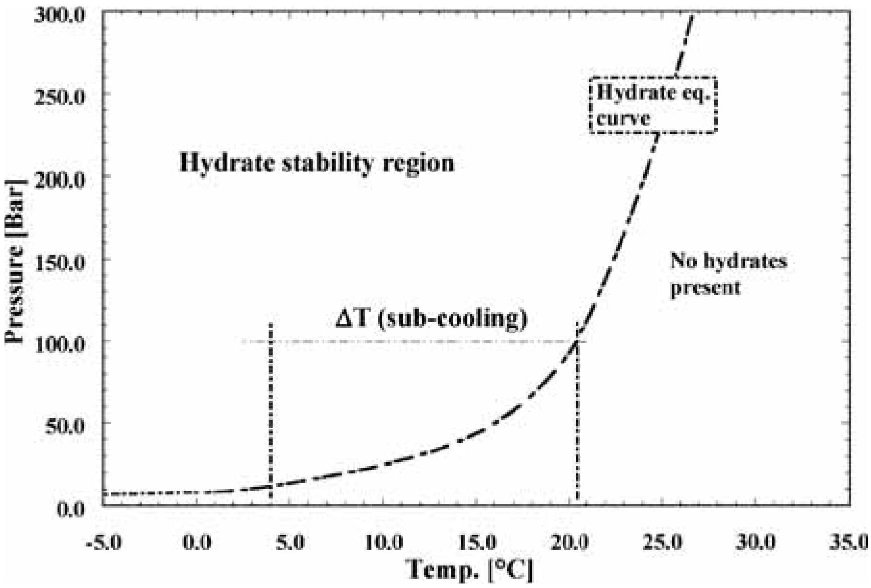

Figure 1. 1 Example of pressure-temperature graph for gas hydrate formation.[8]

For preventing gas hydrates from forming in the flow lines of gas and oil transportation, a range of methods have been proposed, for example, dehydration, keeping operating temperature and pressure out of the hydrate stability region, and chemical inhibition.[3, 4] For many field scenarios where hydrate plug prevention is required, deployment of chemical inhibitors is a comparatively effective and cost-saving method to guarantee the gas and oil products flowing smoothly to their destination. Since the early 1990s low dosage hydrate inhibitors (LDHIs) have attracted more and more attention, as the effective dosage of LDHIs required is in much smaller quantities than that of traditional thermodynamic hydrate inhibitors (THIs), which is beneficial for capital and operating expenses saving as well as for health and environment protection.[8-10]

Kinetic hydrate inhibitors (KHIs) is a class of LDHIs, the other class being anti-agglomerants (AAs). A significant number of KHIs have been reported, and most of them are water-soluble amide-based polymers, but the inhibition mechanism of KHIs is still not fully understood. Therefore, it is crucial to gain more understanding about the mode of action for KHIs as well as develop more effective and compatible KHIs.

2 Theoretical Background

2.1 Gas Hydrate Structures

Gas hydrates are non-stoichiometric crystalline clathrate consisting of cage-like water molecules "host" and trapped gas molecules "guest". Water molecules are connected by hydrogen bonds to make the cavity framework, and usually each cavity can be filled with one gas molecule.[1, 6, 11] (Figure 2.1) However, gas hydrates are stable as long as over 70% of the water cavities are filled with gas molecules, which means some of the water cavities in gas hydrates can be empty.[12]

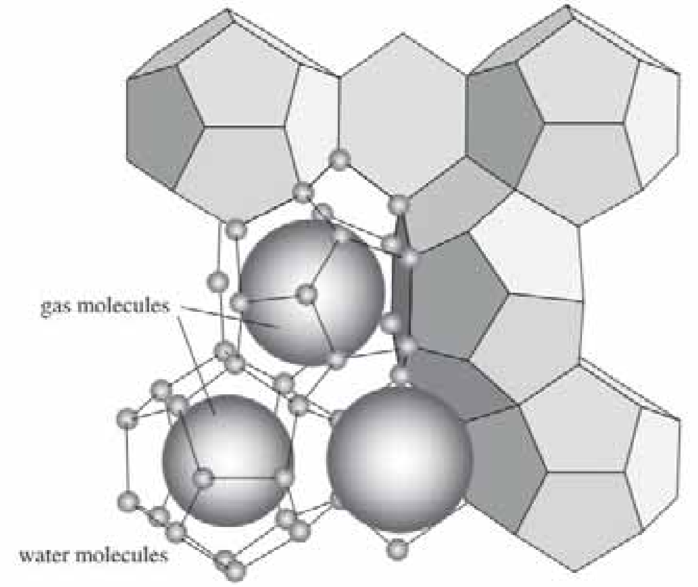

Figure 2. 1 Example of cage-like water molecules trapping gas molecules.[13]

Figure 2.2 shows Structure I, Structure II and Structure H hydrates, abbreviated as sI, sII and sH hydrates, respectively, which are typical structures of gas hydrates. The structures of gas hydrates are classified according to the different cavity types of their composition.

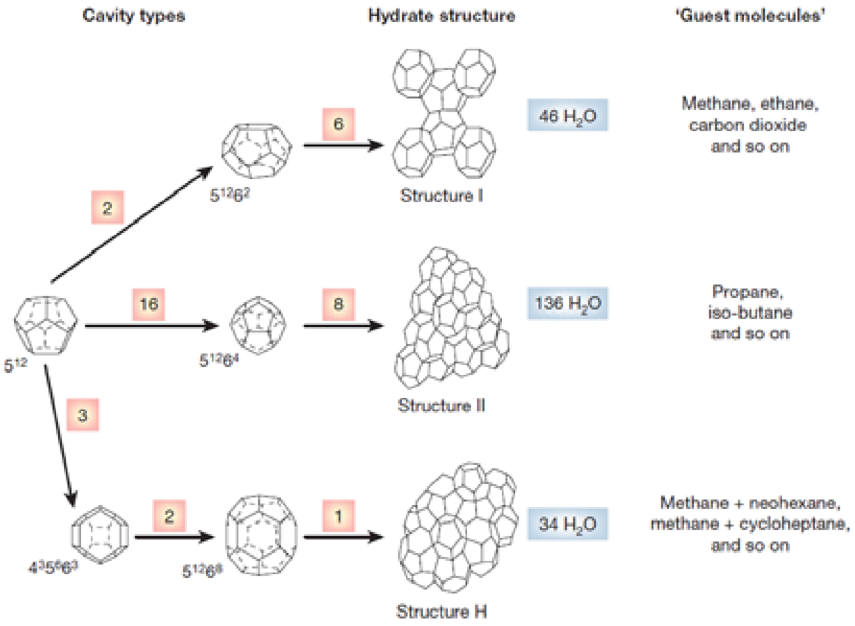
Cavity types
Hydrate structure
'Guest molecules'
5^{12}
2
$5^{12}6^2$
6
Structure I
46 H_2O
Methane, ethane, carbon dioxide and so on
16
$5^{12}6^4$
8
Structure II
136 H_2O
Propane, iso-butane and so on
3
$4^35^66^3$
2
$5^{12}6^8$
1
Structure H
34 H_2O
Methane + neohexane, methane + cycloheptane, and so on

Figure 2. 2 Typical structures of gas hydrates.[6]

The numbers in Figure 2.2, i.e., 5^{12}, $5^{12}6^2$, $5^{12}6^4$, $4^35^66^3$, and $5^{12}6^8$, describe the varying cavity types in gas hydrates. For example, $5^{12}6^2$ indicates the hydrate cavity consisting of twelve pentagonal and two hexagonal faces. Three typical faces formed by water molecules through hydrogen bonds in hydrate cavities can be seen in Figure 2.3. Each structure contains 5^{12} cavities. The smallest unit of sI hydrate is composed of two 5^{12} and six $5^{12}6^2$ cavities, sixteen 5^{12} and eight $5^{12}6^4$ cavities for sII hydrate, and three 5^{12}, two $4^35^66^3$ and one $5^{12}6^8$ cavities for sH hydrate. Notably, when all of the "host" water cages are occupied by the "guest" gas molecules, the component concentrations of sI, sII and sH hydrates are similar: 85 mol% water molecules and 15 mol% gas molecules.

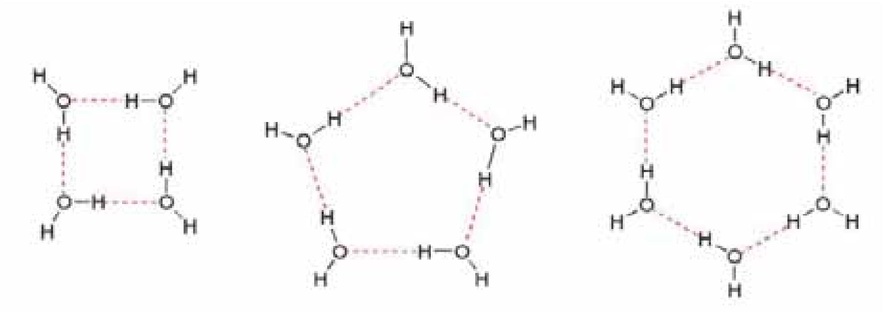

Figure 2. 3 Typical faces formed by water molecules through hydrogen bonds in hydrate cavities.[14]

Different sized gas molecules can fill into the suitable sized gas hydrate structures. System with small gas molecules, i.g., methane, ethane and carbon dioxide, typically produces sI hydrates as they fit the cavities in sI hydrates. System with larger gas molecules, i.g., propane and *iso*-butane, tends to form sII hydrates. sH gas hydrates requires the formation conditions of co-existing of small gas molecules and larger gas molecules than *iso*-butane like methane + cycloheptane.

2.1.1 *Structure I Hydrates*

sI hydrates contain small 5^{12} and large $5^{12}6^{2}$ cavities in the ratio of 1:3. The average radius of 5^{12} and $5^{12}6^{2}$ cavities in sI hydrates is 3.95 and 4.33 Å respectively. Small gas molecules with diameters ranging from approximately 4.4 to 5.5 Å, e.g., methane, hydrogen sulphide, carbon dioxide and ethane preferentially form cubic sI hydrates.[6] It is reported that sI hydrates are the most common gas hydrates in the natural environment due to the enormous amount of methane deposited in deep water sediments and permafrosts.[15, 16] For gas and oil production, sI hydrates can form only when methane gas is rich, and the composition of other hydrocarbon gases is quite low.[4]

2.1.2 *Structure II Hydrates*

The sII unit cell consists of sixteen small 5^{12} and eight larger $5^{12}6^4$ cavities. sII hydrates can form at the presence of large molecules, e.g., propane and *iso*-butane. Also, some binary gas mixtures of small gases, e.g., methane and ethane mixtures, can form stable sII hydrates.[17, 18] However, methane and carbon dioxide mixtures in any combination ratios cannot form stable sII hydrates.[19] sII hydrates are reported to be more stable than sI methane hydrate,[20] and they can be found in nature, especially in thermogenic gas sources[21]. sII is the most common structure that forms in gas and oil fields, as it is the most thermodynamically stable structure even if in the conditions that the methane gas content in the raw natural gas mixture exceeds 90% but there are still some larger gas components like propane and *iso*-butane.[4, 22]

2.1.3 *Structure H Hydrates*

The sH unit cell consists of small 5^{12}, medium $4^35^66^3$ and large $5^{12}6^8$ cavities in the ratio of 3:2:1. sH hydrates can form at the conditions of coexistence of small gases and larger gases than *iso*-butane. Large gas molecules like pentane and hexane are suitable for filling the large $5^{12}6^8$ cavities in sH hydrates, and small gas molecules like methane and hydrogen sulphide can help to stabilize the smaller cavities. sH hydrates have been found in nature, and it is reported that the stability of sH hydrates is between sI and sII hydrates,[20] which means that sH hydrates may exist in a wider pressure-temperature region in the natural environment than sI methane hydrate. However, compared to sI and sII, sH is not a typical structure that forms in the gas and oil industry.[3, 23]

2.1.4 *Coexistence of Hydrate Structures*

Apart from the typical cavities for sI, sII and sH, many uncommon cavity types, such as $5^{12}6^{3}$ and $4^{1}5^{10}6^{2}$, have been discovered by molecular dynamics simulation (MDS) studies. Matthew et al. reported that cavities, including 5^{12}, $5^{12}6^{2}$, $5^{12}6^{3}$, and $5^{12}6^{4}$ exist during the nucleation and growth period of methane hydrate.[24] $5^{12}6^{3}$ cavity acts as a link between the thermodynamically preferred sI hydrate and the kinetically preferred sII hydrate formed initially.[25, 26] (Figure 2.4) Guo et al. reported that at the initial nucleation phase of methane hydrate formation, $4^{1}5^{10}6^{2}$ cavity acts as a link between sI and sH hydrates, and sII hydrate can form from sH hydrate directly.[27, 28] Apart from MDS studies, sII methane hydrates have also been detected by Raman and nuclear magnetic resonance (NMR) spectroscopy in the initial period of methane hydrate formation, and then the sII methane hydrates gradually transform to sI methane hydrates until finally disappeared completely.[29]

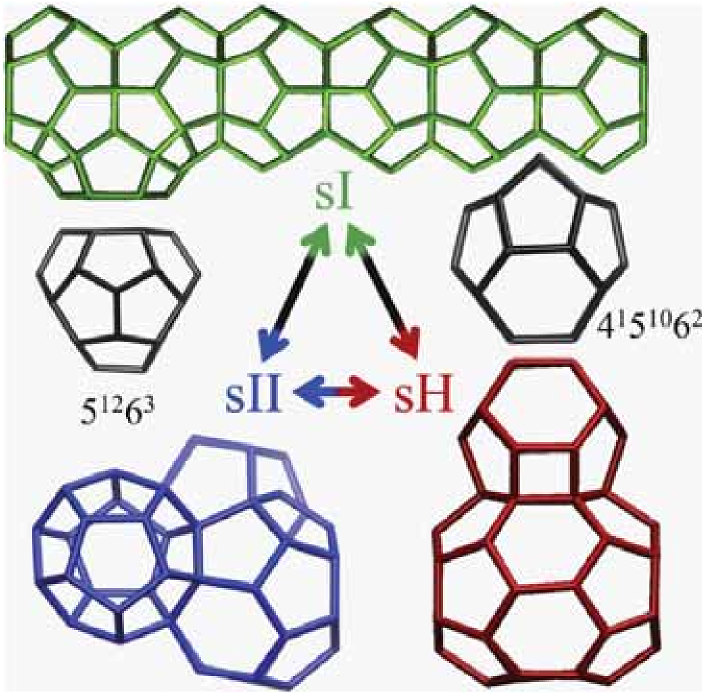

Figure 2. 4 Structural interconversion between sI, sII, and sH via abnormal cavities.[28]

2.2 Gas Hydrate Formation

Theoretically, like the formation procedure of every other crystal, gas hydrate formation includes nucleation and crystal growth two consecutive steps. Predicted by Gibbs in the late 1800s, there is a critical size nucleus which makes the system overcome the free-energy barrier and then allows the crystal to grow smoothly.[30] In Figure 2.5 (a), before reaching the critical size (r_{crit}) the nucleus is metastable (either grow or dissolve) as the total Gibbs free energy (ΔG_{tot}) in the system is unfavourable for increasing its radius. Once the radius of the nucleus is over the r_{crit} size, continued growth becomes favourable (Figure 2.6).

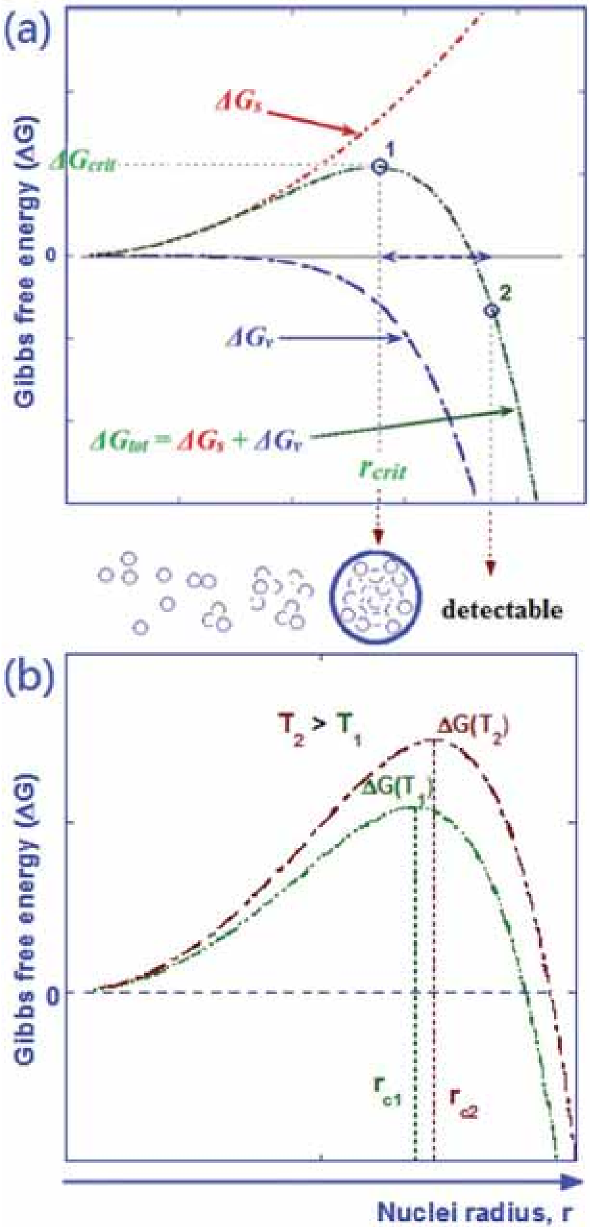

Figure 2. 5 (a) Relationship between free energy barrier and critical nucleus size of hydrate nucleation; (b) Critical nucleus size affected by temperature.[31]

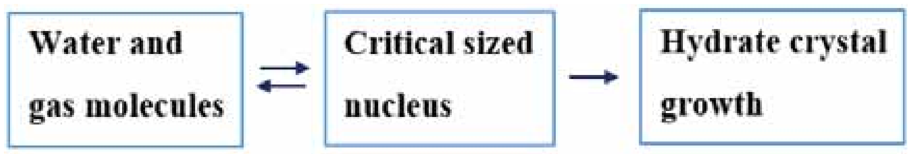

Figure 2. 6 General process of gas hydrate formation.

It seems that finding the critical size is the crucial element for studying the nucleation mechanism of gas hydrate. However, it is challenging to detect the critical-sized nucleus experimentally as it happens on the molecular level and stochastically.[32] Through molecular dynamics simulation studies the critical sizes are reported to be as small as ten molecules to 1000 molecules or even up to several million molecules with the size varying from around 10 to 1000 Å depending on many variables, e.g., temperature, components and supersaturation.[33-36]

Figure 2.5 (b) shows the critical nucleus size can be affected by temperature. The critical size increases, when the temperature gets higher (or supercooling gets lower), which has been proved experimentally, although indirectly. In 2019, using size-controlled graphene oxide nanosheets (GOs) which can be considered as the critical size of the ice nucleus, Bai et al. studied the relationship between the average lateral size (L) of GOs and the sub-cooling (ΔT) of ice formation. They reported that when $L\Delta T \approx 200$ nm K, the ΔT of ice formation decreased as the L of GOs increased.[37]

2.2.1 *Hydrate Nucleation*

As it is difficult to observe the formation procedure of hydrate nucleation directly in the real world, molecular dynamics simulations (MDS) have played an essential role in studying nucleation mechanisms. Several mechanism hypotheses of hydrate nucleation have been proposed via MDS studies. The labile cluster hypothesis (LCH), local structuring hypothesis (LSH), and blob hypothesis are the well-known hydrate nucleation mechanisms.

The labile cluster hypothesis (LCH) is the earliest nucleation mechanism proposed by Sloan et al. in 1991.[38] According to the LCH theory, the nucleation pathway of gas hydrates are as follows. (i) In hydrate forming region, pentamers or hexamers labile ring structures occur in the pure water system. (ii) The labile ring structures form labile clusters immediately when gas molecules dissolve. (iii) The labile clusters agglomerate gradually by sharing faces until reaching the critical size to trigger the subsequent hydrate growth. The LCH supporters believe that the hydrate nucleation starts from the water framework.[39-41]

However, others assume that the hydrate nucleation begins from the dissolved gases as gas hydrate usually starts at the gas/water interface where the concentration of gas is relatively higher.[42-45] Thus, the local structuring hypothesis (LSH) was proposed by Radhakrishnan et al. using molecular dynamics simulations on CO_2 hydrate in 2002.[46] In 2003 the LSH theory has been proved to be also suitable for methane hydrate by MDS.[47] The LSH theory explains the nucleation pathway of gas hydrates as follows. (i) The dissolved gas molecules are locally rearranged to structure similar to that in hydrate clathrate by the mass and thermal fluctuation in the system. At the same time, the water molecules around the rearranged gas molecules are perturbed. (ii) When the size of the locally rearranged gas molecules reaches the critical size, it is energetically favourable for the growth of gas hydrate.

The blob hypothesis was proposed by Jacobson et al. in 2010.[48, 49] Through molecular dynamics simulations, they come up with the nucleation pathway of gas hydrates as follows. (i) In the solution, a blob that aggregates of hydrophobic gas molecules and the water molecules surrounding them forms and dissolves with the fluctuation of mass and thermal of the system. (ii) Amorphous clathrate, which is a mixture of 5^{12}, $5^{12}6^{2}$, $5^{12}6^{3}$, and $5^{12}6^{4}$ cages, occurs when the blob is reaching to the critical size. (iii) Amorphous clathrate becomes a well-organized crystalline clathrate and gas hydrate grows spontaneously. The blob hypothesis considers the gas molecule and water molecule as the same important role at the beginning of gas hydrate nucleation formation.[50-52]

The proposed nucleation pathways of gas hydrates are summarized in Figure 2.7. This scheme was drawn initially by Yoreo to show classical and non-classic nucleation pathways of mineral crystals.[30] It seems a very suitable scheme to show hydrate nucleation pathways. Each of the pathways can explain some phenomenon, but none of them can be fully verified by existing experiment technologies. They are significant conceptual attempts for hydrate nucleation studies and may enlighten the establishment of a predictive hydrate nucleation model in the future.

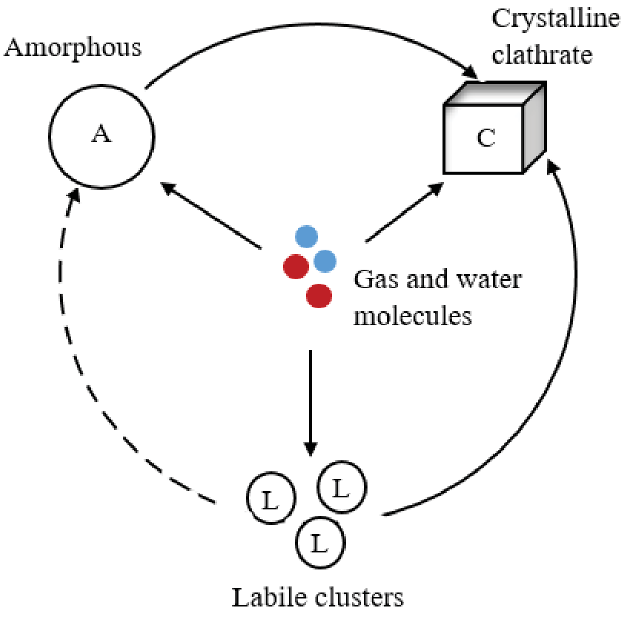

Figure 2. 7 Nucleation pathways from gas and water molecules to the crystalline clathrate.

2.2.2 *Hydrate Crystal Growth*

The formation of hydrate nucleation is a quite stochastic process, as well as it may happen in nanoseconds with the length scale being nanometers. The following hydrate growth process after the nucleation over the critical size may be more intuitive, as it involves a relatively long time and more macro size.[31, 53] However, the hydrate growth process is also more complicated, and it can be affected by many factors, i.g., intrinsic kinetics, surface conditions, mass transfer, and heat transfer. Figure 2.8 shows a typical gas consumption versus time curve of gas hydrate formation in a laboratory-scale reactor. The consumed gas molecules are considered to form gas hydrates. When the pressure and temperature are under hydrate forming region, hydrate crystal growth is a spontaneous process after the critical nucleation size. Thus, the critical research on hydrate crystal growth is the growing rate. In Figure 2.8, at the beginning, some gas molecules are consumed due to the gas dissolution and nucleus formation. Then there is a quick gas consumption when the hydrate crystal growth starts after the stable nucleus. The rates of gas consumption varies during different periods of gas hydrate growth. As there are limited gas or water components in a reaction vessel, it will eventually reach the solid hydrate stable condition.

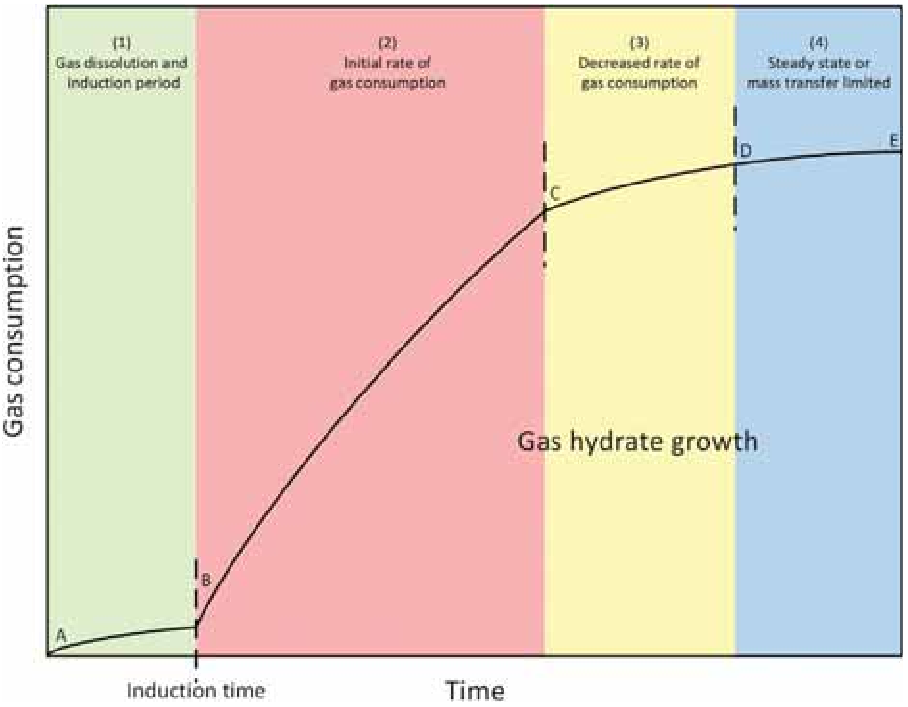

Figure 2. 8 Typical gas consumption versus time curve of gas hydrate formation in a laboratory-scale stirring reactor.[53]

Some models of studying the kinetic rate of gas hydrate growth have been proposed.[53] According to the rate-determining step (RDS) mechanism, those models can be classified into three major categories: (i) Chemical reaction models. Although there is no chemical bond breaking and reformation during the formation of gas hydrates, it is assumed to be chemical reactions when calculating the kinetic growth rate of gas hydrate. The process of gas hydrate formation can be described as several consequent reaction steps, and Arrhenius-type rate equations are utilized to calculate the hydrate growth rate.[54-59] (ii) Mass transfer models. By considering fugacity difference and concentration difference between different phases in gas hydrate formation systems, different mass transfer controlled models were proposed.[60-65] (iii) Heat transfer models. The sub-cooling degree of a system can affect the formation of gas hydrate. Also, heat transfer exists during stirring, flowing, and transportation of gas hydrate. In addition, gas hydrate formation is an exothermic reaction. Thus, heat transfer is one of the critical factors that need to be considered when building gas hydrate growth models.[66-69] Several combined models also have been proposed, such as, mass transfer + reaction kinetics,[70-80] heat transfer + reaction kinetics,[81-83] and fluid flow + heat flow + reaction kinetics model.[84-86] Although most of these proposed models fit well with the experimental results under certain practical conditions, so far, there is no universal model that could explain all the hydrate growth behaviours.

2.3 Gas Hydrate Control

Gas hydrates are non-flowing crystalline solids, so they are unwelcomed during the transportation of gas and oil products. Once gas hydrate blockage forms, the production stoppage may be required to remove the hydrates, and it costs high capital expense (CAPEX) and operating expense (OPEX). The density of hydrate solid is larger than that of the fluid hydrocarbon, so the formation of hydrates may damage the expensive gas and oil facilities and even cause safety problems. The operation of hydrate blockage removal also comes with potential risks of facility damage. Thus, to provide flow assurance, methods for hydrate prevention must be considered, especially for the flow lines in deeper ocean and arctic areas. The formation of gas hydrates requires some certain conditions: (i) Water comes together with light hydrocarbon gases. (ii) Temperature and pressure at the hydrate stability region. The main principles of hydrate prevention are as follows.

- Water control: Remove as much water as possible before the transportation of gas and oil products, e.g., by gas dehydration, water separation and water cut reduction;[5, 87] Minimize free water phase by cold stabilized flow process.[88, 89]

- Gas management: Minimize the gas phase by the application of hydraulic methods; Keep the operational pressure lower than the equilibrium point of gas hydrate formation.[4]
- Thermal methods: Keep the operational temperature high to operate in the no-hydrate region, e.g., by direct heating and isolation.[3]
- Chemical inhibition. (more detailed discussion in Section 2.4)

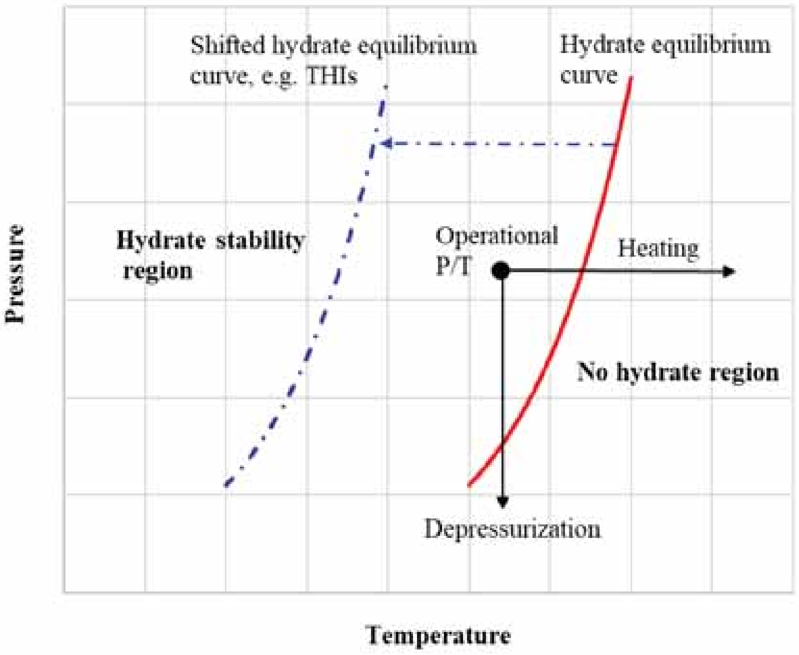
Shifted hydrate equilibrium curve, e.g. THIs
Hydrate equilibrium curve
Hydrate stability region
Operational P/T
Heating
No hydrate region
Depressurization
Pressure
Temperature

Figure 2. 9 Schematic of how THIs, heating and depressurization affect hydrate formation.

For many flow assurance applications, chemical inhibition is more practical than avoidance of the hydrate stability region by water removal, heating, and depressurization (Figure 2.9). As it is impossible to completely eradicate the water in the production well pipes, the presence of some water is usually inevitable. The methods of heating and insulating flowlines are expensive, especially for long-distance transportations. A fairly high pressure is usually required to guarantee the production rate. Chemical inhibition is a comparatively economical CAPEX and OPEX-saving method. More importantly, the application of hydrate inhibition chemicals has been proved to be reliable in many cases.[90-92]

2.4 Chemical Inhibition

Generally speaking, hydrate inhibition chemicals can be divided into two classes: (i) thermodynamic hydrate inhibitors (THIs) and (ii) low dosage hydrate inhibitors (LDHIs).[3, 4] THIs can shift the equilibrium point of hydrate formation to higher pressure or lower temperature, which means that THIs are capable of melting the already formed gas hydrates. However, a very high concentration (ca. 20-80 wt.%) of THIs is required to be effective. LDHIs, as the name implies, are hydrate inhibitors that give considerable performance at low dosages (ca. 0.1-1.0 wt.%). LDHIs have two branches: (i) anti-agglomerants (AAs) and (ii) kinetic hydrate inhibitors (KHIs). AAs enable hydrates to form as small transportable dispersed particles while KHIs delay the hydrate formation rate, thus preventing the blockage of hydrates during the gas and oil transportation.

2.4.1 *Thermodynamic Hydrate Inhibitors*

The application of thermodynamic hydrate inhibitors (THIs) is a traditional method in the gas and oil fields to prevent gas hydrate formation. Typical THIs include alcohols, glycols, and some inorganic salts.[3, 4] Methanol and monoethylene glycol (also called MEG, glycol, or ethyleneglycol) are two of the most commonly used THIs. As the molecular weight of methanol is quite low (32 g/mol), some of it is vaporized into the gas phase when used to prevent gas hydrates from forming in flowlines. In addition, THIs can melt gas hydrates. It is reported that this method was used to solve the hydrate plug problem during the accident of "BP Deep Water Horizon Oil Spill" in 2010: A severe hydrate plug happened due to the leaking well on May 7. When the leaked gas bubbles got contacted with the cold seawater, gas hydrate solids formed and plugged the cofferdam. By June 3, the problem of the gas hydrate plug was solved after the addition of methanol.[93] However, due to the highly flammable, toxic, and refinery catalyst-killing properties of methanol, MEG is preferred many places worldwide. MEG has a comparatively high molecular weight (62 g/mol), so it can be recovered through the removal of water. However, the application of MEG in flowlines may lead to the problem of salt precipitation or a worsening of scaling.[1] In addition, the high concentration requirement of MEG makes high transportation and storage costs. Thus, the alternative method of utilizing significantly lower concentrations of LDHIs for hydrate prevention becomes attractive (Section 2.4.2 - 2.4.3).

2.4.2 *Anti-Agglomerants*

Anti-agglomerants (AAs) are a type of LDHI. AAs do not stop hydrates from forming (unless at very low sub-coolings) but can prevent small hydrate crystals from aggregating into large masses, thus maintaining the fluidity of gas and oil products in the flowlines. This action mode makes AAs useful even at high sub-cooling (>10 ^{o}C) conditions in deepwater applications.[8] Depending on the small hydrate particles dispersed either in the liquid hydrocarbon or in excess of water, AAs can be divided into two classes: (i) production or pipeline AAs and (ii) gas-well AAs.[4]

2.4.2.1 **Pipeline AAs**

The application of pipeline AAs requires a liquid hydrocarbon phase to disperse the formed hydrates, and a water cut below about 80-90% to ensure that the hydrate slurry is not too viscus to transport.[8, 94, 95] Two working mechanisms of pipeline AAs have been proposed: (i) the emulsion mechanism and (ii) the "hydrate-philic" mechanism.[4] In the emulsion mechanism, a water-in-oil emulsion can form when injecting a surfactant. The hydrate particles that form within the water droplets of the emulsion cannot easily get agglomerate. Many series of polymeric surfactants, e.g., polyalkenyl succinic anhydrides and ethoxylated polyamines, are effective emulsion pipeline AAs.[8, 96] In the "hydrate-philic" mechanism, the "hydrate-philic" groups of the amphiphilic surfactants attach to the hydrate surface and then disrupt its growth. The hydrocarbon side of the amphiphilic surfactants makes the attached hydrates hydrophobic. Thus the small hydrate particles can be easily dispersed in the oil phase.[97] Quaternary ammonium and phosphonium surfactants with butyl or pentyl groups are effective "hydrate-philic" AAs.[95, 98] (Figure 2.10)

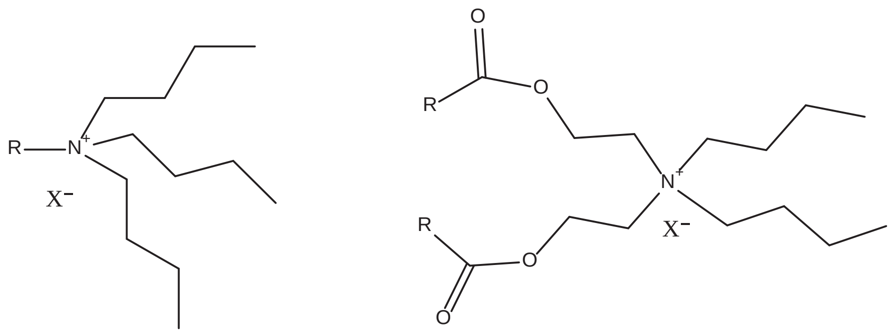

Figure 2. 10 Structures of butylated quaternary ammonium pipeline AAs. R = long alkyl chain and X = counterion.

2.4.2.2 **Gas-well AAs**

Gas-well AAs can disperse hydrates in excess water, and then the small hydrate particles can be transported by the aqueous phase without agglomeration.[99, 100] Thus, the application of gas-well AAs do not require a liquid hydrocarbon phase. Polyetherpolyamines, such as polyetherdiamines, with low molecular weights (<500 g/mol) are excellent gas-well AAs. (Figure 2.11) Polyetheramine gas-well AAs have been used to prevent hydrate blockages in many gas well applications.[101-103]

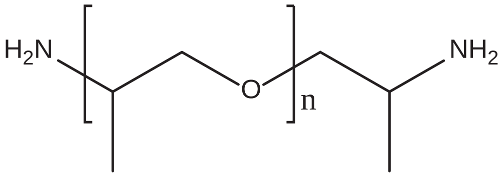

Figure 2. 11 Structure of polyetherdiamine gas-well AA.[104]

2.4.3 *Kinetic Hydrate Inhibitors*

The other class of LDHIs is kinetic hydrate inhibitors (KHIs). KHIs can delay the nucleation onset and/or the crystal growth of hydrate formation for a long enough time to ensure the transportation of gas and oil products to their destination fluently. The commonest and some of the most effective KHIs are water-soluble amide-based polymers, and they include (i) polymers with amide side groups, e.g., poly (*N*-vinyl pyrrolidone) (PVP), poly (*N*-vinyl caprolactam) (PVCap), poly (*N*-isopropyl methacrylamide) (PNIPMAM) and hyperbranched poly (ester amide)s[4, 8-10, 105-107] and (ii) polymers with amide backbones, e.g., anti-freeze proteins, bespoke polypeptides and pseudo-polypeptides.[108-111] PVP, PVCap, PNIPMAM and their copolymers, and hyperbranched poly (ester amide)s have been commercialized in this field. (Figure 2.12) PVP and PVCap have been investigated as KHIs since the early 1990s.[8, 112] Until now, PVP and PVCap, especially the latter, are still used as standards for evaluating the performance of new KHIs. In 1996, Exxon reported a series of polyalkyl(meth)acrylamides and among which PNIPMAM and polyacryloylpyrrolidine (PAPYD) gave the best KHI performance.[113, 114] Since the 2000s, PNIPMAM and its copolymers have been commercially available. Hyperbranched poly (ester amide)s have KHI performance with a sub-cooling up to around 10 °C, not quite as good as the performance of PVCap or PNIPMAM.

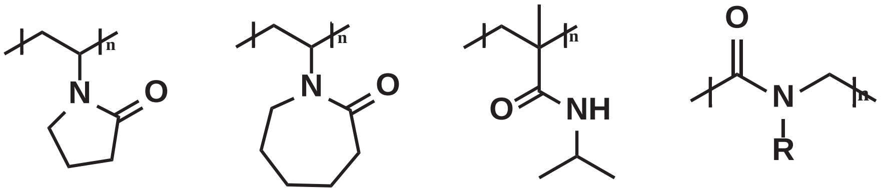

Figure 2. 12 Structures of PVP, PVCap, PNIPMAM and poly (*N*-alkylglycines).

Recently, several kinds of effective non-amide KHI polymers have been reported, e.g., amine *N*-oxide polymers,[115-117] isopropenyloxazolines polymers,[118] and poly (vinyl phosphonate) diesters[119]. (Figure 2.13) Almost all efficient KHI polymers meet the two necessary structural conditions: (i) hydrophilic groups and (ii) hydrophobic groups (alkyl groups) that connected directly or indirectly to the hydrophilic groups.

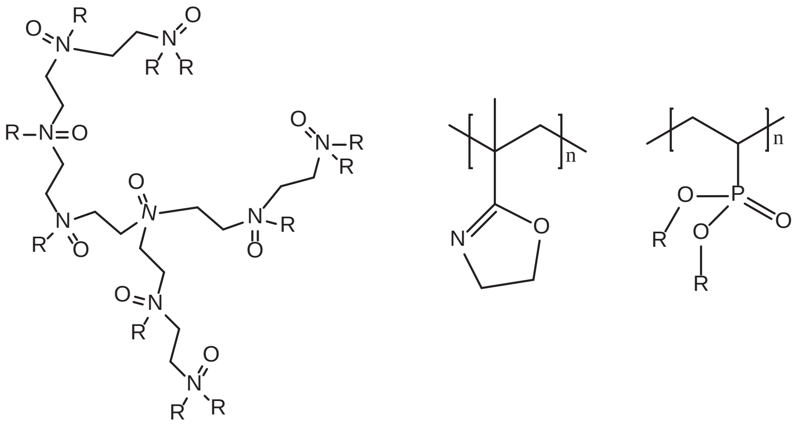

Figure 2. 13 Structures of hyperbranched polyethyleneimine-alkyl-amine oxide (Left), polyisopropenyloxazoline (Middle), and poly (dialkyl vinylphosphonate) (Right).

2.5 Mechanisms for Kinetic Hydrate Inhibition

The hydrate formation process includes nucleation and growth, so KHIs work on nucleation inhibition and growth inhibition, however, depending on the detection method it can be difficult to distinguish the two. Theoretically, for the nucleation inhibition procedure, KHIs prevent water and gas molecules from forming critical-sized nuclei, and for the growth inhibition process, KHIs retard hydrate crystal growth.

2.5.1 *Hypothesized Kinetic Hydrate Inhibition Mechanisms*

Generally speaking, there are two widely accepted inhibition mechanism hypotheses of kinetic hydrate inhibitors: adsorption inhibition hypothesis and perturbation inhibition hypothesis. Figure 2.14 shows the process of hydrate formation and possible working mechanisms of KHIs. Free water in the liquid phase may be prevented from closing to hydrate surface by adsorption or perturbation of KHIs, and then gas hydrate cannot grow further.

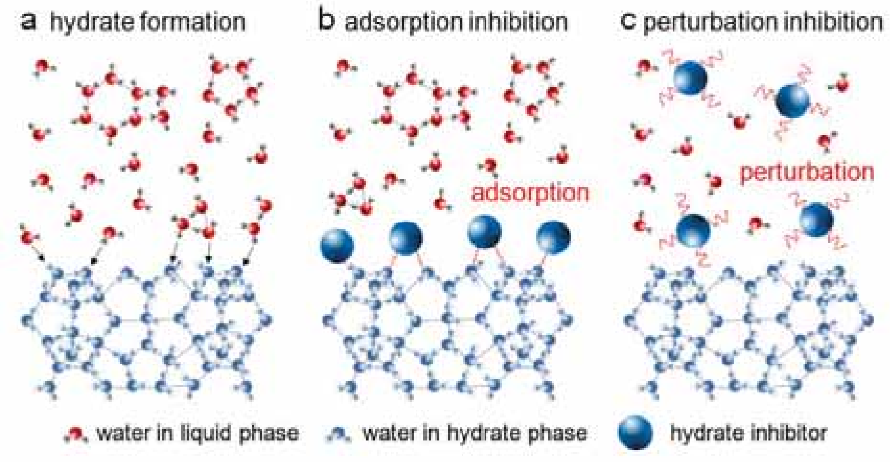
a hydrate formation
b adsorption inhibition
c perturbation inhibition
adsorption
perturbation
water in liquid phase
water in hydrate phase
hydrate inhibitor

Figure 2. 14 Gas hydrate formation and inhibition mechanisms.[120]

Adsorption inhibition theory shown in Figure 2.14 (b) suggests that KHIs adsorb on pre-critical nucleation sites or growing hydrate crystal surface and prevent the hydrate surface from direct contact of water and gas molecules, thus inhibiting hydrate formation.[121] Klomp et al. illustrated a model (Figure 2.15) that KHIs adsorb onto the hydrate crystal surface and divide the surface into small areas. The hydrate growth can only happen in the surface areas that are not covered by KHI, and the formed hydrates in these areas have a larger surface to volume ratio, which is favoured for further hydrate growth. Once the sub-cooling degree is exceeded, the hydrate may grow in between the covered areas. Thus, both the coverage ratio of KHI onto the hydrate surface and the spacing between the coverage areas can affect the KHI performance.

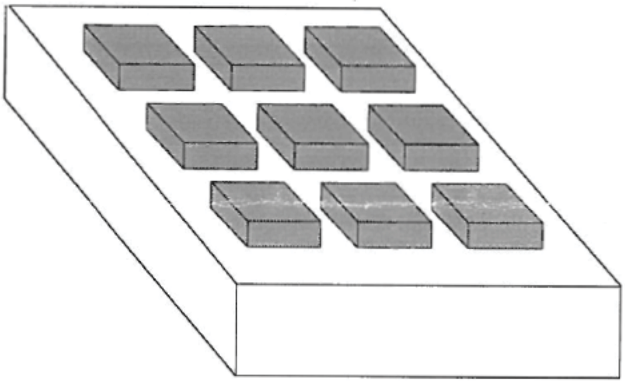

Figure 2. 15 Schematic illustration of KHIs adsorb on the hydrate crystal surface.[122]

The adsorption inhibition theory has been received widespread attention, and there are many evidence both from experimental and computer modelling supporting this theory.[123-127] For example, Zhang et al. demonstrated that on cyclopentane hydrate, the adsorption isotherm of PVP fits well with the Langmuir-type, and that of PVCap accords with the multilayer Brunauer-Emmett-Teller (BET)-type when its concentration is over 0.5 wt.%.[128] Also, when comparing the single adsorption layer of PVP and PVCap, the calculated monolayer density of PVCap is higher due to its larger molecule size. Both the thicker adsorption layer and larger molecule size make PVCap a more powerful KHI than PVP in preventing cyclopentane hydrate from further growing. Also, using molecular dynamics simulations (MDS), Yagasaki et al. observed that PVCap oligomers adsorb to the growing hydrate surface and change gradually the hydrate surface from flat to concave shown in Figure 2.16.[129] According to Gibbs-Thomson equation, the effective sub-cooling decreases with the increasing curvature of the surface. As the effective sub-cooling is the driving force of hydrate growing, the hydrate crystal stops growing when the effective sub-cooling decreases to zero. Only useful KHIs can bind to the hydrate surface for a long enough time to make the curvature over the threshold value. Through small-angle neutron scattering, King et al. reported that KHIs change the conformation of hydrate crystals in liquid, but non-inhibitor polymer does not, which may be a signal of a layer of KHI polymers adsorbed on the hydrate crystal surface.[130]

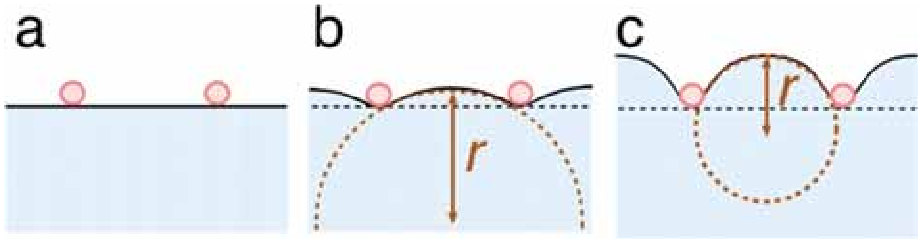

Figure 2. 16 KHI molecules gradually change the hydrate surface from flat to concave. The blue area is hydrate phase, red spheres represents KHI molecules.[129]

It is proposed that the adsorption function of KHIs is attributed to the hydrophilic amide groups. Through molecular simulations, Carver et al. reported that in hydrate/vapour interface KHI monomers adsorb to hydrate surface via the hydrogen bonds between the amide groups and the water molecules at the hydrate surface.[131, 132] However, in the hydrate/water interface, the way of adsorption was found to be different. Yagasaki et al. reported that the strong adsorption affinity between KHIs and hydrate surface is not because of the amide groups but is attributed to the entropic stabilization between the lactam rings of KHIs and the cavities at the hydrate surface.[133] The hydrophobic part in the lactam ring of KHIs is critical to the entropic stabilization as it traps to the hydrate cavity and enhances the structure around the cavity. The reason why PVCap outperforms PVP in inhibiting gas hydrate formation is because of its more suitable size of the hydrophobic part for the open hydrate cavity. There is a little longer distance than the general hydrogen bond between the amide group of PVCap and hydrate surface is reported by Xu et al., indicating that it is not the amide group of PVCap that directly adsorbs to the hydrate surface.[134]

However, studies demonstrated that PVP gives effective inhibition performance even when it has no direct contact with the hydrate surface,[135-137] and PVP can destabilize the pre-critical nucleus.[138] It is implying that there may be other mechanisms of hydrate inhibition, for example, perturbation inhibition.[139] As shown in Figure 2.14 (c), the perturbation inhibition theory suggests that KHIs perturb the organization of local gas and water molecules, thus preventing the formation of critical-sized nucleus and the further crystal growth. By studying hydrophobic amino acids on carbon dioxide hydrates, Sa et al. reported that amino acids with less hydrophobic alkyl side groups give better KHI performance in delaying nucleation and retarding hydrate growth.[120, 140] They demonstrated that the terminal hydrophilic amine and carboxyl acid groups disrupt the hydrogen bonds between the local gas and water molecules, and this is the effect to make the gas hydrate formation slower. The side hydrophobic alkyl groups strengthen the organization of the water structure, and this is the effect to make the gas hydrate formation faster. The balance between the two effects produced by the hydrophilic and hydrophobic groups on the water structure is the critical factor of perturbation inhibition on gas hydrate formation. Custodio et al. reported that pentagon-predominant water structures suggesting the clathrate-like behaviour occur around the isopropyl side groups of PNIPAM hydrogels at low temperature, indicating the hydrophobic alkyl groups may rearrange the behaviour of the nearby water molecules.[141]

2.5.2 *Factors Affecting Kinetic Hydrate Inhibition Performance.*

2.5.2.1 **Hydrate categories.**

(i) sI vs sII gas hydrates.

Methane gas and synthetic natural gas (SNG) mixture whose main components are hydrophobic light alkane gases, are the most common gas types used in hydrate research. Methane gas forms sI hydrates as the most thermodynamically stable phase. The most thermodynamically stable for the SNG mixture is sII hydrates. Using slow constant cooling (SCC) method, Semenov et al. reported that Luvicap 55W and Luvicap EG at 5000 ppm could inhibit methane-propane sII hydrate at the sub-cooling as high as 13-14 °C. But they are only capable of inhibiting methane sI hydrate at sub-coolings lower than 7 ^{o}C.[142] Through the crystal growth inhibition (CGI) method, PVCap has been reported to be an efficient KHI on sII hydrates rather than on sI hydrates, and the reason for its failure may be due to sI hydrates form initially.[143, 144] Through situ Raman spectroscopy, Hong et al. reported that PVCap could interact strongly with the large cavities ($5^{12}6^{2}$), leading to a smaller ratio of the large to small cavities at the early stage of methane hydrates formation.[145] That means to some extent PVCap can retard the formation of sI hydrate, but just not as efficient as it on sII hydrate. Ohno et al. reported that both sI and sII hydrates form during the initial period of methane-ethane hydrates formation, the presence of PVCap influences the structural transition of gas hydrates by disturbing the gas movement and water rearrangement at hydrate crystal interfaces. They observed that PVCap could promote the structural transition to stable sI hydrates when at the sI thermodynamically stable conditions. But it retards the structural transition to stable sII hydrates if sII is the thermodynamically stable phase.[146] Maybe this explains the reason why sI hydrate is harder to inhibit than sII hydrate. In 2012, using several kinds of KHIs, Ohno et al. studied gas hydrates form from methane-ethane-propane mixture.[23] All of those KHIs retarded the structural interconversion from metastable sI to stable sII hydrates.

(ii) Tetrahydrofuran (THF) vs gas sII hydrates.

THF can form sII hydrates at atmospheric pressure, and its equilibrium temperature is approximately 4.4 ^{o}C.[147] THF molecules can occupy the large $5^{12}6^{4}$ cavities of hydrates.[148] THF is usually used to do the preliminary screening of KHIs as its operating procedure is relatively convenient. Using THF in a ball-stop rig equipment, the first efficient PVP was screened out.[149] Also, THF can be used to study the crystal growth procedure of hydrate formation. However, sometimes the KHIs performance on THF may be different from that on hydrophobic gases.[116, 129, 150, 151] For example, when used alone, trialkyl amine oxides are a series of efficient KHIs on inhibiting THF hydrate, but they are poor KHIs on SNG hydrate.[116, 150] This may be due to the different inhibition mechanism between THF and SNG hydrates. As THF is completely miscible with water, the mass transfer limitation of guest molecules is not a problem for the crystal growth of THF hydrate. The binding free energy of THF hydrate surface is relatively lower than that of gas hydrate surface, thus even weakly bound molecules can adsorb to the THF hydrate surface and inhibit it from further growth.[129] Therefore, compared to SNG hydrate, THF hydrate may lower the threshold for KHI screening. However, nearly all classes of KHI polymer are not very good at stopping THF hydrate growth except PVCap. For example, hyperbranched polyesteramides are excellent SNG hydrate inhibitors, but they are not that useful at inhibiting THF hydrate crystal growth,[152] which indicates that the perturbation mechanism may be involved in the nucleus inhibition of SNG hydrate rather than the crystal adsorption mechanism.

(iii) Cyclopentane (CP) vs gas sII hydrates.

CP is a water-insoluble liquid, and it can form sII hydrates at atmospheric pressure. The equilibrium temperature of cyclopentane is approximately 7.7 °C.[153, 154] Using several kinds of KHIs, Dirdal et al. compared their performance on CP hydrate and SNG hydrate.[147] Their KHI performance on CP hydrate correlated fairly well with that on SNG hydrate, but several notable exceptions existed. For example, PVP K-15 gave better performance than Luvicap 55W on CP hydrate, which was the opposite of the result on SNG hydrate. In addition, increasing the concentration of KHIs did not improve the performance on CP hydrate, but it did on SNG hydrate. Thus, the method of using CP hydrate to screen KHIs for natural gas is not always reliable, and this may be because of the less solubility of CP than that of SNG under high pressure and the unlikely structural conversion at the initial stage of CP hydrate formation.

2.5.2.2 Molecular weight (MW).

KHI monomers have little inhibition effect on hydrate formation, and the KHI performance of a polymer increases with increasing repeating units until reaching an optimum size, and then decreases gradually with a longer polymer chain. Generally speaking, the optimum molecular weights of KHIs are approximately 1000-3000 g/mol, indicating that KHI oligomers or polymers with 8-20 monomer units have the best performance.[8, 107, 155] Exxon patented that the KHI performance of polymers with a bimodal distribution of MW is better than that of unimodal MW distribution polymers.[156] Yagasaki came up with a model to explain why KHI polymers have an optimum size and why a bimodal MW distribution polymers perform better via molecular dynamics.[129]

They proposed that a molecule can be a good KHI only if it can strongly bind to the hydrate surface. VCap monomers cannot inhibit hydrate growth as they are weakly bound molecules. On the one hand, the ability of binding to the hydrate surface increases with the increasing number of repeating monomer units in PVCap from one to 20, and it remains the same if over 20 monomer units. On the other hand, the ability of binding to the hydrate surface per monomer unit decreases with the increasing size of PVCap. Thus, an optimum size of PVCap occurs before reaching 20 monomer units because of the balance of the two opposite effects. The low MW polymers and high MW polymers can work complemental on inhibiting the crystal growth of large and small hydrate particles, respectively. Therefore, the bimodal polymers lead to better KHI performance than the polymers with the unimodal distribution of MW. However, although PVP with low MW is best for inhibiting SNG hydrate, PVP with high MW is best to stop THF hydrate crystal growth reported in a patent by Shell Canada Limited.[157] This further confirms that a different inhibition mechanism of THF hydrate from that of SNG hydrate. The different initial locations of PVP molecules have been reported to affect the performance of methane hydrate, e.g., the performance of PVP located at the hydrate solid-liquid phase interface is better than that at gas-liquid phase interface.[158] Thus, the reason why higher MW PVP performs better on THF hydrate is probably because that the completely miscible THF changes the hydrate formation position. The position favours high MW PVP molecules gather at the hydrate solid-liquid phase interface and then prevent THF hydrate from further growth.

2.5.2.3 Polymerization method.

The polymerization method can affect the performance of KHI polymers. For example, adding different chain transfer agents during the free radical polymerization process can make polymers tailed with varying end-capping groups, and these end-capping groups may change their KHI performance.[159, 160] Mercaptoacetic acid and mercaptoethanol end-capping groups have a positive effect on the KHI performance of PVCap. Maybe the end-capping groups change the activity of KHI polymers or themselves can directly work on the cavities of hydrates. It is reported that the polymer tacticity affects the KHI performance.[161] PNIPAM with higher syndiotactic percentage performs better on both THF and SNG hydrates. Also, the random copolymer of poly (*N*-ethyl-β-alanine-co-*N*-propyl-β-alanine) gives better KHI performance than the block copolymer on SNG hydrate.[162] In addition, The KHI performance of linear and hyperbranched polyethylenimines is different. Linear polyethylenimines show better KHI performance on THF hydrate while hyperbranched polyethylenimines are better for inhibiting SNG hydrate.[105, 106] Exxon mobile proposed a model that cage-like water-structures can from around PVCap molecules. (Figure 2.17) The polymer with hydration cages has a large surface area/volume ratio, which makes gas molecules in water uneasy to form cluster. Thus, the KHI performance can be affected by the polymer surface area/volume. In addition, the evidence that the surface area/volume ratio and the molecular spacing of monomer units affect the KHI performance may further confirm Klomp`s theory that both the coverage ratio of KHI onto the hydrate surface and the spacing between the coverage areas can affect the KHI performance, which has been discussed in Section 2.5.1.[122]

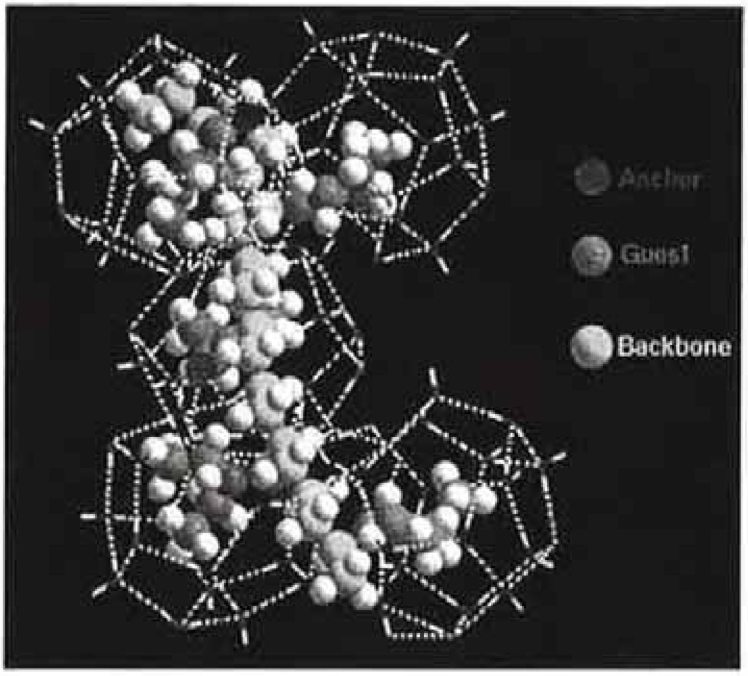

Figure 2. 17 Cage-like water-structures from around PVCap molecule.

2.5.2.4 Hydrophobic alkyl groups.

For many KHI series, e.g., poly (*N*-alkyl(meth)acrylamide)s[163], poly (alkylethylenephosphonate)s[164], poly (*N*-alkyl-*N*-vinylacetamide)s,[165] poly (*N*-alkyl-β-alanine)s[162], and poly (fluoroalkylacrylamide)s[166], the KHI performance depends on the size and shape of the hydrophobic alkyl side groups. Usually, the optimum size is 3-6 C atoms depending on the type and position of the hydrophilic functional group. Hydrophobic groups with 7 or more C atoms are poor KHIs.[167] Also, for the poly (*N*-vinyl lactam) series, the KHI performance increases with the ring size increasing from 5 to 8-membered.[155] Also, the methyl groups on the backbone improve the KHI performance. For example, poly (*N*-isopropylmethacrylamide) (PIPMAM) performed better than poly (*N*-

isopropylacrylamide) (PIPAM)[114], and poly (*N*, *N*-dimethylhydrazidomethacrylamide) (PDMHMAM) outperformed poly (*N*, *N*-dimethylhydrazidoacrylamide) (PDMHAM)[168, 169].

For THF hydrate growth inhibitors, Klomp et al. reported that quaternary ammonium and phosphonium salts with more hydrophobic alkyl groups, such as *n*-butyl and *n*/*iso*-pentyl groups have better performance.[122] In 2012, Chua et al. reported that tetra(*iso*-hexyl)ammonium bromide was the most effective THF inhibitor among the quaternary ammonium-based series. Tetra(*iso*-hexyl)ammonium bromide also gave an excellent synergistic effect for PVCap on SNG hydrate.[150] Recently, Mady and Kelland reported that tris(*tert*-heptyl)(*n*-pentyl)ammonium bromide gave better THF hydrate growth inhibition performance than tetra(*iso*-hexyl)ammonium bromide.[151] Also, the *tert*-heptylated salt gave better synergistic effect for PVCap on SNG hydrate than the *iso*-hexylated salt.[170]

Through molecular simulations, Hudait et al., reported that the alkyl groups could stabilize the ice structure, rigidize the ice-binding site, and slow the water dynamics around the ice-binding site.[171] Arsiccio et al. observed that the destabilizing effect of the ice interface does not require the direct adsorption of the protein but is mediated by the nearby liquid water molecules that may be affected by the non-polar groups.[172] Thus, the hydrophobic alkyl groups of KHIs may have similar effects on the hydrate nucleus and interface. Through thermal analysis on polymer-water interactions, Varma-Nair et al. reported that more hydrophobicity of the pendant group of KHI polymers leads to higher bound water, which favours the KHI performance.[173]

2.5.2.5 Cloud point (T_{Cl}) of KHIs.

KHI formulations include one or more amphiphilic polymers that contain both hydrophilic and hydrophobic groups, so cloud points (T_{Cl}) are often seen if heating the KHI aqueous solutions. It is reported that the low T_{Cl}

temperature of KHI polymer is essential for efficient KHI performance.[167] At typical KHI dosages, PVCap and PNIPMAM have a T_{Cl} of approximately 30-40 °C and 35-45 °C, respectively depending on the molecular weight amongst other factors.[8, 9] According to the paper published by Dirdal and Kelland[167], the reason why low T_{Cl} benefits the performance of a KHI polymer may be as follows. (i) KHI polymers with low T_{Cl} may have the maximum surface area/volume ratio. The advantage of the large surface area/volume ratio of a KHI polymer has been discussed in Section 2.5.2.3. (ii) The hydrophobic interaction of KHI polymers may be strengthened at low temperatures closed to their low T_{Cl}. The effect of hydrophobic interaction on inhibiting hydrate formation has been discussed in Section 2.5.2.4. (iii) KHI polymers with low T_{Cl} tend to concentrate at the gas/water or oil/water interfacial regions where hydrates may initially form, thus giving efficient inhibition performance.

2.5.2.6 Copolymers.

Many effective KHIs are copolymers, such as Luvicap 55W (BASF) and Inhibex BIO-800 (Ashland). Luvicap 55W is an aqueous solution product, and its active ingredient is copolymerized from *N*-vinyl pyrrolidone (VP) and *N*-vinyl caprolactam (VCap) monomers in the ratio of 1:1. The active component of Inhibex BIO-800 is a copolymer of VCap and vinyl alcohol (VOH). Luvicap 55W and Inhibex BIO-800 are powerful KHIs on both sI and sII hydrates.[174] The VP:VCap copolymer has a high cloud point due to the addition of the strongly hydrophilic VP monomer. Copolymerization of VCap with *N*-vinyl-*N*-methylacetamide (VIMA) monomer can also improve the solubility of VCap-based KHIs as well as raise the KHI performance compared to PVIMA or VCap homopolymers given the appropriate VIMA:VCap monomer ratio.[175] This may be due to an opening out of the polymer chain structure giving a higher surface-volume ratio as discussed earlier.

2.5.2.7 Synergists.

Some solvents, nonpolymeric compounds, and even polymers have synergetic effects on KHI polymers. Adding synergists is an efficient and money-saving method to improve the performance of KHIs. It is particularly advantageous if the carrier solvent for the KHI polymers is also a synergist. Typical synergist solvents include small alcohols, alkyl lactates and glycol ethers e.g. *n*-butyl glycol ether, and some ketones.[176,] 4-methyl-1-pentanol was recently shown to be a very powerful synergist.[177] Synergist solvents can be added when making KHI aqueous solution or as a solvent for synthesizing and dissolving KHI polymers.

Besides oxygenated solvents, tetraalkyl ammonium salts, tetraalkyl phosphonium salts, alkylated guanidinium salts, trialkyl amine oxides, and ionic liquids are outstanding nonpolymeric compound synergists.[150, 151, 178-180] The mechanism of the synergetic effect is unclear. It may be because the synergists enhance the reaction of KHIs on the hydrate surface or change the nucleus formation site or decrease the mass transfer rate of the hydrate formation system.[176]

Apart from the above discussion, more factors can affect the KHI performance, such as the gas-liquid interfacial tension of KHI [181], the absolute pressure of the system[182-184], KHI concentration, aqueous volume, stirring rate, test method and experiment equipment.[185, 186] These phenomena are all related to the hydrate formation dynamics and mechanisms. However, the inhibition mechanism of KHIs is still unclear. Thus, to explore more on the inhibition mechanism is of particular importance for the future work in this field.

3 Objectives

Most reported and almost all commercial KHIs are amide-based polymers. However, polyamide KHIs have certain limitations, such as limited inhibition performance for deepwater applications, low cloud point (poor water-solubility) in high salinity produced fluids, and low seawater biodegradability. Also, the inhibition mechanisms of KHIs are still under debate. The function of the amide groups in KHIs is also unsure. As it is difficult to determine directly whether the amide groups have a unique effect on the KHI performance or only make the polymers water-soluble, investigating non-amide KHI polymers may reveal the answer. Therefore, the main objectives for the PhD research were identified as follows.

1. Investigate how *N*-substituents like hydrophobic and hydrophilic groups affect the inhibition performance of tailor-made peptoids. (Paper I)
2. Optimize the inhibition performance of amide-based polymers, including *N*-alkyl-*N*-vinylamide, 3-methylene-2-pyrrolidone, *N*-vinyl caprolactam, *N*-isopropylmethacrylamide, and acrylamide polymers, via one or several of the methods of copolymerization, *N*-alkylation, ring expansion and end-capping modification. (Paper II, III, IV, V).
3. Investigate the inhibition performance of non-amide based polymers, including polyvinylsulphonamides, poly (amine oxide)s, poly (sulfobetaine methacrylate)s, and polyvinylaminals. (Paper VI, VII, VIII, IX, X).

A summary of the results and discussion of the completed studies is presented in Chapter 5. The main conclusions of the completed studies are summarized in Chapter 6. The published papers are attached in the Appendices.

4 Experimental Methods

4.1 Syntheses

4.1.1 Tailor-made Peptoids

A series of poly (glycine-alternating-valine)s with varying glycine *N*-substituents, e.g., alkyl and hydroxyl groups were provided by Professor Yasuhito Koyama (Toyama Prefectural University, Japan). According to the literature[187, 188], the procedure of preparing the glycine *N*-substituted poly (glycine-alternating-valine)s is briefly described as follows. A mixture of isobutyraldehyde, alkyl ammonium chloride, potassium isocyanoacetate, and isopropanol was stirred for eight days at ambient temperature. The mixture was then concentrated under vacuum to get a viscous liquid. The residue was further stirred for six days at ambient temperature to get a viscous crude product. Tetrahydrofuran was used to precipitate the potassium chloride byproduct. After filtration and removing the solvent, the glycine *N*-substituted poly (glycine-alternating-valine) final product was obtained. (Figure 4.1)

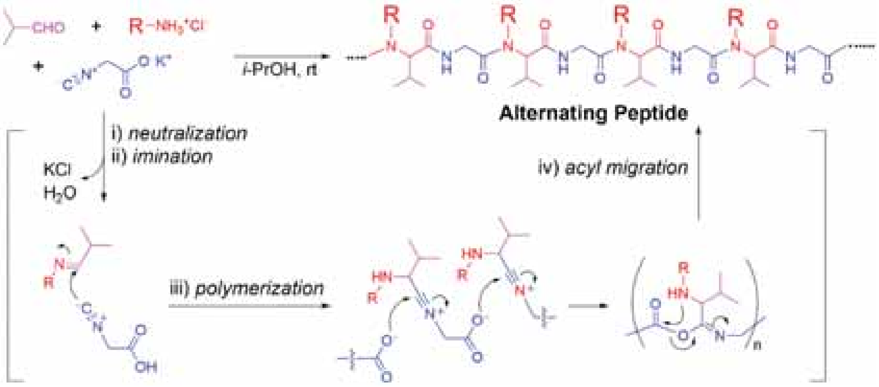
CHO
R–NH₃⁺Cl⁻
O⁻K⁺
i-PrOH, rt
Alternating Peptide
i) neutralization
ii) imination
KCl
H₂O
iv) acyl migration
iii) polymerization
HN
R
OH
n

Figure 4. 1 Synthesis of glycine *N*-substituted poly (glycine-valine)s. R = alkyl group containing 1-3 carbons or hydroxyl group.

4.1.2 *N-alkyl-N-vinylamide Copolymers*

A series of *N*-alkyl-*N*-vinylamide copolymers were provided by Professor Hiroharu Ajiro (Nara Institute of Science and Technology, Japan). The procedure of synthesizing *N*-alkyl-*N*-vinylformamide monomers, e.g., *N*-propyl-*N*-vinylformamide and *N*-butyl-*N*-vinylformamide from *N*-vinylformamide and corresponding alkyl bromides via nucleophilic substitution reaction was reported in literature.[189, 190] The copolymers were synthesized from the *N*-alkyl-*N*-vinylformamide monomers by using the free radical copolymerization method.[165, 190, 191] (Figure 4.2) An example of preparing *N*-vinylformamide and *N*-*n*-butyl-*N*-vinylformamide copolymer is given below. 72.4 mg (0.442 mmol) of 2,2`-azodiisobutyronitrile, 0.97 mL (14.1 mmol) of *N*-vinylformamide monomers, 7.16 mL (56.4 mmol) of *N*-*n*-butyl-*N*-vinylformamide and 2 M toluene were sequential loaded to a 25 mL round-bottom flask under the protection of nitrogen gas. The reacting temperature was at 60 °C. After reacted 24 h, acetone was used to precipitate the polymer. The solid copolymer was obtained after filtration and drying.

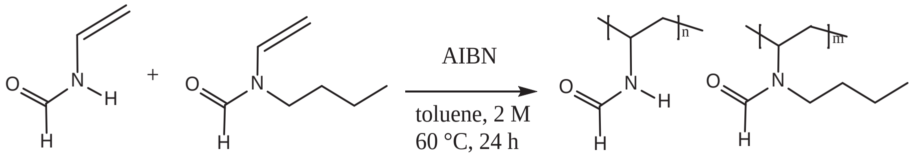

Figure 4. 2 copolymerization of *N*-vinylformamide and *N*-*n*-butyl-*N*-vinylformamide.

4.1.3 *3-Methylene-2-pyrrolidone and 3-Methylene-2-piperidone Polymers*

3-methylene-2-pyrrolidone, *N*-alkyl-3-methylene-2-pyrrolidone, and 3-methylene-2-piperidone polymers were provided by Professor Bert Klumperman (Stellenbosch University, South Africa). The polymers were synthesized from the corresponding monomers via the free radical polymerization method.[192, 193] The reaction procedures toward the monomers were reported in literature.[194-197] An example of the preparation of the 3-methylene-2-piperidone polymer is given as follows. 0.50 g (4.50 mmol) of 3-methylene-2-piperidone monomers, 17 mg (0.06 mmol) of 4, 4′-azobis (4-cyanovaleric acid) and 3 mL dimethyl sulfoxide were added to a 10 mL reaction flask. After 20 min of purge with argon gas, the mixture was heated to 70 °C. The mixture was then kept at 70 ^{o}C and stirred for 24 h. After the reaction, the polymer was purified through dialysis and was isolated via freeze-drying.

4.1.4 *Poly (N-vinyl caprolactam) and Poly (N-isopropyl methacrylamide) with Varying End Caps*

Poly (*N*-vinyl caprolactam) and poly (*N*-isopropyl methacrylamide) with varying mercaptocarboxylic acid end caps were synthesized through the free radical polymerization method by utilizing different chain transfer agents, such as mercaptoacetic acid and mercaptosuccinic acid.[198] (Figure 4.3) A general example of the preparation of the mercaptocarboxylic acid-group-modified poly (*N*-vinyl caprolactam) is given here. 0.1 g of 2, 2`-azodiisobutyronitrile, 10.0 g of *N*-vinyl caprolactam monomers, 0.3 g of mercaptocarboxylic acid, and 30 mL isopropanol were loaded to a round-bottomed flask. After the air in the flask were removed, the mixture was heated to 80 °C. The mixture was then kept at 80 ^{o}C and stirred for seven hours. Then, the isopropanol solvent was removed through a vacuum rotary evaporator. The residue was precipitated in diethyl ether. A solid polymer was obtained after filtration and drying.

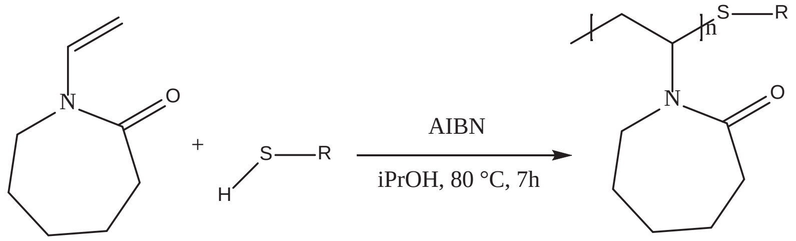

Figure 4. 3 Synthesis of poly (*N*-vinyl caprolactam) with varying mercaptocarboxylic acid end caps. R = carboxylic acid group.

4.1.5 *Direct Synthesis of Acrylamide-based Polymers from Poly (acrylic acid)*

Poly (*N*-isopropylacrylamide) (PNIPAM), poly (*N*-*n*-propylacrylamide) (PNnPAM) and polyacryloylpyrrolidine (PAPYD) were synthesized from poly (acrylic acid) (PAA) via a two-stage process. (Figure 4.4) According to the literature[199], the two-stage process was as follows. First, the polyacrylic acid alkylammonium salts were synthesized from PAA and the corresponding amines, e.g., isopropylamine, *n*-propylamine, and pyrrolidine. Second, the polyacrylic acid alkylammonium salts were intramolecular dehydrated to give the acrylamide polymers (PNIPAM, PNnPAM, and PAPYD). Here we take the PNIPAM synthesized from PAA as an example to show the detailed procedure. PAA (1.004 g, 13.9 mmol, 1.0 eq) was dissolved in anhydrous ethanol (15 mL) at 60 °C. After decreasing the temperature to 30 °C, isopropylamine (1.23 g, 20.8 mmol, 1.5 eq) was added. Under the protection of N_2, the mixture was stirred for 24 h. The mixture was then poured into 50 mL THF solvent. The polyacrylic acid isopropylammonium salt solid was obtained after filtration and vacuum dried. The dry salt was heated to 150 °C, stirred for 6 hours under high vacuum. The target product PNIPAM (1.008 g, 55%) was finally obtained.

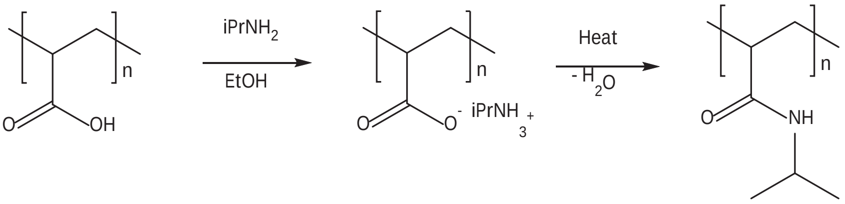

Figure 4. 4 Two-stage synthesis of PNIPAM from PAA.

4.1.6 *N-alkyl-S-vinylsulphonamide Polymers*

A series of *N*-alkyl-*S*-vinylsulphonamide (VSAM) and *N*-vinyl-*N*-methylacetamide (VIMA) copolymers have been synthesized from VSAM and VIMA monomers using the conventional free-radical copolymerization method.[200] (Figure 4.5) According to the literature[201], the procedure of synthesizing *N*-alkyl-*S*-vinylsulphonamide monomer is briefly introduced as follows. Alkylamine (1.0 equivalent) and triethylamine (4.0 equivalent) were mixed in dichloromethane at 0 °C. Under the protection of N_2, 2-chloroethanesulfonyl chloride (1.1 equivalent) was dropwise added to the mixed solution. The mixture was then stirred at 0 °C for four hours. The crude product was washed first with deionized water and then with 3.5 wt.% sodium chloride solution to remove the inorganic compound. After drying with anhydrous sodium sulfate and removing the solvent, the final product was obtained from the organic layer.

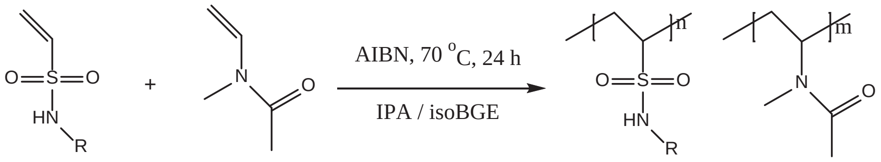

Figure 4. 5 Copolymerization of *N*-alkyl-*S*-vinylsulphonamide and *N*-vinyl-*N*-methylacetamide. R = alkyl group containing 2-4 carbons.

4.1.7 Amine *Oxide Polymers*

Polyamine oxides from alkylated polyethyleneimine were synthesized by using the reported procedure in literature.[105, 106, 202] Glycidyl amine *N*-oxide polyethers were provided by Professor Holger Frey (Johannes Gutenberg-Universität Mainz, Germany). The synthesis procedure of glycidyl amine *N*-oxide polyethers was reported in literature.[203] Two main steps were involved in preparing the amine oxide-based polymers. First, synthesize the corresponding amine polymers. Second, oxidize the amine polymers to amine oxide polymers with hydrogen peroxide being the oxidant.

4.1.8 *Zwitterionic Poly (sulfobetaine methacrylate)s*

A series of zwitterionic poly (sulfobetaine methacrylate)s with varying *N*-alkyl side groups were provided by Professor Bin Zhao (University of Tennessee, United States). The zwitterionic poly (sulfobetaine methacrylate)s were synthesized from the corresponding alkylated sulfobetaine methacrylate monomers by using the free radical polymerization method.[204] An example of the preparation of 3-((2-(Methacryloyloxy)ethyl)-dipentylammonio)propane-1-sulfonate polymers is given below. 0.603 g (2.03 mmol) of 3-((2-(methacryloyloxy)ethyl)-dipentylammonio)propane-1-sulfonate, 7.1 mg (0.043 mmol) of 2, 2`-azodiisobutyronitrile, 2.039 g of 2, 2, 2-trifluoroethanol and 90.5 mg of *N, N*-dimethylformamide were loaded to a 25 mL two-necked flask. The mixture was degassed and heated to 70 °C. After reacted 17 h, the crude product was purified by dialysis. The purified polymer powder was obtained after concentrated and freeze-dried.

4.1.9 *Polyvinylaminals.*

Polyvinylaminals with varying alkyl groups were synthesized from polyvinyl amine and the corresponding aldehydes. (Figure 4.6) The synthesizing procedure was briefly introduced as follows. 2.00 g of 10 wt.% polyvinyl amine in water, 1.0 molar equivalent of aldehyde per amine group, and 1.00 g of isopropanol (IPA) were loaded to a flask. The mixture was heated to 70 °C and then was reacted for 18 hours at this temperature. Usually, a light orange-brown solution containing the target polyvinylaminal product was obtained. The solution was used for KHI tests without further purification.

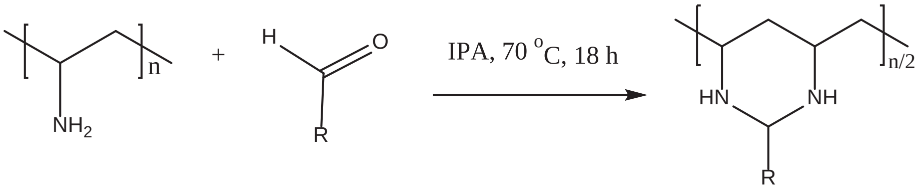

Figure 4. 6 Synthesis of polyvinylaminal from polyvinlyamine and aldehyde. R = chain or cyclic alkyl group.

4.2 Cloud Point (T_{Cl}) Measurement

The cloud point (T_{Cl}) of each polymer was measured according to the following procedure.[190, 198, 205] The polymer aqueous solution (normally at the concentration of 2500 ppm) was heated slowly. The temperature at the first sign of haze observed in the solution was measured as the T_{Cl}

of the polymer. If the T_{Cl} of a polymer was below the room temperature, the polymer solution was cooled to 4 ^{o}C in a cooling room before the heating was applied. The T_{Cl} measurement was repeated for reproducibility.

4.3 Kinetic Hydrate Inhibition Performance Testing

4.3.1 High-pressure Kinetic Hydrate Inhibition Performance Testing

The high-pressure tests were carried out using either pure methane gas or synthetic natural gas (SNG) mixture (Table 4.1). Theoretically, pure methane gas forms structure I hydrate, and the most thermodynamically stable phase for SNG mixture is structure II hydrate.

Table 4. 1 Composition of SNG mixture.

Component	Mol%
Methane	80.67
Ethane	10.20
Propane	4.90
iso-Butane	1.53
n-Butane	0.76
N_2	0.10
CO_2	1.84

4.3.1.1 Rocking Cell 5 Equipment

The high-pressure tests were carried in the rocking cell 5 (RC5) equipment supplied by PSL Systemtechnik, Germany. The RC5 equipment consists of five steel rocking cells positioned in a cooling bath. (Figure 4.7) The inner volume of each cell is 40 mL. Each cell was equipped with a temperature sensor, a pressure sensor, a steel ball for agitation. During the experimental procedure, the gas in/outlet valve of each cell was closed to make sure each cell was a closed system.

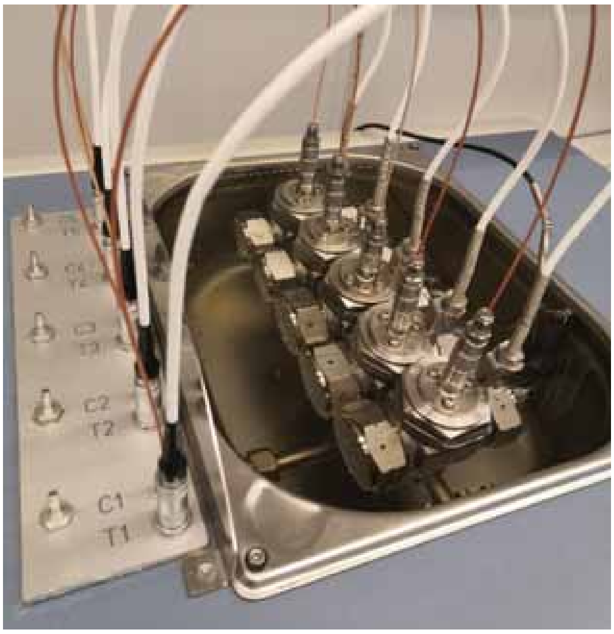

Figure 4. 7 A photo of the RC5 equipment.

4.3.1.2 Slow Constant Cooling Experiment

The slow constant cooling (SCC) method was utilized as the standard screening method to test the inhibition performance of KHIs in my studies, as the variation in results of this test methodology is comparatively low.[1] The SCC method gives some measure of the maximum sub-cooling that a KHI can tolerate before the formation of macroscopic detectable hydrate occurs.[142, 186] The procedure was as follows.[106, 155, 206]

1. Approximately 105 g of KHI polymer aqueous solution was made at least one day before the SCC test to make sure the KHI polymer was totally dissolved. Usually, 20 mL of the KHI solution was loaded to each of the five cells, but only 10 mL for the zwitterionic poly (sulfobetaine methacrylate)s samples. 1 mL of decane was added when doing the gas-water-liquid hydrocarbon multiphase experiments.
2. The air in the cells and the gas lines were removed by applying a vacuum pump, purging with 5-10 bar of SNG (or pure methane gas when doing the experiments on sI hydrate), and using the vacuum pump one more time.
3. The cells were pressurized to 76 bar with SNG or 110 bar with pure methane gas at 20.5 ^{o}C.
4. A temperature control program was run from 20.5 ^{o}C gradually cooling down to 2.0 ^{o}C over the time of 18.5 h to provide the low-temperature atmosphere for gas hydrate formation. The cells were rocked for the solution agitation in it at 20 rocks/min (maximum 40°) during the cooling period.
5. The temperature and pressure sensors for each cell allowed for data recording and storing on a local computer.

Figure 4.8 shows typical temperature-time and pressure-time graphs generated from an SCC experiment. Normally, we can get the information of gas hydrate formation via the temperature-time and pressure-time graphs. As gas molecules are consumed from the gas phase to form gas hydrates, there is a corresponding pressure drop in the pressure-time graph. The gas hydrate formation is an exothermic reaction, so a temperature spike in the temperature-time graph is expected when gas hydrates forming. However, as the cooling bath of RC5 equipment can conduct the heat away quickly enough, the temperature-time curve remains uninfected by the reaction of gas hydrate formation shown in Figure 4.8. Therefore, we can only get the information of gas hydrate formation from the pressure-time graph. In the beginning, the pressure dropped approximately one bar due to the gas dissolved into the aqueous solution. Since this was a closed system, the pressure decreased linearly when the temperature lowered gradually. The point at which the pressure deviated from the linear pressure-time curve indicates the macroscopically detectable formation of gas hydrates. The corresponding temperature at this point was defined as the hydrate onset temperature (T_o). The value of the rapid hydrate growth temperature (T_a) in the temperature-time curve was established according to the steepest drop point of the pressure-time curve.

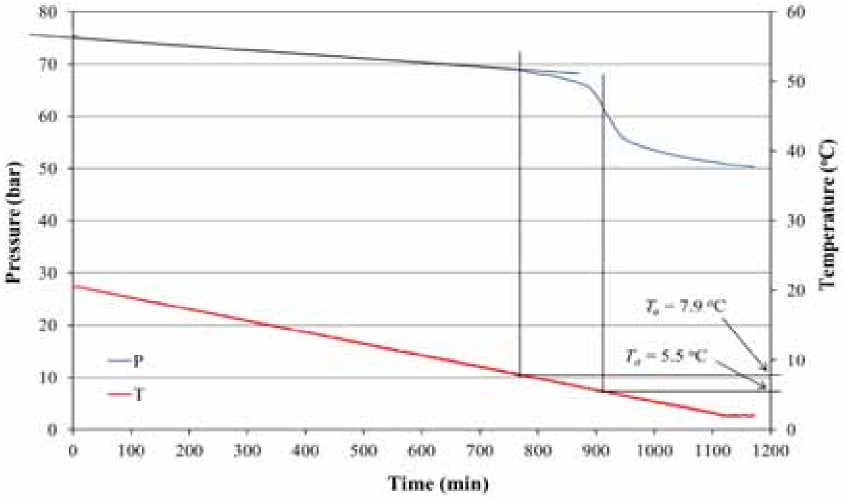

Figure 4. 8 T_o and T_a values determined from the graphs obtained from a SCC experiment.

Typically, 8-10 experiments for each KHI sample were carried out to ensure the statistical validity of the results. Some data scattering was expected since hydrate nucleation is a stochastic event. For the results obtained from the SCC method, usually up to ±10-20 % scattering can be observed from 10 experiments. Data scattering was often much higher for isothermal tests.[202]

4.3.1.3 Isothermal Test

The isothermal tests were carried out to check how long time a KHI solution can hold without detectable gas hydrate formation at a defined sub-cooling condition.[174, 207] The temperature was cooled rapidly down to a desired sub-cooling value, and it was then remained at this sub-cooling throughout the entire test period. The procedure was as follows.[202]

1. Approximately 105 g of KHI polymer aqueous solution was made at least one day before the isothermal test to make sure the KHI polymer was totally dissolved. 20 mL of the KHI solution was loaded to each cell.
2. The air in the cells and the gas lines were removed by applying a vacuum pump, purging with 5-10 bar of pure methane gas, and using the vacuum pump one more.
3. The cells were pressurized to 110 bar with pure methane gas at 20.5 ^{o}C and then were rocked for a few minutes to equalize.
4. The cells were quickly cooled from 20.5 °C down to 4 °C at the cooling rate of 10 °C/h. After reaching 4 °C ($\varDelta T$ = 11.3 °C for sI methane hydrate predicted by the Calsep’s PVTSim software using the cubic equation of state (EOS)), the temperature remained at this value for some time until the gas hydrate formation. The cells were rocked for the solution agitation in it at 20 rocks/min (maximum 40°) throughout the whole test, including the cooling period.

Figure 4.9 shows typical temperature-time and pressure-time graphs generated from an isothermal test. The information on gas hydrate formation can be obtained from the pressure-time curve. During the rapidly cooling period, the pressure also decreased as it was a closed system. Then, the pressure-time curve remained stable due to the temperature was kept at 4 ^{o}C. When the pressure was starting decreasing again, which indicates the formation of gas hydrates, the time from the point where the hydrate forming region reached to the point of the pressure drop was defined as the hydrate induction time (t_i). The hydrate rapid formation time (t_a) was founded according to the steepest drop point of the pressure-time curve. Usually, at least five experiments were carried out to give the average t_i and t_a values for each KHI polymer.

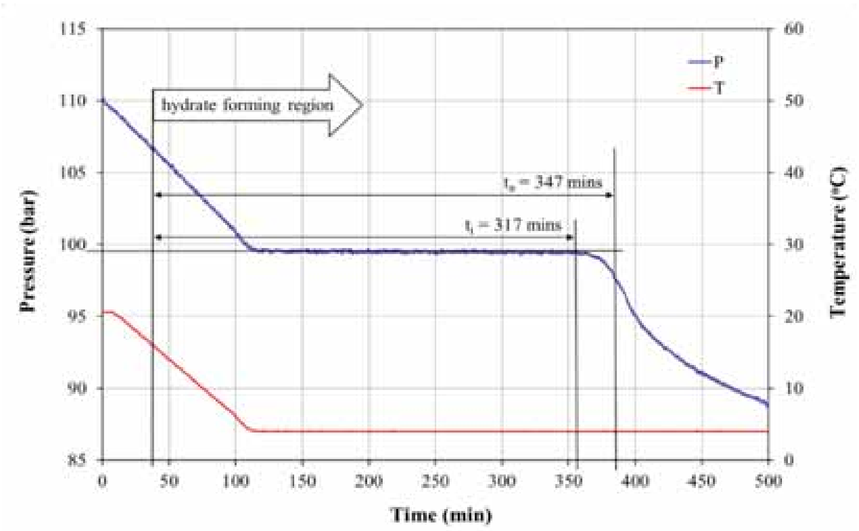

Figure 4. 9 t_i and t_a values determined from the graphs obtained from an isothermal experiment.

4.3.2 *Tetrahydrofuran (THF) Hydrate Crystal Growth Rate Testing*

Tests of THF hydrate crystal growth rate were carried out to check the inhibition effect of KHIs on THF hydrate. As reported in previous publications,[121, 150, 208-210] the THF hydrate crystal growth rate test procedure was as follows.

1. A solution containing 36000 ppm (3.6 wt.%) sodium chloride as well as THF and water in the molar ratio of 1:17 was prepared. The theoretical sub-cooling of this THF/salt solution was about 3.4 ^{o}C.
2. A certain weight of KHI polymer was loaded to a 100 mL glass beaker, and approximately 80 mL of the prepared THF/salt solution was added to the beaker to dissolve the KHI polymer. The beaker was then placed in a cooling bath at -0.5 ^{o}C (accuracy ± 0.05 ^{o}C) and the time recording was started at the same time.
3. The solution in the beaker was stirred every 5 minutes for the first 20 minutes.
4. The ice nucleation used to initiate the THF hydrate was placed in the middle of the solution through the tip of a hollow glass tube filled with crushed ice, and then waited 1 hour for the growth of the THF hydrate crystals from the ice nucleation.
5. The THF hydrate crystals grown on the tip of the tube were cut off and weighed, and the result was calculated as the growth rate of the THF crystals in grams over 1 hour. (Figure 4.10) Typically, over five experiments were carried out to give an average growth rate for each KHI.

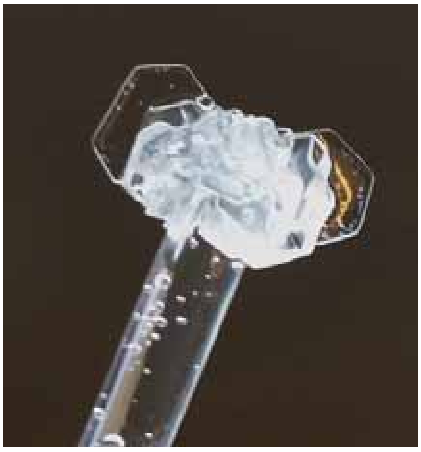

Figure 4. 10 THF hydrate crystals grown on the tip of the hollow glass tube.

5 Completed Studies - Results and Discussion

5.1 Paper I: Kinetic Hydrate Inhibition of Glycyl-valine-based Alternating Peptoids with Tailor-made N-substituents[188]

One of the very first inspirations of investigating KHIs to inhibit the formation of gas hydrates came from the anti-freeze proteins (AFPs) and the anti-freeze glycoproteins (AFGPs) that could allow organisms, such as polar fish, surviving in subzero temperatures.[211, 212] Since the early 1990s a range of AFPs and AFGPs have been investigated as KHIs.[213-217] However, the cost of the natural proteins KHIs is too high for field application.[218, 219] Thus, investigating synthetic KHI polymers is a good way to reduce the capital expense (CAPEX) and operating expense (OPEX). As peptide bonds are the basic structure in AFPs and AFGPs, a series of bespoke or tailor-made polypeptides were investigated as KHIs, and some of them were found to be efficient KHIs, such as peptones and polyglycines with isopropyl or *n*-propyl groups.[108, 167]

We synthesized four kinds of peptoid polymers with glycine and *N*-substituted valine alternating dipeptide repeating units, including poly (glycine-*L*-methylated valine), poly (glycine-*L*-ethylated valine), poly (glycine-*L*-*n*-propylated valine) and poly (glycine-*L*-ethanolated valine), abbreviated as MA-Pep, EA-Pep, PA-Pep and EtA-Pep respectively. (Figure 5.1) These peptoid polymers were investigated as KHIs using the SNG mixture.

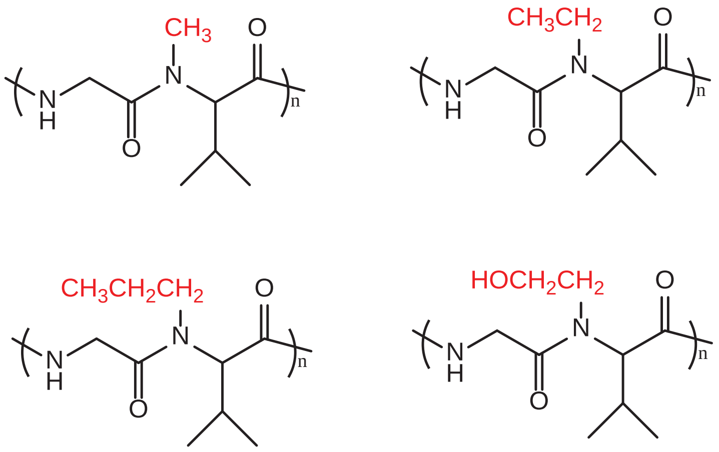

Figure 5. 1 Structures of the alternating peptides with different *N*- substituents. MA-Pep (up left), EA-Pep (up right), PA-Pep (down left) and EtA-Pep (down right).

Table 5.1 summarized the results from the KHI performance tests of MA-Pep, EA-Pep, PA-Pep, and EtA-Pep, as well as the results of pure water, PVP K-15, and PVCap for comparison. As shown in Table 5.1, MA-Pep with *N*-methyl groups and EA-Pep with *N*-ethyl groups gave almost the same KHI performance (p-value > 0.05 from t-test). The average T_o values of MA-Pep and EA-Pep were a little lower than PVP K-15, indicating they were a bit more powerful than PVP K-15 in inhibiting gas hydrate formation. However, MA-Pep and EA-Pep were not good at inhibiting rapid forming hydrate once the detectable gas hydrate formed, as the average T_a values of them were higher than that of PVP K-15. PA-Pep gave better KHI performance than MA-Pep and EA-Pep, which was as efficient as the commercial PVCap. The reasons why PA-Pep with *N*-*n*-propyl groups gave such remarkable KHI performance may be as follows. First, the size of the *n*-propyl group is suitable to penetrate the $5^{12}6^4$ cavity of sII gas hydrate, thus disturbing the structure organization of gas hydrate.[173, 189] Second, hydrophobic *n*-propyl groups trigger the formation of clathrate water structures, resulting in that the water structures prefer to grow around the *n*-propyl groups of the KHI peptoid rather than small gas molecules.[141] Thus, with the competition from the hydrophobic groups, the formation of the gas hydrate nuclei around the gas molecules becomes difficult. We replaced the *n*-propyl group with the hydroxyethyl group in the peptoid, which is similar in size but relatively more hydrophilic. The KHI performance of EtA-Pep with hydroxyethyl is worse than PA-Pep, but better than EA-Pep, which indicates that both the high hydrophobicity and the appropriate size of the *N*-substituents are essential for the KHI performance of the peptoids, while the former is particularly important.

Table 5. 1 Results of SCC tests for KHI polymers at 2500 ppm. Average of 10 tests. The deviations were calculated by using the formula of STDEV.S in Excel.

Polymer	**T_o (av.) ± deviation (°C)**	**ΔT (av.) at T_o (°C)**	**T_a (av.) (°C)**	**T_o (av.) − T_a (av.) (°C)**
Pure Water	16.8 ± 0.6	3.6	16.7	0.1
PVP K-15	13.9 ± 0.5	6.4	10.3	3.6
PVCap	10.4 ± 0.4	9.8	9.9	0.5
MA-Pep	13.0 ± 0.4	7.3	12.9	0.1
EA-Pep	13.3 ± 0.3	7.0	13.0	0.3
PA-Pep	10.4 ± 0.1	9.8	10.2	0.2
EtA-Pep	11.1 ± 0.5	9.1	11.0	0.1

We tested the KHI performance of the best peptoid PA-Pep at different concentrations. Like many other series of KHI polymers,[193, 200, 220] a trend of the improved KHI performance with increasing concentration can be seen for PA-Pep. (Figure 5.2)

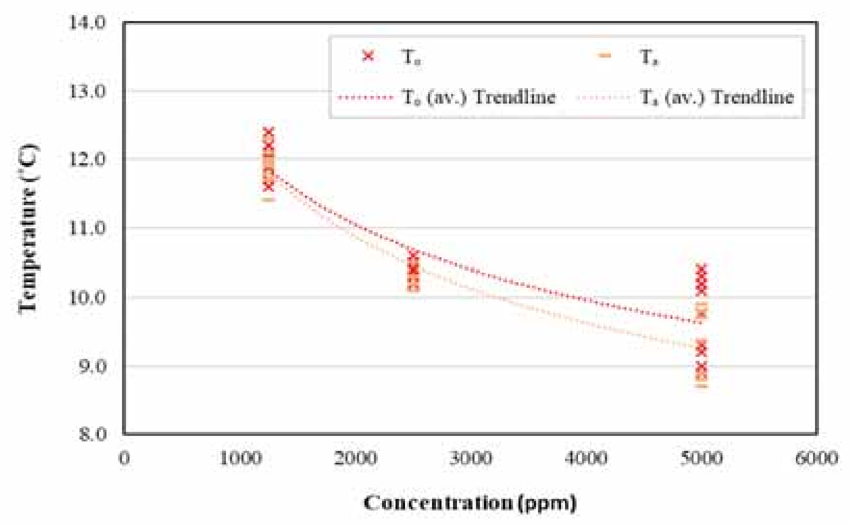

Figure 5. 2 KHI performance of PA-Pep at different concentrations.

5.2 Paper II: Optimizing the Kinetic Hydrate Inhibition Performance of *N*-alkyl-*N*-vinylamide Copolymers[190]

Polyvinyl formamide derivatives have been reported to be effective KHIs, especially the ones with long alkyl chains on the carbon moiety or the nitrogen moiety of the amide groups.[165, 221] The KHI performance of poly (*N*-*n*-propyl-*N*-vinylformamide) with *n*-propyl groups has been proven to be better than poly (*N*-isopropyl-*N*-vinylformamide) with isopropyl groups.[189] Thus, it is of great interest to investigate poly (*N*-*n*-butyl-*N*-vinylformamide) with *n*-butyl groups and poly (*N*-*iso*-butyl-*N*-vinylformamide) with *iso*-butyl groups as KHIs for comparing their KHI performance. However, the *N*-*n*/*iso*-butyl-*N*-vinylformamide homopolymers were water-insoluble. Reports showed that utilizing *N*-vinylformamide monomers to copolymerize with *N*-*n*-propyl-*N*-vinylformamide and *N*-isopropyl-*N*-vinylformamide can improve their cloud points as well as water solubility. The KHI performance of the copolymers with *N*-*n*-propyl side groups still outperform the copolymers with *N*-isopropyl side groups.[189]

Therefore, we synthesized a series of water-soluble *N*-vinylformamide: *N*-*n*-butyl-*N*-vinylformamide (NVF:nBuNVF) copolymers and *N*-vinylformamide: *N*-*iso*-butyl-*N*-vinylformamide (NVF:iBuNVF) copolymers. A series of *N*-methyl-*N*-vinylacetamide: *N*-*n*-propyl-*N*-vinylformamide (MNVA:nPrNVF) copolymers and *N*-methyl-*N*-vinylacetamide: *N*-isopropyl-*N*-vinylformamide (MNVA:iPrNVF) copolymers were also synthesized. These copolymers were investigated as sII hydrate KHIs using the SNG mixture. (Figure 5.3 and Table 5.2)

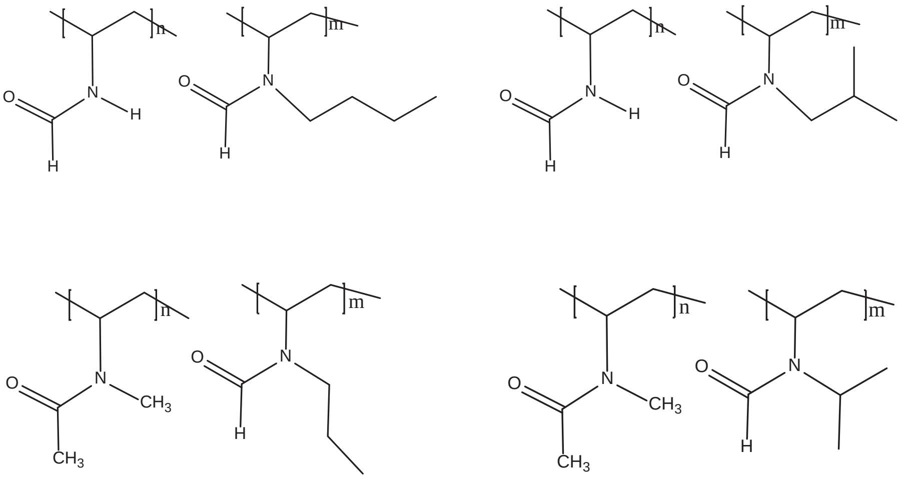

Figure 5. 3 Structures of NVA:nBuNVF copolymer (top left), NVA:iBuNVF copolymer (top right), MNVA:nPrNVF copolymer (bottom left) and MNVA:iPrNVF copolymer (bottom right).

Table 5. 2 Analytical data of *N*-alkyl-*N*-vinylamide copolymers.[a]

Sample	**M1**	**M2**	**Yield (%)**	**Monomer in copolymer**	***Mn*[e]**	**Đ[e]**
RK2-033	NVF	nBuNVF	18[b]	75:25	4200	3.38
RK1-134	NVF	nBuNVF	26[c]	81:19	4500	3.44
RK1-120	NVF	nBuNVF	19[c]	67:33	15400	3.02
RK1-135	NVF	iBuNVF	22[c]	51:49	7400	3.13
RK2-034	NVF	iBuNVF	14[b]	74:26	9700	3.35
RK1-121	NVF	iBuNVF	16[c]	58:42	10500	3.58
RK2-035	MNVA	nPrNVF	27[b]	25:75	2800	2.2
RK1-125	MNVA	nPrNVF	50[d]	56:44	6200	2.08
RK2-037	MNVA	iPrNVF	15[b]	37:63	2000	1.86
RK2-036	MNVA	iPrNVF	17[b]	42:58	2000	2.08
RK1-136	MNVA	iPrNVF	27[d]	28:72	2300	2.94
RK1-126	MNVA	iPrNVF	30[d]	27:73	4500	1.94

[a] Radical polymerization was achieved with azobisisobutyronitrile (AIBN) in toluene at 60 °C at 2 M. [b] Diethyl ether-insoluble part. [c] Acetone-insoluble part. [d] Hexane-insoluble part. [e] Determined by size-exclusion chromatography (SEC) with polystyrene standard in dimethylformamide (DMF).

As can be seen from Table 5.3, the KHI performance of the *N*-alkyl-*N*-vinylamide copolymers generally improves when the percentage of the monomers with long *N*-alkyl side chain increases. Thus, the copolymers with the highest percentage of the propylated or butylated monomers generally gave the best results. Consistent with previously reported results[189], the KHI performance of the copolymers with *N*-*n*-propyl groups surpasses those with *N*-isopropyl groups. The addition of MNVA monomers in the copolymers did not reduce the performance of poly-*N*-*n*-propyl-*N*-vinylformamide but significantly increased its cloud and deposition points.[189] The copolymer with *N*-*iso*-butyl groups gave better KHI performance than the copolymer with *N*-*n*-butyl groups at similar butylated monomer ratios. We surmise that the carbon backbone length of *n*-propyl group and *iso*-butyl group may be the optimum value for penetrating the bulk water structure and causing great interaction with hydrate particles.

Two of the best performing copolymers were further evaluated at different concentrations ranging from 1000 to 7500 ppm. (Figure 5.4 and 5.5) An obvious increasing trend of inhibiting performance can be seen for both of them when their concentrations increased from 1000 to 5000 ppm. However, when the concentration over 5000 ppm, the KHI performance of them either only improved a little bit or even got worse. Thus, considering the overall cost and the KHI performance, the optimal application concentration for this KHI series is approximately 5000 ppm.

Table 5. 3 Cloud point and average KHI performance of *N*-alkyl-*N*-vinylamide copolymers at 2500 ppm. Average of 10 tests. The deviations were calculated by using the formula of STDEV.S in Excel.

Sample	T_{Cl} (˚C)	T_o **(av.) ± deviation (˚C)**	T_a **(av.) (˚C)**	T_o **(av.) -** T_a **(av.) (˚C)**
DIW		16.0 ± 0.7	15.8	0.2
PVP K-15	> 95	13.9 ± 0.5	10.3	3.6
Luvicap 55W	78	7.3 ± 0.4	6.3	1.0
RK2-033	28	9.3 ± 0.2	9	0.3
RK1-134	33	9.9 ± 0.4	9.5	0.4
RK1-120	28	9.1 ± 0.5	8.9	0.2
RK1-135	20	8.2 ± 0.2	8	0.2
RK2-034	41	8.6 ± 0.4	8.4	0.2
RK1-121	34	9.9 ± 0.6	9.4	0.5
RK2-035	66	8.7 ± 0.7	7.4	1.3
RK1-125	59	9.2 ± 0.3	8.6	0.6
RK2-037	94	9.9 ± 0.5	9	0.9
RK2-036	> 95	10.3 ± 0.4	9.2	1.1
RK1-136	86	9.4 ± 0.3	8.8	0.6
RK1-126	83	10.5 ± 0.6	9.4	1.1

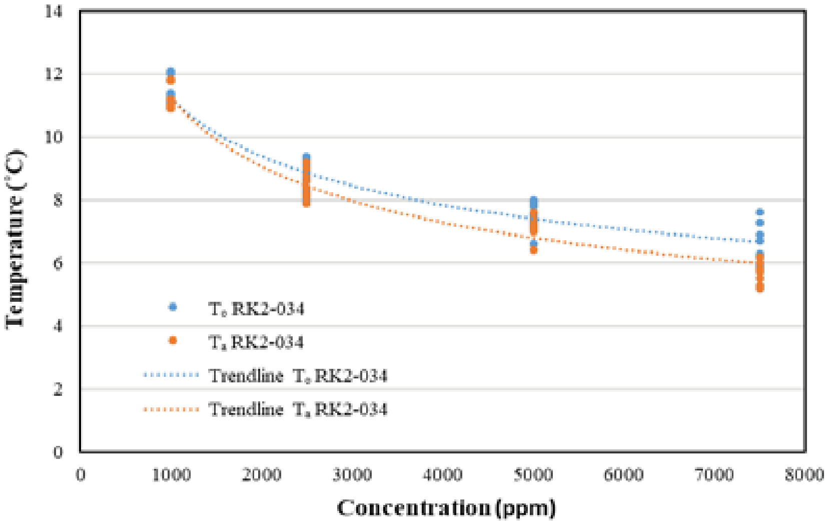

Figure 5. 4 KHI performance of RK2-034 at varying concentrations.

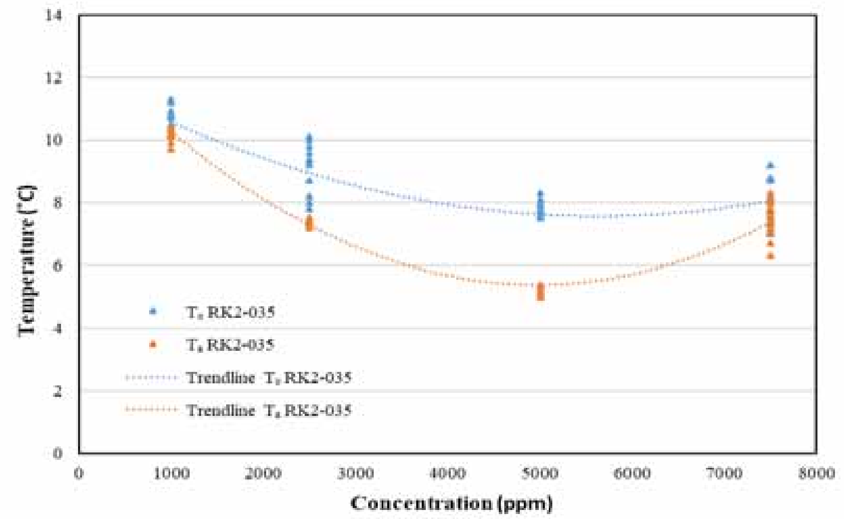

Figure 5. 5 KHI performance of RK2-035 at varying concentrations.

Different synergists were added to the copolymers with the best KHI performance to investigate the synergistic effect. (Table 5.4) Although 2-ethoxyethanol (2-EE) has a good synergistic effect for some KHI polymers, e.g., polyacrylamides,[222] it is not a good synergist for this *N*-alkyl-*N*-vinylamide copolymer series. The synergistic improvement in KHI performance by adding mono-*n*-butyl glycol ether (nBGE) is much greater for the copolymers with *iso*-butyl groups than for the copolymers with *n*-propyl groups. However, the addition of mono-*iso*-butyl glycol ether (iBGE) leads to greater synergistic improvement for the *n*-propylated copolymers than for the *iso*-butylated copolymers. It indicates that a better synergistic effect can be achieved by having one chemical with a straight alkyl chain and one with a branched alkyl group, which probably due to the complementary interaction between the polymer and synergist.

Table 5. 4 Summary of average KHI performance of *N*-alkyl-*N*-vinylamide copolymers with varying synergists. Average of 10 tests. The deviations were calculated by using the formula of STDEV.S in Excel.

Sample + Solvent	**Concn. (ppm)**	**T_o (av.) ± deviation (°C)**	**T_a (av.) (°C)**	**T_o (av.) - T_a (av.) (˚C)**
DIW	0	16.0 ± 0.7	15.8	0.2
DIW + nBGE	0 + 10000	16.1 ± 0.3	15.9	0.2
DIW + iBGE	0 + 10000	16.2 ± 0.2	16.0	0.2
RK1-135	2500	8.2 ± 0.2	8.0	0.2
RK1-135 + nBGE	2500 + 10000	4.7 ± 0.2	4.1	0.6
RK2-034	2500	8.6 ± 0.4	8.4	0.2
RK2-034 + nBGE	2500 + 10000	7.4 ± 0.6	7.0	0.4

RK2-034 + 2-EE	2500 + 10000	9.4 ± 0.6	9.2	0.2
RK1-125	2500	9.2 ± 0.3	8.6	0.6
RK1-125 + nBGE	2500 + 10000	8.5 ± 0.9	8.1	0.4
RK1-125 + iBGE	2500 + 10000	7.5 ± 0.9	6.7	0.8
RK2-035	2500	8.7 ± 0.7	7.4	1.3
RK2-035 + nBGE	2500 + 10000	9.0 ± 0.3	8.9	0.1
RK2-035 + 2-EE	2500 + 10000	8.9 ± 0.8	7.9	1.0
HA8-014A	2500	8.7 ± 0.2	8.2	0.5
HA8-014A + nBGE	2500 + 10000	7.7 ± 0.3	7.3	0.4
HA8-014A + iBGE	2500 + 10000	6.9 ± 0.2	6.5	0.4

5.3 *Paper III: Improving the Kinetic Hydrate Inhibition Performance of 3-Methylene-2-pyrrolidone Polymers by N-alkylation, Ring Expansion and Copolymerization*[193]

Poly (*N*-vinyl lactam)s, such as poly (*N*-vinyl pyrrolidone) (PVP) and poly (*N*-vinyl caprolactam) (PVCap), are a series of traditional KHIs.[8, 9] Nowadays, their homopolymer and copolymer products are still widely used in industry application as well as laboratory studies.[10, 174] 3-methylene-2-pyrrolidone (3M2P) polymer, which is a poly lactam that is structurally similar to PVP, has been investigated as KHI.[223] (Figure 5.6) However, the KHI performance of 3M2P polymer is not very good. The 5-membered ring of 3M2P maybe not the ideal size for inhibiting the formation of gas hydrates as the report showed that poly (*N*-vinyl lactam)s with larger pendant ring size ranging from 5 to 8-member gave better KHI performance.[155] The proton attached to the nitrogen atom in 3M2P can be easily replaced by alkyl groups, and polymers with more hydrophobic alkyl groups have high potential of being efficient KHIs as long as they keep water-soluble.[165, 224] Also, copolymerization with other monomers has been proved to be an effective method to improve the performance of KHIs.[175, 225]

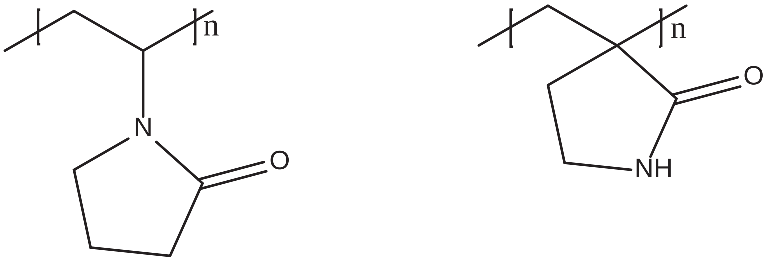

Figure 5. 6 Structure of PVP (left) and 3M2P polymer (right).

Therefore, we were interested in utilizing the methods of ring expansion, *N*-alkylation, and copolymerization to improve the KHI performance of 3M2P polymer. (Figure 5.7) Thus, 3-methylene-2-piperidone (3M2Pip) polymer with 6-membered pendant rings, *N*-alkylated 3M2P polymers including *N*-methyl-3-methylene-2-pyrrolidone (Me-3M2P), *N*-ethyl-3-methylene-2-pyrrolidone (Et-3M2P) and *N*-*n*-propyl-3-methylene-2-pyrrolidone (nPr-3M2P) polymers, and copolymers including 3M2P:*N*-*n*-butyl methacrylamide (BuMAAm), 3M2P:VCap and Me-3M2P:VCap have been synthesized and investigated as sII hydrate KHIs using the SNG mixture. (Table 5.5)

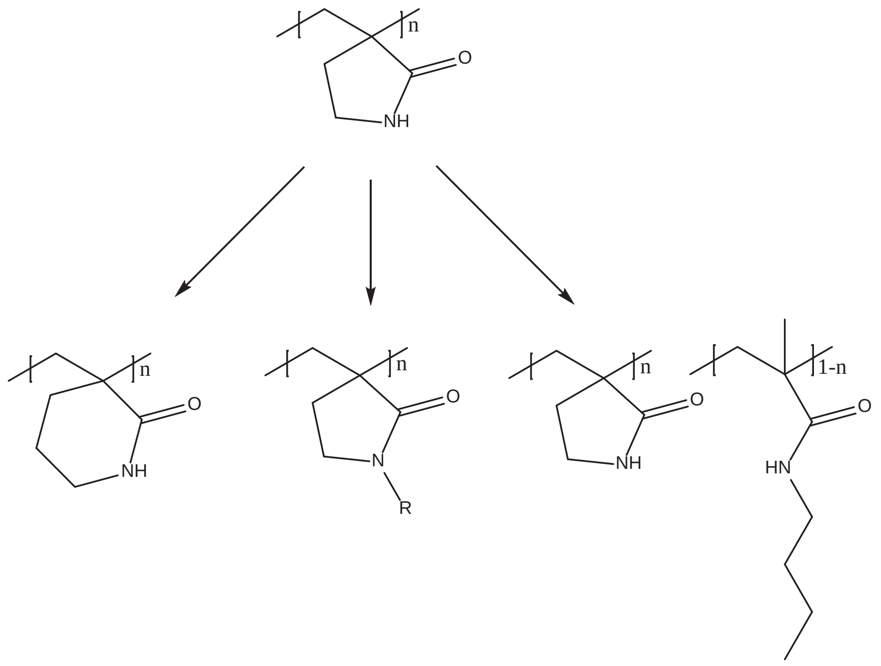

Figure 5. 7 Three methods to improve the KHI performance of 3M2P polymer. R = alkyl groups containing 1-3 carbon atoms.

Table 5. 5 Analytical data of the synthesized polymers in this study.

Polymer	**Monomer 1 (n)**	**Monomer 2 (1-n)**	**n**	***Đ***	***Mn* (g/mol)**
1	Me-3M2P			2.27	4000[a]
2a	Et-3M2P			2.20	1100[a]
2b	Et-3M2P			1.63	9000[a]
3	nPr-3M2P			2.08	6100[a]
4	3M2Pip				<12900
A	3M2P	BuMAAm	0.97		4300[b]
B	3M2P	BuMAAm	0.91		5500[b]

C	3M2P	BuMAAm	0.88		2400[b]
D	3M2P	BuMAAm	0.77		4500[b]
E	3M2P	BuMAAm	0.75		3300[b]
i	3M2P	VCap	0.53	1.37	4800[a]
ii	Me-3M2P	VCap	0.50	1.22	7600[a]

[a] Number average molecular weights obtained from DMAc SEC.

[b] Number average molecular weights obtained from ^{1}H NMR spectroscopy.

As can be seen from Table 5.6, the 3M2Pip polymer with 6-membered pendant rings gave significantly better KHI performance than the 3M2P with 5-membered rings. The addition of methyl group on the pendant ring of 3M2P polymer did not improve its KHI performance. The *N*-alkylated 3M2P polymers with more hydrophobic groups, such as ethyl and propyl groups, gave significantly better KHI performance than the 3M2P polymer. The copolymerization with BuMAAm or VCap monomer can also improve the KHI performance of 3M2P polymer. There is a trend showing that the KHI performance improved when the percentage of BuMAAm monomers in the copolymers increased.

The reason why the KHI performance of 3M2P polymer achieved significantly improvement maybe because that all of the three methods: (i) ring expansion with more carbon-containing lactam, (ii) N-alkylation and (iii) copolymerization with more hydrophobic monomers lead to more hydrophobic side groups in the KHI polymer. As the hydrophobic groups can strengthen the organization of the water structure,[120, 140, 173] the water structure may prefer to grow around the hydrophobic groups leading to fragile hydrate cavities formed around the gas molecules. Thus, with the competition of the hydrophobic groups the critical-sized hydrate nucleus cannot easy to form. The hydrophobic side groups hang on the backbone of a KHI polymer, which may make them swing here and there in the KHI solution, so the formed water structures around them cannot easily accumulate to the critical size. A more hydrophobic side group of a polymer can be more competitive and swingable, resulting in better KHI performance.

Table 5. 6 Summary of the KHI performance of the polymers at 5000 ppm and cloud points. Average of 10 tests. The deviations were calculated by using the formula of STDEV.S in Excel.

Additive	**T_o (av.) ± deviation °C**	**ΔT at T_o °C**	**T_a (av.) °C**	**T_o (av.) - T_a (av.) °C**	**T_{Cl} °C**
No additive	17.3 ± 0.3	3.1	17.2	0.1	
PVP K-15	13.3 ± 0.9	7.0	9.1	4.2	>95
VP:VCap	6.2 ± 1.0	13.9	3.3	2.9	78
3M2P	15.2 ± 0.4	5.1	15.0	0.2	>85
3M2Pip	9.5 ± 0.7	10.7	9.3	0.2	37.6
Me-3M2P	15.4 ± 0.5	4.9	12.5	2.9	>85
Et-3M2P-a	9.2 ± 1.0	11.0	8.5	0.7	>80
Et-3M2P-b	8.3 ± 0.4	11.9	5.8	2.5	71.5
nPr-3M2P	7.8 ± 0.7	12.3	5.9	1.9	19.8
3M2P:BuMAAm-A	13.0 ± 0.4	7.3	12.6	0.4	>85
3M2P:BuMAAm-B	9.5 ± 0.9	10.7	9.2	0.3	>85
3M2P:BuMAAm-C	8.4 ± 0.3	11.8	8.3	0.1	47.6
3M2P:BuMAAm-D	8.1 ± 0.7	12.1	8.0	0.1	33
3M2P:BuMAAm-E	7.2 ± 0.2	12.9	7.0	0.2	30
3M2P:VCap-i	8.0 ± 0.4	12.2	7.5	0.5	67.2
Me-3M2P:VCap-ii	8.4 ± 0.3	11.8	7.2	1.2	41

Two of the best copolymers in this study were chosen to test at varying concentrations and the results are shown in Figure 5.8. Figure 5.8 also includes the results of KHI performance tests of Luvicap 55W at different concentrations for comparison. The same trend can be seen that all the three copolymers gave better KHI performance at higher concentrations ranging from 500 to 5000 ppm.

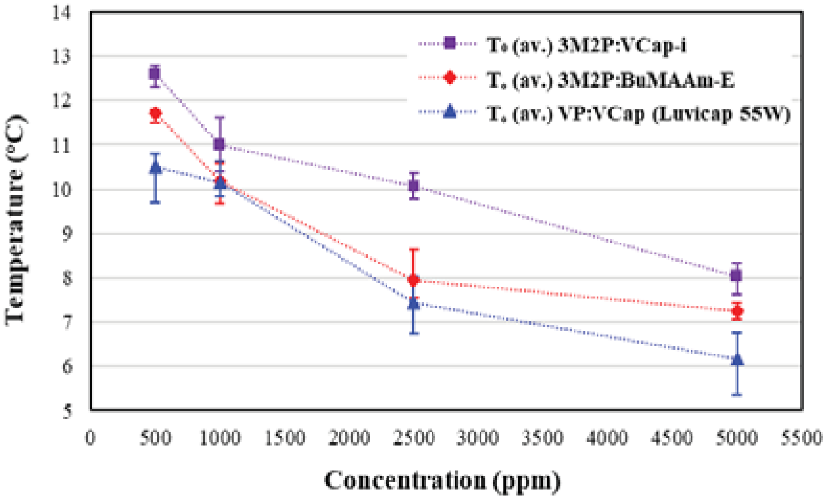

Figure 5. 8 Average T_o values of 3M2P:VCap, 3M2P:BuMAAm and VP:VCap copolymers versus concentration.

5.4 *Paper IV: Study of the Kinetic Hydrate Inhibitor Performance of Poly (N-vinyl caprolactam) and Poly (N-isopropyl methacrylamide) with Varying End Caps*[198]

The discovery of poly (*N*-vinyl caprolactam) (PVCap) is one of the very important milestones in KHI development history.[3, 8, 9] PVCap has become a market-leading KHI for many years and by nowadays it is still a standard by which newly developed KHIs would be compared in both industry application and laboratory studies.[10] PVCap has efficient KHI performance for both sI and sII hydrate.[174] For sII hydrates, PVCap homopolymers can be useful at the sub-coolings up to 10-12 °C, depending on the methods of manufacture.[8] PVCap would lose its KHI performance in deepwater applications with higher sub-coolings. the low cloud point (T_{Cl}) of PVCap is also a limitation for its application. The T_{Cl} of PVCap is around 35 °C and it would be precipitated at the injection points in the industry where the temperature may be as high as 60-120 °C.[189] Several methods have been utilized to improve the performance of PVCap, e.g., adding synergists and copolymerizing it with other monomers.[175, 177] Ieong et al. reported that utilizing chain transfer agents (CTAs) to modify the polymers during the synthesizing procedure is an effective technique to improve their thermoresponsive, amphiphilic and biocompatible properties.[226] The modified PVCap with mercaptoacetic acid end-capping group has been proved to be a better KHI than the normal PVCap.[159] Thus, it is of great interest to investigate KHI polymers modified with more categories of CTAs.

In this study, several mercaptocarboxylic acids have been used as CTAs during the procedure of synthesizing PVCaps and poly (*N*-isopropyl methacrylamide)s (PNIPMAMs). (Table 5.7) The mercaptocarboxylic acid groups modified polymers have been investigated as KHIs using both pure methane gas and SNG mixture in gas + water system as well as in gas + water + decane multiphase system.

Table 5. 7 Summary of mercaptocarboxylic acids modified polymers and molecular weight results.

Polymer	**Chain transfer agent**	***Mn***	***Đ***
PVCap		4403	2.42
$PVCapSCH_2COOH$	Mercaptoacetic acid	3350	2.25
$PVCapSCH(COOH)CH_2COOH$	Mercaptosuccinic acid	4006	2.55

$PVCapSC_6H_4COOH$	4-Mercaptobenzoic acid	5404	2.03
$PVCapSC_{11}H_{22}COOH$	12-Mercaptododecanoic acid	5586	2.02
$PVCapSC_{15}H_{30}COOH$	16-Mercaptohexadecanoic acid	6530	2.01
PNIPMAM		12088	2.18
$PNIPMAMSCH_2COOH$	Mercaptoacetic acid	10812	29.34
$PNIPMAMSCH(COOH)CH_2COOH$	Mercaptosuccinic acid	1965	4.7

As shown in Table 5.8 and Figure 5.9, $PVCapSCH_2COOH$ and $PNIPMAMSCH_2COOH$ with mercaptoacetic acid end-capping groups gave significantly better KHI performance than the normal PVCap and PNIPMAM for both sI and sII hydrates. We surmise that the carboxylic acid groups in the end of PVCap molecules may be able to enter and bond to open hydrate cavities in a semi-clathrate manner, thus inhibiting the gas hydrate formation.[227] $PVCapSCH(COOH)CH_2COOH$ and $PNIPMAMSCH(COOH)CH_2COOH$ with mercaptosuccinic acid end-capping groups even gave better KHI performance than the SCH_2COOH end group modified polymers for sII hydrate. It may be because that the large $5^{12}6^4$ cavities in sII hydrates are big enough for the $SCH(COOH)CH_2COOH$ groups and the carboxylic acid groups in $SCH(COOH)CH_2COOH$ are twice as many as in SCH_2COOH. However, for sI hydrate, $PVCapSCH(COOH)CH_2COOH$ and $PNIPMAMSCH(COOH)CH_2COOH$ only gave slightly better KHI performance than the normal PVCap and PNIPMAM, and the mercaptosuccinic acid end group modified polymer was worse than the mercaptoacetic acid end group modified polymer. It probably due to the 5^{12} and $5^{12}6^2$ cavities of sI hydrate are only big enough for the

SCH_2COOH groups but not for the $SCH(COOH)CH_2COOH$ groups, and the extra CHCOOH in the $SCH(COOH)CH_2COOH$ group may sterically interfere its interaction with the cavities of sI hydrate. $PVCapSC_{11}H_{22}COOH$ with 12-mercaptododecanoic acid end-capping groups gave the same KHI performance as the normal PVCap for both sI and sII hydrates, as the long fatty acid group is not the suitable size for the hydrate cavities. $PVCapSC_{15}H_{30}COOH$ with 16-mercaptohexadecanoic acid end-capping groups gave better KHI performance than the normal PVCap for sII hydrate but gave almost the same performance as the normal PVCap for sI hydrate. It may be because that the low cloud point of $PVCapSC_{15}H_{30}COOH$ is useful for the KHI performance on sII hydrate.[167] $PVCapSC_6H_4COOH$ with 4-mercaptobenzoic acid end-capping groups performed even worse than the normal PVCap for both sI and sII hydrates. The reason probably due to the π orbitals in the benzene rings interact with each other, thus reducing the freedom of the PVCap molecules to disturb the water structure.

Table 5. 8 Summary KHI performance results for the end group-modified polymers at 2500 ppm both in methane + water and in SNG + water systems. Average of 10 tests.

		sII		**sI**	
Sample	**T_{CI} (ºC)**	**T_o (av.) (ºC)**	**T_a (av) (ºC)**	**T_o (av) (ºC)**	**T_a (av.) (ºC)**
DIW		16.9	16.7	12.2	12.1
PVCap	35.5	9.7	9.4	7.2	7.0
$PVCapSCH_2COOH$	37.8	8.7	8.2	6.3	6.2
$PVCapSCH(COOH)CH_2COOH$	36.8	8.5	8.2	6.9	6.7
$PVCapSC_{11}H_{22}COOH$	35.5	9.7	9.3	7.1	7.0
$PVCapSC_{15}H_{30}COOH$	<4 [a]	8.7	8.4	7.1	7.0

PVCapSC$_6$H$_4$COOH	32.8	10.5	10.1	7.9	7.7
PNIPMAM	34.1	9.3	9.1	7.7	7.5
PNIPMAMSCH$_2$COOH	39.2	8.3	8.0	6.7	6.3
PNIPMAMSCH(COOH)CH$_2$COOH	42.5	7.6	7.3	7.2	7.0

[a] Cloudy at 4 °C.

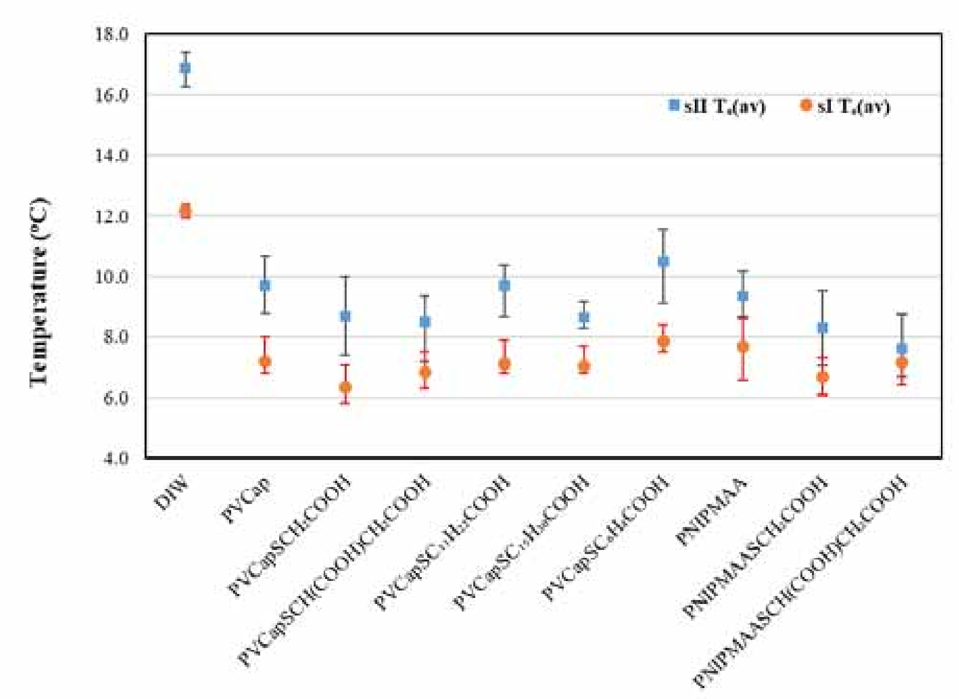

Figure 5. 9 Summary of the average T_o values for KHI polymers at 2500 ppm both in methane + water and in SNG + water systems.

We further investigated the KHI performance of PVCapSCH(COOH)CH$_2$COOH at different concentrations in the SNG + water system. Figure 5.10 shows a trend that the KHI performance of

$PVCapSCH(COOH)CH_2COOH$ increases when the concentration increases from 2500 to 5000 to 7500 ppm.

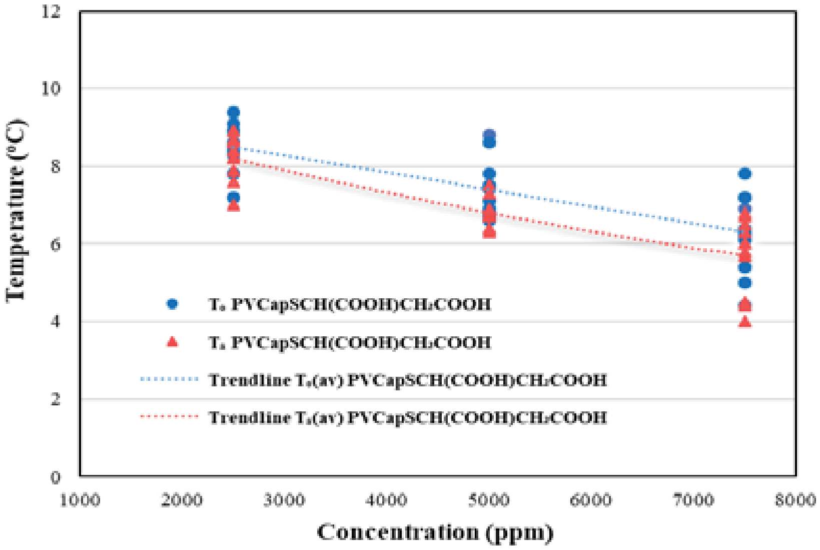

Figure 5. 10 The KHI performance of $PVCapSCH(COOH)CH_2COOH$ at varying concentrations in SNG + water system.

We wondered whether the end group-modified polymers would give an advantage for the system with the liquid hydrocarbon phase, so we tested the KHI performance in the SNG + water + decane multiphase system, and the results show in Figure 5.11. However, only $PVCapSCH_2COOH$ and $PVCapSC_{15}H_{30}COOH$ gave significantly better KHI performance than the normal PVCap on sII hydrate in the multiphase system, and the KHI performance of $PVCapSCH(COOH)CH_2COOH$, $PVCapSC_6H_4COOH$ and $PVCapSC_{11}H_{22}COOH$ were almost the same as the normal PVCap in this system. The mediocre performance of $PVCapSCH(COOH)CH_2COOH$ in the multiphase system was unexpected and the reason why this happened maybe because that organic phase changed the formation route of gas hydrates, resulting in a different KHI mechanism from the gas + water system.[228-230]

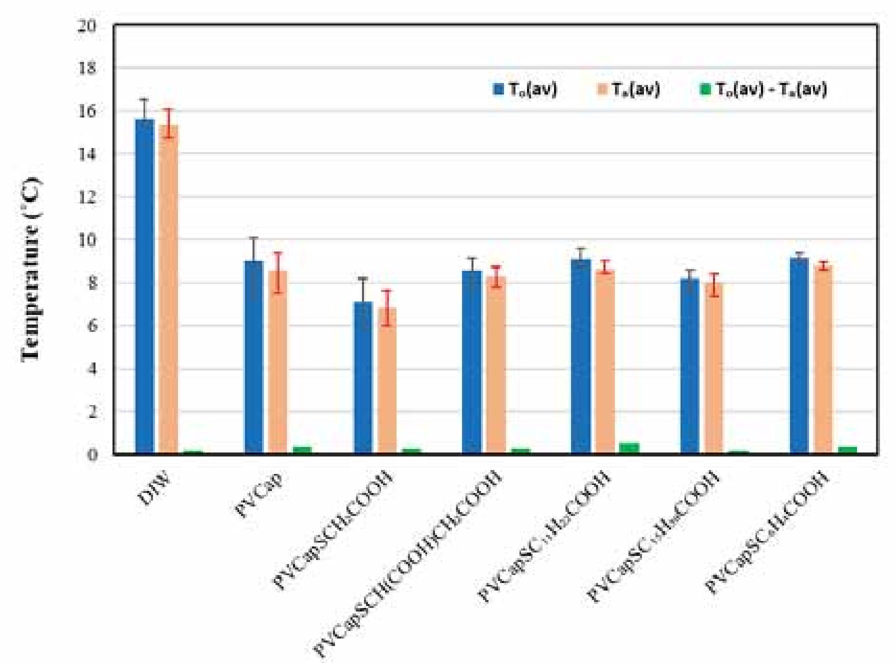

Figure 5. 11 Summary KHI performance results for the end groups modified polymers at 2500 ppm in SNG + water + decane system.

5.5 Paper V: A Simple and Direct Route to High Performance Acrylamide-based Kinetic Gas Hydrate Inhibitors from Poly (acrylic acid)[205]

(Meth)acrylamide-based polymers are a series of KHIs that have been used commercially in the gas hydrate inhibiting field, and among which the *N*-alkyl(meth)acrylamide polymers with the alkyl being isopropyl, *n*-propyl, and pyrrolidinyl groups were reported to be the best KHIs.[231-235]

Normally, the (meth)acrylamide-based polymers are made from the corresponding (meth)acrylamide monomers. Few manufacturers and/or limited applications outside the oil industry of the (meth)acrylamide monomers make their KHI polymer products being relatively expensive. Thus, the methods of making (meth)acrylamide-based polymers directly from relatively cheaper polymeric starting materials, such as poly (acrylic acid) (PAA), poly (methacrylic acid) (PMAA) and poly (methyl acrylate) (PMA), which have been reported to be experimentally feasible,[199, 236-238] are possible to reduce the cost of the (meth)acrylamide-based KHI polymers. In addition, the same starting material polymers ensure the fixed molecular weights of the (meth)acrylamide-based KHI products, thus allowing a better comparison of the pendant functional groups.

Therefore, we tried making polyalkylacrylamides from poly (acrylic acid) (PAA) and amines, polyalkylmethacrylamides from poly (methacrylic acid) (PMAA) and amines, and poly (isopropylmethacrylamide) from poly (methylmethacrylate) (PMA) and isopropylamine using triazabicyclodecene (TBD) as catalyst. However, we only successfully got the target products of polyalkylacrylamides from PAA and the corresponding amines. (Figure 5.12) The failed attempts of making polyalkylmethacrylamides probably due to the steric hindrance of the methyl groups in the backbone of PMAA and PMA affected the reaction of the acid or ester pendant groups with amines. The synthesized acrylamide-based polymers were investigated as KHIs using SNG mixture.

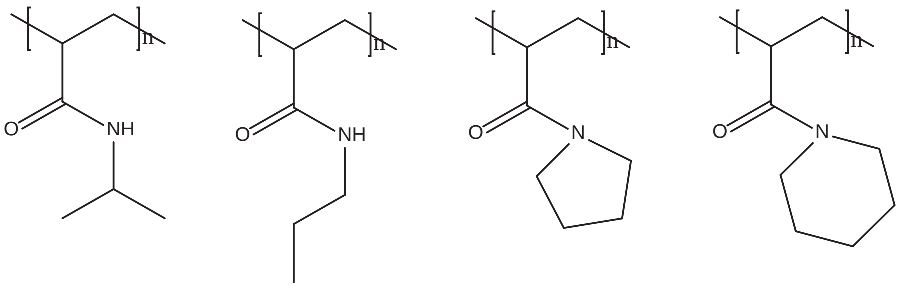

Figure 5. 12 From left to right: poly (*N*-isopropylacrylamide) (PNIPAM), poly (*N*-*n*-propylacrylamide) (PNnPAM), polyacryloylpyrrolidine (PAPYD) and polyacryloylpiperidine (PAPPD)

The results from the KHI performance tests of the acrylamide-based polymers directly made from PAA are listed in Table 5.9, as well as the results of deionized water (DIW), PVCap (*Mw* 2000-4000 g/mol), PNIPAM (*Mw* 2509 g/mol) made from NIPAM monomers and PAPYD (*Mw* 5000 g/mol) made from APYD monomers are also included for comparison.

We chose two kinds of PAAs with similar molecular weights but provided by different suppliers to make the acrylamide-based KHI polymers. Both the two series of acrylamide-based polymers made from PAA1 and PAA2 respectively gave considerable KHI performance, indicating the route of making acrylamide-based polymers from PAAs was successful. In addition, the low cloud points of these KHI polymers imply the good conversion of the acrylamide-based polymers from PAAs, as the addition of the pendant hydrophobic groups could lead to low cloud point and the previous study reported that even 10% unconverted acrylic acid groups in the polymer would lead to a much higher cloud point.[235]

Normally, as reported in many publications, the *n*-propylated polymers gave better KHI performance than the isopropylated polymers.[189, 190, 200, 224] However, in this study, both PNnPAM1 and PNnPAM2 could not be fully soluble, resulting in the worse KHI performance of them than that of PNIPAM1 and PNIPAM2. PAPYD1 and PAPYD2 gave the best KHI performance, and reason for such good KHI performance may be due to the pyrrolidinyl groups in the acrylamide-based polymers. Perhaps the pyrrolidinyl group is a suitable size to enter the $5^{12}6^4$ cavity of the sII hydrate and/or the suitable hydrophobic group for disturbing the water structure of gas hydrate, thus preventing gas hydrate from forming. The KHI performance of PAPPD1 with piperidinyl groups was not very good, maybe because of its poor water solubility. We believe that the KHI performance of PAPPD1 should be better if it could have been fully water-soluble, as the better KHI performance of the polymers with 6-membered rings than the polymers with 5-membered rings has been reported in many KHI series, such as the polyvinyl lactam series and the amine oxide polymers with cyclic amines series.[155, 239]

Polyacrylic acid pyrrolidinylammonium salt (PAPYD2 salt) was the neutralization product of poly (acrylic acid) with pyrrolidine that has not converted to the polyacryloylpiperidine acrylamide polymer. The PAPYD2 salt gave no inhibition performance, indicating that the *N*-alkylated amide groups are critical for the outstanding KHI performance of the acrylamide-based polymer final products.

Table 5. 9 The KHI performance of the acrylamide-based polymers at 2500 ppm and their cloud points and corresponding original main materials. Average of 10 tests unless otherwise stated. The deviations were calculated by using the formula of STDEV.S in Excel.

Name	**Original material**	**T_{Cl} (ºC)**	**T_o (av.) ± deviation (°C)**	**T_a (av.) (°C)**
DIW			16.4 ± 0.6	16.3
PVCap		40	10.4 ± 0.4	9.9
PNIPAM	NIPAM monomer	39 [a]	9.5 [a]	9.3 [a]

PAPYD	APYD monomer	60	9.8 ± 0.7	9.6
PNIPAM1	PAA1 (*Mw* 1800 g/mole) + isopropylamine	42	8.5 ± 0.2	8.3
PNnPAM1 [#]	PAA1 (*Mw* 1800 g/mole) + n-propylamine	< 4	9.1 ± 0.3	9.0
PAPYD1	PAA1 (*Mw* 1800 g/mole) + pyrrolidine	23	7.1 ± 0.5	6.8
PAPPD1 [#]	PAA1 (*Mw* 1800 g/mole) + piperidine	< 4	11.6 ± 0.5	11.5
PNIPAM2	PAA2 (*Mw* 2000 g/mole) + isopropylamine	35	8.5 ± 0.2 [b]	8.3 [b]
PNnPAM2 [#]	PAA2 (*Mw* 2000 g/mole) + *n*-propylamine	< 4	10.0 ± 0.2	9.9
PAPYD2 [#]	PAA2 (*Mw* 2000 g/mole) + pyrrolidine	35-40	8.1 ± 1.0 [b]	7.8 [b]
PAPYD2 salt	PAA2 (*Mw* 2000 g/mole) + pyrrolidine	> 90	17.3 ± 0.5 [b, c]	16.8 [b, c]

[#] Not fully soluble. [a] Results from a previous publication.[169] [b] Results from RC5-1. [c] Two tests. Other results are obtained from RC5-2.

We further tested the KHI performance of PNIPAM1 at different concentrations, and the results of the SCC tests are shown in Figure 5.13 From Figure 5.13 there is a trend showing that the KHI performance of PNIPAM1 increases when the concentration increases from 1250 to 5000 ppm, which is consistent with the reported results of poly (*N*-isopropylacrylamide).[189]

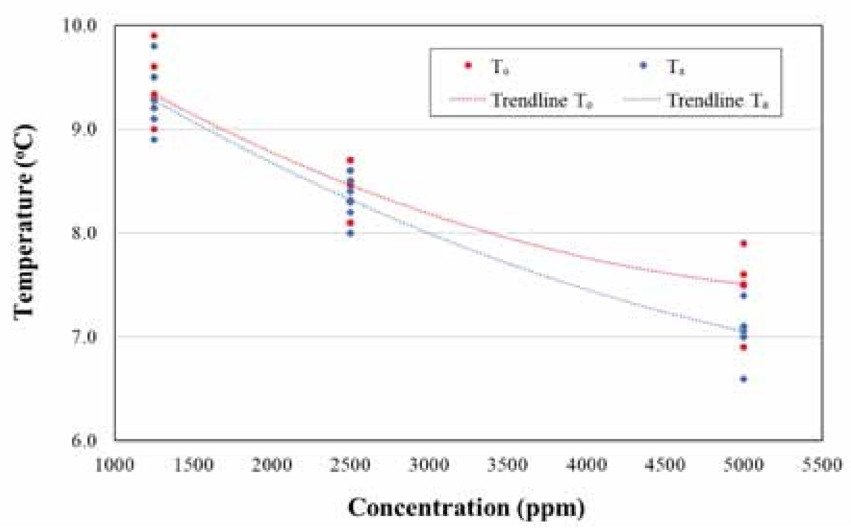

Figure 5. 13 KHI performance of PNIPAM1 at different concentrations.

5.6 Paper VI: Polyvinylsulphonamides as Kinetic Hydrate Inhibitors[200]

Base on the fact that most effective KHIs are amide-containing polymers, the amide group seems to be an indispensable element for KHIs.[155, 165, 219] Although in recent years some other functional groups, e.g., hydroxyl, sulfonic acid, phosphoric acid, and carboxyl acid groups, have been introduced into KHI polymers to improve their properties, the main active components of these KHIs are still the amide group-containing part.[9, 159, 160] (Figure 5.14)

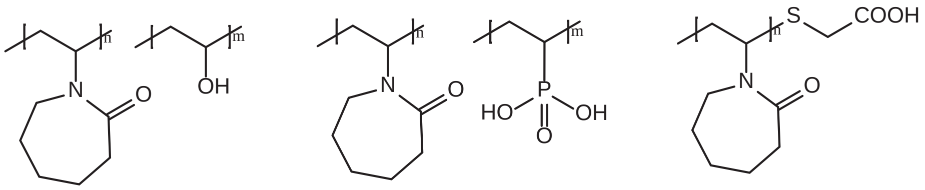

Figure 5. 14 Structures of modified KHIs by different functional groups. From left to right: VCap: vinyl alcohol copolymer, VCap: vinyl phosphoric acid copolymer, and carboxyl-terminated PVCap.

The sulphonamide group (-NH-S(=O)$_2$-) has a similar structure to the amide group (-NH-C(=O)-),[240] and sulphonamide compounds have been widely used in medicinal science,[241, 242] thus the sulphonamide group-containing polymers may have potential to be efficient and environmentally friendly KHIs.

Therefore, it is of great interest to investigate *N*-alkylvinylsulphonamide polymers as KHIs. We first attempted to make *N*-alkylvinylsulphonamide homopolymers, including *N*-ethylvinylsulphonamide (EtVSAM), *N*-*n*-propylvinylsulphonamide (nPrVSAM), and *N*-*iso*-butylvinylsulphonamide (iBuVSAM) homopolymers, but none of them were water-soluble. Therefore, *N*-vinyl-*N*-methylacetamide (VIMA) monomers were utilized to copolymerize with the *N*-alkylvinylsulphonamide monomers to improve the water solubility. The KHI performance of these sulphonamide group-containing copolymers was investigated as KHIs using the SNG mixture. In addition, *n*-propylmethacrylamide: *N*-vinyl-*N*-methylacetamide copolymers (co(nPrMAM:VIMA)) and *n*-propylmethacrylate: *N*-vinyl-*N*-methylacetamide copolymer (co(nPrMA:VIMA)) were also investigated as KHIs in this study for comparison. (Table 5.10)

Table 5. 10 Analytic results of the synthesized polymers as well as their cloud points (T_{Cl}) and deposition point (T_{dp}) at 2500 ppm.

Name	**Monomer ratio**	**Solvent**	**Concn. (wt.%)**	***Mw* (Da)**	***Đ***	**T_{Cl} (ºC)**	**T_{dp} (ºC)**
VIMA homopolymer	0:1	IPA	23.2	3400	3.09	> 90	> 90
co(nPrVSAM:VIMA)*	1:2	IPA	27.9	4700	1.68	< 4	< 4
co(nPrVSAM:VIMA)*	1:3	IPA	22.1	7097	1.66	< 4	< 4
co(nPrVSAM:VIMA)	1:4	IPA	22.3	5100	1.65	> 90	> 90
co(nPrVSAM:VIMA)	1:5	IPA	23.6	3400	2.43	> 90	> 90
co(nPrVSAM:VIMA)	1:8	IPA	22.0	2500	2.78	< 4#	> 90
co(nPrVSAM:VIMA)	1:12	IPA	21.5	5000	3.57	> 90	> 90
co(nPrVSAM:VIMA)	1:18	IPA	21.6	2700	2.45	> 90	> 90
co(EtVSAM:VIMA)	1:5	IPA	22.7	3100	1.72	> 90	> 90
co(iPrVSAM:VIMA)	1:5	IPA	23.2	2700	2.45	> 90	> 90
co(iBuVSAM:VIMA)	1:5	IPA	22.2	3800	2.11	< 4#	> 90
co(iBuVSAM:VIMA)	1:8	IPA	23.0	3500	3.18	< 4#	> 90
co(nPrMAM:VIMA)	1:5	IPA	23.3	1600	2.29	31	31
co(nPrMAM:VIMA)	1:8	IPA	22.2	1300	3.25	35	35
co(nPrMAM:VIMA)	1:12	IPA	22.6	2600	2.00	51	51
co(nPrMAM:VIMA)	1:18	IPA	22.0	3300	3.00	45	45
co(nPrMA:VIMA)	1:5	IPA	21.7	2800	2.80	< 4	> 90
co(nPrMA:VIMA)	1:8	IPA	22.5	3100	2.58	< 4	> 90
co(nPrMA:VIMA)	1:12	IPA	22.8	2900	2.90	< 4#	> 90
co(nPrMA:VIMA)	1:18	IPA	22.9	3300	3.00	< 4#	> 90
co(nPrVSAM:VIMA)*	1:4	iBGE	21.2	5500	3.67	< 4	< 4

Note: * Not fully soluble in water. # Opaque solution from 4 to 90 ºC.

As shown in Table 5.11, co(nPrVSAM:VIMA)s with *N*-*n*-propyl pendant groups gave better KHI performance than co(EtVSAM:VIMA), co(iPrVSAM:VIMA) and co(iBuVSAM:VIMA), when compared at the same mole ratio of *N*-alkylated vinylsulphonamide monomers to VIMA monomers in the copolymers. This indicates that for the vinylsulphonamide polymer series, the KHI performance can be affected by the varying *N*-alkyl pendant groups and of which most affected by the *N*-*n*-propyl groups. We presume that the *n*-propyl group with suitable hydrophobic property or optimum size interacts properly with the water structures, thus disturbing the formation of gas hydrate.[189, 190] Although there is a trend showing that the less percentage of nPrVSAM monomers in co(nPrVSAM:VIMA) copolymers leads to worse KHI performance, the copolymer with approximately 5% mole ratio of nPrVSAM (co(nPrVSAM:VIMA) 1:18) still gave KHI performance as good as PVCap. This implies that even a low percentage of nPrVSAM in the copolymer can be very powerful in inhibiting the gas hydrate formation. Co(nPrVSAM:VIMA) gave better KHI performance than co(nPrMAM:VIMA) and co(nPrMA:VIMA), indicating that the sulphonamide functional groups in the copolymers may have a more powerful inhibition effect on gas hydrate formation than the ester and amide functional groups. The more powerful KHI effect of the sulphonamide group than the ester and amide groups is properly due to its higher hydrophobicity, as hydrophobic groups are critical for the performance of inhibitors.[171] Mono-*iso*-butyl glycol ether (iBGE) showed good synergistic effect on co(nPrVSAM:VIMA), as the co(nPrVSAM:VIMA) copolymer synthesized in iBGE gave significantly better KHI performance than those made in isopropanol (IPA).

Table 5. 11 Summary results from the SCC tests for KHI polymers at 2500 ppm. Average of 10 tests. The deviations were calculated by using the formula of STDEV.S in Excel.

Name	**Monomer ratio**	**Solvent**	**T_o (av.) ± deviation (°C)**	**ΔT (av.) at T_o (°C)**	**T_a (av.) (°C)**
Pure water			16.9 ± 0.6	3.5	16.8
PVCap			10.4 ± 0.4	9.8	9.9
PVIMA homopolymer	0:1	IPA	16.7 ± 0.3	3.7	16.4
co(nPrVSAM:VIMA)*	1:2	IPA	11.2 ± 0.1	9.0	11.2
co(nPrVSAM:VIMA)*	1:3	IPA	10.1 ± 0.0	10.1	9.9
co(nPrVSAM:VIMA)	1:4	IPA	10.1 ± 0.1	10.1	10.0
co(nPrVSAM:VIMA)	1:5	IPA	9.5 ± 0.1	10.7	9.3
co(nPrVSAM:VIMA)	1:8	IPA	9.7 ± 0.2	10.5	9.4
co(nPrVSAM:VIMA)	1:12	IPA	9.8 ± 0.3	10.4	9.4
co(nPrVSAM:VIMA)	1:18	IPA	10.3 ± 0.2	9.9	10.1
co(EtVSAM:VIMA)	1:5	IPA	12.4 ± 0.1	7.9	12.3
co(iPrVSAM:VIMA)	1:5	IPA	10.9 ± 0.2	9.3	10.0
co(iBuVSAM:VIMA)	1:5	IPA	10.0 ± 0.3	10.2	9.6
co(iBuVSAM:VIMA)	1:8	IPA	10.2 ± 0.3	10.0	9.8
co(nPrMAM:VIMA)	1:5	IPA	10.4 ± 0.1	9.8	9.9
co(nPrMAM:VIMA)	1:8	IPA	10.8 ± 0.2	9.4	10.2
co(nPrMAM:VIMA)	1:12	IPA	11.2 ± 0.2	9.0	10.5
co(nPrMAM:VIMA)	1:18	IPA	11.3 ± 0.1	8.9	10.8
co(nPrMA:VIMA)	1:5	IPA	12.5 ± 0.1	7.8	12.3
co(nPrMA:VIMA)	1:8	IPA	11.7 ± 0.1	8.5	11.5
co(nPrMA:VIMA)	1:12	IPA	11.8 ± 0.2	8.4	11.7
co(nPrMA:VIMA)	1:18	IPA	11.3 ± 0.1	8.9	11.1
co(nPrVSAM:VIMA)*	1:4	iBGE	7.1 ± 0.1	13.0	6.9

Note: * Not fully soluble in water.

One of the best copolymers in this study, the co(nPrVSAM:VIMA) copolymer with the nPrVSAM to VIMA monomer mole ratio of 1:12

synthesized in IPA, was chosen for further investigating the KHI performance at varying concentrations. (Figure 5.15) There is a trend showing that co(nPrVSAM:VIMA) gave better KHI performance when its concentration increases, which is typical of many other KHI classes.[193, 220, 243]

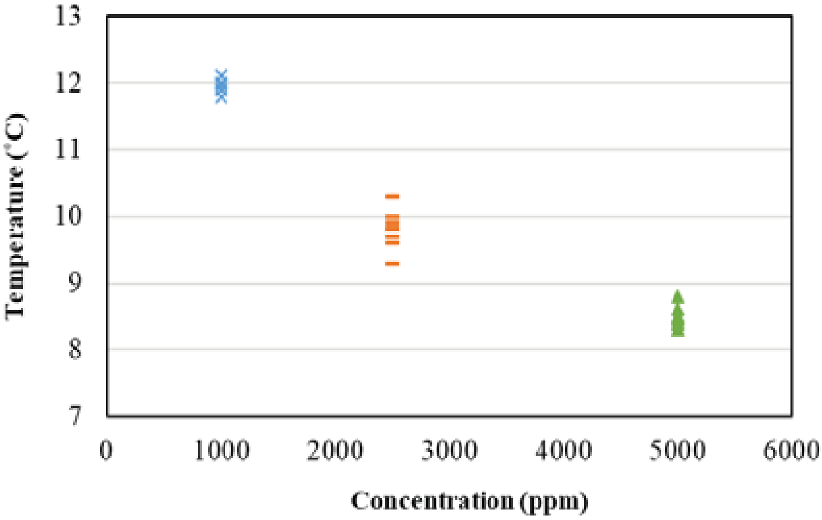

Figure 5. 15 T_o values of the co(nPrVSAM:VIMA) 1:12 synthesized in IPA at different concentrations in water.

5.7 *Paper VII: Kinetic Inhibition Performance of Alkylated Polyamine Oxides on Structure I Methane Hydrate*[202]

Amine oxide compounds, such as tri (*n*-butyl) amine oxide (TBAO), *n*-butylated bis-amine oxides, *n*-butylated tris-amine oxides, *n*-butylated polyethyleneimine oxide, have been proved to be efficient tetrahydrofuran (THI) hydrate inhibitors. In addition, the KHI performance of these amine oxide compounds on THF hydrate gradually increases when the *n*-butylated amine oxide groups increase in a molecule from one to two to three to several repeating units.[105, 115-117] TBAO itself has been reported to be poor KHI on sII gas hydrate when using SNG mixture, but it has a remarkable synergistic effect for PVCap in inhibiting sII gas hydrate.[116] Tri(*n*-pentyl) amine oxide (TPAO) with more hydrophobic pentyl groups gave a better synergistic effect for PVCap on sII gas hydrate than TBAO. Amine oxide derivatives of *n*-butylated oligoethyleneamines and polyethyleneamines gave excellent KHI performance on sII gas hydrate.[106, 107] In addition, some amine oxide compounds, such as amido-bis amine oxides containing 13-17 carbon atoms have shown reasonable anti-agglomerant performance when investigated as AAs in the SNG system.[8, 244] Thus, it is of particular interest in exploring the inhibition ability of amine oxide compounds on the structure I hydrate.

Therefore, a series of alkylated oligo- and polyamine oxides, including tetraethylenepentamine-alkyl-amine oxides (TEPA-alkyl-AO) and hyperbranched polyethyleneimine-alkyl-amine oxides (HPEI-alkyl-AO) were synthesized and investigated as sI methane hydrate KHIs. (Figure 5.16 and Table 5.12) In addition, the alkyl groups in these amine oxide oligomers and polymers were expanded from the *n*-butyl group that was almost exclusively used in past studies to more hydrophobic pentyl and hexyl groups. HPEI-alkyl-quaternary ammonium bromide and HPEI-alkyl-propylenesulfonate were also synthesized and tested for comparison.

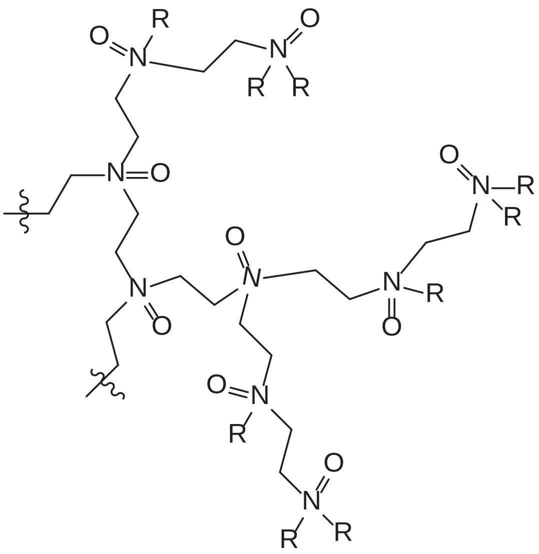

Figure 5. 16 Structure of HPEI-alkyl-AO. R = alkyl groups containing 2 to 6 carbons.

Table 5. 12 Summary of the synthesized oligomers and polymers, as well as their active concentrations in the solvent carriers.

Additive	Solvent	Concn. (wt.%)
TEPA-Ethyl-AO	IPA/H_2O	29.4
TEPA-(*n*-Propyl)-AO	IPA/H_2O	39.2
TEPA-(*n*-Butyl)-AO	IPA/H_2O	38.7
TEPA-(*iso*-Pentyl)-AO	IPA/H_2O	30.3
TEPA-(*n*-Pentyl)-AO	IPA/H_2O	39.0
TEPA-(*iso*-Pentyl)-AO	nBGE/H_2O	27.3
HPEI-0.3k-Ethyl-AO	IPA/H_2O	27.8
HPEI-0.3k-(*n*-Propyl)-AO	IPA/H_2O	28.9
HPEI-0.3k-(*n*-Butyl)-AO	IPA/H_2O	30.6
HPEI-0.3k-(*iso*-Pentyl)-AO	IPA/H_2O	31.7
HPEI-0.3k-(*n*-Pentyl)-AO	IPA/H_2O	31.4
HPEI-0.3k-(*iso*-Hexyl)-AO	IPA/H_2O	28.5
HPEI-0.3k-(*tert*-Hexyl)-AO	IPA/H_2O	25.1

HPEI-0.3k-(*n*-Hexyl)-AO*	IPA/H_2O	42.4
HPEI-0.6k-(*iso*-Pentyl)-AO	IPA/H_2O	31.0
HPEI-1.2k-(*iso*-Pentyl)-AO	IPA/H_2O	31.0
HPEI-10k-(*iso*-Pentyl)-AO	IPA/H_2O	32.1
HPEI-0.6k-(*n*-Pentyl)-AO	IPA/H_2O	29.5
HPEI-1.2k-(*n*-Pentyl)-AO	IPA/H_2O	30.7
HPEI-10k-(*n*-Pentyl)-AO	IPA/H_2O	31.7
HPEI-1.2k-(*iso*-Hexyl)-AO	IPA/H_2O	30.5
HPEI-0.3k-(*n*-Butyl)-AO	nBGE/H_2O	31.2
HPEI-0.3k-(*iso*-Pentyl)-AO	nBGE/H_2O	31.3
HPEI-0.3k-(*n*-Pentyl)-AO	nBGE/H_2O	30.6
HPEI-0.3k-(*iso*-Hexyl)-AO	nBGE/H_2O	31.3
HPEI-0.3k-(*tert*-Hexyl)-AO	nBGE/H_2O	26.5
HPEI-0.3k-(*iso*-Pentyl) quaternary ammonium Br		100 %
HPEI-0.3k-(*iso*-Pentyl)-propylenesulfonate		100 %

* Water-insoluble

As seen in Table 5.13, a trend was showing that the increasing size of the alkyl groups led to an improvement in the KHI performance for both the TEPA-alkyl-AO series and the HPEI-alkyl-AO series. TEPA-(*iso*-Pentyl)-AO with *iso*-pentyl groups gave better KHI performance than TEPA-(*n*-Pentyl)-AO with *n*-pentyl groups. 2500 ppm of HPEI-0.3k-(*n*-Butyl)-AO, HPEI-0.3k-(*iso*-Pentyl)-AO, HPEI-0.3k-(*n*-Pentyl)-AO, HPEI-0.3k-(*iso*-Hexyl)-AO, and HPEI-0.3k-(*t*-Hexyl)-AO gave such good KHI performance that the T_o values were out of the measurement limitation (3.1 °C) of the SCC method, so they were tested at a lower concentration of 1500 ppm. The HPEI-alkyl-AO with *iso*-pentyl, *iso*-hexyl and *tert*-hexyl gave better KHI performance than the HPEI-alkyl-AO with *n*-butyl and *n*-pentyl groups. We presume the reason why the amine oxide oligomers and polymers with long and branched alkyl groups gave excellent KHI performance may be because these alkyl groups can strongly disturb the water structure of gas hydrate, resulting in inhibiting the formation of gas hydrates. Studies reported that both sI and sII hydrate occurred during the initial period of methane hydrate formation and growth.[26, 29, 245] We presume that although these long and branched alkyl groups are too big for the $5^{12}6^{2}$ cavities of sI hydrate, they probably be the correct size to enter the $5^{12}6^{4}$ cavities of sII hydrate, thus preventing the gas hydrate from forming. HPEI-0.3k-(*iso*-Pentyl)-quaternary ammonium bromide and HPEI-0.3k-(*iso*-Pentyl)-propylenesulfonate gave worse KHI performance than HPEI-0.3k-(*iso*-Pentyl)-AO, indicating that the amine oxide functional group is also critical for the performance in inhibiting gas hydrate formation. The hydrogen-bonding amine oxide groups and the hydrophobic alkyl groups in HPEI-0.3k-(*iso*-Pentyl)-AO contribute equally to its KHI performance.

Table 5. 13 Summary results of the oligomers and polymers in IPA solvent from SCC tests at 1500 ppm and 2500 ppm in water. Average of 10 tests unless otherwise stated.

Additive	**Concn. (ppm)**	**T_o (°C)**	**ΔT at T_o (°C)**	**T_a (°C)**
pure water		12.0 ± 0.6	3.6 ± 0.6	11.9 ± 0.6
Luvicap 55W	2500	5.4 ± 0.8	10.0 ± 0.8	4.6 ± 0.4
Inhibex 101	2500	4.9 ± 0.8	10.5 ± 0.8	4.3 ± 0.6
Inhibex BIO-800	2500	4.4 ± 0.3	11.0 ± 0.3	4.0 ± 0.2
TEPA-Et-AO	2500	11.3 ± 0.3	4.3 ± 0.3	11.2 ± 0.3
TEPA-(*n*-Propyl)-AO	2500	8.5 ± 0.5	7.0 ± 0.5	8.2 ± 0.5

TEPA-(*n*-Butyl)-AO	2500	6.1 ± 0.3	9.4 ± 0.3	5.4 ± 0.2
TEPA-(*iso*-Pentyl)-AO	2500	3.1 ± 0.2	12.2 ± 0.2	2.3 ± 0.4
TEPA-(*n*-Pentyl)-AO	2500	4.2 ± 0.3	11.2 ± 0.3	4.0 ± 0.2
HPEI-0.3k-Ethyl-AO	2500	10.7 ± 0.4	4.8 ± 0.4	10.6 ± 0.2
HPEI-0.3k-(*n*-Propyl)-AO	2500	5.5 ± 0.4	9.9 ± 0.4	5.3 ± 0.4
HPEI-0.3k-(*n*-Butyl)-AO	2500	3.2 ± 0.2	12.1 ± 0.2	3.1 ± 0.1
HPEI-0.3k-(*iso*-Pentyl)-AO	2500	2.0 ± 0.0 [a]	13.3 ± 0.0	2.0 ± 0.0
HPEI-0.3k-(*n*-Pentyl)-AO	2500	3.3 ± 0.1	12.0 ± 0.1	2.7 ± 0.5
HPEI-0.3k-(*iso*-Hex)-AO	2500 [b]	2.2 ± 0.2 [c]	13.1± 0.2 [c]	2.0 ± 0.0 [c]
HPEI-0.3k-(*tert*-Hexyl)-AO	2500	2.0 ± 0.0 [d, e]	13.3 ± 0.0 [d]	2.0 ± 0.0 [d]
HPEI-0.3k-(*iso*-Pentyl)-quaternary ammonium Br	2500 [b]	10.2 ± 0.1	5.3 ± 0.1	10.0 ± 0.1
HPEI-0.3k-(*iso*-Pentyl)-propylenesulfonate	2500	8.8 ± 0.1	6.7 ± 0.1	6.9 ± 0.1
HPEI-0.3k-(*n*-Butyl)-AO	1500	5.5 ± 0.2	9.9 ± 0.2	5.3 ± 0.2

HPEI-0.3k-(*iso*-Pentyl)-AO	1500	3.3 ± 0.9	12.0 ± 0.9	3.1 ± 1.1
HPEI-0.3k-(*n*-Pentyl)-AO	1500	5.5 ± 0.2	9.9 ± 0.2	5.4 ± 0.2
HPEI-0.3k-(*iso*-Hexyl)-AO	1500	4.0 ± 0.6	11.3 ± 0.6	3.9 ± 0.6
HPEI-0.3k-(*tert*-Hexyl)-AO	1500	4.1 ± 0.5	11.2 ± 0.5	4.0 ± 0.5

[a] The average time at 2 °C before hydrate onset for the five cells is 1143 mins. [b] Not fully soluble in water. [c] Calculated from the results of two cells, no gas hydrate detected from the resting three cells. [d] Calculated from the results of four cells, no gas hydrate detected from the rest cell. [e] The average time at 2 °C before hydrate onset for the four cells with hydrate formation is 1151 mins.

We further carried out the isothermal tests to evaluate the KHI performance of the amine oxide oligomers and polymers with the alkyl groups containing four or more carbons. As shown in Table 5.14, when at the same molecular weight, the amine oxide polymers with more carbons in the alkyl groups led to longer induction time (t_i). nBGE gave a remarkable synergistic effect on the HPEI-alkyl-AO KHI series, especially for HPEI-0.3k-(*tert*-Hexyl)-AO. Reports showed that the molecular weight (MW) of KHI polymers might have some effects on their KHI performance and normally the polymers with the MW of around 1000-3000 g/mole gave the best KHI performance.[107, 129, 155] Therefore, we evaluated the inhibition performance of a range of HPEI-Pentyl-AOs (*n*-pentyl or *iso*-pentyl) with different MWs. HPEI-1.2k-(*iso*-Pentyl)-AO and HPEI-0.6k-(*n*-Pentyl)-AO performed the best in each series, respectively.

Table 5. 14 Summary results of the oligomer and polymers from isothermal tests at 2500 ppm in water. Average of at least 5 tests.

Additive	**Solvent**	**t_i (min)**	**t_a (min)**
Luvicap 55W		87 ± 7	106 ± 4
Luvicap 55W with added 5500ppm BGE		88 ± 3	109 ± 6
Inhibex BIO800 in 5500ppm BGE		93 ± 9	113 ± 8
TEPA-(*iso*-Pentyl)-AO	IPA	227 ± 8	237 ± 8
HPEI-0.3k-(*n*-Butyl)-AO	IPA	158 ± 28	172 ± 32
HPEI-0.3k-(*iso*-Pentyl)-AO	IPA	300 ± 60	356 ± 54
HPEI-0.3k-(*n*-Pentyl)-AO	IPA	380 ± 195	688 ± 322
HPEI-0.3k-(*iso*-Hexyl)-AO*	IPA	807 ± 953	826 ± 954
HPEI-0.3k-(*tert*-Hexyl)-AO	IPA	730 ± 110	1026 ± 56
HPEI-0.6k-(*n*-Pentyl)-AO	IPA	486 ± 156	2412 ± 572
HPEI-1.2k-(*n*-Pentyl)-AO	IPA	120 ± 35	130 ± 35
HPEI-10k-(*n*-Pentyl)-AO*	IPA	110 ± 12	121 ± 10
HPEI-0.6k-(*iso*-Pentyl)-AO	IPA	518 ± 72	2496 ± 254
HPEI-1.2k-(*iso*-Pentyl)-AO	IPA	864 ± 526	1639 ± 719
HPEI-10k-(*iso*-Pentyl)-AO*	IPA	88 ± 3	93 ± 2
HPEI-1.2k-(*iso*-Hexyl)-AO*	IPA	73 ± 3	76 ± 1

TEPA-(*iso*-Pentyl)-AO	nBGE	238 ± 22	281 ± 29
HPEI-0.3k-(*n*-Butyl)-AO	nBGE	109 ± 21	119 ± 21
HPEI-0.3k-(*iso*-Pentyl)-AO	nBGE	702 ± 349	878 ± 298
HPEI-0.3k-(*n*-Pentyl)-AO	nBGE	583 ± 548	1198 ± 1032
HPEI-0.3k-(*iso*-Hextyl)-AO*	nBGE	581 ± 550	598 ± 543
HPEI-0.3k-(*tert*-Hextyl)-AO	nBGE	2976 ± 756	4876 ± 2606

***** Not fully soluble in water.

5.8 Paper VIII: Amine N-oxide Kinetic Hydrate Inhibitor Polymers for High Salinity Applications[239]

Hundreds of KHI molecules have been reported since the early 1990s and most of them are amide-containing polymers, such as poly (*N*-vinyl caprolactam) (PVCap) with cyclic amide, and poly (*N*-isopropyl methacrylamide) (PNIPMAM) with acyclic amide.[3, 4] The reason why most reported KHI polymers contain repeating amide groups is maybe because the highly hydrophilic amide group renders the polymers water-soluble, and good water solubility is the essential requirement for KHIs. In addition, the amide group can offer three covalent bonds (one from the carbon moiety and two from the nitrogen moiety) that allow it to connect with different groups, thus providing immense structural diversities.[240] Therefore, the development of KHI research was mainly based on amide polymers. The amine oxide group is also highly hydrophilic and strongly hydrogen-bonding and can offer three covalent bonds for connecting with other groups. Thus, it is of particular interest to investigate amine oxide-containing polymers as KHIs. In addition, cyclic amine oxides have not been investigated previously.

A range of amine oxide polymers with cyclic or acyclic amines, i.e., poly (propylene oxide): poly (*N*, *N*-diethyl glycidyl amine *N*-oxide) block copolymers (PPO-*b*-PDEGAO), poly (propylene oxide): poly (piperidine glycidyl amine *N*-oxide) block copolymers (PPO-*b*-PPiGAO) and poly (piperidine glycidyl amine *N*-oxide) homopolymers (PPiGAO) oxidized from the corresponding amine polymers were synthesized and investigated as KHIs using SNG mixture in this study. (Figure 5.17 and Table 5.15)

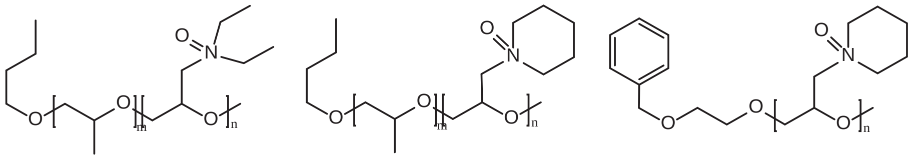

Figure 5. 17 Structures of PPO-*b*-PDEGAO (left), PPO-*b*-PPiGAO (middle) and PPiGAO (right).

Table 5. 15 Analytical results of PPO-*b*-PDEGA, PPO-*b*-PPiGA and PPiGA as well as the corresponding amine oxide polymers (PGAO).

Sample	**GA (mol %)**	**M_n[a] (kg/mol)**	**M_n[b] (kg/mol)**	**Đ[b]**	**M_n (PGAO)[a] (kg/mol)**
PPO_{21}-*b*-$PDEGA_6$	22	2.1	1.4	1.08	2.2
PPO_{21}-*b*-$PDEGA_{12}$	36	2.9	1.5	1.10	3.0
PPO_{47}-*b*-$PDEGA_{11}$	23	4.3	2.6	1.17	4.4
PPO_{47}-*b*-$PDEGA_{20}$	30	5.4	2.7	1.19	5.7
PPO_{21}-*b*-$PPiGA_3$	13	1.8	1.4	1.05	1.8
PPO_{21}-*b*-$PPiGA_{13}$	38	3.1	1.7	1.05	3.3

PPO$_{21}$-*b*-PPiGA$_{20}$	49	4.2	1.7	1.08	4.4
PPO$_{47}$-*b*-PPiGA$_{14}$	23	4.7	2.5	1.18	5.0
PPO$_{47}$-*b*-PPiGA$_{25}$	35	6.4	2.3	1.25	6.7
PPiGA$_{20}$	100	3.0	1.1	1.03	3.3
PPiGA$_{24}$	100	3.5	1.4	1.03	3.9

[a] Composition and molecular weights determined by ^{1}H NMR (400 MHz, C*D*Cl$_3$). [b] Determined by SEC (DMF, PEO-calibration).

As seen in Table 5.16, the four PPO-*b*-PDEGAO copolymers gave little KHI performance with the average T_o values being only a little lower than pure water. The poly (*N*, *N*-diethyl glycidyl amine *N*-oxide) part in PPO-*b*-PDEGAO copolymers probably gave negligible effect on the KHI performance as PPO$_{21}$-*b*-PDEGAO$_{12}$ with 12 units of *N*, *N*-diethyl glycidyl amine *N*-oxide gave no better (p-value > 0.05 from t-test) KHI performance than PPO$_{21}$-*b*-PDEGAO$_6$ with six units of *N*, *N*-diethyl glycidyl amine *N*-oxide. Also, compared to PPO$_{47}$-*b*-PDEGAO$_{11}$, more units of *N*, *N*-diethyl glycidyl amine *N*-oxide in PPO$_{47}$-*b*-PDEGAO$_{20}$ did not increase its KHI performance. However, more percentage of the poly (propylene oxide) part in the PPO-*b*-PDEGAO copolymers may benefit the KHI performance as PPO$_{47}$-*b*-PDEGAO$_{11}$ gave significantly better (p-value < 0.05 from t-test) KHI performance than PPO$_{21}$-*b*-PDEGAO$_{12}$.

The PPO-*b*-PPiGAO copolymer series gave remarkable KHI performance, and among which PPO$_{47}$-*b*-PPiGAO$_{14}$ performed the best. This means that both the poly (propylene oxide) part and the poly (piperidine glycidyl amine *N*-oxide) part, especially the latter, in the PPO-*b*-PPiGAO copolymers contributed to the better KHI performance. This may be because that the cyclic piperidine ring can disturb the water structure efficiently or the 6-membered ring is the suitable size to enter the open $5^{12}6^4$ cavity of sII hydrate, thus inhibiting the gas hydrate formation.[133] More units of propylene oxide in PPO-*b*-PPiGAO copolymers led to better KHI performance. However, the optimum number of the piperidine glycidyl amine *N*-oxide units in the PPO-*b*-PPiGAO copolymers or the PPiGAO homopolymers to give the best KHI performance may be between 3 and 20, as either without PPiGAO unit or with more than 20 units of PPiGAO led to worse KHI performance.

None of the amine *N*-oxide polymers at 2500 ppm in this study had a cloud point when heating up to 95 °C. Also, when heated up to 95 °C, the best amine *N*-oxide homopolymer $PPiGAO_{20}$ gave no cloud point even in 15 wt.% (150 000 ppm) sodium chloride solution. The excellent compatible property of $PPiGAO_{20}$ with sodium chloride solution gave it the potential to be applied in high-salinity- and high-temperature-produced fluids.

Table 5. 16 Summary of the KHI performance results of each amine *N*-oxide polymer at 2500 ppm from SCC tests. Average of 10 tests. The deviations were calculated by using the formula of STDEV.S in Excel.

Name	**T_o (av.) ± deviation (°C)**	**ΔT (av.) at T_o (°C)**	**T_a (av.) (°C)**	**T_o (av.) - T_a (av.) (°C)**
DIW	16.6 ± 0.6	3.8	16.5	0.1
PVCap	10.4 ± 0.4	9.8	9.9	0.5
PPO_{21}-*b*-$PDEGAO_6$	15.2 ± 0.7	5.2	15.1	0.1
PPO_{21}-*b*-$PDEGAO_{12}$	15.7 ± 0.7	4.7	15.6	0.1
PPO_{47}-*b*-$PDEGAO_{11}$	14.9 ± 0.5	5.5	14.8	0.1
PPO_{47}-*b*-$PDEGAO_{20}$	14.8 ± 0.5	5.6	14.7	0.1
PPO_{21}-*b*-$PPiGAO_3$	12.5 ± 0.5	7.8	11.1	1.4
PPO_{21}-*b*-$PPiGAO_{13}$	10.6 ± 0.1	9.6	10.0	0.6
PPO_{21}-*b*-$PPiGAO_{20}$	11.3 ± 0.5	8.9	10.8	0.5
PPO_{47}-*b*-$PPiGAO_{14}$	9.8 ± 0.3	10.4	9.7	0.1

PPO_{47}-*b*-$PPiGAO_{25}$	10.8 ± 0.2	9.4	10.6	0.2
$PPiGAO_{20}$	9.9 ± 0.3	10.3	8.7	1.2
$PPiGAO_{24}$	11.4 ± 0.2	8.8	10.3	1.1

The KHI performance of one of the best amine *N*-oxide polymers $PPiGAO_{24}$ was tested at different concentrations ranging from 1250 to 7500 ppm. The average T_o values of $PPiGAO_{24}$ almost decreased linearly when the concentration increased from 1250 to 5000 ppm. The KHI performance of $PPiGAO_{24}$ only improved a little when the concentration increased from 5000 to 7500 ppm. (Figure 5.18)

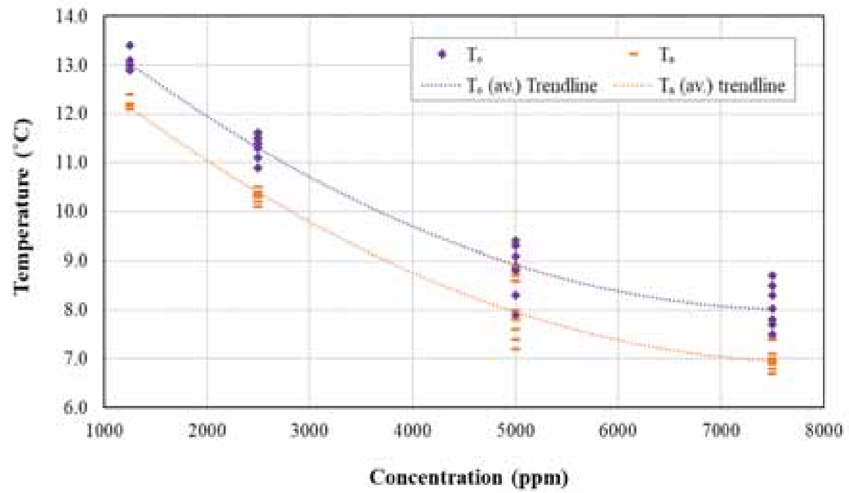

Figure 5. 18 Results of KHI performance tests for $PPiGAO_{24}$ at different concentrations.

5.9 Paper IX: Zwitterionic Poly (sulfobetaine methacrylate)s as Kinetic Hydrate Inhibitors

Zwitterionic poly (sulfobetaine methacrylate)s (PSBMAs) are a series of ultralow biofouling polymers that have been widely used in nanomedicine, biomaterial and healthcare applications.[246-248] Also, the sulfonate anions and amine cations in PSBMAs make them have the properties of superior hydrophilicity as well as antipolyelectrolyte effect.[249-253] One of the limitations of traditional amide-based KHI polymers is the low cloud point or poor water solubility in high concentrated brine solution.[254-256] PSBMAs may have the potential to conquer this limitation and become a new series of environmentally friendly KHIs.

Past studies showed that the size of the alkyl pendant groups is important to the inhibition performance of a KHI polymer and the general assumption is that the increased size of alkyl groups (or hydrophobicity) leads to improved KHI performance as long as the KHI polymer is kept water-soluble.[165, 220, 231] However, the reported alkylated polymers are usually water-insoluble if there are more than four carbon atoms in the alkyl group. Low molecular weight hyperbranched polyethyleneimine-alkyl-amine oxides (HPEI-alkyl-AO) with *iso*-hexyl or *tert*-hexyl groups were reported to be water-soluble, and they gave remarkable KHI performance, but the HPEI-(*n*-hexyl)-AO with *n*-hexyl pendant groups was water-insoluble.[202] The excellent hydrophilicity of PSBMAs may render the polymers with long *n*-alkyl groups water-soluble,[204] thus make it possible to compare the KHI performance of PSBMA polymers with different *n*-alkyl groups.

We synthesized zwitterionic 3-((2-methacryloyloxyethyl)(methyl)(*n*-butyl)ammonio)propane-1-sulfonate, 3-((2-methacryloyloxyethyl)(methyl)(*n*-pentyl)ammonio)propane-1-sulfonate, 3-((2-methacryloyloxyethyl)(methyl)(*n*-hexyl)ammonio)propane-1-sulfonate, and 3-((2-

methacryloyloxyethyl)(dipentyl)ammonio)propane-1-sulfonate homopolymers abbreviated as P4, P5, P6 and P55 respectively. Copolymers containing different molar ratios of 3-((2-methacryloyloxyethyl)(methyl)(*n*-hexyl)ammonio)propane-1-sulfonate monomer units and *N*-isopropylmethacrylamide (NIPMAM) monomer units were also synthesized. (Figure 5.19 and Table 5.17) These homopolymers and copolymers were investigated as KHIs using the SNG mixture.

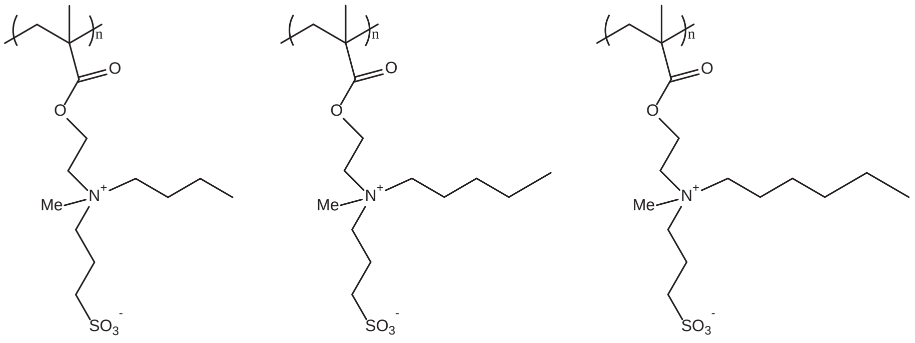

(P4) (P5) (P6)

Figure 5. 19 Structures of zwitterionic 3-((2-methacryloyloxyethyl)(methyl)(*n*-alkyl)ammonio)propane-1-sulfonate homopolymers with *n*-butyl, *n*-pentyl and *n*-hexyl groups.

Table 5. 17 Summary of characterization results of zwitterionic polymers.

Polymer	**Monomer(s)**	**Synthesis Method** [a]	**Polymer's Molecular Characteristics**	**T_{CI} (3 wt.%)** [e]	**T_{CI} (1 wt.%)** [e]
P4	M4	RAFT	$M_{n,\mathrm{SEC}}$ = 3.4 kDa; $Đ$ = 3.80 [b]	Soluble	Soluble
P5	M5	RAFT	$M_{n,\mathrm{SEC}}$ = 2.3 kDa; $Đ$ = 4.69 [b]	51 °C	NA

P6-1	M6	RAFT	$M_{n,\mathrm{SEC}}$ = 7.5 kDa; $Đ$ = 3.51 [b]	18 °C	NA
P6-2	M6	RAFT	[η] = 0.116 dL/g [c]	14 °C	18 °C
P6-3	M6	RAFT	[η] = 0.166 dL/g [c]	15 °C [f]	21 °C [f]
P6-4	M6	AIBN	[η] = 0.442 dL/g [c]	10 °C	11 °C
P55	M55	AIBN	$M_{n,\mathrm{SEC}}$ = 64.9 kDa; $Đ$ = 2.36 [d] [η] = 0.490 dL/g [c]	NA	37 °C
PCO-1	M6 + NIPMAM	AIBN	[η] = 0.350 dL/g [c]	NA	27 °C
PCO-2	M6 + NIPMAM	AIBN	[η] = 0.286 dL/g [c]	NA	30 °C

[a] RAFT: reversible addition-fragmentation chain transfer polymerization; AIBN: α,α'-azobisisobutyronitrile (AIBN)-initiated conventional free radical polymerization. [b] Determined by an aqueous SEC system relative to PEO standards. [c] Intrinsic viscosity in 2,2,2-trifluoroethanol at 25 °C determined using the Wolf method.[257, 258] [d] Determined by a DMF SEC system relative to polystyrene standards. [e] T_{Cl}: cloud point in Milli-Q water determined by visual inspection. [f] P6-3 exhibited a broad LCST transition in water upon heating.

As shown in Table 5.18, comparing the polymers synthesized from the RAFT method, the KHI performance of the zwitterionic 3-((2-methacryloyloxyethyl)(methyl)(*n*-alkyl)ammonio)propane-1-sulfonate homopolymers increased as the size of the alkyl groups increased from C_4 to C_5 to C_6. This maybe further confirm the hydrophobic group-gas molecule competition inhibiting mechanism that has been discussed in Section 5.3. P6-1, P6-2 and P6-3 were all made from the same zwitterionic 3-((2-methacryloyloxyethyl)(methyl)(*n*-hexyl)ammonio)propane-1-sulfonate monomers using the same RAFT method, thus they gave quite similar KHI performance. The KHI performance of P6-4 made by the AIBN method was a little, but statistically significantly, worse ($p<0.05$ from *t*-test) than P6-1, P6-2 and

P6-3 made by the RAFT method. This maybe because of the high molecular weight reflected by the intrinsic viscosity or the different end cap group of P6-4. Studies showed that both molecular weight and end cap group of a polymer could affect its KHI performance.[198, 259] P55 with *N*-di-*n*-pentyl groups gave no better KHI performance than P5 with *N*-*n*-pentyl groups. The extra *n*-pentyl group could maybe increase the KHI performance of P55, but the high molecule weight or different end cap group probably decreases the KHI performance of P55, thus no increased or decreased performance was observed as a result. Both PCO-1 and PCO-2 copolymers gave better KHI performance than homopolymer P6-4 synthesized by the same AIBN polymerisation method.

Table 5. 18 Summary of KHI performance results from SCC tests of polymers at 2500 ppm, as well as their cloud points (T_{Cl}). Average of 10 tests. The deviations were calculated by using the formula of STDEV.S in Excel.

Name	**Monomer(s)**	**T_{Cl} (ºC) (1 wt.%)**	**T_o (av.) ± deviation (°C)**	**T_a (av.) (°C)**	**T_o (av.) − T_a (av.) (°C)**
DIW			16.9 ± 0.7	16.8	0.1
PVCap		31	11.2 ± 0.1	10.6	0.6
P4	M4	>90	14.0 ± 0.2	13.6	0.4
P5	M5	>51	12.1 ± 0.1	11.8	0.3
P6-1	M6	>18	11.6 ± 0.3	11.3	0.3
P6-2	M6	18	11.6 ± 0.3	11.3	0.3
P6-3	M6	21	11.0 ± 0.2	10.5	0.5
P6-4	M6	11	12.0 ± 0.1	11.8	0.2
P55	M55	37	12.2 ± 0.4	11.9	0.3
PCO-1	M6 (58%) + NIPMAM (42%)	27	10.4 ± 0.3	10.3	0.1
PCO-2	M6 (56%) + NIPMAM (44%)	30	11.5 ± 0.3	11.4	0.1

We further tested the KHI performance of P6-1, P6-3 and PCO-1 at different concentrations. (Figure 5.20) The increased concentrations from 1500 to 5000 ppm led to the increased KHI performance of P6-1 and P6-3. However, when the concentration increased from 5000 to 7500 ppm, the KHI performance of P6-1 and P6-3 did not get increased. This may be because molecular micelles were formed in the solution of the zwitterionic polymers at high concentrations, so the number of the active polymer molecules was kept stable.[260, 261] The KHI performance of PCO-1 increased when the concentration increased from 1500 to 7500 ppm.

Also, the improvement of PCO-1 with increasing concentration was much greater than the zwitterionic homopolymers. In addition to amine and amine oxide polymers, many other non-amide based KHI polymers, e.g., polyvinylsulphonamides, poly (alkylethylenephosphonate)s and cationic polymers, also gave a relatively small increase in KHI performance at increasing concentration compared to amide polymers.[164, 200, 239, 262] We speculate that the strong hydrogen-bonding groups, such as amide, amine, and amine oxide groups, maybe lead to better water perturbation and/or, hydrate particle growth inhibition. Thus, it appears that strong hydrogen-bonding groups in KHI polymers are a necessity for reaching very high sub-cooling performance when relatively high dosages are applied.

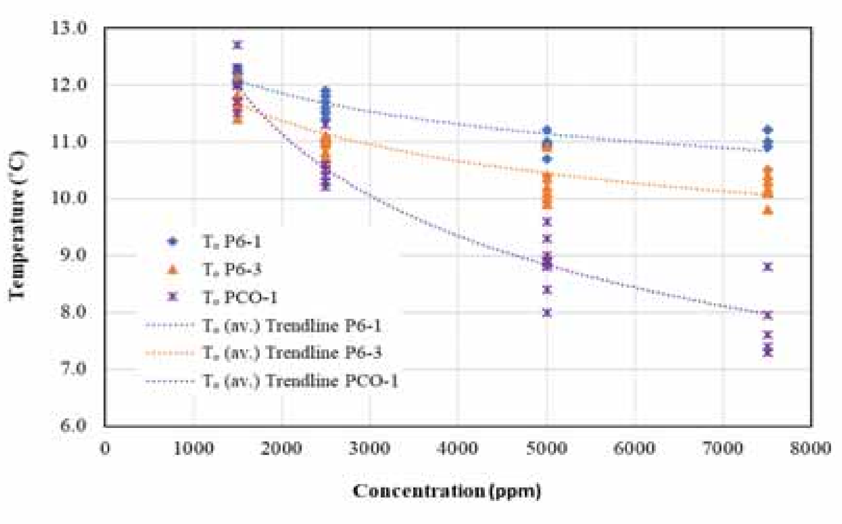

Figure 5. 20 The KHI performance of P6-1, P6-3 and PCO-1 at different concentrations.

5.10 Paper X: High Cloud Point Polyvinylaminals as Non-amide Based Kinetic Gas Hydrate Inhibitors

Polyvinylamine (PVAm) is a kind of desirable intermediate polymer as it has high chemical reactivity due to the primary amine functional groups in it.[263-265] Previously, a series of poly (vinylalkanamide)s have been synthesized from PVAm in our laboratory, and these poly (vinylalkanamide)s with long pendant alkyl groups, such as isopropyl and *n*-propyl groups, gave excellent KHI performance.[221] However, the poly (vinylalkanamide)s with the pendant alkyl groups containing four or more carbon atoms became water-insoluble. We believe hydrophobic alkyl groups larger than propyl group can give improved KHI performance.[190, 220] Polyvinylaminals have been reported to be easily made from PVAm with aldehydes using the one-step process.[263, 266] Polyvinylaminals have aminal (or aminoacetal) groups with secondary amine groups which offer the possibility of great hydrophilicity, thus they maybe allow the polymers with long sized alkyl groups to be water-soluble.

Therefore, we synthesized a series of polyvinylaminals with chain or cyclic alkyl groups from PVAms and the corresponding aldehydes. (Figure 5.21) The synthesized polyvinylaminals were investigated as THF hydrate crystal growth inhibitors as well as KHIs using SNG mixture in both sapphire and steel rocking cells.

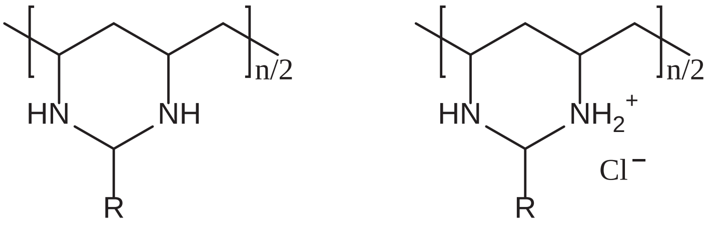

Figure 5. 21 Structures of polyvinylaminals (left) and protonated polyvinylaminals in acidic solution. R = chain or cyclic alkyl group.

As can be seen in Table 5.19, all the polyvinylaminals gave considerable performance in inhibiting the crystal growth of THF hydrate at pH 7. Some of the polyvinylaminals were also tested at pH 3, and results showed that the inhibition performance improved a little when in the acidic solutions. Perhaps for this polyvinylaminal series, some of the protonated quaternary ammonium groups in the polymers can only give a minor advantage for inhibiting THF hydrate growth. (Figure 5.21) The polyvinylaminals with pendant *n*-butyl and cyclohexyl groups gave the best inhibition performance. Also, the inhibition performance of the best polyvinylaminals were tested at both 4000 and 2000 ppm, and results showed that the polyvinylaminals at the higher concentration gave lower growth rates as well as more and thinner hexagonal plates in general.

Table 5. 19 Summary results of THF hydrate crystal growth tests. All polyvinylaminals made from the polyvinylamine with *Mw* = 10000 g/mole.

Polyvinylaminal	**Concn. (ppm)**	**pH**	**Rate (g/h)**	**Crystal shape**
No additive		7	1.59	Rhombic
No additive		3	1.30	Rhombic
Tetrabutylammonium bromide	4000	7	0.45	Distorted rhombic
Tetrapentylammonium bromide	4000	7	0.04	Very distorted
Polyvinylamine, *Mw* 10000 g/mole	4000	7	1.81	Rhombic
Polyvinylaminal, R= *n*-Propyl	4000	6.5	0.72	Rhombic
Polyvinylaminal, R = *n*-Butyl	2000	3	0.80	Mostly rhombic
Polyvinylaminal, R = *n*-Butyl	4000	7	0.34	Hexagonal plates
Polyvinylaminal, R = *n*-Butyl	4000	3	0.23	Hexagonal plates
Polyvinylaminal, R = *n*-Pentyl	2000	3	1.25	Rhombic crystals + hexagonal plates
Polyvinylaminal, R = *n*-Pentyl	4000	7	0.65	Rhombic crystals + hexagonal plates
Polyvinylaminal, R = *n*-Pentyl	4000	3	0.38	Hexagonal plates
Polyvinylaminal, R = Cyclopentyl	4000	7	0.58	Rhombic crystals + Hexagonal plates
Polyvinylaminal, R = Cyclohexyl	4000	7	0.39	Hexagonal plates
Polyvinylaminal, R = Cyclohexyl	4000	3	0.33	Hexagonal plates

Table 5.20 summarized the KHI performance of the polyvinylaminals from SCC tests using SNG mixture in both steel and sapphire cells. The reason why we used two types of cells is because that one rig needed maintenance, and we had to move to the other one to continue our study. The maximum inner volume of the sapphire cells was 20 mL, and 10 mL solution was loaded into each sapphire cell to keep the same ratio of

gas/solution volume (50/50) as was the case with the steel cells. The results obtained from both rigs generally agreed quite well within a 95% confidence limit when using the same solutions. As shown in Table 5.20, the KHI performance of the polyvinylaminals with pendant alkyl groups generally increased when the carbon atoms in the alkyl groups increased from 3 to 4 to 5 to 6. The branched *iso*-pentyl groups improved the KHI performance even more compared to the *n*-pentyl groups, which has been reported in previous studies.[150, 177] This indicates that the *iso*-pentyl group may be able to give a better interaction with the water structure, thus rendering a better inhibition effect. The best polyvinylaminal with pendant cyclohexyl groups gave KHI performance almost as good as the famous commercial PVCap. Many polymers with cyclohexyl groups, such as poly (ethylene citramide), polytartramide and hyperbranched poly (ester amide), were reported to give excellent KHI performance.[267-269] This may be because the cyclohexyl group has good interaction with the water structure as well as its possibility to form sII hydrate.[270] The polyvinylaminals in acidic solution gave slightly worse KHI performance than that in neutral solution, and this may be because that the protonation of the amine groups made the polymers less hydrophobic. Similar to many other KHI polymer series,[118, 193, 220] the higher concentration of the polyvinylaminals led to better KHI performance. The presence of two amine groups per hydrophobic group give good hydrogen-bonding possibilities to the bulk water or hydrate particle surfaces. This ability is good for high performance at increasing KHI dosages, as discussed in Paper IX.

Table 5. 20 Summary results from SCC tests. Average of 6 tests unless otherwise stated. All polyvinylaminals made from the polyvinylamine with *Mw* = 10000 g/mole.

Polyvinylaminal	**Concn. (ppm)**	**pH**	**T_o (av.) (°C)**	**T_a (av.) (°C)**	**Cell type**
No additive		7.0	17.1	16.6	Steel

No additive		7.0	16.8	16.4	Sapphire
PVP K-15, *Mw* 8000 g/mole	2500	7.0	11.6	10.9	Sapphire
PVP K-15, *Mw* 8000 g/mole	2500	7.0	11.1	9.9	Steel
PVCap, *Mw* 10000 g/mole	2500	7.0	9.6	9.2	Steel
PVCap, *Mw* 10000 g/mole	2500	7.0	9.9	8.9	Sapphire
Polyvinylamine, *Mw* 10000 g/mole	2500		16.9	16.8	Sapphire
Polyvinylaminal, R = *n*-Propyl	2500	6.5	15.1	15.0	Sapphire
Polyvinylaminal, R = *iso*-Butyl	2500	6.5	11.6	11.2	Steel
Polyvinylaminal, R = *iso*-Butyl	2500	6.5	11.8	11.5	Sapphire
Polyvinylaminal, R = *iso*-Butyl	5000	6.5	10.0	9.7	Sapphire
Polyvinylaminal, R = *tert*-Butyl	2500	6.5	15.2	15.1	Sapphire
Polyvinylaminal, R = *n*-Butyl	2500	6.5	11.8	11.7	Sapphire
Polyvinylaminal, R = *n*-Butyl	2500	2.9	11.5	11.4	Sapphire
Polyvinylaminal, R = *n*-Pentyl	2500	6.5	11.9	11.8	Sapphire
Polyvinylaminal, R = *iso*-Pentyl (8 tests)	2500	6.5	10.3	10.0	Steel
Polyvinylaminal, R = Cyclopentyl	2500	6.5	11.6	11.5	Sapphire
Polyvinylaminal, R = Cyclohexyl	2500	6.5	9.8	9.4	Steel
Polyvinylaminal, R = Cyclohexyl	2500	6.5	10.4	10.2	Sapphire
Polyvinylaminal, R = Cyclohexyl	2500	3.1	11.2	10.8	Sapphire
Polyvinylaminal, R = Cyclohexyl	5000	6.5	7.0	6.5	Steel
Polyvinylaminal, R = Cyclohexyl	5000	6.5	7.6	7.1	Sapphire

6 Conclusions and Future Work

In the work presented in this thesis, the kinetic hydrate inhibition performance of various amide based and non-amide based polymers has been reported. The inhibition performance of amide based KHI polymers, i.e., *N*-alkyl-*N*-vinylamide polymers, 3-methylene-2-pyrrolidone polymers, poly (*N*-vinyl caprolactam) and poly (*N*-isopropyl methacrylamide), has been improved. In addition, several categories of non-amide polymers, including polyvinylsulphonamides, polyamine oxides, poly (sulfobetaine methacrylate)s and polyvinylaminals, were investigated as KHIs. The work made a better understanding of the inhibition mechanisms of KHIs, which is also beneficial for designing high-performance KHIs for future work.

6.1 Main Conclusions

The main conclusions of the work that have been done during my PhD study period can be summarized as follows.

1. Non-amide polymers, such as polyvinylsulphonamides, polyamine oxides, poly (sulfobetaine methacrylate)s, and polyvinylaminals, can be efficient KHIs. In addition, most of the non-amide KHI polymers gave high cloud points.
2. The inhibition performance of KHI polymers including both amide and non-amide polymers largely depends on the size of the hydrophobic alkyl groups connected directly or close to the functional groups, such as amide, amine oxide, sulphonamide, and amine groups. Generally, as long as the alkylated polymers maintained to be water-soluble, the more carbon atoms in the alkyl groups (up to 6), the more split branches at the end of the chain alkyl groups (*iso*- or *tert*-), and the larger size of the cyclic alkyl or heterocyclic groups (up to 6-membered ring) led to better inhibition performance.

3. The KHI polymers containing strong hydrogen-bonding functional groups, e.g., amide, amine and amine oxide groups, gave more increase in the inhibition performance with increasing concentration, compared to polyvinylsulphonamides and poly (sulfobetaine methacrylate)s.
4. The effective synergist solvent can be chosen according to the structure of a KHI polymer, as usually a better synergistic effect has been found with having one chemical with a straight alkyl chain and one with a branched or cyclic alkyl group.
5. The inhibition performance of KHI polymers with different end cap functional groups in the polymer molecules can vary. Mercaptoacetic acid end-capping group increased the inhibition performance of PVCap and PNIPMAM, while 4-mercaptobenzoic acid end-capping group decreased the performance of PVCap and PNIPMAM for both sI and sII gas hydrates. However, mercaptosuccinic acid end-capping group only increased the performance of PVCap and PNIPMAM for sII gas hydrate but had little effect on sI gas hydrate.
6. Apart from synthesizing KHI polymers from their corresponding monomers, making efficient KHIs from other readily available polymeric starting materials can be an alternative entry point, e.g., the acrylamide-based polymers from poly (acrylic acid)s, the alkylated polyamine oxides from polyethyleneimine and the polyvinylaminals from polyvinylamines. In addition, the KHI polymers from the same starting polymeric materials gave the same polymer backbone and number of monomer units, which allowed us to focus on comparing the effects of the alkyl groups.

6.2 Future Work

Based on the results and conclusions from the work presented in this thesis, future work can be carried out as follows.

1. As the polymers with 6-membered rings gave better inhibition performance than that with 5-membered rings, to expand the ring size from 6 to 7 or even 8-membered may increase the performance. This is particularly feasible for the poly (glycidyl amine *N*-oxide) series, because the superior solubility of this type of polymer may make the poly (glycidyl amine *N*-oxide)s with large rings water-soluble.
2. More types of end-capping groups can be introduced to modify PVCap and PNIPMAM. In addition, the end-capping groups with good effects can be used to modify other classes of KHI polymers.
3. Methacrylamide-based polymers failed to synthesize directly from poly (methacrylic acid)s or poly (methyl methacrylate)s, but it is possible to make them from poly (thiomethacrylate)s via the amidation reaction. This method is worth trying because methacrylamide-based polymers were reported to be better KHIs than the equivalent acrylamide-based ones.
4. The work presented on *N*-alkyl-*S*-vinylsulphonamide polymer series was just our initial results, so it is interesting to continue the study of the reversed *N*-vinyl-*S*-alkyl sulphonamide polymers to check if reversed sulphonamide polymers have improved properties such as solubility and KHI performance.
5. Copolymerisation, as well as the addition of synergists, including solvents, salts or polymers, could be investigated to further improve the inhibition performance of non-amide based polymer series, such as polyvinylsulphonamides, polyamine oxides, poly (sulfobetaine methacrylate)s, and polyvinylaminals.
6. If possible to synthesis, amide based polymers and amine oxide-based polymers with otherwise similar structures could be investigated to compare the different effects in KHI performance between the two hydrogen-bonding functional groups.

7 References

1. Sloan, E. D.; Koh, C. A., *Clathrate hydrates of natural gases. 3rd Ed.* CRC Press: Boca Raton, Florida, 2008.
2. Hammerschmidt, E., Formation of gas hydrates in natural gas transmission lines. *Industrial & Engineering Chemistry* **1934,** *26* (8), 851-855.
3. Sloan, E. D., *Natural gas hydrates in flow assurance*. Gulf Professional Publishing: 2010.
4. Kelland, M. A., *Production Chemicals for the Oil and Gas Industry. 2nd Ed.* CRC Press: Boca Raton, Florida, 2014; p 219-245.
5. Carroll, J., *Natural gas hydrates: a guide for engineers*. Gulf Professional Publishing: 2014.
6. Jr, E. D. S., Fundamental principles and applications of natural gas hydrates. *Nature* **2003,** *426*.
7. Arjmandi, M.; Tohidi, B.; Danesh, A.; Todd, A. C., Is subcooling the right driving force for testing low-dosage hydrate inhibitors? *Chemical Engineering Science* **2005,** *60* (5), 1313-1321.
8. Kelland, M. A., History of the Development of Low Dosage Hydrate Inhibitors. *Energy & Fuels* **2006,** *20* (3), 825-847.
9. Perrin, A.; Musa, O. M.; Steed, J. W., The chemistry of low dosage clathrate hydrate inhibitors. *Chem Soc Rev* **2013,** *42* (5), 1996-2015.
10. Wang, Y.; Fan, S.; Lang, X., Reviews of gas hydrate inhibitors in gas-dominant pipelines and application of kinetic hydrate inhibitors in China. *Chinese Journal of Chemical Engineering* **2019,** *27* (9), 2118-2132.
11. Englezos, P., Clathrate hydrates. *Industrial & engineering chemistry research* **1993,** *32* (7), 1251-1274.
12. Gudmundsson, J.; Borrehaug, A. In *Frozen hydrate for transport of natural gas*, NGH 96: 2nd international conference on natural gaz hydrates (Toulouse, June 2-6, 1996), 1996; pp 415-422.
13. Maslin, M.; Owen, M.; Betts, R.; Day, S.; Dunkley Jones, T.; Ridgwell, A., Gas hydrates: Past and future geohazard? *Philosophical Transactions of the Royal Society A: Mathematical, Physical Engineering Sciences* **2010,** *368* (1919), 2369-2393.

14. Steed, J.; Atwood, J., Molecular guests in solution. In *Supramolecular chemistry, 2nd ed.*, Wiley: London, 2009.

15. Ginsburg, G.; Soloviev, V., Submarine gas hydrates. Translated from Russian. Norma Publishers, St. Petersburg, Russia: 1998.

16. Kvenvolden, K. A., Gas hydrates—geological perspective and global change. *Reviews of geophysics* **1993,** *31* (2), 173-187.

17. Subramanian, S.; Kini, R. A.; Dec, S. F.; Jr, E. D. S., Evidence of structure II hydrate formation from methane + ethane mixtures. *Chemical Engineering Science* **2000,** *55*, 1981-1999.

18. Hester, K. C.; Sloan, E. D., sII Structural Transitions from Binary Mixtures of Simple sI Formers. *International Journal of Thermophysics* **2005,** *26* (1), 95-106.

19. Staykova, D. K.; Hansen, T.; Salamatin, A. N.; Kuhs, W. F. In *Kinetic diffraction experiments on the formation of porous gas hydrates*, Proc. 4th Int. Conf. Gas Hydrates, 2002.

20. Lu, H.; Seo, Y.-t.; Lee, J.-w.; Moudrakovski, I.; Ripmeester, J. A.; Chapman, N. R.; Coffin, R. B.; Gardner, G.; Pohlman, J., Complex gas hydrate from the Cascadia margin. *Nature* **2007,** *445* (7125), 303-306.

21. Zhang, X.; Du, Z.; Luan, Z.; Wang, X.; Xi, S.; Wang, B.; Li, L.; Lian, C.; Yan, J. J. G., Geophysics, Geosystems, In situ Raman detection of gas hydrates exposed on the seafloor of the South China Sea. **2017,** *18* (10), 3700-3713.

22. Schicks, J. M.; Naumann, R.; Erzinger, J.; Hester, K. C.; Koh, C. A.; Sloan, E. D., Jr., Phase transitions in mixed gas hydrates: experimental observations versus calculated data. *J Phys Chem B* **2006,** *110* (23), 11468-74.

23. Ohno, H.; Moudrakovski, I.; Gordienko, R.; Ripmeester, J.; Walker, V. K., Structures of Hydrocarbon Hydrates during Formation with and without Inhibitors. *Journal of Physical Chemistry A* **2012,** *116* (5), 1337-1343.

24. Walsh, M. R.; Koh, C. A.; Sloan, E. D.; Sum, A. K.; Wu, D. T., Microsecond Simulations of Spontaneous Methane Hydrate Nucleation and Growth. *science* **2009,** *326*, 1095-1098.

25. Vatamanu, J.; Kusalik, P. G., Unusual crystalline and polycrystalline structures in methane hydrates. *J. Am. Chem. Soc.* **2006,** *128* (49), 15588-15589.

26. Nguyen, A. H.; Jacobson, L. C.; Molinero, V., Structure of the clathrate/solution interface and mechanism of cross-nucleation of clathrate hydrates. *The Journal of Physical Chemistry C* **2012,** *116* (37), 19828-19838.

27. Guo, G.-J.; Zhang, Y.-G.; Liu, C.-J.; Li, K.-H., Using the face-saturated incomplete cage analysis to quantify the cage compositions and cage linking structures of amorphous phase hydrates. *Physical Chemistry Chemical Physics* **2011,** *13* (25), 12048-12057.

28. Liang, S.; Kusalik, P. G., Communication: Structural interconversions between principal clathrate hydrate structures. AIP Publishing LLC: 2015.

29. Schicks, J. M.; Ripmeester, J. A. J. A. C. I. E., The coexistence of two different methane hydrate phases under moderate pressure and temperature conditions: Kinetic versus thermodynamic products. **2004,** *43* (25), 3310-3313.

30. Yoreo, J. D., crystal nucleation: more than one pathway. *Nature Materials* **2013,** *12*, 284-285.

31. Ke, W.; Svartaas, T. M.; Chen, D., A review of gas hydrate nucleation theories and growth models. *Journal of Natural Gas Science and Engineering* **2019,** *61*, 169-196.

32. Warrier, P.; Khan, M. N.; Srivastava, V.; Maupin, C. M.; Koh, C. A., Overview: Nucleation of clathrate hydrates. *The Journal of chemical physics* **2016,** *145* (21), 211705.

33. Fletcher, N., Size effect in heterogeneous nucleation. *The Journal of chemical physics* **1958,** *29* (3), 572-576.

34. Garten, V.; Head, R., Homogeneous nucleation and the phenomenon of crystalloluminescence. *Philosophical Magazine* **1966,** *14* (132), 1243-1253.

35. Otpushchennikov, N., Determination of the size of the elementary crystal nucleus from acoustic measurement. *Soviet Phys. Cryst* **1962,** *7*, 237-240.

36. Adamski, T., Commination of crystal nucleation by a precipitation method. *Nature* **1963,** *197* (4870), 894-894.

37. Bai, G.; Gao, D.; Liu, Z.; Zhou, X.; Wang, J., Probing the critical nucleus size for ice formation with graphene oxide nanosheets. *Nature* **2019,** *576* (7787), 437-441.

38. Sloan Jr, E.; Fleyfel, F., A molecular mechanism for gas hydrate nucleation from ice. *AIChE Journal* **1991,** *37* (9), 1281-1292.

39. CHRISTIANSEN, R. L.; E. DENDY SLOAN, J., Mechanisms and Kinetics of Hydrate Formation. *ANNALS NEW YORK ACADEMY OF SCIENCES* **1994**, 283-305.
40. Kvamme, B. In *A new theory for the kinetics of hydrate formation*, NGH 96: 2nd international conference on natural gaz hydrates (Toulouse, June 2-6, 1996), 1996; pp 139-146.
41. Kvamme, B., A unified nucleation theory for the kinetics of hydrate formation. *Annals of the New York Academy of Sciences* **2000,** *912* (1), 496-501.
42. Guo, G.-J.; Zhang, Y.-G.; Li, M.; Wu, C.-H., Can the dodecahedral water cluster naturally form in methane aqueous solutions? A molecular dynamics study on the hydrate nucleation mechanisms. *The Journal of chemical physics* **2008,** *128* (19), 194504.
43. Koh, C. A.; Wisbey, R. P.; Wu, X.; Westacott, R. E.; Soper, A. K., Water ordering around methane during hydrate formation. *The Journal of Chemical Physics* **2000,** *113* (15), 6390-6397.
44. Zhang, J. F.; Hawtin, R. W.; Yang, Y.; Nakagava, E.; Rivero, M.; Choi, S. K.; Rodger, P. M., Molecular dynamics study of methane hydrate formation at a water/methane interface. *Journal of Physical Chemistry B* **2008,** *112* (34), 10608-10618.
45. Hawtin, R. W.; Quigley, D.; Rodger, P. M., Gas hydrate nucleation and cage formation at a water/methane interface. *Physical Chemistry Chemical Physics* **2008,** *10* (32), 4853-4864.
46. Radhakrishnan, R.; Trout, B. L., A new approach for studying nucleation phenomena using molecular simulations: application to CO 2 hydrate clathrates. *The Journal of chemical physics* **2002,** *117* (4), 1786-1796.
47. Moon, C.; Taylor, P. C.; Rodger, P. M., Molecular dynamics study of gas hydrate formation. *J. Am. Chem. Soc.* **2003,** *125* (16), 4706-4707.
48. Jacobson, L. C.; Hujo, W.; Molinero, V., Amorphous precursors in the nucleation of clathrate hydrates. *J. Am. Chem. Soc.* **2010,** *132* (33), 11806-11811.
49. Jacobson, L. C.; Hujo, W.; Molinero, V., Nucleation pathways of clathrate hydrates: effect of guest size and solubility. *The Journal of Physical Chemistry B* **2010,** *114* (43), 13796-13807.
50. Lauricella, M.; Meloni, S.; English, N. J.; Peters, B.; Ciccotti, G., Methane clathrate hydrate nucleation mechanism by advanced

molecular simulations. *The Journal of Physical Chemistry C* **2014,** *118* (40), 22847-22857.

51. Walsh, M. R.; Rainey, J. D.; Lafond, P. G.; Park, D.-H.; Beckham, G. T.; Jones, M. D.; Lee, K.-H.; Koh, C. A.; Sloan, E. D.; Wu, D. T., The cages, dynamics, and structuring of incipient methane clathrate hydrates. *Physical Chemistry Chemical Physics* **2011,** *13* (44), 19951-19959.

52. Vatamanu, J.; Kusalik, P. G., Observation of two-step nucleation in methane hydrates. *Physical Chemistry Chemical Physics* **2010,** *12* (45), 15065-15072.

53. Yin, Z.; Khurana, M.; Tan, H. K.; Linga, P., A review of gas hydrate growth kinetic models. *Chemical Engineering Journal* **2018,** *342*, 9-29.

54. Vysniauskas, A.; Bishnoi, P., A kinetic study of methane hydrate formation. *Chemical Engineering Science* **1983,** *38* (7), 1061-1072.

55. Vysniauskas, A.; Bishnoi, P., Kinetics of ethane hydrate formation. *Chemical Engineering Science* **1985,** *40* (2), 299-303.

56. Lekvam, K.; Ruoff, P., A reaction kinetic mechanism for methane hydrate formation in liquid water. *J. Am. Chem. Soc.* **1993,** *115* (19), 8565-8569.

57. Boxall, J.; Davies, S.; Koh, C.; Sloan, E. D., Predicting when and where hydrate plugs form in oil-dominated flowlines. Society of Petroleum Engineers: SPE Projects, Facilities & Construction, 2009; Vol. 4, pp 80-86.

58. Zerpa, L. E.; Sloan, E. D.; Sum, A. K.; Koh, C. A., Overview of CSMHyK: A transient hydrate formation model. *Journal of Petroleum Science and Engineering* **2012,** *98*, 122-129.

59. Yang, D.; Le, L. A.; Martinez, R. J.; Currier, R. P.; Spencer, D. F., Kinetics of CO2 hydrate formation in a continuous flow reactor. *Chemical engineering journal* **2011,** *172* (1), 144-157.

60. Englezos, P.; Kalogerakis, N.; Dholabhai, P.; Bishnoi, P., Kinetics of gas hydrate formation from mixtures of methane and ethane. *Chemical Engineering Science* **1987,** *42* (11), 2659-2666.

61. Englezos, P.; Kalogerakis, N.; Dholabhai, P.; Bishnoi, P., Kinetics of formation of methane and ethane gas hydrates. *Chemical Engineering Science* **1987,** *42* (11), 2647-2658.

62. Skovborg, P.; Rasmussen, P., A mass transport limited model for the growth of methane and ethane gas hydrates. *Chemical Engineering Science* **1994,** *49* (8), 1131-1143.

63. Herri, J.-M.; Pic, J.-S.; Gruy, F.; Cournil, M., Methane hydrate crystallization mechanism from in ‐ situ particle sizing. *AIChE Journal* **1999,** *45* (3), 590-602.

64. Clarke, M. A.; Bishnoi, P. J. C. e. s., Determination of the intrinsic kinetics of CO2 gas hydrate formation using in situ particle size analysis. **2005,** *60* (3), 695-709.

65. Turner, D. J.; Miller, K. T.; Sloan, E. D., Methane hydrate formation and an inward growing shell model in water-in-oil dispersions. *Chemical Engineering Science* **2009,** *64* (18), 3996-4004.

66. Uchida, T.; Ebinuma, T.; Kawabata, J. i.; Narita, H., Microscopic observations of formation processes of clathrate-hydrate films at an interface between water and carbon dioxide. *J. Cryst. Growth* **1999,** *204* (3), 348-356.

67. Mori, Y. H., Estimating the thickness of hydrate films from their lateral growth rates: application of a simplified heat transfer model. *J. Cryst. Growth* **2001,** *223* (1-2), 206-212.

68. Peng, B.; Dandekar, A.; Sun, C.; Luo, H.; Ma, Q.; Pang, W.; Chen, G., Hydrate film growth on the surface of a gas bubble suspended in water. *The Journal of Physical Chemistry B* **2007,** *111* (43), 12485-12493.

69. Mochizuki, T.; Mori, Y. H., Clathrate-hydrate film growth along water/hydrate-former phase boundaries—numerical heat-transfer study. *J. Cryst. Growth* **2006,** *290* (2), 642-652.

70. Mork, M.; Gudmundsson, J. S. In *Hydrate formation rate in a continuous stirred tank reactor: experimental results and bubble-to-crystal model*, 4th International Conference on Gas Hydrates, Citeseer: 2002.

71. Hashemi, S.; Macchi, A.; Servio, P., Gas hydrate growth model in a semibatch stirred tank reactor. *Industrial engineering chemistry research* **2007,** *46* (18), 5907-5912.

72. Bergeron, S.; Servio, P., Reaction rate constant of propane hydrate formation. *Fluid Phase Equilib.* **2008,** *265* (1-2), 30-36.

73. Salamatin, A. N.; Hondoh, T.; Uchida, T.; Lipenkov, V. Y., Post-nucleation conversion of an air bubble to clathrate air–hydrate crystal in ice. *J. Cryst. Growth* **1998,** *193* (1-2), 197-218.

74. Salamatin, A. N.; Kuhs, W. F. In *Formation of porous gas hydrates*, the Fourth International Conference on Gas Hydrates, Yokohama, Yokohama, 2015.

75. Shindo, Y.; Lund, P.; Fujioka, Y.; Komiyama, H., Kinetics of formation of CO2 hydrate. *Energy conversion and management* **1993,** *34* (9-11), 1073-1079.

76. Shindo, Y.; Lund, P. C.; Fujioka, Y.; Komiyama, H., Kinetics and mechanism of the formation of CO2 hydrate. *International journal of chemical kinetics* **1993,** *25* (9), 777-782.

77. Shindo, Y.; Sakaki, K.; Fujioka, Y.; Komiyama, H., Kinetics of the formation of CO2 hydrate on the surface of liquid CO2 droplet in water. *Energy conversion and management* **1996,** *37* (4), 485-489.

78. Lund, P.; Shindo, Y.; Fujioka, Y.; Komiyama, H., Study of the pseudo‐steady‐state kinetics of CO2 hydrate formation and stability. *International Journal of Chemical Kinetics* **1994,** *26* (2), 289-297.

79. Teng, H.; Kinoshita, C.; Masutani, S., Hydrate formation on the surface of a CO2 droplet in high-pressure, low-temperature water. *Chemical Engineering Science* **1995,** *50* (4), 559-564.

80. Dalmazzone, D.; Hamed, N.; Dalmazzone, C., DSC measurements and modelling of the kinetics of methane hydrate formation in water-in-oil emulsion. *Chemical Engineering Science* **2009,** *64* (9), 2020-2026.

81. Freer, E. M.; Selim, M. S.; Sloan Jr, E. D., Methane hydrate film growth kinetics. *Fluid Phase Equilib.* **2001,** *185* (1-2), 65-75.

82. Mu, L.; Li, S.; Ma, Q.-L.; Zhang, K.; Sun, C.-Y.; Chen, G.-J.; Liu, B.; Yang, L.-Y., Experimental and modeling investigation of kinetics of methane gas hydrate formation in water-in-oil emulsion. *Fluid Phase Equilib.* **2014,** *362*, 28-34.

83. Liu, X.; Flemings, P. B., Dynamic multiphase flow model of hydrate formation in marine sediments. *Journal of Geophysical Research: Solid Earth* **2007,** *112* (B3).

84. Moridis, G., User's manual of the TOUGH+ core code v1. 5: A general-purpose simulator of non-isothermal flow and transport through porous and fractured media. **2014**.

85. Zerpa, L. E.; Rao, I.; Aman, Z. M.; Danielson, T. J.; Koh, C. A.; Sloan, E. D.; Sum, A. K., Multiphase flow modeling of gas hydrates with a simple hydrodynamic slug flow model. *Chemical Engineering Science* **2013,** *99*, 298-304.

86. Kim, H.; Bishnoi, P. R.; Heidemann, R. A.; Rizvi, S. S., Kinetics of methane hydrate decomposition. *Chemical engineering science* **1987,** *42* (7), 1645-1653.
87. Bringedal, B.; Ingebretsen, T.; Haugen, K. In *Subsea separation and reinjection of produced water*, Offshore Technology Conference, Offshore Technology Conference: 1999.
88. Talley, L. D.; Turner, D. J.; Priedeman, D. K., Method of generating a non-plugging hydrate slurry. Google Patents: 2013.
89. Lund, A.; Lysne, D.; Larsen, R.; Hjarbo, K. W., Method and system for transporting a flow of fluid hydrocarbons containing water. Google Patents: 2004.
90. Phillips, N. J.; Grainger, M.; Services, T. O., Development and Application of Kinetic Hydrate Inhibitors in the North Sea. In *the 1998 SPE Gas Technology Symposium*, Calgary, Alberta, Canada, 1998.
91. Fu, S.; Cenegy, L.; Neff, C. In *A summary of successful field applications of a kinetic hydrate inhibitor*, SPE international symposium on oilfield chemistry, Society of Petroleum Engineers: 2001.
92. Klomp, U. In *The world of LDHI: From conception to development to implementation*, Proceedings of the 6th International Conference on Gas hydrates, Vancouver, Canada, 2008.
93. Giavarini, C.; Hester, K., *Gas hydrates: Immense energy potential and environmental challenges*. Springer Science & Business Media: 2011.
94. Webber, P. A.; Conrad, P.; Lewis, D.; Jagneaux, R. L. In *Continuous anti-agglomerant LDHI application for deepwater Subsea Tieback: a study on water quality and low water cut scenarios*, Offshore Technology Conference, Offshore Technology Conference: 2012.
95. Webber, P. A. In *Fundamental Understanding on the Effects of Anti-Agglomerants Towards Overboard Water Quality*, Offshore Technology Conference, Offshore Technology Conference: 2010.
96. Sugier, A.; Bourgmayer, P.; Durand, J.-P., Process for delaying the formation and/or reducing the agglomeration tendency of hydrates. Google Patents: 1993.
97. Klomp, U.; Kruka, V.; Reijnhart, R. In *Low dosage hydrate inhibitors and how they work*, Proceedings of the symposium Controlling Hydrates, Waxes and Asphaltenes, IBC Conference, Aberdeen, 1997.

98. Maccioni, F.; Passucci, C.; Milanese, S. In *Torque moment as indicator of low dosage hydrates inhibitors: Effects on multiphase systems. Experimental study on quaternary ammonium and phosphonium compounds*, Proceedings of the 7th International Conference on Gas Hydrates (ICGH 2011), 2011; pp 17-21.

99. Pakulski, M.; Szymczac, S. In *Twelve years of laboratory and field experience for polyether polyamine gas hydrate inhibitors*, Proceedings of international conference on gas hydrates, 2008.

100. Pakulski, M. K., Method for controlling gas hydrates in fluid mixtures. Google Patents: 1998.

101. Lovell, D.; Pakulski, M. In *Hydrate inhibition in gas wells treated with two low dosage hydrate inhibitors*, SPE Gas Technology Symposium, Society of Petroleum Engineers: 2002.

102. Budd, D.; Hurd, D.; Pakulski, M.; Schaffer, T. D. In *Enhanced hydrate inhibition in Alberta gas field*, SPE Annual Technical Conference and Exhibition, Society of Petroleum Engineers: 2004.

103. Pakulski, M. K.; Dawson, J. C., Well service composition and method. Google Patents: 2004.

104. Pakulski, M. K., Method for controlling gas hydrates in fluid mixtures. Google Patents: 2001.

105. Kelland, M. A.; Mady, M. F., Acylamide and Amine Oxide Derivatives of Linear and Hyperbranched Polyethylenimines. Part 1: Comparison of Tetrahydrofuran Hydrate Crystal Growth Inhibition Performance. *Energy & Fuels* **2016,** *30* (5), 3934-3940.

106. Kelland, M. A.; Magnusson, C.; Lin, H.; Abrahamsen, E.; Mady, M. F., Acylamide and Amine Oxide Derivatives of Linear and Hyperbranched Polyethylenimine. Part 2: Comparison of Gas Kinetic Hydrate Inhibition Performance. *Energy & Fuels* **2016,** *30* (7), 5665-5671.

107. Magnusson, C. D.; Kelland, M. A., Nonpolymeric Kinetic Hydrate Inhibitors: Alkylated Ethyleneamine Oxides. *Energy & Fuels* **2015,** *29* (10), 6347-6354.

108. Reyes, F. T.; Guo, L.; Hedgepeth, J. W.; Zhang, D.; Kelland, M. A., First Investigation of the Kinetic Hydrate Inhibitor Performance of Poly(N-alkylglycine)s. *Energy & Fuels* **2014,** *28* (11), 6889-6896.

109. Perfeldt, C. M.; Chua, P. C.; Daraboina, N.; Friis, D.; Kristiansen, E.; Ramløv, H.; Woodley, J. M.; Kelland, M. A.; von Solms, N., Inhibition of gas hydrate nucleation and growth: efficacy of

an antifreeze protein from the longhorn beetle Rhagium mordax. *Energy & Fuels* **2014,** *28* (6), 3666-3672.
110. Zeng, H.; Moudrakovski, I. L.; Ripmeester, J. A.; Walker, V. K., Effect of antifreeze protein on nucleation, growth and memory of gas hydrates. *AIChE journal* **2006,** *52* (9), 3304-3309.
111. Jensen, L.; Thomsen, K.; von Solms, N., Inhibition of structure I and II gas hydrates using synthetic and biological kinetic inhibitors. *Energy & Fuels* **2011,** *25* (1), 17-23.
112. Kelland, M. A., A review of kinetic hydrate inhibitors-Tailor-made water-soluble polymers for oil and gas industry applications. In *Advances in Materials Science Research*, Wytherst, M. C., Ed. Nova Science Publishers Inc.: New York, 2011; Vol. 8.
113. Colle, K. S.; Costello, C. A.; Oelfke, R. H.; Talley, L. D.; Longo, J. M.; Berluche, E. A method for inhibiting hydrate formation. 1996.
114. Colle, K. S.; Costello, C. A.; Talley, L. D.; Oelfke, R. H.; Berluche, E. Method for inhibiting hydrate formation. WO 96/41786. 1996.
115. Klug, P. Method of Inhibiting Gas Hydrate Formation. 6,102,986, 2000.
116. Kelland, M. A.; Kvaestad, A. H.; Astad, E. L., Tetrahydrofuran Hydrate Crystal Growth Inhibition by Trialkylamine Oxides and Synergism with the Gas Kinetic Hydrate Inhibitor Poly(N-vinyl caprolactam). *Energy & Fuels* **2012,** *26* (7), 4454-4464.
117. Kelland, M. A., Tetrahydrofuran hydrate crystal growth inhibition by bis-and tris-amine oxides. *Chemical Engineering Science* **2013,** *98*, 1-6.
118. Reyes, F. T.; Malins, E. L.; Becer, C. R.; Kelland, M. A., Non-amide kinetic hydrate inhibitors: Performance of a series of polymers of isopropenyloxazoline on structure II gas hydrates. *Energy & Fuels* **2013,** *27* (6), 3154-3160.
119. Magnusson, C. D.; Liu, D. J.; Chen, E. Y. X.; Kelland, M. A., Non-Amide Kinetic Hydrate Inhibitors: Investigation of the Performance of a Series of Poly(vinylphosphonate) Diesters. *Energy & Fuels* **2015,** *29* (4), 2336-2341.
120. Sa, J.-H.; Kwak, G.-H.; Lee, B. R.; Park, D.-H.; Han, K.; Lee, K.-H., Hydrophobic amino acids as a new class of kinetic inhibitors for gas hydrate formation. *Scientific Reports* **2013,** *3* (1).

121. Larsen, R.; Knight, C. A.; Sloan Jr, E. D., Clathrate hydrate growth and inhibition. *Fluid Phase Equilib.* **1998,** *150*, 353-360.

122. Klomp, U.; Kruka, V.; Reinjhart, R. In *Low Dosage Inhibitors:(How) Do They Work*, 2nd International Conference on Controlling Hydrates, Waxes and Asphaltenes, Aberdeen, Oct, 1997; pp 20-21.

123. Peng, B.-Z.; Sun, C.-Y.; Liu, P.; Liu, Y.-T.; Chen, J.; Chen, G.-J., Interfacial properties of methane/aqueous VC-713 solution under hydrate formation conditions. *Journal of colloid interface science* **2009,** *336* (2), 738-742.

124. Anderson, B. J.; Tester, J. W.; Borghi, G. P.; Trout, B. L., Properties of inhibitors of methane hydrate formation via molecular dynamics simulations. *J. Am. Chem. Soc.* **2005,** *127* (50), 17852-17862.

125. Yang, J.; Tohidi, B., Characterization of inhibition mechanisms of kinetic hydrate inhibitors using ultrasonic test technique. *Chemical Engineering Science* **2011,** *66* (3), 278-283.

126. Xu, P.; Lang, X.; Fan, S.; Wang, Y.; Chen, J., Molecular dynamics simulation of methane hydrate growth in the presence of the natural product pectin. *The journal of physical chemistry C* **2016,** *120* (10), 5392-5397.

127. Li, Z.; Jiang, F.; Qin, H.; Liu, B.; Sun, C.; Chen, G., Molecular dynamics method to simulate the process of hydrate growth in the presence/absence of KHIs. *Chemical Engineering Science* **2017,** *164*, 307-312.

128. Zhang, J.; Lo, C.; Couzis, A.; Somasundaran, P.; Wu, J.; Lee, J. W., Adsorption of kinetic inhibitors on clathrate hydrates. *The Journal of Physical Chemistry C* **2009,** *113* (40), 17418-17420.

129. Yagasaki, T.; Matsumoto, M.; Tanaka, H., Molecular Dynamics Study of Kinetic Hydrate Inhibitors: The Optimal Inhibitor Size and Effect of Guest Species. *The Journal of Physical Chemistry C* **2018,** *123* (3), 1806-1816.

130. King Jr, H.; Hutter, J. L.; Lin, M. Y.; Sun, T., Polymer conformations of gas-hydrate kinetic inhibitors: A small-angle neutron scattering study. *The Journal of Chemical Physics* **2000,** *112* (5), 2523-2532.

131. Michael, G.; MarkáRodger, P., Characterisation of the {111} growth planes of a type II gas hydrate and study of the mechanism of

kinetic inhibition by poly (vinylpyrrolidone). *Journal of the Chemical Society, Faraday Transactions* **1996,** *92* (24), 5029-5033.

132. Carver, T. J.; Drew, M. G.; Rodger, P. M., Configuration‐biased Monte Carlo simulations of poly (vinylpyrrolidone) at a gas hydrate crystal surface. *Annals of the New York Academy of Sciences* **2000,** *912* (1), 658-668.

133. Yagasaki, T.; Matsumoto, M.; Tanaka, H., Adsorption Mechanism of Inhibitor and Guest Molecules on the Surface of Gas Hydrates. *J Am Chem Soc* **2015,** *137* (37), 12079-85.

134. Xu, J.; Li, L.; Liu, J.; Wang, X.; Yan, Y.; Zhang, J., The molecular mechanism of the inhibition effects of PVCaps on the growth of sI hydrate: an unstable adsorption mechanism. *Physical Chemistry Chemical Physics* **2018,** *20* (12), 8326-8332.

135. Moon, C.; Taylor, P. C.; Rodger, P. M., Clathrate nucleation and inhibition from a molecular perspective. *Canadian journal of physics* **2003,** *81* (1-2), 451-457.

136. Moon, C.; Hawtin, R. W.; Rodger, P. M., Nucleation and control of clathrate hydrates: insights from simulation. *Faraday Discussions* **2007,** *136*, 367-382.

137. Kvamme, B.; Kuznetsova, T.; Aasoldsen, K., Molecular simulations as a tool for selection of kinetic hydrate inhibitors. *Molecular Simulation* **2005,** *31* (14-15), 1083-1094.

138. Duffy, D.; Moon, C.; Rodger, P., Computer-assisted design of oil additives: hydrate and wax inhibitors. *Molecular Physics* **2004,** *102* (2), 203-210.

139. Ide, M.; Maeda, Y.; Kitano, H., Effect of Hydrophobicity of Amino Acids on the Structure of Water. *J. Phys. Chem. B* **1997,** (101), 7022-7026.

140. Sa, J. H.; Kwak, G. H.; Han, K.; Ahn, D.; Lee, K. H., Gas hydrate inhibition by perturbation of liquid water structure. *Sci Rep* **2015,** *5*, 11526.

141. Custodio, K. K. S.; Claudio, G. C.; Nellas, R. B., Structural Dynamics of Neighboring Water Molecules of N-Isopropylacrylamide Pentamer. *ACS Omega* **2020,** *5* (3), 1408-1413.

142. Semenov, A. P.; Medvedev, V. I.; Gushchin, P. A.; Vinokurov, V. A., Kinetic Inhibition of Hydrate Formation by Polymeric Reagents: Effect of Pressure and Structure of Gas Hydrates. *Chemistry and Technology of Fuels and Oils* **2016,** *51* (6), 679-687.

143. Mozaffar, H.; Anderson, R.; Tohidi, B., Reliable and repeatable evaluation of kinetic hydrate inhibitors using a method based on crystal growth inhibition. *Energy & Fuels* **2016,** *30* (12), 10055-10063.
144. Glénat, P.; Anderson, R.; Mozaffar, H.; Tohidi, B. In *Application of a new crystal growth inhibition based KHI evaluation method to commercial formulation assessment*, Proceedings of the 7th International Conference on Gas hydrates, Domestic Organizing Committee ICGH-4, Edinburgh: 2011; pp 17-21.
145. Hong, S. Y.; Lim, J. I.; Kim, J. H.; Lee, J. D., Kinetic Studies on Methane Hydrate Formation in the Presence of Kinetic Inhibitor via in Situ Raman Spectroscopy. *Energy & Fuels* **2012**, 121031111023001.
146. Ohno, H.; Strobel, T. A.; Dec, S. F.; Sloan, E. D.; Jr.; Koh, C. A., Raman Studies of Methane-Ethane Hydrate Metastability. *J. Phys. Chem. A* **2009,** (113), 1711–1716.
147. Dirdal, E. G.; Arulanantham, C.; Sefidroodi, H.; Kelland, M. A., Can cyclopentane hydrate formation be used to rank the performance of kinetic hydrate inhibitors? *Chemical Engineering Science* **2012,** *82*, 177-184.
148. Tohidi, B.; Danesh, A.; Todd, A.; Burgass, R.; Østergaard, K., Equilibrium data and thermodynamic modelling of cyclopentane and neopentane hydrates. *Fluid Phase Equilib.* **1997,** *138* (1-2), 241-250.
149. Sloan Jr, E. D., Method for controlling clathrate hydrates in fluid systems. Google Patents: 1995.
150. Chua, P. C.; Kelland, M. A., Tetra(iso-hexyl)ammonium Bromide-The Most Powerful Quaternary Ammonium-Based Tetrahydrofuran Crystal Growth Inhibitor and Synergist with Polyvinylcaprolactam Kinetic Gas Hydrate Inhibitor. *Energy & Fuels* **2012,** *26* (2), 1160-1168.
151. Mady, M. F.; Kelland, M. A., Tris(tert-heptyl)-N-alkyl-1-ammonium bromides—Powerful THF hydrate crystal growth inhibitors and their synergism with poly-vinylcaprolactam kinetic gas hydrate inhibitor. *Chemical Engineering Science* **2016,** *144*, 275-282.
152. Del Villano, L.; Kelland, M. A., Tetrahydrofuran hydrate crystal growth inhibition by hyperbranched poly (ester amide) s. *Chemical engineering science* **2009,** *64* (13), 3197-3200.
153. Nicholas, J. W.; Dieker, L. E.; Sloan, E. D.; Koh, C. A., Assessing the feasibility of hydrate deposition on pipeline walls—

Adhesion force measurements of clathrate hydrate particles on carbon steel. *Journal of Colloid Interface Science* **2009,** *331* (2), 322-328.
154. Nakajima, M.; Ohmura, R.; Mori, Y. H., Clathrate hydrate formation from cyclopentane-in-water emulsions. *Industrial engineering chemistry research* **2008,** *47* (22), 8933-8939.
155. Chua, P. C.; Kelland, M. A., Poly(N-vinyl azacyclooctanone): A More Powerful Structure II Kinetic Hydrate Inhibitor than Poly(N-vinyl caprolactam). *Energy & Fuels* **2012,** *26* (7), 4481-4485.
156. Colle, K. S.; Talley, L. D.; Longo, J. M. A method for inhibiting hydrate formation. WO2005005567A1. 2005.
157. Anselme, M.; Reijnhout, M.; Muijs, H.; Klomp, U. A method for inhibiting gas hydrate formation. WO1993025798A1. 1993.
158. Cheng, L.; Wang, L.; Li, Z.; Liu, B.; Chen, G., Inhibition Effect of Kinetic Hydrate Inhibitors on the Growth of Methane Hydrate in Gas–Liquid Phase Separation State. *Energies* **2019,** *12* (23), 4482.
159. Zhang, Q.; Shen, X.; Zhou, X.; Liang, D., Inhibition Effect Study of Carboxyl-Terminated Polyvinyl Caprolactam on Methane Hydrate Formation. *Energy & Fuels* **2017,** *31* (1), 839-846.
160. Wan, L.; Liang, D.-Q.; Ding, Q.; Hou, G., Investigation into the inhibition of methane hydrate formation in the presence of hydroxy-terminated poly(N-vinylcaprolactam). *Fuel* **2019,** *239*, 173-179.
161. Chua, P. C.; Kelland, M. A.; Hirano, T.; Yamamoto, H., Kinetic Hydrate Inhibition of Poly(N-isopropylacrylamide)s with Different Tacticities. *Energy & Fuels* **2012,** *26* (8), 4961-4967.
162. Reyes, F. T.; Kelland, M. A.; Kumar, N.; Jia, L., First Investigation of the Kinetic Hydrate Inhibition of a Series of Poly(β-peptoid)s on Structure II Gas Hydrate, Including the Comparison of Block and Random Copolymers. *Energy & Fuels* **2015,** *29* (2), 695-701.
163. Chua, P. C.; Kelland, M. A.; Hirano, T.; Kamigaito, M., Kinetic hydrate inhibition of poly(N-alkyl(meth)acrylamide)s with different tacticities. In *Proceedings of the International Conference on Gas Hydrates (ICGH7)*, Edinburgh, U.K., 2011.
164. Lin, H.; Wolf, T.; Wurm, F. R.; Kelland, M. A., Poly(alkyl ethylene phosphonate)s: A New Class of Non-amide Kinetic Hydrate Inhibitor Polymers. *Energy & Fuels* **2017,** *31* (4), 3843-3848.
165. Ajiro, H.; Takemoto, Y.; Akashi, M.; Chua, P. C.; Kelland, M. A., Study of the Kinetic Hydrate Inhibitor Performance of a Series of

Poly(N-alkyl-N-vinylacetamide)s. *Energy & Fuels* **2010,** *24* (12), 6400-6410.
166. Mady, M. F.; Min Bak, J.; Lee, H.-i.; Kelland, M. A., The first kinetic hydrate inhibition investigation on fluorinated polymers: Poly(fluoroalkylacrylamide)s. *Chemical Engineering Science* **2014,** *119*, 230-235.
167. Dirdal, E. G.; Kelland, M. A., Does the Cloud Point Temperature of a Polymer Correlate with Its Kinetic Hydrate Inhibitor Performance? *Energy & Fuels* **2019,** *33* (8), 7127-7137.
168. Mady, M. F.; Kelland, M. A., N,N-Dimethylhydrazidoacrylamides. Part 1: Copolymers with N-Isopropylacrylamide as Novel High-Cloud-Point Kinetic Hydrate Inhibitors. *Energy & Fuels* **2014,** *28* (9), 5714-5720.
169. Ree, L. H. S.; Mady, M. F.; Kelland, M. A., N,N-Dimethylhydrazidoacrylamides. Part 3: Improving Kinetic Hydrate Inhibitor Performance Using Polymers of N,N-Dimethylhydrazidomethacrylamide. *Energy & Fuels* **2015,** *29* (12), 7923-7930.
170. Mady, M. F.; Kelland, M. A., Synergism of tert-Heptylated Quaternary Ammonium Salts with Poly(N-vinyl caprolactam) Kinetic Hydrate Inhibitor in High-Pressure and Oil-Based Systems. *Energy & Fuels* **2018,** *32* (4), 4841-4849.
171. Hudait, A.; Qiu, Y.; Odendahl, N.; Molinero, V., Hydrogen-Bonding and Hydrophobic Groups Contribute Equally to the Binding of Hyperactive Antifreeze and Ice-Nucleating Proteins to Ice. *J Am Chem Soc* **2019,** *141* (19), 7887-7898.
172. Arsiccio, A.; McCarty, J.; Pisano, R.; Shea, J.-E., Heightened Cold-Denaturation of Proteins at the Ice-Water Interface. *J. Am. Chem. Soc.* **2020**.
173. Varma‐Nair, M.; Costello, C. A.; Colle, K. S.; King, H. E., Thermal analysis of polymer–water interactions and their relation to gas hydrate inhibition. *Journal of applied polymer science* **2007,** *103* (4), 2642-2653.
174. Abrahamsen, E.; Kelland, M. A., Comparison of Kinetic Hydrate Inhibitor Performance on Structure I and Structure II Hydrate-Forming Gases for a Range of Polymer Classes. *Energy & Fuels* **2018,** *32* (1), 342-351.

175. Colle, K. S.; Oelfke, R. H.; Kelland, M. A. Method for Inhibiting Hydrate Formation. 1999.
176. Ree, L. H. S.; Kelland, M. A., Investigation of Solvent Synergists for Improved Kinetic Hydrate Inhibitor Performance of Poly(N-isopropyl methacrylamide). *Energy & Fuels* **2019,** *33* (9), 8231-8240.
177. Kelland, M. A.; Dirdal, E. G.; Ree, L. S., Solvent Synergists for Improved Kinetic Hydrate Inhibitor Performance of Poly (N-vinyl caprolactam). *Energy & Fuels* **2020**.
178. Mady, M. F.; Kelland, M. A., Fluorinated Quaternary Ammonium Bromides: Studies on Their Tetrahydrofuran Hydrate Crystal Growth Inhibition and as Synergists with Polyvinylcaprolactam Kinetic Gas Hydrate Inhibitor. *Energy & Fuels* **2013**, 130828090238002.
179. Kamal, M. S.; Hussein, I. A.; Sultan, A. S.; von Solms, N., Application of various water soluble polymers in gas hydrate inhibition. *Renewable and Sustainable Energy Reviews* **2016,** *60*, 206-225.
180. Magnusson, C. D.; Kelland, M. A., Performance Enhancement ofN-Vinylcaprolactam-Based Kinetic Hydrate Inhibitors by Synergism with Alkylated Guanidinium Salts. *Energy & Fuels* **2016,** *30* (6), 4725-4732.
181. Qin, H. B.; Sun, C. Y.; Sun, Z. F.; Liu, B.; Chen, G. J., Relationship between the interfacial tension and inhibition performance of hydrate inhibitors. *Chemical Engineering Science* **2016,** *148*, 182-189.
182. Peytavy, J.-L.; Glenat, P.; Bourg, P., Kinetic Hydrate Inhibitors - Sensitivity towards Pressure and Corrosion Inhibitors. In *Proceedings of the International Petroleum Technology Conference*, Dubai, U.A.E., 2007.
183. Kelland, M. A.; Mønig, K.; Iversen, J. E.; Lekvam, K., Feasibility Study for the Use of Kinetic Hydrate Inhibitors in Deep-Water Drilling Fluids. *Energy & Fuels* **2008,** *22*, 2405–2410.
184. Kelland, M. A.; Svartaas, T. M.; Dybvik, L., Experiments Related to the Performance of Gas Hydrate Kinetic Inhibitors. *Ann. N. Y. Acad. Sci.* **2000,** *912*, 744−752
185. Lone, A.; Kelland, M. A., Exploring Kinetic Hydrate Inhibitor Test Methods and Conditions Using a Multicell Steel Rocker Rig. *Energy & Fuels* **2013,** *27* (5), 2536-2547.

186. Ke, W.; Kelland, M. A., Kinetic Hydrate Inhibitor Studies for Gas Hydrate Systems: A Review of Experimental Equipment and Test Methods. *Energy & Fuels* **2016,** *30* (12), 10015-10028.

187. Ihsan, A. B.; Nargis, M.; Koyama, Y., Effects of the Hydrophilic–Lipophilic Balance of Alternating Peptides on Self-Assembly and Thermo-Responsive Behaviors. *International journal of molecular sciences* **2019,** *20* (18), 4604.

188. Zhang, Q.; Koyama, Y.; Ihsan, A. B.; Kelland, M. A., Kinetic Hydrate Inhibition of Glycyl-valine-based Alternating Peptoids with Tailor-made N-substituents. *Energy & Fuels* **2020**.

189. Kelland, M. A.; Abrahamsen, E.; Ajiro, H.; Akashi, M., Kinetic Hydrate Inhibition withN-Alkyl-N-vinylformamide Polymers: Comparison of Polymers to n-Propyl and Isopropyl Groups. *Energy & Fuels* **2015,** *29* (8), 4941-4946.

190. Zhang, Q.; Kawatani, R.; Ajiro, H.; Kelland, M. A., Optimizing the Kinetic Hydrate Inhibition Performance of N-Alkyl-N-vinylamide Copolymers. *Energy & Fuels* **2018,** *32* (4), 4925-4931.

191. Kawatani, R.; Kan, K.; Kelland, M. A.; Akashi, M.; Ajiro, H., Remarkable Effect on Thermosensitive Behavior Regarding Alkylation at the Amide Position of Poly(N-vinylamide)s. *Chemistry Letters* **2016,** *45* (6), 589-591.

192. David, G.; Loubat, C.; Boutevin, B.; Robin, J.; Moustrou, C., Radical polymerization of ethyl acrylate with dead end polymerization conditions. *European polymer journal* **2003,** *39* (1), 77-83.

193. Zhang, Q.; Heyns, I. M.; Pfukwa, R.; Klumperman, B.; Kelland, M. A., Improving the Kinetic Hydrate Inhibition Performance of 3-Methylene-2-pyrrolidone Polymers by N-Alkylation, Ring Expansion, and Copolymerization. *Energy & Fuels* **2018,** *32* (12), 12337-12344.

194. Heyns, I. M.; Pfukwa, R.; Klumperman, B., Synthesis, Characterization, and Evaluation of Cytotoxicity of Poly(3-methylene-2-pyrrolidone). *Biomacromolecules* **2016,** *17* (5), 1795-800.

195. Iskander, G. M.; Ovenell, T. R.; Davis, T. P., Synthesis and properties of poly (1 ‐ alkyl ‐ 3 ‐ methylene ‐ 2 ‐ pyrrolidone) s. *Macromolecular Chemistry Physics* **1996,** *197* (10), 3123-3133.

196. Harrison, T. J.; Dake, G. R., An expeditious, high-yielding construction of the food aroma compounds 6-acetyl-1, 2, 3, 4-tetrahydropyridine and 2-acetyl-1-pyrroline. *The Journal of organic chemistry* **2005,** *70* (26), 10872-10874.

197. Riofski, M. V.; John, J. P.; Zheng, M. M.; Kirshner, J.; Colby, D. A., Exploiting the facile release of trifluoroacetate for the α-methylenation of the sterically hindered carbonyl groups on (+)-sclareolide and (−)-eburnamonine. *The Journal of organic chemistry* **2011,** *76* (10), 3676-3683.

198. Zhang, Q.; Kelland, M. A., Study of the Kinetic Hydrate Inhibitor Performance of Poly(N-vinylcaprolactam) and poly(N-isopropylmethacrylamide) with Varying End Caps. *Energy & Fuels* **2018,** *32* (9), 9211-9219.

199. Mumick, P. S.; Chang, Y.; Wang, J. H. Temperature sensitive polymers and water-dispersible products containing the polymers. US006451429B2. 2002.

200. Zhang, Q.; Kelland, M. A.; Ajiro, H., Polyvinylsulfonamides as Kinetic Hydrate Inhibitors. *Energy & Fuels* **2020,** *34* (2), 2230-2237.

201. Rogachev, V. O.; Metz, P., Thermal and high pressure intramolecular Diels–Alder reaction of vinylsulfonamides. *Nature Protocols* **2007,** *1* (6), 3076-3087.

202. Zhang, Q.; Kelland, M. A., Kinetic inhibition performance of alkylated polyamine oxides on structure I methane hydrate. *Chemical Engineering Science* **2020,** *220*.

203. Blankenburg, J.; Stark, M.; Frey, H., Oxidation-responsive polyether block copolymers lead to non-ionic polymer surfactants with multiple amine N-oxides. *Polymer Chemistry* **2019,** *10* (13), 1569-1574.

204. Wang, N.; Seymour, B. T.; Lewoczko, E. M.; Kent, E. W.; Chen, M.-L.; Wang, J.-H.; Zhao, B., Zwitterionic poly (sulfobetaine methacrylate) s in water: from upper critical solution temperature (UCST) to lower critical solution temperature (LCST) with increasing length of one alkyl substituent on the nitrogen atom. *Polymer Chemistry* **2018,** *9* (43), 5257-5261.

205. Zhang, Q.; Ree, L. S.; Kelland, M. A., A simple and direct route to high performance acrylamido-based kinetic gas hydrate inhibitors from poly (acrylic acid). *Energy & Fuels* **2020,** *34* (5), 6279-6287.

206. Ree, L. H. S.; Kelland, M. A.; Roth, P. J.; Batchelor, R., First investigation of modified poly(2-vinyl-4,4-dimethylazlactone)s as kinetic hydrate inhibitors. *Chemical Engineering Science* **2016,** *152*, 248-254.

207. Qin, H.-B.; Sun, Z.-F.; Wang, X.-Q.; Yang, J.-L.; Sun, C.-Y.; Liu, B.; Yang, L.-Y.; Chen, G.-J., Synthesis and Evaluation of Two New Kinetic Hydrate Inhibitors. *Energy & Fuels* **2015,** *29* (11), 7135-7141.
208. Anselme, M.; Muijs, H.; Klomp, U., Method for inhibiting the plugging of conduits by gas hydrates. International Patent Application WO93/25798, 1993.
209. Makogon, T. Y.; Larsen, R.; Knight, C. A.; E. Dendy Sloan, J., Melt growth of tetrahydrofuran clathrate hydrate and its inhibition: method and first results. *Journal of Crystal Growth* **1997,** *179* 258-262.
210. Del Villano, L.; Kelland, M. A., An investigation into the kinetic hydrate inhibitor properties of two imidazolium-based ionic liquids on Structure II gas hydrate. *Chemical engineering science* **2010,** *65* (19), 5366-5372.
211. Yeh, Y.; Feeney, R. E., Antifreeze proteins: Structures and mechanisms of function. *Chem. Rev.* **1996,** *96* (2), 601-617.
212. Edwards, A. R., A molecular modeling study of the winter flounder antifreeze peptide as a potential kinetic hydrate inhibitor. *Annals of the New York Academy of Sciences* **1994,** *715* (1), 543-544.
213. Zeng, H.; Wilson, L. D.; Walker, V. K.; Ripmeester, J. A., Effect of antifreeze proteins on the nucleation, growth, and the memory effect during tetrahydrofuran clathrate hydrate formation. *J. Am. Chem. Soc.* **2006,** *128* (9), 2844-2850.
214. Sun, T.; Davies, P. L.; Walker, V. K., Structural basis for the inhibition of gas hydrates by α-helical antifreeze proteins. *Biophysical journal* **2015,** *109* (8), 1698-1705.
215. Perfeldt, C. M.; Chua, P. C.; Daraboina, N.; Friis, D.; Kristiansen, E.; Ramlov, H.; Woodley, J. M.; Kelland, M. A.; von Solms, N., Inhibition of Gas Hydrate Nucleation and Growth: Efficacy of an Antifreeze Protein from the Longhorn Beetle Rhagium mordax. *Energy & Fuels* **2014,** *28* (6), 3666-3672.
216. Al-Adel, S.; Dick, J. A.; El-Ghafari, R.; Servio, P., The effect of biological and polymeric inhibitors on methane gas hydrate growth kinetics. *Fluid Phase Equilib.* **2008,** *267* (1), 92-98.
217. Sharifi, H.; Walker, V. K.; Ripmeester, J.; Englezos, P., Insights into the behavior of biological clathrate hydrate inhibitors in aqueous saline solutions. *Crystal growth design* **2014,** *14* (6), 2923-2930.

218. Kelland, M. A., A Review of Kinetic Hydrate Inhibitors from an Environmental Perspective. *Energy & Fuels* **2018,** *32* (12), 12001-12012.
219. Kelland, M. A.; Zhang, Q.; Chua, P. C., A Study of Natural Proteins and Partially Hydrolyzed Derivatives as Green Kinetic Hydrate Inhibitors. *Energy & Fuels* **2018,** *32* (9), 9349-9357.
220. Abrahamsen, E.; Kelland, M. A., Carbamate Polymers as Kinetic Hydrate Inhibitors. *Energy & Fuels* **2016,** *30* (10), 8134-8140.
221. Chua, P. C.; Kelland, M. A.; Ajiro, H.; Sugihara, F.; Akashi, M., Poly(vinylalkanamide)s as Kinetic Hydrate Inhibitors: Comparison of Poly(N-vinylisobutyramide) with Poly(N-isopropylacrylamide). *Energy & Fuels* **2013,** *27* (1), 183-188.
222. Carlise, J. R.; Lindeman, O. E. S.; Reed, P. E.; Conrad, P. G.; ver Vers, L. M. Method of Controlling Gas Hydrates in Fluid Systems. WO 2010/045520. 2010.
223. Abrahamsen, E.; Heyns, I. M.; von Solms, N.; Pfukwa, R.; Klumperman, B.; Kelland, M. A., First Study of Poly(3-methylene-2-pyrrolidone) as a Kinetic Hydrate Inhibitor. *Energy & Fuels* **2017,** *31* (12), 13572-13577.
224. Reyes, F. T.; Kelland, M. A., First Investigation of the Kinetic Hydrate Inhibitor Performance of Polymers of Alkylated N-Vinyl Pyrrolidones. *Energy & Fuels* **2013,** *27* (7), 3730-3735.
225. Namba, T.; Fujii, Y.; Saeki, T.; Kobayashi, H., Clathrate hydrate inhibitor and method of inhibiting the formation of clathrate hydrates using it. Google Patents: 2001.
226. Ieong, N. S.; Redhead, M.; Bosquillon, C.; Alexander, C.; Kelland, M.; O'Reilly, R. K., The Missing Lactam-Thermoresponsive and Biocompatible Poly(N-vinylpiperidone) Polymers by Xanthate-Mediated RAFT Polymerization. *Macromolecules* **2011,** *44* (4), 886-893.
227. Rodionova, T. V.; Komarov, V. Y.; Villevald, G. V.; Karpova, T. D.; Kuratieva, N. V.; Manakov, A. Y., Calorimetric and structural studies of tetrabutylammonium bromide ionic clathrate hydrates. *J Phys Chem B* **2013,** *117* (36), 10677-85.
228. Shin, K.; Kim, J.; Seo, Y.; Kang, S. P., Effect of kinetic hydrate inhibitor and liquid hydrocarbon on the heterogeneous segregation and deposition of gas hydrate particles. *Korean J. Chem. Eng.* **2014,** *31* (12), 2177-2182.

229. Stoporev, A. S.; Manakov, A. Y.; Kosyakov, V. I.; Shestakov, V. A.; Altunina, L. K.; Strelets, L. A., Nucleation of Methane Hydrate in Water-In-Oil Emulsions: Role of the Phase Boundary. *Energy & Fuels* **2016,** *30* (5), 3735-3741.

230. Stoporev, A. S.; Semenov, A. P.; Medvedev, V. I.; Sizikov, A. A.; Gushchin, P. A.; Vinokurov, V. A.; Manakov, A. Y., Visual observation of gas hydrates nucleation and growth at a water - organic liquid interface. *J. Cryst. Growth* **2018,** *485*, 54-68.

231. Ree, L. H. S.; Opsahl, E.; Kelland, M. A., N-Alkyl Methacrylamide Polymers as High Performing Kinetic Hydrate Inhibitors. *Energy & Fuels* **2019,** *33* (5), 4190-4201.

232. Colle, K. S.; Costello, C. A.; Oelfke, R. H.; Talley, L. D.; Longo, J. M.; Berluche, E. Method for Inhibiting Hydrate Formation. US005600044A. 1997.

233. Colle, K. S.; Costello, C. A.; Berluche, E.; Oelfke, R. H.; Talley, L. D. Method for Inhibiting Hydrate Formation. US006028233A. 2000.

234. Bartels, J. W.; Jones, R. A.; Servesko, J. M. Kinetic Hydrate Inhibitors for Controlling Gas Hydrate Formation in Wet Gas System. WO 2019/036671 A1. 2019.

235. Kelland, M. A.; Svartaas, T. M.; Øvsthus, J.; Namba, T., A new class of kinetic hydrate inhibitor. *Annals of the New York Academy of Sciences* **2000,** *912* (1), 281-293.

236. Easterling, C. P.; Kubo, T.; Orr, Z. M.; Fanucci, G. E.; Sumerlin, B. S., Synthetic upcycling of polyacrylates through organocatalyzed post-polymerization modification. *Chemical science* **2017,** *8* (11), 7705-7709.

237. Van Guyse, J. F.; Verjans, J.; Vandewalle, S.; De Bruycker, K.; Du Prez, F. E.; Hoogenboom, R., Full and Partial Amidation of Poly (methyl acrylate) as Basis for Functional Polyacrylamide (Co) Polymers. *Macromolecules* **2019,** *52* (14), 5102-5109.

238. Aksakal, S.; Liu, R.; Aksakal, R.; Becer, C. R., Nitroxide-mediated polymerisation of thioacrylates and their transformation into poly (acrylamide) s. *Polymer Chemistry* **2020**.

239. Zhang, Q.; Kelland, M. A.; Frey, H.; Blankenburg, J.; Limmer, L., Amine N-Oxide Kinetic Hydrate Inhibitor Polymers for High-Salinity Applications. *Energy & Fuels* **2020,** *34* (5), 6298-6305.

240. DeRuiter, J., Amides and Related Functional Groups. *Principles of Drug Action* **2005,** *1*, 1-16.

241. Owa, T.; Nagasu, T., Novel sulphonamide derivatives for the treatment of cancer. *Expert Opinion on Therapeutic Patents* **2000,** *10* (11), 1725-1740.

242. Wang, S.; Zhang, H. y.; Wang, L.; Duan, Z. J.; Kennedy, I., Analysis of sulphonamide residues in edible animal products: A review. *Food Additives & Contaminants* **2006,** *23* (4), 362-384.

243. Ree, L. H. S.; Sirianni, Q. E. A.; Gillies, E. R.; Kelland, M. A., Systematic Study of Polyglyoxylamides as Powerful, High-Cloud-Point Kinetic Hydrate Inhibitors. *Energy & Fuels* **2019,** *33* (3), 2067-2075.

244. Kelland, M. A. Method of Inhibiting the Formation of Gas Hydrates Using Amine Oxides. 2013.

245. Vatamanu, J.; Kusalik, P. G., Unusual Crystalline and Polycrystalline Structures in Methane Hydrates. *J. AM. CHEM. SOC.* **2006,** *128*, 15588-15589.

246. Blackman, L. D.; Gunatillake, P. A.; Cass, P.; Locock, K. E., An introduction to zwitterionic polymer behavior and applications in solution and at surfaces. *Chemical Society Reviews* **2019,** *48* (3), 757-770.

247. Kao, C.-W.; Cheng, P.-H.; Wu, P.-T.; Wang, S.-W.; Chen, I.-C.; Cheng, N.-C.; Yang, K.-C.; Yu, J., Zwitterionic poly (sulfobetaine methacrylate) hydrogels incorporated with angiogenic peptides promote differentiation of human adipose-derived stem cells. *RSC advances* **2017,** *7* (81), 51343-51351.

248. Zhang, L.; Cao, Z.; Bai, T.; Carr, L.; Ella-Menye, J.-R.; Irvin, C.; Ratner, B. D.; Jiang, S., Zwitterionic hydrogels implanted in mice resist the foreign-body reaction. *Nature biotechnology* **2013,** *31* (6), 553-556.

249. Jiang, S.; Cao, Z., Ultralow‐fouling, functionalizable, and hydrolyzable zwitterionic materials and their derivatives for biological applications. *Advanced materials* **2010,** *22* (9), 920-932.

250. Shao, Q.; Jiang, S., Molecular understanding and design of zwitterionic materials. *Advanced materials* **2015,** *27* (1), 15-26.

251. Mary, P.; Bendejacq, D. D.; Labeau, M.-P.; Dupuis, P., Reconciling low-and high-salt solution behavior of sulfobetaine polyzwitterions. *The Journal of Physical Chemistry B* **2007,** *111* (27), 7767-7777.

252. Laschewsky, A. J. P., Structures and synthesis of zwitterionic polymers. **2014,** *6* (5), 1544-1601.

253. Laschewsky, A.; Rosenhahn, A., Molecular design of zwitterionic polymer interfaces: searching for the difference. *Langmuir* **2018,** *35* (5), 1056-1071.
254. Kelland, M. A., Additives for Kinetic Hydrate Inhibitor Formulations To Avoid Polymer Fouling at High Injection Temperatures: Part 1. A Review of Possible Methods. *Energy & Fuels* **2020,** *34* (3), 2643-2653.
255. Güner, A.; Ataman, M., Effects of inorganic salts on the properties of aqueous poly (vinylpyrrolidone) solutions. *Colloid Polymer Science* **1994,** *272* (2), 175-180.
256. Moghaddam, S. Z.; Thormann, E., The Hofmeister series: Specific ion effects in aqueous polymer solutions. *Journal of colloid interface science* **2019,** *555*, 615-635.
257. Eckelt, J.; Knopf, A.; Wolf, B. A., Polyelectrolytes: Intrinsic viscosities in the absence and in the presence of salt. *Macromolecules* **2008,** *41* (3), 912-918.
258. Wolf, B. A. J. M. r. c., Polyelectrolytes revisited: reliable determination of intrinsic viscosities. **2007,** *28* (2), 164-170.
259. Seo, S. D.; Paik, H. J.; Lim, D. H.; Lee, J. D., Effects of Poly(N-vinylcaprolactam) Molecular Weight and Molecular Weight Distribution on Methane Hydrate Formation. *Energy & Fuels* **2017,** *31* (6), 6358-6363.
260. Herrmann, K., Micellar properties of some zwitterionic surfactants. *Journal of Colloid Interface Science* **1966,** *22* (4), 352-359.
261. Chevalier, Y.; Melis, F.; Dalbiez, J. P., Structure of zwitterionic surfactant micelles: micellar size and intermicellar interactions. *The Journal of Physical Chemistry B* **1992,** *96* (21), 8614-8619.
262. Nakarit, C.; Kelland, M. A.; Liu, D. J.; Chen, E. Y. X., Cationic kinetic hydrate inhibitors and the effect on performance of incorporating cationic monomers into N-vinyl lactam copolymers. *Chemical Engineering Science* **2013,** *102*, 424-431.
263. Pinschmidt Jr, R. K., Polyvinylamine at last. *Journal of Polymer Science Part A: Polymer Chemistry* **2010,** *48* (11), 2257-2283.
264. JONES, G. D.; ZOMLEFER, J.; HAWKINS, K., ATTEMPTED PREPARATION OF POLYVINYLAMINE (1). *The Journal of Organic Chemistry* **1944,** *9* (6), 500-512.
265. Pelton, R., Polyvinylamine: a tool for engineering interfaces. *Langmuir* **2014,** *30* (51), 15373-15382.

266. Titherley, A. W.; Branch, G. E. K., XLI.—Hexahydropyrimidine and its benzoyl derivatives. *Journal of the Chemical Society, Transactions* **1913,** *103*, 330-340.
267. Reyes, F. T.; Kelland, M. A.; Sun, L.; Dong, J., Kinetic Hydrate Inhibitors: Structure–Activity Relationship Studies on a Series of Branched Poly (ethylene citramide) s with Varying Lipophilic Groups. *Energy & Fuels* **2015,** *29* (8), 4774-4782.
268. Li, D.; Ma, S.; Laroui, A.; Zhang, Y.; Wang, J.; Lu, P.; Dong, J., Controlling water dynamics for kinetic inhibition of clathrate hydrate. *Fuel* **2020,** *271*, 117588.
269. Klomp, U. C. METHOD FOR INHIBITING THE PLUGGING OF CONDUITS BY GAS HYDRATES. U.S. Patent 6905605. 2005.
270. Sun, Z.-G.; Fan, S.-S.; Guo, K.-H.; Shi, L.; Guo, Y.-K.; Wang, R.-Z., Gas hydrate phase equilibrium data of cyclohexane and cyclopentane. *Journal of Chemical Engineering Data* **2002,** *47* (2), 313-315.

Appendices

Paper I.	Kinetic Hydrate Inhibition of Glycyl-valine-based Alternating Peptoids with Tailor-made *N*-substituents.
Paper II.	Optimizing the Kinetic Hydrate Inhibition Performance of *N*-Alkyl-*N*-vinylamide Copolymers.
Paper III.	Improving the Kinetic Hydrate Inhibition Performance of 3-Methylene-2-pyrrolidone Polymers by *N*-Alkylation, Ring Expansion, and Copolymerization.
Paper IV.	Study of the Kinetic Hydrate Inhibitor Performance of Poly (*N*-vinyl caprolactam) and Poly (*N*-isopropyl methacrylamide) with Varying End Caps.
Paper V.	A Simple and Direct Route to High Performance Acrylamide-based Kinetic Gas Hydrate Inhibitors from Poly (acrylic acid).
Paper VI.	Polyvinylsulfonamides as Kinetic Hydrate Inhibitors.
Paper VII.	Kinetic Inhibition Performance of Alkylated Polyamine Oxides on Structure I Methane Hydrate.
Paper VIII.	Amine N-Oxide Kinetic Hydrate Inhibitor Polymers for High-Salinity Applications.
Paper IX.	Zwitterionic Poly (sulfobetaine methacrylate)s as Kinetic Hydrate Inhibitors.
Paper X.	High Cloud Point Polyvinylaminals as Non-amide Based Kinetic Gas Hydrate Inhibitors.

Paper I

Kinetic Hydrate Inhibition of Glycyl-valine-based Alternating Peptoids with Tailor-made *N*-substituents

Authors:

Qian Zhang*, Yasuhito Koyama, Abu Bin Ihsan, and Malcolm A. Kelland

Published in Energy & Fuels 2020, 34 (4), 4849-4854.

This paper is not in Brage due to copyright.

Paper II

Optimizing the Kinetic Hydrate Inhibition Performance of *N*-Alkyl-*N*-vinylamide Copolymers

Authors:

Qian Zhang, Ryo Kawatani, Hiroharu Ajiro, and Malcolm A. Kelland*

Published in Energy & Fuels 2018, 32 (4), 4925-4931.

This paper is not in Brage due to copyright.

Paper III

Improving the Kinetic Hydrate Inhibition Performance of 3-Methylene-2-pyrrolidone Polymers by *N*-Alkylation, Ring Expansion, and Copolymerization

Authors:

Qian Zhang, Ingrid M. Heyns, Rueben Pfukwa, Bert Klumperman, and Malcolm A. Kelland*

Published in Energy & Fuels 2018, 32 (12), 12337-12344.

Improving the Kinetic Hydrate Inhibition Performance of 3-methylene-2-pyrrolidone polymers by *N*-Alkylation, Ring Expansion and Copolymerization

Qian Zhang,[#] Ingrid M. Heyns,[§] Rueben Pfukwa, [§] Bert Klumperman, [§] Malcolm A. Kelland[#]*

[#] Department of Chemistry, Bioscience and Environmental Engineering, Faculty of Science and Technology, University of Stavanger, N-4036 Stavanger, Norway

[§] Department of Chemistry and Polymer Science, Stellenbosch University, Private Bag X1, Matieland 7602, South Africa

* Corresponding author: Tel.: +47 51831823; fax +47 51831750

E-mail address: malcolm.kelland@uis.no (M.A. Kelland)

ABSTRACT

Poly(*N*-vinyl lactam)s has been the dominant class of kinetic hydrate inhibitor (KHI) polymer for many years in oil and gas flow assurance applications. Recently, we reported on the KHI performance of a new but closely related polymer, poly(3-methylene-2-pyrrolidone), P(3M2P). (Abrahamsen, E.; Heyns, I. M.; von Solms, N.; Pfukwa, R.; Klumperman, B.; Kelland, M. A., First Study of Poly(3-methylene-2-pyrrolidone) as a Kinetic Hydrate Inhibitor. Energy & Fuels 2017, 31 (12), 13572-13577). It was suggested that, like poly(*N*-vinyl pyrrolidone), the polymer is not sufficiently hydrophobic for optimum KHI performance. We now report on three improvements to this class 1) by alkylating the pyrrolidone ring 2) by expanding the ring size from 5 to 6 atoms 3) by copolymerization with more hydrophobic monomers. All new polymers were tested in high pressure rocking cells with a Structure II-forming gas mixture. When methyl, ethyl and n-propyl groups were introduced onto the pyrrolidone ring the poly(5-n-propyl-3-methylene-2-pyrrolidone) homopolymer, with lowest cloud point of the three polymers, showed the best KHI efficacy. Expanding the ring size to the 6-ring piperidone group, also lowered the polymer cloud point and improved the KHI performance relative to P(3M2P). Copolymers of 3M2P with *N*-vinyl caprolactam and *N*-n-butyl methacrylamide (n-BuMAm) were also synthesised. All copolymers showed good improvements over P(3M2P). The best copolymer was the n-BuMAm:3M2P copolymer with highest n-BuMAm content and lowest cloud point. The best two copolymers were further investigated at different concentrations (1000, 2500, and 5000 ppm) showing an increase in performance with increasing concentration.

INTRODUCTION

When water is present with natural gases under conditions of low temperatures and elevated pressures conditions, gas hydrates tend to form. Gas hydrates are ice-like host-guest compounds composed of hydrogen bonded water molecules "cages", into which small guest gas molecules such as methane, ethane, propane and acid gases such as carbon dioxide and hydrogen sulphide, are held.[1-2] Pipeline blockage caused by gas hydrates is considered as a major flow assurance problem in oil and gas operations. Avoidance of gas hydrate formation is a necessity, which attracts increasing research on gas hydrates inhibition methods because once generated, gas hydrates can be difficult to remove and cause large losses in revenue.[3-5]

Injection of kinetic hydrate inhibitors (KHIs) is a well-known technology to control gas hydrates, which has been successfully used in the oil and gas industry for more than two decades.[6] KHIs are a class of low dosage hydrate inhibitors (LDHIs), the other being anti-agglomerants (AAs). Being LDHIs, KHIs are injected at low concentration typically 0.1-2 wt. %

active materials in solvents. The exact inhibition mechanism of KHIs is still the subject of discussion but there is much evidence for both hydrate nucleation and crystal growth inhibition.[3, 7-8] The main ingredient in KHI formulations is one or more water-soluble oligomers or polymers, most of which containing repeating amide groups with neighbouring hydrophobic groups. Amongst the linear polyvinyl polymers this includes poly(*N*-vinyl pyrrolidone) (PVP), poly(*N*-vinylcaprolactam) (PVCap), poly(*N*-alkyl(meth)acrylamide)s, poly(*N*-alkyl-*N*-vinylalkanamide)s and their copolymers (Figures 1 and 2).

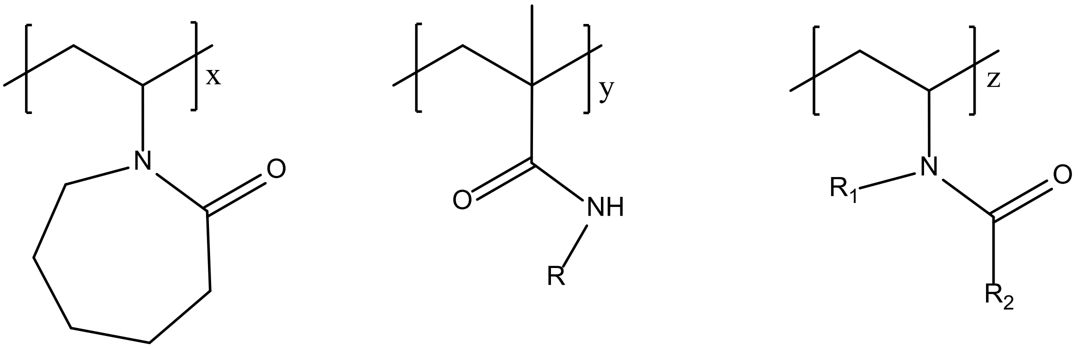

Figure 1. Structure of poly(N-vinylcaprolactam) (left), poly(N-alkyl(meth)acrylamide)s (middle) and poly(N-alkyl-N-vinylalkanamide)s (right).

The suitable size of the pendant hydrophobic groups are critical to the KHI performance, either too short or too long are unfavorable.[9-12] This is probably related to the various cage sizes in gas hydrates structures and the ability of the hydrophobic groups to disrupt hydrate clustering and/or crystal growth while at the same time maintaining water-solubility. If we take poly(*N*-alkyl-*N*-vinylalkanamide)s derivatives as an example: poly(*N*-vinylmethylamide), that contains small pendant methyl groups, is a poor KHI, whilst poly(*N*-vinyl-n-propylamide) with longer propyl pendant hydrophobic groups performs quite well as KHI, but when it comes to polymers with more carbon atoms pendant alkyls such as poly(*N*-vinylisobutylamide) become insoluble in water.[10]

Recently, an interesting new polyamide poly(3-methylene-2-pyrrolidone) (P(3M2P)) homopolymer was synthesized. Besides other potential applications it was investigated as a KHI (Figure 2).[13-15] This polymer has a very similar structure to PVP, one of the earliest commercialized KHIs. However, like PVP, the KHI performance of 3M2P polymer was not very high. The 3M2P monomer unit has actually less pendant hydrophobicity than PVP as one of the ring carbon atoms in P(3M2P) is part of the polymer backbone and the nitrogen is more sterically available for hydrogen-bonding. Therefore, we decided to investigate methods to improve the performance of P(3M2P) and came up with three possibilities to increase the hydrophobicity, *i.e.* 1) ring alkylation, 2) copolymerization and 3) ring expansion. We will now discuss these three options.

We have shown in previous work that the performance of PVP can be improved by alkylating the pyrrolidone ring.[12] For P(3M2P), the NH group gives added flexibility compared to PVP, as the proton on the nitrogen atom can readily be replaced by other hydrophobic groups. In this work we have investigated alkylated derivatives of 3M2P homopolymer with methyl, ethyl and n-propyl groups.

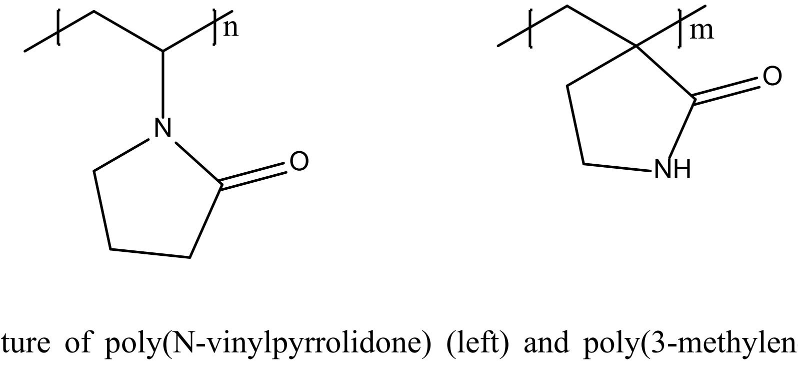

Figure 2. Structure of poly(N-vinylpyrrolidone) (left) and poly(3-methylene-2-pyrrolidone) (right).

Copolymers with different kinds of monomers can ameliorate some limitations of homopolymers.[11,16-19] Poor solubility in water is one of these limitations, especially for homopolymers with large pendant hydrophobic groups. For example, poly(*N*-vinylisobutylamide) mentioned earlier is not soluble in water, but the copolymer of *N*-vinylisobutylamide with *N*-vinylisopropylamide is water-soluble and was shown to have good performance as a KHI.[10] Another limitation of homopolymers can be the low cloud point (T_{Cl}) or deposition point (T_{dp}). As the temperature of the well fluids near the inhibitor injection point are often as high as 60-120 °C, a KHI polymer with low T_{Cl} may precipitate and cause its own blockage. For example, PVCap is a very effective and efficient KHI, and it is often the comparative standard for evaluating new KHIs in laboratory studies. However, the T_{Cl} and T_{dp} of PVCap is only 31-40 °C. Thus, for industry applications VCap is often copolymerized with more hydrophilic monomers to avoid injection problems. This can present a new problem in that too much comonomer can reduce the performance as a KHI. VP:VCap is a common commercial copolymer KHI in which the use of VP has little effect on the performance compared to PVCap. The 1:1 VCap:*N*-vinyl-*N*-methyl acetamide (VCap:VIMA) is rare of a VCap copolymer which has better KHI effect than either PVCap or PVIMA homopolymers.[20]

Conversely, VP can be copolymerized with more hydrophobic monomers to increase the KHI efficacy. An example is VP:n-butyl acrylate copolymer.[21-22] This is the second technique we used in this work to improve the performance of P(3M2P). We made copolymers of 3M2P monomer with VCap (an obvious choice to compare to VP:VCap copolymer) and *N*-n-butyl(meth)acrylamide. We chose this acrylamide as the amide gives more hydrophilicity than the ester in n-butyl acrylate allowing us to make copolymers with a higher percentage of *N*-n-butyl(meth)acrylamide whilst still keeping water-solubility.

The last method to attempt to improve the performance of P(3M2P) was to expand the pyrrolidone ring to six or even seven-membered rings. Previously we showed that expanding the lactam ring in poly(*N*-vinyl lactam)s from 5 ring atoms to 6, 7 and 8 atoms by adding extra ring methylene groups improves the KHI performance. All these new homopolymers and copolymers have been tested as KHIs in high-pressure rocking cells using a natural gas mixture that forms Structure II hydrates as the most stable phase.

EXPERIMENTAL SECTION

Materials

Poly(*N*-vinylpyrrolidone) (PVP K15) pure powder and molecular weight of 8000 g/mol was obtained from Ashland chemical company. *N*-vinylpyrrolidone:*N*-vinylcaprolactam 1:1 copolymer (VP:VCap) was obtained as an aqueous solution of 53.8 wt. % from BASF with tradename Luvicap 55W. All chemicals for monomer synthesis were purchased from commercial sources.

^{1}H and ^{13}C NMR spectra were obtained with a Varian VXR-Unity (300 MHz) spectrometer, unless stated otherwise. Majority of the compounds were dissolved in $CDCl_3$ or D_2O with tetramethylsilane (TMS) as an internal reference. Liquid Chromatography Mass Spectrometry (LC-MS) was obtained with a Waters Synapt G2 with Electron Spray Ionization (ESI) in the positive mode. The column used was Waters UPLC C18, 2.1×100 mm. Molecular weights of 3M2P and *N*-vinylcaprolactam copolymers and *N*-alkylated-3M2P homopolymers were obtained via SEC analysis, in DMAc. The instrument used was an Agilent 1260 fitted with a PSS guard column (50 × 8 mm) in series with three analytical PSS GRAM columns (300 × 8 mm, 10 µm, 2 × 3000 Å and 1 × 100 Å), which was kept at 40 °C. DMAc was stabilized with 0.05% BHT (w/v) and 0.03 % LiCl (w/v). The instrument was equipped with an Agilent 1260

Quad pump and a refractive index detector. The flow rate was 0.800 mL/min and the injection volume, 100 µL. The SEC system was calibrated using narrow dispersity PMMA standards obtained from Polymer Laboratories. Molecular weights of 3M2P and *N*-BuMAAm copolymers were calculated from ^{1}H NMR spectroscopy.

Monomer and Polymer characterization

3-methylene-2-pyrrolidone (3M2P). The procedure was adapted from literature.[23] ^{1}H NMR (300 MHz, DMSO) δ: 8.05 (s, 1H, $-N\underline{H}$), 5.67 (td, J = 2.9, 1.4 Hz, 1H, $=C\underline{H}_{2a}$), 5.27 (tt, J = 2.5, 1.3 Hz, 1H, $=C\underline{H}_{2b}$), 3.28 – 3.21 (m, 2H, $-C\underline{H}_2-NH$), 2.78 – 2.70 (m, 2H, $-C\underline{H}_2-C=$). 13C NMR (300 MHz, DMSO-d6) δ: 175.45, 141.62, 114.47, 38.90, 26.32. MS (ESI): m/z = 98.1 (calculated: 98.06 for [M + H]+).

N-methyl-3-methylene-2-pyrrolidone (N-M3M2P). The procedure was carried out as described in the literature.[24] Purification was performed via column chromatography using ethyl acetate as the eluent ($R_f = 0.36$), giving the product as a yellow liquid. ^{1}H NMR (300 MHz, $CDCl_3$) δ: 5.87 (td, J = 2.8, 0.8 Hz, 1H, $=C\underline{H}_{2a}$), 5.23 (td, J = 2.3, 0.7 Hz, 1H, $=C\underline{H}_{2b}$), 3.35 – 3.29 (m, 2H, $-N-C\underline{H}_2-$), 2.87 (s, 3H, $-C\underline{H}_3$), 2.73 – 2.66 (m, 2H, $-C\underline{H}_2-C=$). ^{13}C NMR (300 MHz, CDC13-d1) δ: 168.03, 139.52, 114.84, 46.21, 30.15, 23.98. MS (ESI): m/z = 112.1 (calculated: 112.08 for $[M + H]^+$). *Poly(N-M3M2P).* ^{1}H NMR (300 MHz, $CDCl_3$) δ: 3.5 - 3.1 (broad), 2.9 – 2.6 (broad), 2.2 – 1.1 (broad).

N-ethyl-3-methylene-2-pyrrolidone (N-E3M2P). The procedure was carried out as described in the literature.[24] Purification was performed via column chromatography, with ethyl acetate/pentane as eluent (1:1 v/v, $R_f = 0.28$), yielding the product as a yellow liquid. ^{1}H NMR (300 MHz,$CDCl_3$) δ: 5.96 (td, J = 2.8, 0.8 Hz, 1H, $=C\underline{H}_{2a}$), 5.30 (td, J = 2.4, 0.7 Hz, 1H, $=C\underline{H}_{2b}$), 3.42 (dt, J = 13.3, 7.2 Hz, 4H, $-C\underline{H}_2-N-C\underline{H}_2-$), 2.80 – 2.72 (m, 2H, $-C\underline{H}_2-C=$), 1.16 (t, J = 7.2 Hz, 3H, $-C\underline{H}_3$).^{13}C NMR (300 MHz, $CDCl_3$) δ: 171.31, 139.99, 115.17, 43.52, 37.87, 24.09, 12.39. MS (ESI): m/z = 126.1 (calculated: 126.09 for $[M + H]^+$). *Poly(N-E3M2P).* ^1H NMR (300 MHz, $CDCl_3$) δ: 3.5 – 3.0 (broad), 2.4 – 1.3 (broad), 1.2 – 0.9 (broad).

N-n-propyl-3-methylene-2-pyrrolidone (N-Pr3M2P). The monomer was obtained by *N*-alkylation of 3M2P with 1-bromopropane as follows: Sodium hydride (50 mg, 2.08 mmol) was added to 3M2P (0.20 g, 2.06 mmol) in DMF (20 mL). The reaction mixture was allowed to stir for 20 min. Subsequently, 1-bromopropane (0.20 mL, 2.20 mmol) was added to the reaction mixture and allowed to stir overnight at 95 °C, where after the solvent was removed under reduced pressure. The crude mixture was purified by column chromatography, with ethyl acetate as eluent ($R_f = 0.58$), yielding the product as a brown-yellow liquid (0.19 g, 66 %). ^1H NMR (300 MHz,$CDCl_3$) δ: 5.97 (td, J = 2.9, 0.6 Hz, 1H, $=C\underline{H}_{2a}$), 5.31 (td, J = 2.4, 0.5 Hz, 1H, $=C\underline{H}_{2b}$), 3.40 – 3.32 (m, 4H, $-C\underline{H}_2-N-C\underline{H}_2-$), 2.79 – 2.72 (m, 2H, $-C\underline{H}_2-C=$), 1.65 – 1.51 (m, 2H, $-C\underline{H}_2-CH_3$), 0.91 (t, J = 7.4 Hz, 3H, $-C\underline{H}_3$). ^{13}C NMR (300 MHz, $CDCl_3$) δ: 168.09, 140.01, 115.11, 44.92, 44.10, 24.25, 20.58, 11.43. MS (ESI): m/z = 140.1 (calculated: 140.11 for $[M + H]^+$), 162.1 (calculated: 162.10 for $[M + Na]^+$). *Poly(N-Pr3M2P).* ^1H NMR (300 MHz, $CDCl_3$) δ: 3.5 – 3.0 (broad), 2.1 – 1.2 (broad), 1.0 – 0.7 (broad).

N-n-butyl methacrylamide (N-BuMAAm). The synthesis was adapted from a literature procedure.[25] ^1H NMR (300 MHz, $CDCl_3$) δ: 6.03 (s, 1H, $-N\underline{H}$), 5.62 (s, 1H, $=C\underline{H}_{2a}$), 5.25 (s, 1H, $=C\underline{H}_{2b}$), 3.26 (q, J = 6.7 Hz, 2H, $-NH-C\underline{H}_2-$), 1.90 (s, 3H, $=C-C\underline{H}_3$), 1.48 (m, 2H, $-CH_2-C\underline{H}_2-CH_2-$), 1.32 (m, 2H, $-C\underline{H}_2-CH_3$), 0.88 (t, J = 7.3 Hz, 3H, $-CH_2-C\underline{H}_3$). ^{13}C NMR (300 MHz, $CDCl_3$) δ: 168.58, 140.31, 119.09, 39.46, 31.67, 20.14, 18.73, 13.78. MS (ESI): m/z = 142.1 (calculated: 142.22 for $[M + H]^+$), 164.1 (calculated: 164.20 for $[M + Na]^+$).

3-Methylene-2-piperidone (3M2Pip). The reactions towards the monomer were adapted from literature procedures.[26-27] ^1H NMR (300 MHz, $CDCl_3$) δ: 6.23 (dd, J = 3.3, 1.6 Hz, 1H, $=C\underline{H}_{2b}$), 5.84 (s, 1H, $-N\underline{H}$), 5.34 – 5.31 (m, 1H, $=C\underline{H}_{2a}$), 3.42 – 3.36 (m, 2H, $-C\underline{H}_2-N-$), 2.58 (ddt, J = 7.9, 4.5, 1.6 Hz, 2H, -C$\underline{H_2}$-C=), 1.88 (dt, J = 12.1, 6.0 Hz, 2H, -CH_2-C$\underline{H_2}$-CH_2-). ^{13}C NMR (300 MHz, $CDCl_3$) δ: 171.00, 137.48, 122.37, 42.90, 29.93, 23.29. MS (ESI): m/z = 112.1 (calculated: 112.08 for $[M + H]^+$), 134.1 (calculated: 134.07 for $[M + Na]^+$). Poly(N-Pr3M2P). 1H NMR (300 MHz, D_2O) δ: 3.5 – 3.2 (broad), 2.5 – 1.2 (broad).

Synthesis Method for Polymers (Figure 3, Table 1)

Polymerization. Homo-and copolymerizations were performed with similar conditions as described in literature.[28] The copolymer, poly(3M2P-*co*-*N*-BuMAAm) with 9 % incorporated *N*-BuMAAm prepared will be used as an example. 3M2P (0.73 g, 7.52 mmol) dissolved in 4.4 mL DMSO was added to a 25 mL pear-shaped flask. Subsequently, *N*-BuMAAm (0.19 g, 1.33 mmol) and ACVA (0.50 g, 1.77 mmol) were added and the polymerization mixture was purged with argon gas for 15 min, where after the reaction flask was placed in a heated oil bath at 90 °C for 2h. The polymerization was stopped by allowing it to cool and opening the flask to air. The crude mixture was placed in dialysis tubing (3 500 molecular weight cut-off) and dialyzed against water for 24 h, replacing the water every 8 h. The polymer was isolated by freeze-drying, in > 80% yield.

Homopolymerizations of *N*-alkylated monomers were carried using the same protocol as the copolymerization above, with the following monomer:initiator ratios: 7.5:1 for *N*-M3M2P, 5:1 and 10:1 for *N*-E3M2P, and 7.5:1 for *N*-Pr3M2P.

Preparation of poly(3M2Pip). To a 10 mL reaction flask was added, 3M2Pip (0.50 g, 4.50 mmol), ACVA (17 mg, 0.06 mmol) dissolved in 3 mL DMSO. The reaction mixture was purged with argon gas for 20 min, where after the reaction flask was placed in a heated oil bath at 70 °C. The reaction mixture was left stirring for 24 h, subsequently the polymerization flask was opened and allowed to reach room temperature. The polymer was purified by dialysis (dialysis tubing with molecular weight cut-off of 3 500 g/mol) against water. The polymer was isolated by freeze-drying.

Cloud Point (Tcl) Measurement

Turbidimetry measurements were performed with UV/vis instrument with a constant heating rate of 0.2 °C/min and monitored at a wavelength of 500 nm. Polymer concentrations of 10 mg/mL in distilled, deionized water was used. UV/vis spectroscopy was performed on a Specord® 210 Plus spectrophotometer. The instrument was equipped with two Peltier cooled cell holders (without stirrers) and the software used was WinASPECT® plus. The T_{cl} was taken at 50 % transmittance of the heating turbidimetry curves.

Table 1. Homopolymers and copolymers synthesized in this study.

Polymer	Monomer 1 (n)	Monomer 2 (1-n)	n	*Đ*	Mn g/mol	T_{cl} °C
1	*N*-M3M2P		-	2.27	4000	>80
2a	*N*-E3M2P			2.20	1100	>80
2b	*N*-E3M2P			1.63	9000	71.5
3	*N*-Pr3M2P			2.08	6100	19.8
4	3M2Pip				<12900	See discussion
E	3M2P	*N*-BuMAAm	0.75	1.36	4900	30
D	3M2P	*N*-BuMAAm	0.77	1.41	4800	33
C	3M2P	*N*-BuMAAm	0.88		*	47.6
B	3M2P	*N*-BuMAAm	0.91		*	>80
A	3M2P	*N*-BuMAAm	0.97		*	>80
i	3M2P	VCap	0.53	1.37	3500	67.2
ii	*N*-M3M2P	VCap	0.50	1.22	6200	41

* Polymers A-C could not be analysed due to P(3M2P)'s incompatibility with the mobile phase of the SEC; however, polymers D and E should be a good guideline to the molecular weight of A-C, as the polymers were synthesized in exactly the same way.

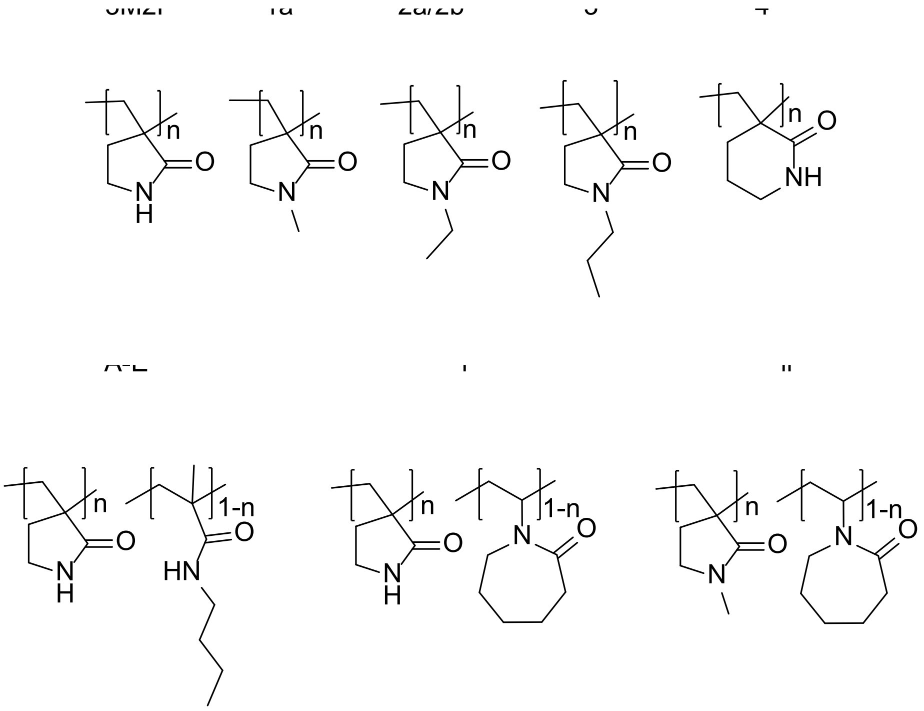

Figure 3. Homopolymers and copolymers investigated in this study.

Experimental Equipment

The experimental equipment mainly included five steel rocking cells, which were parallelly held up by a rocker rig in a cooling bath. (Figure 4) The maximum effective volume of each cell was 40 mL. A steel ball was used to agitate the solution in each cell when rocking. Each cell was equipped with a pressure sensor with an uncertainty of ± 0.2 bar and a temperature sensor with an uncertainty of ± 0.1 °C. Data collected by the pressure and temperature sensors were saved in a computer. This KHI performance testing equipment was supplied by PSL Systemtechnik, Germany. For structure II gas hydrate at 76 bar, the equilibrium temperature

(Teq) tested in this equipment has been reported to be 20.2 ± 0.05 °C in the previous work of our group, which is similar to 20.5 °C calculated by the PVTSim software from Calsep.[14.16-18] We have recently re-evaluated Teq in the rocking cells. Using the slow ramping method recommended by Tohidi *et al*, rather than constant warming, we obtained a value of 20.5 ºC for Teq, exactly in line with the software prediction.[29-30]

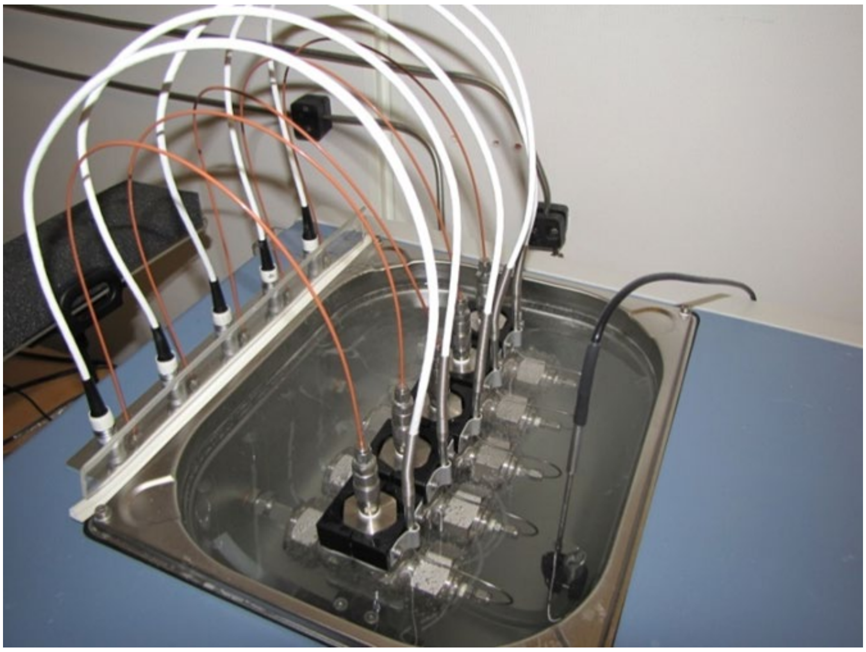

Figure 4. Five steel rocking cells in a cooling bath.

Slow Constant Cooling Method

As operators wish to avoid hydrate formation completely, the delay time of hydrate nucleation is considered the most critical factor for field applications, which largely depends upon the amount of subcooling in the system. Therefore, a method to determine the maximum subcooling that an inhibitor can prevent hydrate formation could be measured by slowly cooling the test fluids until hydrate nucleation occurs.[31-33] Similar to the previous work of our group, this slow constant cooling method was used to evaluate the KHI performance ranking of the polymers in this study.[34-36] Synthetic nature gas (SNG) mixture, which theoretically forms a Structure II hydrate as the most thermodynamically stable phase, was used to form gas hydrate (Table 2).

Table 2. Synthetic Nature Gas (SNG) mixture used in this study.

Component	**mol %**
methane	80.67
ethane	10.20
propane	4.90
CO_2	1.84
isobutane	1.53
n-butane	0.76
N_2	0.10

The procedure of the slow constant cooling (SCC) method was as follows: (1) 20 ml of KHI aqueous solution was loaded to each cell. (2) Air in the cells was removed by a pump. Approximately 5 bar of the SNG mixture was then purged into the cells. Then, the system was evacuated once more. (3) The cells were pressurized up to 76 bar with the SNG at the temperature of 20.5 °C and then the valve of each cell was closed. (4) The cells were slowly cooled from 20.5 °C to 2 °C at an average rate of 1 °C/h and were continuously rocked with a maximum angle of 40° at a rocking rate of 20 full swings/min. Typical graphs of the temperature and pressure versus time obtained during this procedure are shown in Figure 5.

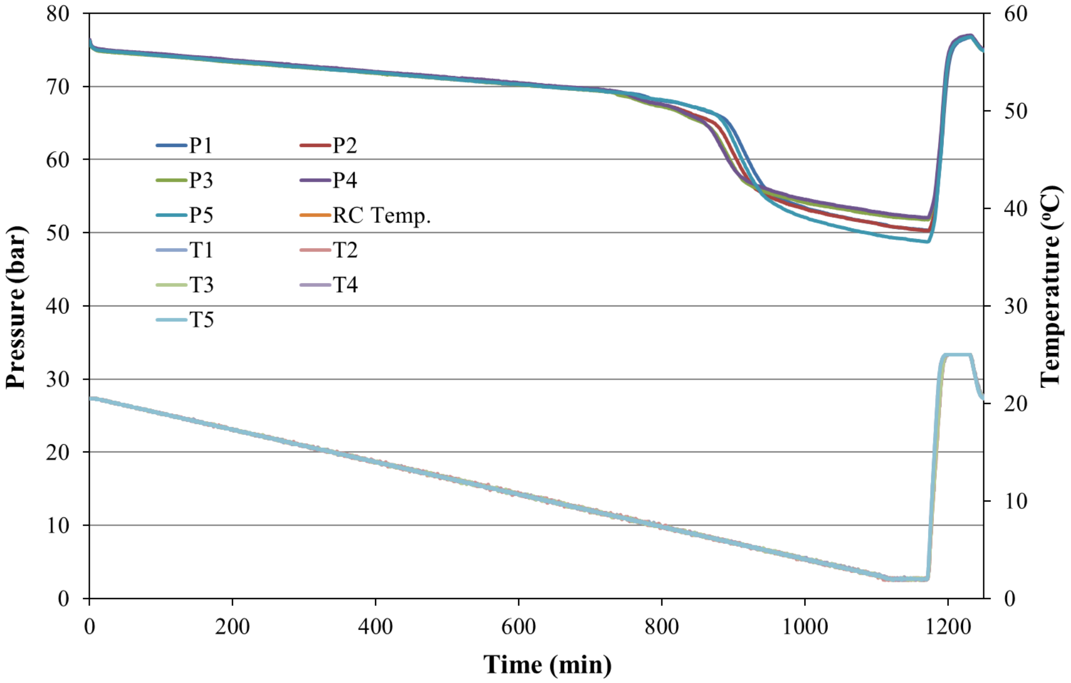

Figure 5. Typical graphs of the temperature and pressure versus time from all 5 cells. (The example shown is for a 5000 ppm solution of polymer 2b).

The temperature and pressure versus time data of each cell can be obtained and used to analyze the onset temperatures (To) and rapid hydrate formation temperatures (Ta), as shown in Figure 5. The pressure dropped a little when the rocking started, because some of the SNG mixture becomes dissolved in the aqueous phase. Then, the pressure gradually decreased in accord with the constant cooling of the cell temperature in this closed system. When gas hydrates are generated the pressure deviated from the original linear trajectory because some gas is now trapped in gas hydrate solid. The temperature corresponding to this graphical turning point is called the hydrate onset temperature (To). When the pressure curve became steepest, the temperature corresponding to this point is called the rapid hydrate formation temperature (Ta). Analyzed from Figure 6, To and Ta values of 5000 ppm of polymer 2b from cell No. 1 are 7.8

°C and 5.5 °C respectively. The subcoolings at To were also calculated compensating for the drop of pressure and the consequential drop of the equilibrium temperature at To.

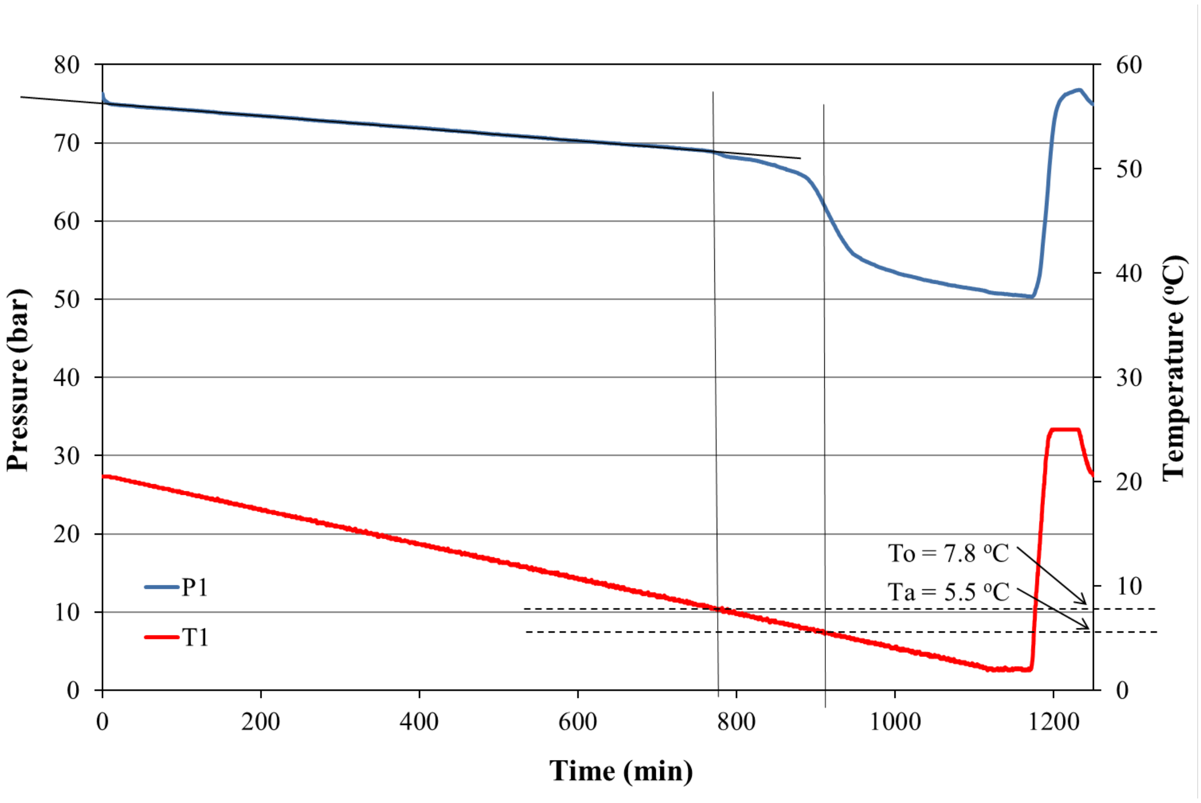

Figure 6. Typical graph of the temperature and pressure versus time data of cell No. 1. (5000 ppm of 2b solution inside).

RESULTS AND DISCUSSION

Table 3 lists a summary of the average To (and subcooling at To) and Ta values for polymers at 5000 ppm in deionized water as well as cloud point values. The results of pure water, PVP and the VP:VCap copolymer at the same concentration are also included for comparison. The average To and Ta values of each polymer were determined from minimum 8-10 standard constant cooling tests for each polymer. The experimental deviation from the average To value, giving an indication of reproducibility, was maximum ±12.6% except for the VP:VCap copolymer which was 20.1%. This is because the deviation increases as the average To value decreases and the To values for the VP:VCap copolymer are comparatively low in Table 2. However, using the subcooling data, the experimental deviation from the average subcooling value at To was maximum ±14.6% for polymer (1), Me-3M2P homopolymer. For VP:VCap copolymer the deviation is now ±8.9% based on the subcooling. Examples of the deviation in To values are given in Figure 7. The polymer with greatest deviation in this graph is polymer (B) with ±12.6% deviation for To. The subcooling deviation for this polymer is 11.2%.

Table 3. Summary of the Average To and Ta Values for Polymers at 5000 ppm and Cloud Point Values.

Additive	**Mn g/mol**	**To (av.) °C**	**ΔT at To °C**	**Ta (av.) °C**	**To (av.) - Ta (av.) °C**	**T_{Cl} °C**
No additive		17.3	3.1	17.2	0.1	
PVP K15	8000	13.3	7.0	9.1	4.2	>95
VP:VCap	<5000	6.2	13.9	3.3	2.9	78
3M2P	5500	15.2	5.1	15.0	0.2	>85
Me-3M2P	4000[a]	15.4	4.9	12.5	2.9	>85
Et-3M2P-a	1100[a]	9.2	11.0	8.5	0.7	>80
Et-3M2P-b	9000[a]	8.3	11.9	5.8	2.5	71.5
n-Pr-3M2P	6100[a]	7.8	12.3	5.9	1.9	19.8
3M2Pip	<12900*	9.5	10.7	9.3	0.2	37.6
3M2P:*N*-BuMAAm-A	4300[b]	13.0	7.3	12.6	0.4	>85

3M2P:*N*-BuMAAm-B	5500[b]	9.5	10.7	9.2	0.3	>85
3M2P:*N*-BuMAAm-C	2400[b]	8.4	11.8	8.3	0.1	47.6
3M2P:*N*-BuMAAm-D	4500[b]	8.1	12.1	8.0	0.1	33
3M2P: *N*-BuMAAm-E	3300[b]	7.2	12.9	7.0	0.2	30
3M2P: VCap-i	4800[a]	8.0	12.2	7.5	0.5	67.2
Me-3M2P: VCap-ii	7600[a]	8.4	11.8	7.2	1.2	41

[a] Number average molecular weights obtained from DMAc SEC.

[b] Number average molecular weights obtained from ^1H NMR spectroscopy.

* See discussion about molecular weight of this polymer.

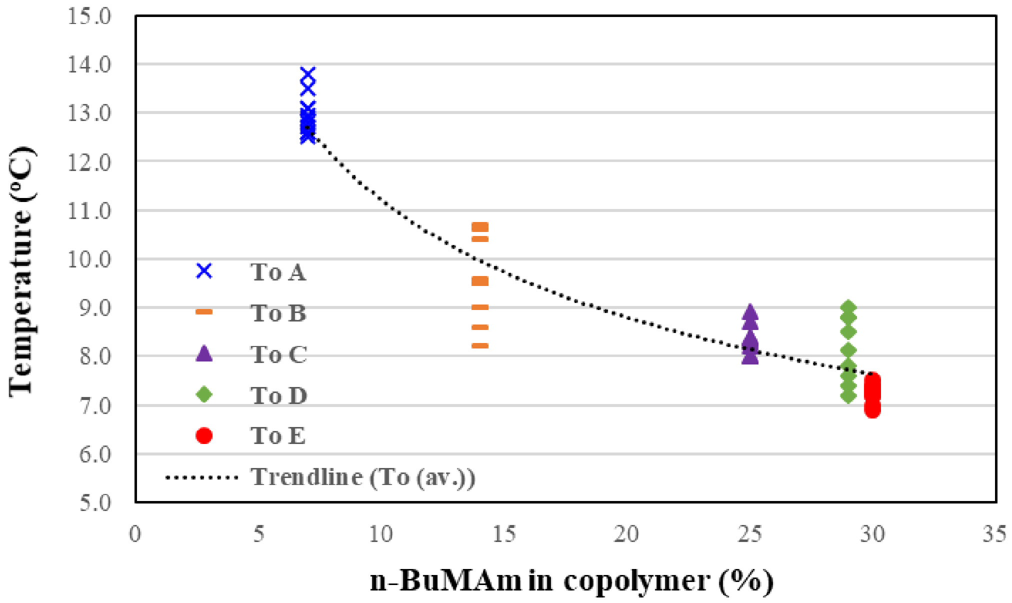

Figure 7. Onset temperatures for 3M2P: n-BuMAm copolymers with different n-BuMAm ratios at 5000 ppm.

To determine whether one polymer had performed better as a KHI than another we used statistical t-tests based on the To values, which for the reproducibility obtained in our experiments usually requires a minimum of 8-10 tests for statistical significance at the 95% confidence level ($p < 0.05$).[37] The To value is considered the most important temperature parameter of evaluating the performance of KHIs as it refers to the first detectable gas hydrate formation. The Ta value is the temperature of the rapid gas hydrate formation, which illustrates the threshold of a KHI preventing the gas hydrate growth. To-Ta is the difference between the To and Ta values, which can give an indication of the ability of a KHI to delay the rapid gas hydrate growth after the first detection of gas hydrate formation. However, caution must be used because the growth rate will depend on the subcooling in the system at To.

All polymers gave better KHI performance than pure water. Concerning the alkylated 3M2P polymers, poly(*N*-methyl-3-methylene-2-pyrrolidone) (Me-3M2P) gave a To (av.) value of 15.4 °C, which was similar to the KHI performance of poly(3-methylene-2-pyrrolidone) (P(3M2P)) (To(av.) = 15.2 °C, at 5000 ppm) reported previously in our group.[14] However, when the pendant hydrophobic alkyl groups became longer, the To values dropped significantly. For example, poly(*N*-ethyl-3-methylene-2-pyrrolidone) (Et-3M2P-a) which has a low M_n value of 1100 g/mol gave a To (av.) value of 9.2 °C, which was statistically significantly lower than that of Me-3M2P and PVP using a comparative t-test. This shows the importance of a larger hydrophobic group than methyl to obtain a significant effect on the KHI performance. As the molecular weight may have an effect on the KHI performance, a second homopolymer Et-3M2P-b was synthesised with higher molecular weight (9000 g/mole). Results show that there was statistically significantly lower To (av.) value for Et-3M2P-b. In general, a higher molecular weight gives a lower KHI performance with low molecular weights in the region 1500−3000 g/mol often performing the best for monomodal distributions.[12,16,34,38] However, in this case, an M_n value of 1100g/mol for polymer 2a may be under the limit for optimum KHI performance. In addition, the good performance of the Et-3M2P-a with higher molecular weight maybe due to its lower cloud point, as the cloud point of polymers also play an important role on KHI performance.[11] Thus, the lower cloud point of polymer Et-3M2P-b (71.5 ºC) compared to Et-3M2P-a (> 80 ºC), suggests greater hydrophobic interaction with the water phase for Et-3M2P-b which may contribute to the better KHI performance.

The next polymer up in the alkylated 3M2P series, poly(N-n-propyl-3-methylene-2-pyrrolidone) (n-Pro-3M2P) gave a To (av.) value of 8.3 ºC, which was statistically significantly lower ($p < 0.05$ by t-tests) than that of 2a. However, there was no statistically significantly difference between n-Pro-3M2P and 2b as $p > 0.05$ from the t-test. The iso-propylated polymer proved difficult to make. Larger alkyl groups (butyl etc.) were considered too large for the homopolymer to remain water-soluble at KHI test temperatures. Copolymerization with more hydrophilic groups is possible but we have not explored this yet.

Ring expansion was the next potential improvement we investigated. Synthesis of the 7-ring monomer 3-methylene-2-azepanone was successful. However, the polymer was very hydrophobic and polymerizations had very low conversions, likely due to the steric hindrance of the large ring. We did manage to synthesise both the 6-ring monomer and its polymer, poly(3-methylene-2-piperidone) (3M2Pip) via conventional radical polymerization, using 4,4′-azobis(4-cyanovaleric acid) (ACVA) as initiator. The solubility trend of poly(3M2Pip) resembled poly(3M2P)'s resistance to solubilize in various organic solvents, and indicated to also only being soluble in hexafluoroisopropanol (HFIP) and water. The exact molecular weight was not obtained as we required size exclusion chromatography (SEC) with HFIP as mobile phase, which was not available. However, in a smaller preliminary study using azobisisobutyronitrile (AIBN) as initiator (monomer:initiator = 220:1) the Mn value of that polymer was 12 900 g/mol with a dispersity of 1.64. The sample of poly(3M2Pip) used in this study used a monomer:ACVA ratio 75:1. So we assumed the tested sample would have a lower Mn than 12900 g/mol.

The 6-membered ring 3M2Piperidone homopolymer was water-soluble at room temperature and seemed to have a cloud point temperature on warming. However, on closer investigation we realized it was not thermoresponsive behaviour but the cloudiness-to-clear transition on cooling the solution was attributed by the pH of the water (polyampholyte).

The 3M2Piperidone homopolymer gave superior KHI performance to P(3M2P) with To (av.) of 9.5 °C. This confirms the hypothesis that the KHI performance improves as the lactam ring size increases, as reported for 5−8-ring poly(*N*-vinyl lactam)s.[34,38]

The third potential method to improve the performance of P(3M2P) was to copolymerize the 3M2P monomer with more hydrophobic monomers. VCap was an obvious choice since it is widely used as the more hydrophobic component in a range of VCap:VP based co- and terpolymers. We made one VCap copolymer with 3M2P with monomer ratio 53:47, and one VCap copolymer with Me-3M2P with monomer ratio 50:50.

The two copolymers gave very similar KHI performance with To values of 8.0 °C and 8.4 °C, respectively. Two factors may be operating against each other to give this result. Firstly, Me-3M2P:VCap copolymer had a lower cloud point value (Tcl = 41 °C) due to the higher percentage of VCap monomer and the extra methyl group in the pyrrolidone ring in the Me-3M2P monomer. This means Me-3M2P:VCap copolymer has higher hydrophobicity than 3M2P:VCap copolymer which can be helpful for KHI performance as discusssed earlier. However, Me-3M2P:VCap copolymer has a higher molecular weight which is detrimental for KHI efficacy. These two factors may be cancelling each other out, giving the result of similar To (av.) values. We also speculate that the Me-3M2P: VCap copolymer was not at the ideal monomers ratio, as early studies shown that there is an optimal molar ratio for a copolymer with two KHI-active monomers giving the best KHI effect.[3,20]

For the copolymers of 3M2P with *N*-n-butyl(meth)acrylamide (3M2P:n-BuMAm), a trend can be seen that the KHI performance of the copolymers increased with increasing percentage of n-BuMAm in the copolymer. When the percentage of n-BuMAm in the copolymer increased from 7 to 30 %, the To (av.) value dropped considerably from 13.0 to 7.2 °C. The To values for 3M2P:n-BuMAm copolymers are also illustrated in Figures 6 showing the spread of results. The increase in KHI performance is also in line with the decrease in cloud point. For the two copolymers with similar low cloud points, D and E, copolymer E probably gives a lower To value due to the lower molecular weight (2200 g/mol).

Two of the best copolymers in this study, 3M2P:n-BuMAm-E and 3M2P:VCap, were evaluated at varying concentrations. The To (av.) values at 1000, 2500, and 5000 ppm are summarized in Table 4 and Figure 8. The data for the VP:VCap copolymer are also included for comparison. The results indicate that the KHI effect of the three copolymers became stronger as the concentration increased within the range from 1000 to 5000 ppm. At low concentration (1000 ppm), 3M2P:n-BuMAm-E almost had the same good KHI performance as the commercialized VP:VCap copolymer. However, as the concentration was increased the performance gap (i.e. the difference in To (av.) values) between the copolymers increased. The 3M2P:VCap copolymer showed worse KHI performance than VP:VCap copolymer at all concentrations tested in this study.

The reason why the new copolymers give lower KHI performance compared to the VP:VCap copolymer may be as follows: firstly, the 3M2P unit, which is the constant monomer in the new copolymers, is not as good as *N*-vinylpyrrolidone (NVP) in Luvicap 55W. Although 3M2P is structural similar to NVP, the pendant hydrophobic group in the former is shorter than that in the latter, which may be the main reason leading to its relatively poor KHI effect. The detailed explanations of why PVP perform slightly better than P(3M2P) were reported in our previous study.[14] Second, the new copolymers may have not reached their optimal monomer ratio to get the best KHI performance as discussed earlier.

Table 4. Summary of the Average To and Ta at 1000, 2500, and 5000 ppm for i and E and VP:VCap copolymer for comparison.

Entry at 1000 ppm	**To (av.) (ºC)**	**Ta (av.) (ºC)**	**To (av.) - Ta (av.) (ºC)**
3M2P:VCap	11.0	10.5	0.5
3M2P:n-BuMAm-E	10.2	10.0	0.2
VP:VCap	10.1	9.0	1.1
Entry at 2500 ppm	**To (av.) (ºC)**	**Ta (av.) (ºC)**	**To (av.) - Ta (av.) (ºC)**
3M2P:VCap	10.1	8.9	1.2
3M2P:n-BuMAm-E	7.9	7.6	0.3
VP:VCap	7.4	6.0	1.4
Entry at 5000 ppm	**To (av.) (ºC)**	**Ta (av.) (ºC)**	**To (av.) - Ta (av.) (ºC)**
3M2P:VCap	8.0	7.5	0.5
3M2P:n-BuMAm-E	7.2	7.0	0.2
VP:VCap	6.2	3.3	2.9

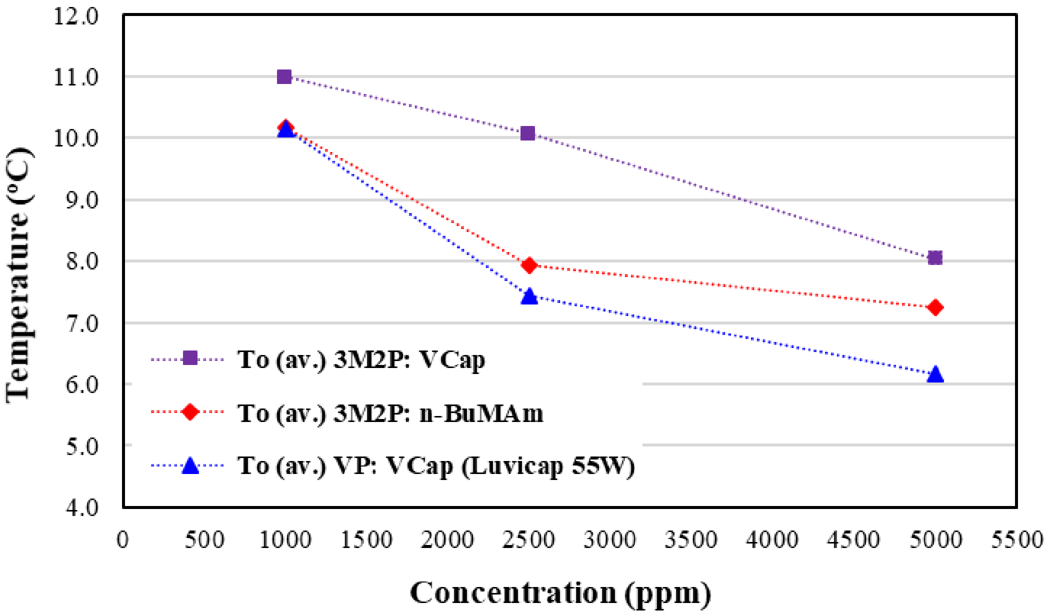

Figure 8. Average To values of i, E and VP:VCap copolymer versus concentration.

CONCLUSION

In this study, we have synthesized a series of water-soluble alkylated 3-methylene-2-pyrrolidone homopolymers, 3-methylene-2-pyrrolidone copolymers with PVCap or n-BuMAm, as well as poly(3-methylene-2-piperidone). These polymers were investigated as structure II gas hydrate inhibitors for the first time. Their KHI performance were studied in high-pressure rocking cells using slow constant cooling method.

It was found that the alkylated 3-methylene-2-piperidone homopolymers with large hydrophobic alkyl groups, such as ethyl and n-propyl groups, performed the best. The *N*-vinylcaprolactam and N-n-butyl(meth)acrylamide comonomers could improve the KHI performance considerably. For 3-methylene-2-pyrrolidone with N-n-butyl(meth)acrylamide (3M2P: n-BuMAm) copolymer series, there was a trend shown that the KHI performance improved as the percentage of n-BuMAm increased. In addition, the best two copolymers were tested at varying concentrations range from 1000 to 5000 ppm. Better KHI performance came out when the solution contained higher doses. The poly(3-methylene-2-piperidone) that with one more carbon atom in each pendant group unit than the poly(3-methylene-2-pyrrolidone) also shown obviously better KHI performance.

Based on the discoveries above, we believe that adding suitable size alkyl groups and copolymerizing with other monomers are easy and effective methods to explore new KHIs. We are currently investigating more alkylated 3-methylene-2-pyrrolidone homopolymers with larger alkyl groups, such as n-butyl and isopentyl, as well as more copolymers for further confirming our findings. In addition, adding synergists is worth trying to improve KHI performance of these new polymers.

REFERENCES

1. Jr, E. D. S., Fundamental principles and applications of natural gas hydrates. *NATURE* **2003,** *426*.

2. Sloan, E. D., Clathrate Hydrates of Natural Gases. **2007**.

3. Kelland, M. A., History of the development of low dosage hydrate inhibitors. *Energy & Fuels* **2006,** *20* (3), 825-847.

4. Chong, Z. R.; Yang, S. H. B.; Babu, P.; Linga, P.; Li, X. S., Review of natural gas hydrates as an energy resource: Prospects and challenges. *Applied Energy* **2016,** *162*, 1633-1652.

5. Sloan, E. D., A changing hydrate paradigm - from apprehension to avoidance to risk management. *Fluid Phase Equilib.* **2005,** *228*, 67-74.

6. Kelland, M. A., Production Chemicals for the Oil and Gas Industry, Second Edition. *CRC Press* **2014**, 219-245.

7. Perrin, A.; Musa, O. M.; Steed, J. W., The chemistry of low dosage clathrate hydrate inhibitors. *Chem Soc Rev* **2013,** *42* (5), 1996-2015.

8. Creek, J. L., Efficient Hydrate Plug Prevention. *Energy & Fuels* **2012,** *26* (7), 4112-4116.

9. Ajiro, H.; Takemoto, Y.; Akashi, M.; Chua, P. C.; Kelland, M. A., Study of the Kinetic Hydrate Inhibitor Performance of a Series of Poly(N-alkyl-N-vinylacetamide)s. *Energy & Fuels* **2010,** *24* (12), 6400-6410.

10. Chua, P. C.; Kelland, M. A.; Ajiro, H.; Sugihara, F.; Akashi, M., Poly(vinylalkanamide)s as Kinetic Hydrate Inhibitors: Comparison of Poly(N-vinylisobutyramide) with Poly(N-isopropylacrylamide). *Energy & Fuels* **2013,** *27* (1), 183-188.

11. Kelland, M. A.; Abrahamsen, E.; Ajiro, H.; Akashi, M., Kinetic Hydrate Inhibition with N-Alkyl-N-vinylformamide Polymers: Comparison of Polymers ton-Propyl and Isopropyl Groups. *Energy & Fuels* **2015,** *29* (8), 4941-4946.

12. Reyes, F. T.; Kelland, M. A., First Investigation of the Kinetic Hydrate Inhibitor Performance of Polymers of Alkylated N-Vinyl Pyrrolidones. *Energy & Fuels* **2013,** *27* (7), 3730-3735.

13. Heyns, I. M.; Pfukwa, R.; Klumperman, B., Synthesis, Characterization, and Evaluation of Cytotoxicity of Poly(3-methylene-2-pyrrolidone). *Biomacromolecules* **2016,** *17* (5), 1795-800.

14. Abrahamsen, E.; Heyns, I. M.; von Solms, N.; Pfukwa, R.; Klumperman, B.; Kelland, M. A., First Study of Poly(3-methylene-2-pyrrolidone) as a Kinetic Hydrate Inhibitor. *Energy & Fuels* **2017,** *31* (12), 13572-13577.

15. Klumperman, L.; Pfukwa, R.; Heyns, I. M. 3-Methylene-2-pyrrolidone based polymers. International Patent Application WO 2017/029630.

16. Reyes, F. T.; Kelland, M. A., Investigation of the Kinetic Hydrate Inhibitor Performance of a Series of Copolymers of N-Vinyl Azacyclooctanone on Structure II Gas Hydrate. *Energy & Fuels* **2013,** *27* (3), 1314-1320.

17. Mady, M. F.; Kelland, M. A., N,N-Dimethylhydrazidoacrylamides. Part 1: Copolymers with N-Isopropylacrylamide as Novel High-Cloud-Point Kinetic Hydrate Inhibitors. *Energy & Fuels* **2014,** *28* (9), 5714-5720.

18. Ree, L. H. S.; Mady, M. F.; Kelland, M. A., N,N-Dimethylhydrazidoacrylamides. Part 3: Improving Kinetic Hydrate Inhibitor Performance Using Polymers of N,N-Dimethylhydrazidomethacrylamide. *Energy & Fuels* **2015,** *29* (12), 7923-7930.

19. Zhang, Q.; Kawatani, R.; Ajiro, H.; Kelland, M. A., Optimizing the Kinetic Hydrate Inhibition Performance of N-Alkyl-N-vinylamide Copolymers. *Energy & Fuels* **2018,** *32* (4), 4925-4931.

20. Colle, K. S.; Oelfke, R. H.; Kelland, M. A. METHOD FOR INHIBITING HYDRATE FORMATION. 1999.

21. Angel, M.; Neubecker, K.; Stein, S. World Patent Application WO 2004/042190, 2004.

22. Namba, T.; Fujii, Y.; Saeki, T.; Kobayashi, H. WO Patent Application 96/37684, 1996.

23. Heyns, I. M.; Pfukwa, R.; Klumperman, B., Synthesis, Characterization, and Evaluation of Cytotoxicity of Poly(3-methylene-2-pyrrolidone. *Biomacromolecules* **2016**, *17* (5), 1795-800.

24. Iskander, G. M.; Ovenell, T. R.; Davis, T. *Macromol. Chem. Phys.* **1996**, *197*, 3123–3133.

25. Ritter, H.; Schwarz-Barac, S.; Stein, P. *Macromolecules* **2003**, *36* (2), 318–322.

26. Harrison, T. J.; Dake, G. R. *J. Org. Chem.* **2005**, *70* (26), 10872–10874.

27. Riofski, M. V; John, J. P.; Zheng, M. M.; Kirshner, J.; Colby, D. A. *J. Org. Chem.* **2011**, *76*, 3676–3683.

28. David, G.; Loubat, C.; Boutevin, B.; Robin, J. J.; Moustrou, C. *Eur. Polym. J.* **2003**, *39* (1), 77–83.

29. Gjertsen, L. H.; Fadnes, F. H., Measurements and predictions of hydrate equilibrium conditions. In *Gas Hydrates: Challenges for the Future*, Holder, G. D.; Bishnoi, P. R., Eds. New York Acad Sciences: New York, 2000; Vol. 912, pp 722-734.

30. Tohidi, B.; Burgass, R. W.; Danesh, A.; Østergaard, K. K.; Todd, A. C. Improving the Accuracy of Gas Hydrate Dissociation Point Measurements, Annals of the New York Academy of Sciences **2006**, *912*(1), 924 – 931.

31. Arjmandi, M.; Tohidi, B.; Danesh, A.; Todd, A. C., Is subcooling the right driving force for testing low-dosage hydrate inhibitors? *Chem. Eng. Sci.* **2005,** *60* (5), 1313-1321.

32. Zhang, Q.; Shen, X.; Zhou, X.; Liang, D., Inhibition Effect Study of Carboxyl-Terminated Polyvinyl Caprolactam on Methane Hydrate Formation. *Energy & Fuels* **2017,** *31* (1), 839-846.

33. Ke, W.; Kelland, M. A., Kinetic Hydrate Inhibitor Studies for Gas Hydrate Systems: A Review of Experimental Equipment and Test Methods. *Energy & Fuels* **2016,** *30* (12), 10015-10028.

34. Chua, P. C.; Kelland, M. A., Poly(N-vinyl azacyclooctanone): A More Powerful Structure II Kinetic Hydrate Inhibitor than Poly(N-vinyl caprolactam). *Energy & Fuels* **2012,** *26* (7), 4481-4485.

35. Mady, M. F.; Min Bak, J.; Lee, H.-i.; Kelland, M. A., The first kinetic hydrate inhibition investigation on fluorinated polymers: Poly(fluoroalkylacrylamide)s. *Chem. Eng. Sci.* **2014,** *119*, 230-235.

36. Abrahamsen, E.; Kelland, M. A., Carbamate Polymers as Kinetic Hydrate Inhibitors. *Energy & Fuels* **2016,** *30* (10), 8134-8140.

37. Walpole, R. E.; Myers, R. H.; Myers, S. L.; Walpole, R. E.; Ye, K. Probability and Statistics for Engineers and Scientists, 8th ed.; Pearson Education: Upper Saddle River, NJ, USA, 2007.

38. O'Reilly, R.; Ieong, N. S.; Chua, P. C.; Kelland, M. A., Missing Poly(N-vinyl lactam) Kinetic Hydrate Inhibitor: High-Pressure Kinetic Hydrate Inhibition of Structure II Gas Hydrates with Poly(N-vinyl piperidone) and Other Poly(N-vinyl lactam) Homopolymers. *Energy & Fuels* **2011,** *25* (10), 4595-4599.

Paper IV

Study of the Kinetic Hydrate Inhibitor Performance of Poly (*N*-vinyl caprolactam) and Poly (*N*-isopropyl methacrylamide) with Varying End Caps

Authors:

Qian Zhang and Malcolm A. Kelland*

Published in Energy & Fuels 2018, 32 (9), 9211-9219.

Study of the Kinetic Hydrate Inhibitor Performance of Poly(*N*-vinylcaprolactam) and poly(*N*-isopropylmethacrylamide) with Varying End-caps

Qian Zhang and Malcolm A. Kelland*

Department of Mathematics and Natural Science, Faculty of Science and Technology, University of Stavanger, N-4036 Stavanger, Norway

* Corresponding author: Tel.: +47 51831823; fax +47 51831750

E-mail address: malcolm.kelland@uis.no (M.A. Kelland)

ABSTRACT

Poly(*N*-vinylcaprolactam) (PVCap) is an effective kinetic hydrate inhibitor (KHI) that has been widely used in both industry applications and laboratory studies. Industrially, organic peroxides are often used as the VCap polymerization initiator. In our own past studies we usually make PVCap by polymerizing VCap with azoisobutyronitrile (AIBN) giving a 2-cyanoprop-2-yl polymer end cap. In this study, VCap was polymerized with AIBN and a series of mercaptocarboxylic acid chain transfer agents (CTAs) to modify the end groups of PVCap. These end-group-modified PVCaps were investigated as KHIs in high-pressure rocking cells. Some of them showed better KHI performance than PVCap made with AIBN alone. The mercaptoacetic acid-group-modified PVCap (PVCapSCH$_2$COOH) had significantly better inhibition performance than the normal PVCap on both structure I (sI) and structure II (sII) gas hydrate-forming systems in aqueous solution, as well as a SII hydrate-forming system containing added decane. However, the most powerful sII gas hydrate inhibitor among these end-group-modified PVCaps in this study was found to be the mercaptosuccinic acid-group-modified PVCap ($\text{PVCapSCH(COOH)CH}_2\text{COOH}$). For example, in slow constant cooling tests at 76 bar with the sII gas hydrate-forming gas mixture, 2500 ppm $\text{PVCapSCH(COOH)CH}_2\text{COOH}$ in deionized water gave first detectable hydrate formation at an average temperature (To(av)) of 8.5 °C. In contrast, PVCap made with AIBN alone gave a statistically significant and higher To(av) value of 9.7 °C. In contrast, 4-mercaptobenzoic acid-group-modified PVCap ($\text{PVCapSC}_6\text{H}_4\text{COOH}$) in deionized water increased the To(av) value to 10.5 °C. We also introduced the mercaptoacetic acid and mercaptosuccinic acid groups into poly(*N*-isopropylmethacrylamide) (PNIPMAA) polymers, again using AIBN as initiator. Both of the end-group-modified PNIPMAAs gave superior KHI performance than PNIPMAA made using AIBN alone.

INTRODUCTION

In pipelines and wells where water is present with natural gas at elevated pressure and low temperature conditions, the conditions are thermodynamically suitable for gas hydrates formation.[1-2] Gas hydrate is an ice-like solid, which can block the flow in pipelines, causing dramatic economic loss and even lead to explosion disasters if not handled correctly.[3-4] From the microstructure point of view, gas hydrates are made of cages formed by water molecules via hydrogen bonds, and there are guest gas molecules trapped through van der Waal forces inside these water cages. Based on the size and category of guest gas molecules, gas hydrates form three main types of clathrate crystal structures: structure I (sI), structure II (sII) and structure H (sH).[5]

In order to control gas hydrate formation in oil and gas production flow lines, plenty of hydrate prevention methods have been proposed, among which injecting low dosage hydrate inhibitors

(LDHIs) is now a well-known and reliable method. Both CAPEX and OPEX savings can be made compared to the use of traditional technology such as the use of thermodynamic inhibitors.[6-7] Kinetic hydrate inhibitors (KHIs) is one of the two classes of LDHI, the other being anti-agglomerants (AAs). KHIs can delay the gas hydrate nucleation and/or growth for a period of time, thus guaranteeing oil and gas production pipeline flow to the destination.[8-13]

Effective KHIs include water-soluble polymers contain several repeating amides groups, such as poly(*N*-vinylcaprolactam) (PVCap), poly(*N*-alkyl(meth)acrylamide)s, and poly(*N*-alkylvinylamide)s and copolymers thereof. (Figure 1)[14-17] Although a great number of KHIs have been discovered, their inhibition mechanisms are not fully understood. However, some theories have been suggested.[18-21]

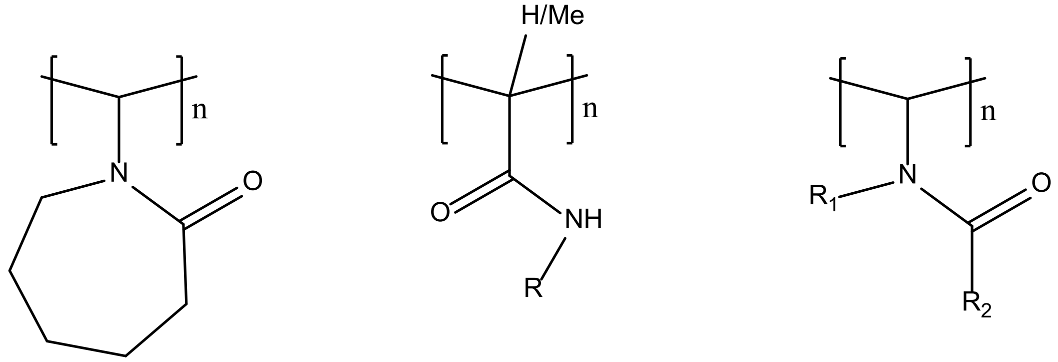

Figure 1. From left to right, poly(*N*-vinylcaprolactam) (PVCap), poly(*N*-alkyl(meth)acrylamide)s and poly(*N*-alkylvinylamide)s.

Homopolymers and copolymers of N-vinyl caprolactam (VCap) are among the most common KHIs and are commercially available from several companies. Industrially, organic peroxides are often used as the VCap polymerization initiator. In our own past studies we usually make PVCap by polymerizing VCap with azoisobutyronitrile (AIBN) giving a 2-cyanoprop-2-yl polymer end cap (Table 1). PVCap homopolymer has good kinetic inhibition effect and depending on the method of manufacture has been suggested useful for subcoolings up to 10-12 °C for sII hydrates.[4] In addition, the cloud point (Tcl) of PVCap is approximately 35 °C, while the temperature of injection points in industry may be as high as 60-120 °C.[7] The two weak points mentioned above limit the application range of PVCap. Some methods to improve the performance have been studied, such as copolymerizing it with other KHIs, adding synergists, etc.[22-25] Nga Sze Ieong et al showed that the use of chain-transfer agents can significantly change the biocompatible, thermoresponsive and amphiphilic nature of polymers.[26] Qian Zhang et al showed that polymerization with addition of chain-transfer agent (CTA) mercaptoacetic acid, can significantly improve the inhibition performance of PVCap on sI hydrates.[27] Although CTAs are used to produce lower polymer molecular weights, GPC studies showed that the performance improvement was not due to differences in polymer molecular weight. CTAs are chemicals that can cause chain transfer effects on the growing activity polymer chains during the free radical polymerization reaction.[28] They can react with the free radicals at the end of polymer chains, therefore, different function groups can possibly be added to the end of the polymers.[29] This kind of end-capping method maybe an easier synthetic route to improve the KHI performance.

Table 1. Common commercial polymerization initiators.

Initiator	Chemicals Structure	Radical generated
Benzoyl peroxide (BPO)	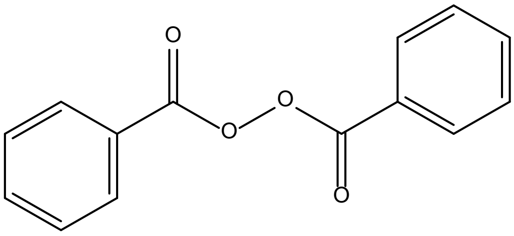	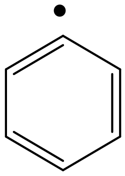

Di-tert-butyl peroxide (DTBP)	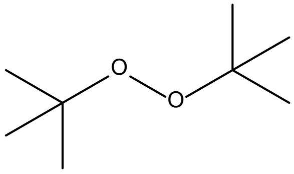	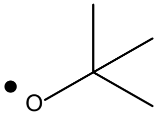
Azoisobutyronitrile (AIBN)	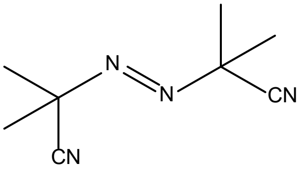	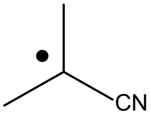

In this paper, we reported the KHI performance results of a series of end-group-modified PVCaps and poly N-isopropylmethacrylamides (PNIPMAAs) using both pure methane gas, forming sI hydrates, and synthetic natural gas (SNG) forming sII hydrates. We studied these modified KHIs not only in gas + water system, but also in gas + water + decane system. All KHI performance studies were carried out in high-pressure steel rocking cells.

EXPERIMENTAL SECTION

Materials

N-vinyl caprolactam monomer (NPVCap) was obtained from Ashland and *N*-isopropylmethacrylamide monomer (NIPMAA) was obtained from Evonik. Both were 99+% pure by NMR spectroscopic analysis. 2-propanol (iPrOH), diethyl ether (EE), and chloroform-D ($CDCl_3$) were obtained from VWR. Decane, 2,2`-azodiisobutyronitrile (AIBN), mercaptoacetic acid, mercaptosuccinic acid, 4-mercaptobenzonic acid, 12-mercaptododecanoic acid, and 16-mercaprohexadecanoic acid were obtained from Merck (Sigma-Aldrich). All chemicals were used without further purification. A balance with an uncertainty of ± 0.001 g was used to weigh chemicals. The deionized water was our lab-made, with a resistivity of around 18 mΩ cm^{-1}.

Polymer characterization

Nuclear magnetic resonance (NMR) spectrograms were measured by a Bruker ASCEnd™ 400 system. The Mw values of polymers were measured by an A JASCO Chem NAV size-exclusion chromatography (SEC) system at 40 °C with DMF as the eluent.

Synthesis Method for Polymers

(1) Synthesis method of normal PVCap and PNIPMAA (with no CTAs added): 0.1 g AIBN, 10.0 g NPVCap (or NIPMAA when synthesizing PNIPMAA), and 30 mL iPrOH were introduced into a 100 mL round-bottomed flask. Then, the system was vacuumed/flushed 3-5 times with N_2. Under N_2, the mixture was heated to 80 °C and stirred for about 7 hours. The iPrOH solvent was then removed using a vacuum rotary evaporator. Then, 50 mL EE was added into the solid residue, the mixture stirred overnight and filtered to obtain the solid product. ^1H NMR spectroscopy indicated that greater than 99% monomer was converted into polymer. PVCap. ^1H NMR ($CDCl_3$) δ: 1.2−1.9 ppm (broad), 2.2−2.6 ppm (broad), 2.8−3.4 ppm (broad), 4.2−4.6 ppm (broad).

(2) Synthesis method of end-group-modified PVCaps and PNIPMAAs was carried out in an identical way and scale except that 0.3g mercaptocarboxylic acid was also added to the mixture (Figure 2, Table 2). ^1H NMR spectroscopy indicated that greater than 99% monomer was conversed into polymer. Besides the characteristic peaks of the polymer, a peak in the location of 9.7 ppm could also be observed in the respective ^1H NMR spectra of mercaptoacetic acid-

group-modified PVCap (PVCapSCH$_2$COOH), mercaptosuccinic acid-group-modified PVCap (PVCapSCH(COOH)CH$_2$COOH), 4-mercaptobenzonic acid-group-modified PVCap (PVCapSC$_6$H$_4$COOH), 12-mercaptododecanoic acid-group-modified PVCap (PVCapSC$_{11}$H$_{22}$COOH), and 16-mercaprohexadecanoic acid-group-modified PVCap (PVCapSC$_{15}$H$_{30}$COOH). This peak indicates that there are carboxyl groups in these modified polymers, showing that the target mercaptocarboxylic acid group was successfully introduced into the corresponding polymer molecule. Table 2 summarizes the polymers made and their SEC molecular weight analysis. The PVCap polymers have similar molecular weights to avoid this factor affecting the KHI performance. We were less successful with the PNIPMAA polymers in getting similar molecular weights, in particular the mercaptosuccinic acid polymer gave a much lower Mn value than the other two polymers. The consequences of this are discussed later.

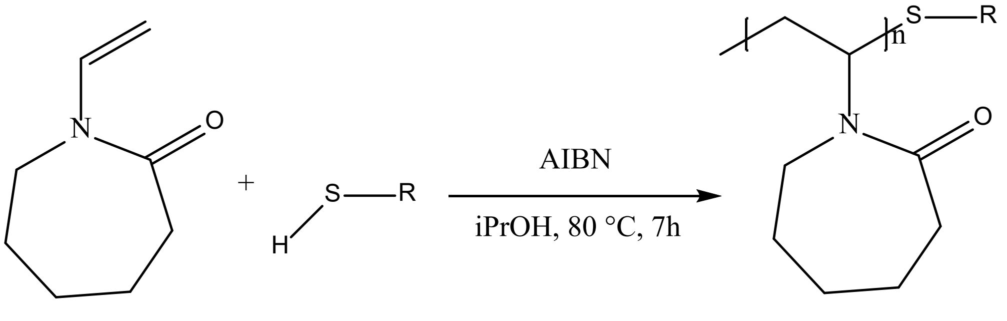

Figure 2. Synthesis of mercaptocarboxylic acid group modified PVCap. R = acetic acid group, succinic acid group, benzoic acid group, dodecanoic acid group and hexadecanoic acid group.

Table 2. Summary of synthesized polymers and molecular weight data.

Polymer	**Chain transfer agent**	**Mn[a]**	**PDI[a]**

PVCap		4403	2.42
PVCapSCH$_2$COOH	Mercaptoacetic acid	3350	2.25
PVCapSCH(COOH)CH$_2$COOH	Mercaptosuccinic acid	4006	2.55
PVCapSC$_6$H$_4$COOH	4-Mercaptobenzoic acid	5404	2.03
PVCapSC$_{11}$H$_{22}$COOH	12-Mercaptododecanoic acid	5586	2.02
PVCapSC$_{15}$H$_{30}$COOH	16-Mercaptohexadecanoic acid	6530	2.01
PNIPMAA		12088	2.18
PNIPMAASCH$_2$COOH	Mercaptoacetic acid	10812	29.34
PNIPMAASCH(COOH)CH$_2$COOH	Mercaptosuccinic acid	1965	4.7

[a] Determined by size-exclusion chromatography (SEC).

Cloud Point (Tcl) Measurement

0.25 g of polymer was dissolved in 100 mL of deionized water. 10 mL of this solution was loaded in a test tube and heated slowly. The solution in the tube was stirred and was observed carefully throughout the heating procedure. The cloud point (Tcl) was obtained at the temperature at which the first visual sign of clouding (haze) appeared. Each test was repeated three times.

High-pressure Rocker Rig Tests with Synthetic Natural Gas (SNG) Mixture and Pure Methane Gas

Similar to previous KHI studies from our group,[9, 13, 30-32] a rocker rig supplied by PSL Systemtechnik, Germany, was used to evaluate the inhibition performance of the end-group-modified KHIs. This rocker rig equipment contains five separate steel cells, with a volume of

40ml for each cell. Normally 20ml aqueous solution was loaded into each cell for testing. When starting rocking, the steel ball in each cell agitates the solution inside. Pure methane gas was used as the sI hydrate-forming gas, while a synthetic natural gas (SNG) mixture was used as the sII hydrate-forming material (Table 3).

Table 3. Composition of SNG mixture used in this study.

Component	**mol %**
methane	80.67
ethane	10.20
propane	4.90
CO_2	1.84
isobutane	1.53
n-butane	0.76
N_2	0.10

The slow constant cooling method was used to evaluate the polymer KHI performance. The critical parameters determined were the hydrate onset temperature (To) and the rapid hydrate formation temperature (Ta).[12, 27] The procedure of slow constant cooling method is as follows: (1) Solution loading: 20.0 mL aqueous polymer KHI solution was loaded into each cell. 1 mL decane was added on the top of the polymer solution only when testing the KHI performance in the gas + water + liquid hydrocarbon multiphase system. (2) System cleaning: A pump was used to remove the air in the system. Then, 3-5 bars gas, which was the same type of gas used to synthesize hydrates, was used to flush the system. The system was then evacuated one more time. (3) Gas loading: When the temperature was stable at 20.5 °C, 76 bars of SNG mixture or 110 bars of pure methane gas was purged in to each cell. A higher pressure was used with methane to give sufficient subcooling to evaluate the polymers. (4) Constant cooling: The temperature of the system was lowered from 20.5 °C to 2 °C over 18.5 hours, with a cooling rate of approximately 1 °C/h. Pressure and temperature data for each cell during the cooling procedure were collected by a computer. Typical graphs from one rocker rig test (i.e. 5 cells) using constant cooling method can be found in Figure 3.

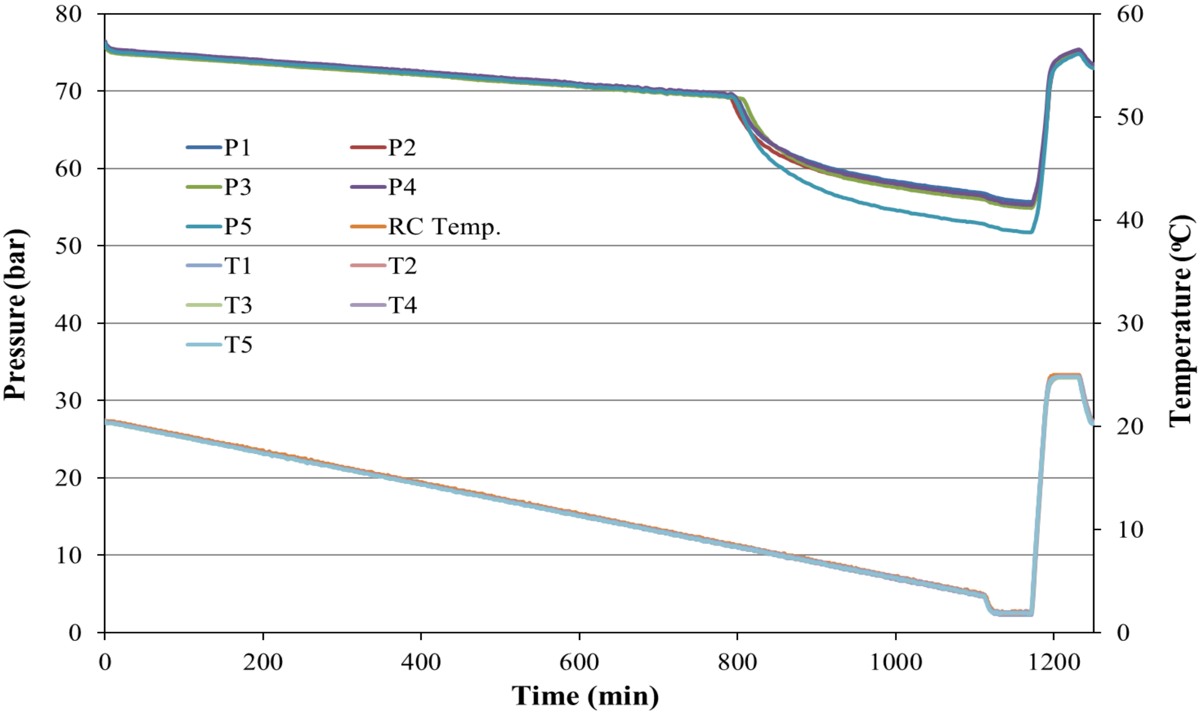

Figure 3. Pressure and temperature versus time graphs for all five cells using 2500 ppm $PVCapSC_{15}H_{30}COOH$.

At 76 bar, the equilibrium temperature (Teq) of the sII hydrate system obtained in previous studies was 20.2 ± 0.05 °C, which agrees quite well with the calculated Teq value of 20.5 °C by Calsep's PVTSim software.[9, 33] At 110 bar, the equilibrium temperature (Teq) of sI hydrates predicted by the software was 16.0 °C.

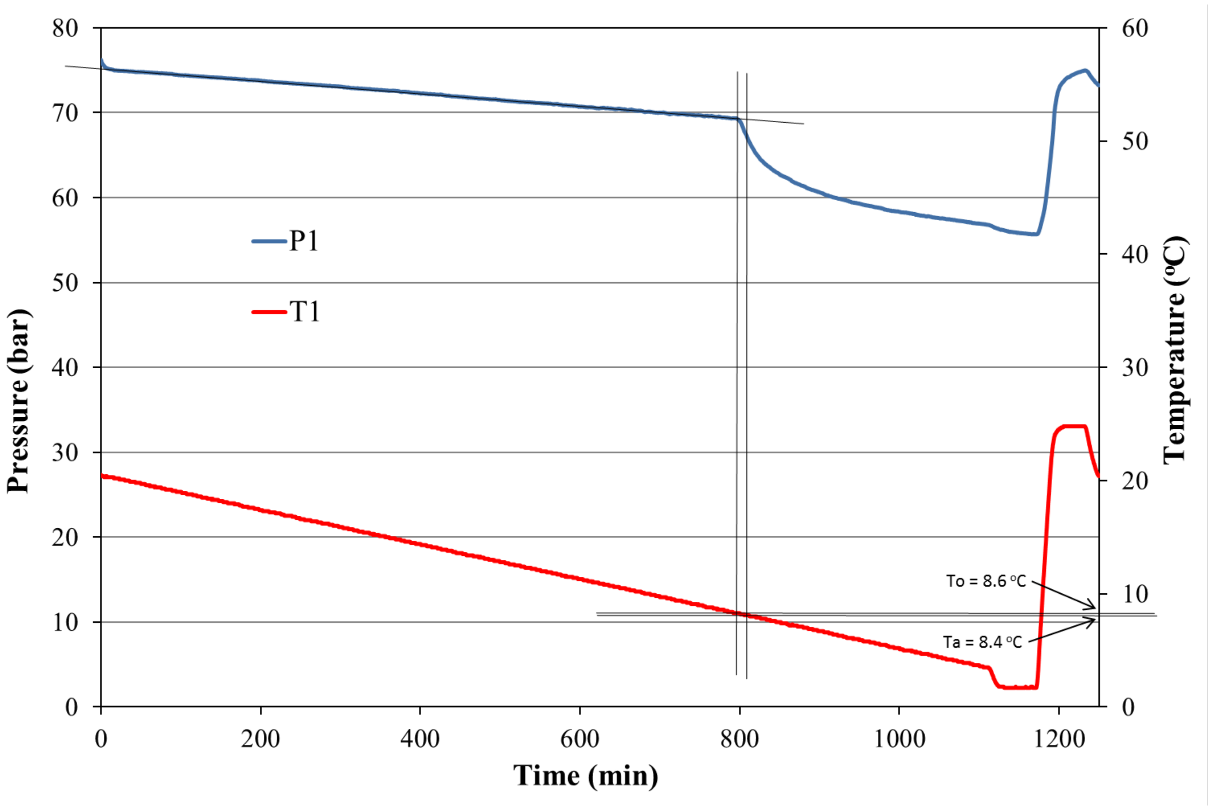

Figure 4. Typical pressure and temperature versus time graphs showing analysis of the To and Ta values from one cell.

Figure 4 shows typical pressure-time and temperature-time graphs from one cell (cell 1 in our rig). We can see from this figure that, at the very beginning, the pressure dropped a little for the reason that gas dissolves slightly in water during the initial agitation. Then the pressure decreased continuously as the temperature decreased linearly. Finally, when the gas hydrates are generated, the pressure dropped very quickly as much gas in the system gets trapped into the formed hydrate cages. The temperature corresponding to the turning point of the pressure is considered to be the To value (first observed hydrate onset temperature), while the temperature corresponding to the steepest pressure drop is called the Ta value (most rapid hydrate formation temperature).

In order to reduce the results deviations, each KHI polymer was tested 8-10 times to obtain average To and Ta values. No cell gave consistently better or worse results than others, so there was no systematic errors of these cells.

RESULTS AND DISCUSSION

The average To and Ta values (based on 8-10 constant cooling tests) for different end-group-modified KHI polymers on both sI and sII hydrates are summarized in Table 4. The To values varied by no more than ±15% whilst the Ta values varied by ±12%. This table also includes the cloud point of these KHIs. The To rather than Ta value is considered the most critical evaluation parameter for KHI performance as operators are keen to avoid any sign of hydrate formation in their flow lines in case this could gradually build up and cause a plug. Nucleation may have occurred somewhat earlier than To in our slow constant cooling laboratory tests but could not be detected on the microscopic scale. The average To values are also shown graphically in Figure 5 for easier visual comparisons. Results for deionized water (DIW) are also added to Table 4 and Figure 5.

Table 4. Summary data of the average To and Ta values for different polymers tested at 2500 ppm in deionized water for both sI and sII hydrate forming systems.

Sample	Cloud point (°C)	To(av) (°C)	Ta(av) (°C)	To(av) - Ta(av) (°C)	To(av) (°C)	Ta(av) (°C)	To(av) - Ta(av) (°C)
		sII			sI		
DIW		16.9	16.7	0.2	12.2	12.1	0.1
PVCap	35.5	9.7	9.4	0.3	7.2	7.0	0.2
PVCapSCH$_2$COOH	37.8	8.7	8.2	0.5	6.3	6.2	0.1

PVCapSCH(COOH)CH_2COOH	36.8	8.5	8.2	0.3	6.9	6.7	0.2
PVCapS$C_{11}H_{22}$COOH	35.5	9.7	9.3	0.4	7.1	7.0	0.1
PVCapS$C_{15}H_{30}$COOH	<4[a]	8.7	8.4	0.2	7.1	7.0	0.1
PVCapSC_6H_4COOH	32.8	10.5	10.1	0.4	7.9	7.7	0.2
PNIPMAA	34.1	9.3	9.1	0.2	7.7	7.5	0.2
PNIPMAASCH_2COOH	39.2	8.3	8.0	0.3	6.7	6.3	0.4
PNIPMAASCH(COOH)CH_2COOH	42.5	7.6	7.3	0.3	7.2	7.0	0.2

[a] Cloudy at 4 °C.

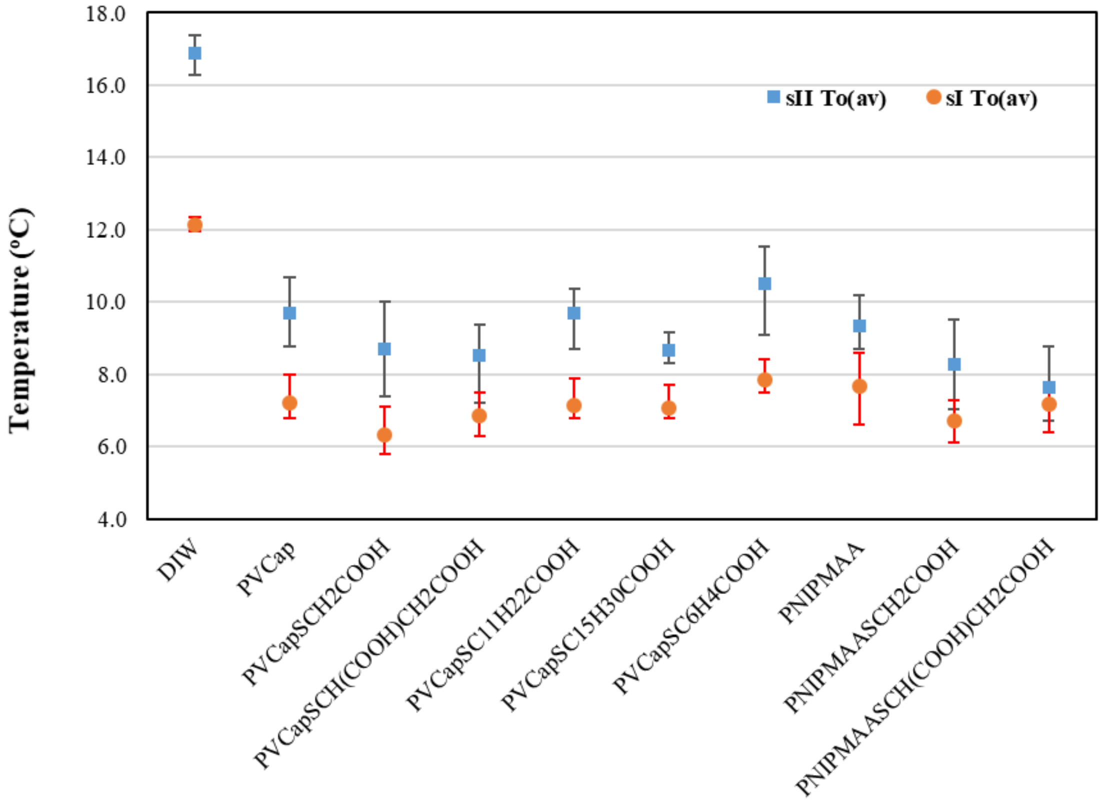

Figure 5. Summary data of the average To values for different polymers at 2500 ppm in deionized water.

As Table 4 shows, all polymers at the concentration of 2500 ppm gave a significantly better inhibition performance than pure water. Regarding the various PVCap polymers, it should be noted that PVCap in Table 4 also has an end-cap, i.e. the 2-cyanoprop-2-yl group (Table 1). Also, we attempted to keep the molecular weight and PDI values as close as possible for a set of polymers to be compared. This is because the molecular weight and molar concentration can affect KHI performance. Apart from the standard PVCap, the other PVCaps are made using added CTA, which gives them various thio-organic acid end groups instead. The same is true for PNIPMAA. Although it is fair to say that there are no dramatic differences between the performances of the polymers with different end caps (the biggest range of average To values is 8.5-10.5 °C for PVCap polymers in the sII hydrate system), there are some statistically significant results when t-test analysis is applied at the 95% confidence level ($p < 0.05$).[34]

We will discuss the results for the two small thio-acid end groups, SCH_2COOH and $SCH(COOH)CH_2COOH$ first. Thus, both these end groups improved the KHI performance of PVCap for both sI and sII hydrates. Note that the molecular weight of these three polymers is fairly similar. In particular the M_n value for normal PVCap is 4403 g/mole and for $PVCapSCH(COOH)CH_2COOH$ is 4006 g/mole, indicating that it is unlikely that molecular weight is the primary cause of the improved KHI performance with the thiosuccinic acid end group. The molecular weight distributions also looked similar with no apparent bimodal distribution, which also could have affected the performance.[35] For sII hydrates, the average To value of normal PVCap was 9.7 °C. The average To value for $PVCapSCH_2COOH$ was 8.7 °C, which was statistically significantly different from that of normal PVCap by t-test analysis. $PVCapSCH(COOH)CH_2COOH$ also lowered the sII hydrates average To value by a significant amount, to 8.5 °C, but we cannot say that $PVCapSCH(COOH)CH_2COOH$ gave better KHI performance than $PVCapSCH_2COOH$ at the 95% confidence level. Compared with normal PNIPMAA, which gave sII hydrates an average To value of 9.3 °C, $PNIPMAASCH_2COOH$ and $PNIPMAASCH(COOH)CH_2COOH$ both significantly reduced the average To values to 8.3 °C and 7.6 °C respectively. However, the value of 7.6 °C for

PNIPMAASCH(COOH)CH_2COOH may at least in part be due to the significantly lower polymer molecular weight compared to normal PNIPMAA. For sI hydrates, the average To value of PVCapSCH_2COOH was 6.3 °C, which is also statistically significantly different from the To value of normal PVCap (7.2 °C). This is consistent with the conclusion in a previous article, that the mercaptoacetic acid modified PVCap is superior to the normal PVCap, made using AIBN with CTA, in inhibiting sI hydrates.[27] Although PVCapSCH(COOH)CH_2COOH gave sI hydrates an average To value to 6.9 °C, a little lower than the normal PVCap, this is not a significant difference because $p > 0.05$ from t-test analysis. We have the same situation for PNIPMAASCH(COOH)CH_2COOH on sI hydrates: adding the SCH(COOH)CH_2COOH end group to the polymer end only slightly improved the performance compared to normal PNIPMAA. But the p value was 0.07 in a t-test between these two polymers, which gives only confidence at the 93% level. However, PNIPMAASCH_2COOH could significantly increase the inhibition performance compared with normal PNIPMAA.

In contrast to the PVCap polymers with thioacetic and thiosuccinic acid end groups, the PVCap with thiobenzoic acid (PVCapSC_6H_4COOH) end group performed worse than the standard PVCap made with added CTA. For sII hydrate the average To value of PVCapSC_6H_4COOH was 10.5 °C, which is statistically significantly worse than 9.7 °C for standard PVCap. The performance was also significantly worse with PVCapSC_6H_4COOH for the sI hydrate system. Since all the CTA used contain a terminal carboxylic acid group, we suggest that the aromatic benzene ring in the chain end worsens the KHI activity of PVCap, and that this may be related to the π-bonding character of the aromatic ring. Thus, the π-orbitals in the aromatic rings may possibly interact with each other (as seen in graphite or asphaltene stacking) causing weak polymer-polymer interactions and reducing the freedom of the polymer strands to perturb the water structure or interact with hydrate crystal surfaces.

The reason why SCH_2COOH and $SCH(COOH)CH_2COOH$ functional end groups can improve the KHIs performance compared to the normal PVCap with 2-cyanoprop-2-yl end group, must surely lie with the carboxylic acid groups. However, all the CTAs used have carboxylic acid end groups but in the case of SCH_2COOH and $SCH(COOH)CH_2COOH$ they are small end groups, giving negligible effect on the molar concentration of polymer, and do not contain any aromatic groups. We presume the carboxylic acid groups being sterically fairly adjacent to the nearest caprolactam group can also interact via hydrogen bonds with hydrate clusters. This could possibly involve carboxylic acid groups entering and bonding to open hydrate cages in a semi-clathrate bonding manner.[36] This could help preventing the hydrate nuclei from reaching the critical size for further growth or reduce the rate of crystal growth once the particles have reached super critical size. A possible reason why SCH_2COOH end group significantly improved the KHI effect for both sI and sII hydrate systems, whilst $SCH(COOH)CH_2COOH$ only significantly affected the sII hydrate system, maybe be due to the different cage sizes between sI and sII hydrates. For sII hydrates, which consist of sixteen 5^{12} and eight $5^{12}6^4$ cages, the larger cage size is big enough for both SCH_2COOH and $SCH(COOH)CH_2COOH$ groups. In addition, there are twice as many carboxylic acid groups in $SCH(COOH)CH_2COOH$ as in SCH_2COOH. However, when it comes to sI hydrates, which consist of two 5^{12} and six $5^{12}6^2$ cages, the cage is suitably sized for SCH_2COOH. For $SCH(COOH)CH_2COOH$ groups, which also contain a CH_2COOH group, we presume that the extra CHCOOH group sterically interferes with interactions to the $5^{12}6^2$ cages. Computer modelling studies would be needed to help confirm this.

We also included two fatty acid thiol end groups in the study on PVCap to introduce a more amphiphilic nature to the polymer chain. These polymers are $PVCapSC_{11}H_{22}COOH$ and $PVCapSC_{15}H_{30}COOH$. The CTA end group represents 4.0 and 4.4% of the polymer molecular weight, compared to 1.6 wt.% for the normal PVCap with 2-cyanoprop-2-yl end group. Thus, the affect on the molar concentration is quite small. The average To values for PVCapS$C_{11}H_{22}$COOH on both sI and sII hydrate systems were not significantly different from normal PVCap. The same is true for PVCapS$C_{15}H_{30}$COOH for the sI hydrate system but this PVCap with a thiohexadecanoic end group did give a significantly better To values for sII hydrates. Due to this anomaly we carried out further tests and obtained the same result.

The question is, can we explain these results? Clearly these thiofatty acid end groups are both too large to occupy hydrate cages. Due to the long hydrophobic C11 or C15 alkyl chains, these polymers could congregate more at the gas-water interface than the normal PVCap which is where gas hydrate formation is believed to be initiated. But the PVCapS$C_{11}H_{22}$COOH polymer showed no improvement over the normal PVCap, which diminishes that theory. The answer may possibly lie in the polymer water-solubility. At first it seems surprising that PVCapS$C_{15}H_{30}$COOH improved the KHI performance as the 2500ppm solution is cloudy above 4 °C. (The PVCapS$C_{11}H_{22}$COOH polymer was fully soluble at the test conditions). However, we have carried out several studies which indicate that a low cloud point can be useful for good KHI performance.[7] We have also previously encountered polymers with excellent KHI performance that were still cloudy in solution under the test conditions.[19] We speculate that this is due to a thin layer of polymer deposition on the surfaces of the cell, particular rough areas, which can affect the availability of heteronucleation sites. However, for sI, no KHI performance improvement was observed with PVCapS$C_{15}H_{30}$COOH. However, the kinetics are generally faster for formation of sI hydrate as it is more symmetrical and has a lower percentage of the large cages than sII hydrates. It is also possible is that the polymerisation procedure is affected by the different surfactant chain transfer agents (CTAs), and the C15-based CTA gives a better distribution of polymer molecular weights even though the weight averages are the same for both polymer. But again this doesn’t explain why the effect doesn’t work for tests with SI hydrate. A possibility that does address the supposed anomaly with SI hydrates is that the solubility of the hydrate-forming alkanes at the interfacial varies between the C11-capped and C15.-capped polymers for SI and SII hydrate. i.e. the C15-capped polymer has little effect on the solubility of methane (hence the lack of performance enhancement for SI hydrate) but does lower the solubility of the C2-C4 hydrate-forming components that make SII hydrate. Finally, the shape of the polymers themselves (straight or more coiled) may vary between the depending on the size of the alkyl end-capping and the shape is also affected by the hydrate-forming alkanes dissolved in the water at the interfacial area.

Since PVCapSCH(COOH)CH_2COOH gave the greatest lowering of the average To values for the PVCap polymer series, we investigated this polymer at varying concentration. Figure 6 shows all the individual To values and Ta values for PVCapSCH(COOH)CH_2COOH at concentrations of 2500, 5000, and 7500 ppm. From this figure, we can see an obvious trend that PVCapSCH(COOH)CH_2COOH performs better as the concentration becomes higher. Although some of the data are overlapping among these three concentrations, the p values still remains < 0.05 from t-test analysis, illustrating that there are statistical differences between the results at different concentrations.

As mentioned earlier, and according to previous studies, scattering of about ±15 % of the To values is normal for tests on any one polymer at the same set of conditions.[6, 10] This is because of the stochastic nature for gas hydrate formation in a small reactor. However, some of the data shown in Figure 6 deviate more than a 15% scattering. We think this maybe because of foaming of the solution especially at the higher 7500ppm concentration.

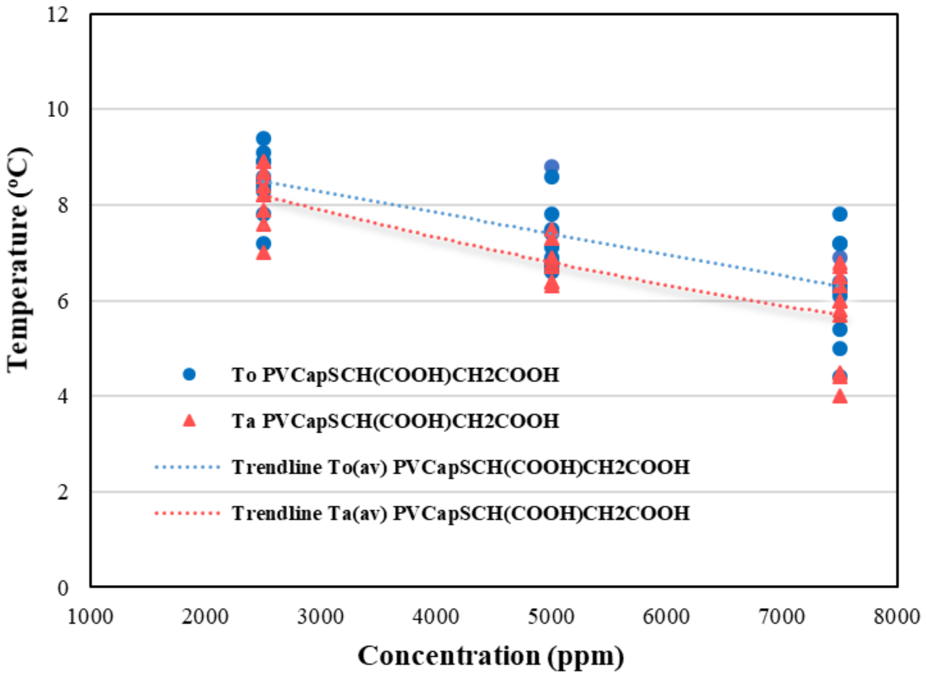

Figure 6. To and Ta values of PVCapSCH(COOH)CH_2COOH versus concentration in deionized water under SNG mixture.

Since two of the CTAs contain long hydrophobic groups, PVCapS$C_{11}H_{22}$COOH and PVCapS$C_{15}H_{30}$COOH, we wondered whether this might be an advantage for systems with liquid hydrocarbon phases. Although the terminal groups is a carboxylic acid we imagined that the C12 or C16 chain could hang in the hydrocarbon and the rest of the polymer in the water phase. In this way, a higher concentration of polymer could be obtained at the hydrocarbon-water interface where hydrate formation is expected to occur, which in theory could improve the KHI performance compared to normal PVCap. We also tested the other CTA-modified PVCap polymers for further comparison. The To(av) and Ta(av) values (based on 8-10 constant cooling test) from SNG + water + decane multiphase tests are listed in Table 5 and also summarized graphically in Figure 7. The To result for DIW (15.6 °C) was lower than in the SNG-water system since the addition of decane lowers the equilibrium temperature of the system. All the polymers gave considerably lower To values than DIW (no polymer). Of the six polymers tested PVCapSCH_2COOH clearly gave the lowest average To value of 7.1 °C, almost 2 °C lower than the normal PVCap made without added CTA. Compared to normal PVCap, there was no significant effect on KHI performance from PVCap$SCH(COOH)CH_2COOH$, PVCap$SC_{11}H_{22}COOH$ and PVCapSC_6H_4COOH, but there was a significantly lower average To value for PVCap$SC_{15}H_{30}COOH$. As with the gas-water systems we think this is related to the lower solubility of PVCap$SC_{15}H_{30}COOH$. Thus, the theory that the amphiphilic nature of long alkyl chain hydrophobically capped KHI polymers would enhance the performance by increasing the polymer concentration at the hydrocarbon-water interface appears to be false. In addition, one further observation was that when the cells were opened there was no sign of emulsion formation when using the two PVCaps with C12 and C16 fatty acid end groups. Therefore, there does not appear to be any advantage in using long hydrophobic tails on the KHI polymer. Finally, we are not sure why PVCap$SCH(COOH)CH_2COOH$ did not enhance the KHI performance when adding 1mL decane into the solution compared to studies without decane. Studies reported that the presence of hydrocarbons could affect the formation process of hydrates, possibly because the growth route of gas hydrates in water + organic phases is different from that without organic phases, thus leading to differences in the primary KHI mechanism.[37-40]

Table 5. Average Ta and To values of different end-group-modified KHIs at 2500 ppm in SNG + water + decane system.

Sample	To(av) (°C)	Ta(av) (°C)	To(av) - Ta(av) (°C)
DIW	15.6	15.4	0.2
PVCap	9.0	8.6	0.4

$\mathrm{PVCapSCH_2COOH}$	7.1	6.8	0.3
$\mathrm{PVCapSCH(COOH)CH_2COOH}$	8.6	8.3	0.3
$\mathrm{PVCapSC_{11}H_{22}COOH}$	9.1	8.6	0.5
$\mathrm{PVCapSC_{15}H_{30}COOH}$	8.2	8.0	0.2
$\mathrm{PVCapSC_6H_4COOH}$	9.2	8.8	0.4

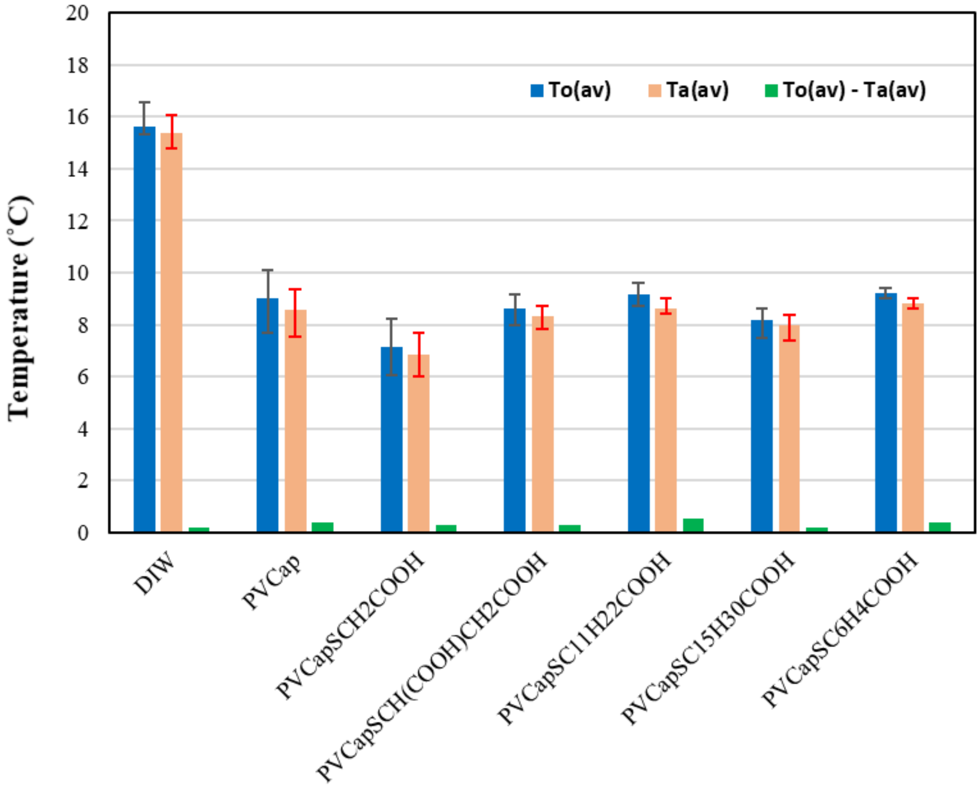

Figure 7. Summary data of different end-group-modified KHIs at 2500 ppm in SNG + water + decane phases.

CONCLUSION

A series of end-group-modified PVCaps and PNIPMAAs have been synthesized using CTAs and investigated as gas hydrate kinetic inhibitors in high-pressure rocking cells. Their inhibition effect on both sI and sII gas hydrate-forming systems was evaluated by using pure methane gas and SNG mixture respectively.

The mercaptoacetic acid-group-modified PVCap ($PVCapSCH_2COOH$) had significantly better inhibition performance than the normal PVCap on both structure I (sI) and structure II (sII) gas hydrate-forming systems in aqueous solution, as well as a SII hydrate-forming system containing added decane. These results are in line with earlier results with thioacetic acid end-capped PVCap although this current study shows a weaker KHI enhancement.[27]

The other powerful sII gas hydrate inhibitor among these end-group-modified PVCap polymers in this study was found to be the mercaptosuccinic acid-group-modified PVCap ($PVCapSCH(COOH)CH_2COOH$) although it showed negligible effect on the system with added decane. We also introduced the mercaptoacetic acid and mercaptosuccinic acid groups into poly(*N*-isopropylmethacrylamide) (PNIPMAA) polymers, again using AIBN as initiator. Both of the end-group-modified PNIPMAAs gave superior KHI performance than PNIPMAA made using AIBN alone. The 4-mercaptobenzoic acid-group-modified PVCap ($PVCapSC_6H_4COOH$) was the only PVCap polymer that consistently increased the average To(av) value compared to the normal PVCap made without CTA, and consequently gave worse KHI performance. We propose that the aromatic rings are detrimental to the polymer performance, possibly due to stacking of the rings via π-π interactions, reducing the freedom of the polymer chains to kinetically inhibit gas hydrate formation. Extending this theory, it may also be best to avoid using aromatic initiators such as benzoyl peroxide in making KHI polymers as this may decrease the KHI performance.

Finally, the PVCap polymers with long chain C12 fatty acid did not improve the KHI performance compared to the normal PVCap. However, the PVCap with C16 fatty acid end group did improve the KHI performance but this may be related to the low solubility of the polymer. We tentatively propose that this is due to a thin layer of polymer deposition on the surfaces of the cell which can affect the availability of heteronucleation sites for hydrate formation.

We believe that adding the correct function groups to the chain end of polymers such as PVCap and PNIPMAA polymers is an effective way to improve their KHI performance. We will continue to investigate these effective end groups with other KHI polymers as well as explore other end-capping groups. These will be very helpful for industry operations as well as KHI mechanisms studies.

REFERENCES

1. Sloan, E. D., Clathrate Hydrates of Natural Gases. **2007**.

2. Kelland, M. A., Production Chemicals for the Oil and Gas Industry, Second Edition. *CRC Press* **2014**, 219-245.

3. Sloan, E. D., A changing hydrate paradigm - from apprehension to avoidance to risk management. *Fluid Phase Equilib.* **2005,** *228*, 67-74.

4. Kelland, M. A., History of the development of low dosage hydrate inhibitors. *Energy & Fuels* **2006,** *20* (3), 825-847.

5. Jr, E. D. S., Fundamental principles and applications of natural gas hydrates. *NATURE* **2003,** *426*.

6. Abrahamsen, E.; Kelland, M. A., Carbamate Polymers as Kinetic Hydrate Inhibitors. *Energy & Fuels* **2016,** *30* (10), 8134-8140.

7. Kelland, M. A.; Abrahamsen, E.; Ajiro, H.; Akashi, M., Kinetic Hydrate Inhibition withN-Alkyl-N-vinylformamide Polymers: Comparison of Polymers ton-Propyl and Isopropyl Groups. *Energy & Fuels* **2015,** *29* (8), 4941-4946.

8. Ajiro, H.; Takemoto, Y.; Akashi, M.; Chua, P. C.; Kelland, M. A., Study of the Kinetic Hydrate Inhibitor Performance of a Series of Poly(N-alkyl-N-vinylacetamide)s. *Energy & Fuels* **2010,** *24* (12), 6400-6410.

9. Chua, P. C.; Kelland, M. A., Poly(N-vinyl azacyclooctanone): A More Powerful Structure II Kinetic Hydrate Inhibitor than Poly(N-vinyl caprolactam). *Energy & Fuels* **2012,** *26* (7), 4481-4485.

10. Chua, P. C.; Kelland, M. A.; Ajiro, H.; Sugihara, F.; Akashi, M., Poly(vinylalkanamide)s as Kinetic Hydrate Inhibitors: Comparison of Poly(N-vinylisobutyramide) with Poly(N-isopropylacrylamide). *Energy & Fuels* **2013,** *27* (1), 183-188.

11. Daraboina, N.; Ripmeester, J.; Walker, V. K.; Englezos, P., Natural Gas Hydrate Formation and Decomposition in the Presence of Kinetic Inhibitors. 3. Structural and Compositional Changes. *Energy & Fuels* **2011,** *25* (10), 4398-4404.

12. Ke, W.; Kelland, M. A., Kinetic Hydrate Inhibitor Studies for Gas Hydrate Systems: A Review of Experimental Equipment and Test Methods. *Energy & Fuels* **2016,** *30* (12), 10015-10028.

13. Lin, H.; Wolf, T.; Wurm, F. R.; Kelland, M. A., Poly(alkyl ethylene phosphonate)s: A New Class of Non-amide Kinetic Hydrate Inhibitor Polymers. *Energy & Fuels* **2017,** *31* (4), 3843-3848.

14. Kelland, M. A.; Magnusson, C.; Lin, H.; Abrahamsen, E.; Mady, M. F., Acylamide and Amine Oxide Derivatives of Linear and Hyperbranched Polyethylenimine. Part 2: Comparison of Gas Kinetic Hydrate Inhibition Performance. *Energy & Fuels* **2016,** *30* (7), 5665-5671.

15. Mady, M. F.; Kelland, M. A., Tris(tert-heptyl)-N-alkyl-1-ammonium bromides—Powerful THF hydrate crystal growth inhibitors and their synergism with poly-vinylcaprolactam kinetic gas hydrate inhibitor. *Chem. Eng. Sci.* **2016,** *144*, 275-282.

16. Magnusson, C. D.; Kelland, M. A., Performance Enhancement of N-Vinylcaprolactam-Based Kinetic Hydrate Inhibitors by Synergism with Alkylated Guanidinium Salts. *Energy & Fuels* **2016,** *30* (6), 4725-4732.

17. Ree, L. H. S.; Kelland, M. A.; Roth, P. J.; Batchelor, R., First investigation of modified poly(2-vinyl-4,4-dimethylazlactone)s as kinetic hydrate inhibitors. *Chem. Eng. Sci.* **2016,** *152*, 248-254.

18. Sa, J. H.; Kwak, G. H.; Han, K.; Ahn, D.; Lee, K. H., Gas hydrate inhibition by perturbation of liquid water structure. *Sci. Rep.* **2015,** *5*, 11526.

19. Reyes, F. T.; Guo, L.; Hedgepeth, J. W.; Zhang, D.; Kelland, M. A., First Investigation of the Kinetic Hydrate Inhibitor Performance of Poly(N-alkylglycine)s. *Energy & Fuels* **2014,** *28* (11), 6889-6896.

20. Yagasaki, T.; Matsumoto, M.; Tanaka, H., Adsorption Mechanism of Inhibitor and Guest Molecules on the Surface of Gas Hydrates. *J. Am. Chem. Soc.* **2015,** *137* (37), 12079-85.

21. Zeng, H.; Lu, H.; Huva, E.; Walker, V. K.; Ripmeester, J. A., Differences in nucleator adsorption may explain distinct inhibition activities of two gas hydrate kinetic inhibitors. *Chem. Eng. Sci.* **2008,** *63* (15), 4026-4029.

22. Qin, H. B.; Sun, Z. F.; Wang, X. Q.; Yang, J. L.; Sun, C. Y.; Liu, B.; Yang, L. Y.; Chen, G. J., Synthesis and Evaluation of Two New Kinetic Hydrate Inhibitors. *Energy & Fuels* **2015,** *29* (11), 7135-7141.

23. Kelland, M. A.; Hartanti, A. R. D.; Ruysschaert, W. G. Z.; Thorsen, H. B., Tetrahydrofuran Hydrate Crystal Growth Inhibition with Synergistic Mixtures: Insight into Gas Hydrate Inhibition Mechanisms. *Energy & Fuels* **2017,** *31* (8), 8109-8115.

24. Kelland, M. A.; Moi, N.; Howarth, M., Breakthrough in Synergists for Kinetic Hydrate Inhibitor Polymers, Hexaalkylguanidinium Salts: Tetrahydrofuran Hydrate Crystal Growth Inhibition and Synergism with Polyvinylcaprolactam. *Energy & Fuels* **2013,** *27* (2), 711-716.

25. Sefidroodi, H.; Chua, P. C.; Kelland, M. A., THF hydrate crystal growth inhibition with small anionic organic compounds and their synergistic properties with the kinetic hydrate inhibitor poly(N-vinylcaprolactam). *Chemical Engineering Science* **2011,** *66* (10), 2050-2056.

26. Ieong, N. S.; Redhead, M.; Bosquillon, C.; Alexander, C.; Kelland, M.; O'Reilly, R. K., The Missing Lactam-Thermoresponsive and Biocompatible Poly(N-vinylpiperidone) Polymers by Xanthate-Mediated RAFT Polymerization. *Macromolecules* **2011,** *44* (4), 886-893.

27. Zhang, Q.; Shen, X.; Zhou, X.; Liang, D., Inhibition Effect Study of Carboxyl-Terminated Polyvinyl Caprolactam on Methane Hydrate Formation. *Energy & Fuels* **2017,** *31* (1), 839-846.

28. Nakabayashi, K.; Mori, H., Recent progress in controlled radical polymerization of N-vinyl monomers. *Eur. Polym. J.* **2013,** *49* (10), 2808-2838.

29. Bartolozzi, I.; Solaro, R.; Schacht, E.; Chiellini, E., Hydroxyl end-capped macromers of N-vinyl-2-pyrrolidinone as precursors of amphiphilic block copolymers. *Eur. Polym. J.* **2007,** *43* (11), 4628-4638.

30. Mady, M. F.; Kelland, M. A., Fluorinated Quaternary Ammonium Bromides: Studies on Their Tetrahydrofuran Hydrate Crystal Growth Inhibition and as Synergists with Polyvinylcaprolactam Kinetic Gas Hydrate Inhibitor. *Energy & Fuels* **2013**, 130828090238002.

31. Ree, L. H. S.; Mady, M. F.; Kelland, M. A., N,N-Dimethylhydrazidoacrylamides. Part 3: Improving Kinetic Hydrate Inhibitor Performance Using Polymers of N,N-Dimethylhydrazidomethacrylamide. *Energy & Fuels* **2015,** *29* (12), 7923-7930.

32. Reyes, F. T.; Kelland, M. A., First Investigation of the Kinetic Hydrate Inhibitor Performance of Polymers of Alkylated N-Vinyl Pyrrolidones. *Energy & Fuels* **2013,** *27* (7), 3730-3735.

33. Chua, P. C.; Kelland, M. A., Tetra(iso-hexyl)ammonium Bromide-The Most Powerful Quaternary Ammonium-Based Tetrahydrofuran Crystal Growth Inhibitor and Synergist with Polyvinylcaprolactam Kinetic Gas Hydrate Inhibitor. *Energy & Fuels* **2012,** *26* (2), 1160-1168.

34. Walpole, R. E. Probability & Statistics for Engineers & Scientists, 9th ed.; Pearson: Boston, MA, 2012.

35. Colle, K.; Talley, L. D.; Longo, J. M. World Patent Application WO 2005/005567, 2005.

36. Terekhova, I. S.; Manakov, A. Y.; Komarov, V. Y.; Villevald, G. V.; Burdin, A. A.; Karpova, T. D.; Aladko, E. Y. *J. Phys. Chem. B* **2013**, 117, 2796–2806.

37. Shin, K.; Kim, J.; Seo, Y.; Kang, S. P., Effect of kinetic hydrate inhibitor and liquid hydrocarbon on the heterogeneous segregation and deposition of gas hydrate particles. *Korean J. Chem. Eng.* **2014,** *31* (12), 2177-2182.

38. Stoporev, A. S.; Manakov, A. Y.; Kosyakov, V. I.; Shestakov, V. A.; Altunina, L. K.; Strelets, L. A., Nucleation of Methane Hydrate in Water-In-Oil Emulsions: Role of the Phase Boundary. *Energy & Fuels* **2016,** *30* (5), 3735-3741.

39. Seo, Y.; Shin, K.; Kim, H.; Wood, C. D.; Tian, W.; Kozieski, K. A., Preventing Gas Hydrate Agglomeration with Polymer Hydrogels. *Energy & Fuels* **2014,** *28* (7), 4409-4420.

40. Stoporev, A. S.; Semenov, A. P.; Medvedev, V. I.; Sizikov, A. A.; Gushchin, P. A.; Vinokurov, V. A.; Manakov, A. Y., Visual observation of gas hydrates nucleation and growth at a water - organic liquid interface. *J. Cryst. Growth* **2018,** *485*, 54-68.

Paper V

A Simple and Direct Route to High Performance Acrylamide-based Kinetic Gas hydrate Inhibitors from Poly (acrylic acid)

Authors:

Qian Zhang*, Lilian S. Ree, and Malcolm A. Kelland

Published in Energy & Fuels 2020, 34 (5), 6279-6287.

This paper is not in Brage due to copyright.

Paper VI

Polyvinylsulfonamides as Kinetic Hydrate Inhibitors

Authors:

Qian Zhang*, Malcolm A. Kelland, and Hiroharu Ajiro

Published in Energy & Fuels 2020, 34 (2), 2230-2237.

This paper is not in Brage due to copyright.

Paper VII

Kinetic Inhibition Performance of Alkylated Polyamine Oxides on Structure I Methane Hydrate

Authors:

Qian Zhang*, and Malcolm A. Kelland

Published in Chemical Engineering Science 2020, 220 (2020), 115652.

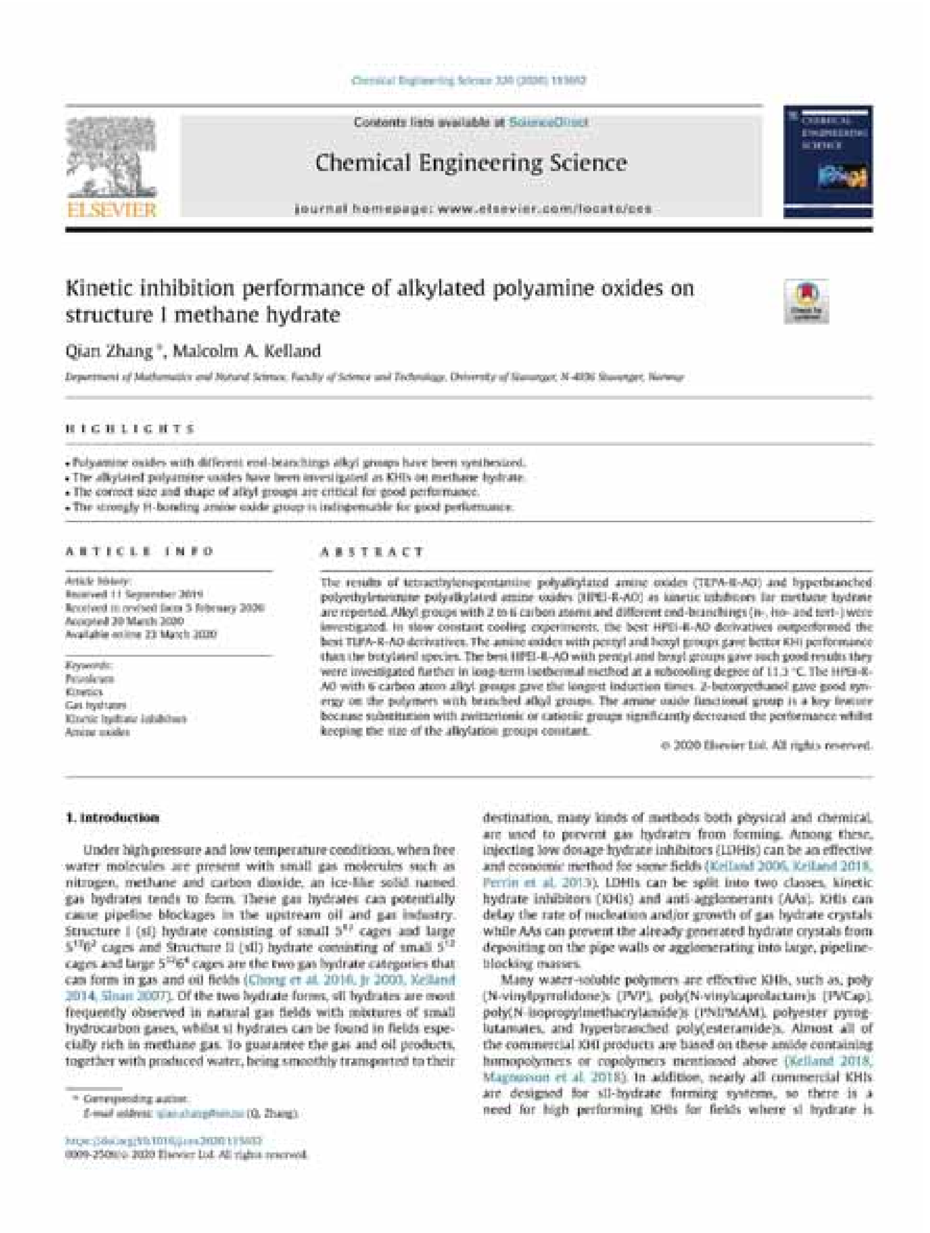

Chemical Engineering Science 220 (2020) 115632

Contents lists available at ScienceDirect

Chemical Engineering Science

journal homepage: www.elsevier.com/locate/ces

Kinetic inhibition performance of alkylated polyamine oxides on structure I methane hydrate

Qian Zhang *, Malcolm A. Kelland

Department of Mathematics and Natural Science, Faculty of Science and Technology, University of Stavanger, N-4036 Stavanger, Norway

HIGHLIGHTS

- Polyamine oxides with different end-branchings alkyl groups have been synthesized.
- The alkylated polyamine oxides have been investigated as KHIs on methane hydrate.
- The correct size and shape of alkyl groups are critical for good performance.
- The strongly H-bonding amine oxide group is indispensable for good performance.

ARTICLE INFO

Article history:
Received 11 September 2019
Received in revised form 5 February 2020
Accepted 20 March 2020
Available online 23 March 2020

Keywords:
Petroleum
Kinetics
Gas hydrates
Kinetic hydrate inhibitors
Amine oxides

ABSTRACT

The results of tetraethylenepentamine polyalkylated amine oxides (TEPA-R-AO) and hyperbranched polyethyleneimine polyalkylated amine oxides (HPEI-R-AO) as kinetic inhibitors for methane hydrate are reported. Alkyl groups with 2 to 6 carbon atoms and different end-branchings (n-, iso- and tert-) were investigated. In slow constant cooling experiments, the best HPEI-R-AO derivatives outperformed the best TEPA-R-AO derivatives. The amine oxides with pentyl and hexyl groups gave better KHI performance than the butylated species. The best HPEI-R-AO with pentyl and hexyl groups gave such good results they were investigated further in long-term isothermal method at a subcooling degree of 11.3 °C. The HPEI-R-AO with 6 carbon atom alkyl groups gave the longest induction times. 2-butoxyethanol gave good synergy on the polymers with branched alkyl groups. The amine oxide functional group is a key feature because substitution with zwitterionic or cationic groups significantly decreased the performance whilst keeping the size of the alkylation groups constant.

© 2020 Elsevier Ltd. All rights reserved.

1. Introduction

Under high pressure and low temperature conditions, when free water molecules are present with small gas molecules such as nitrogen, methane and carbon dioxide, an ice-like solid named gas hydrates tends to form. These gas hydrates can potentially cause pipeline blockages in the upstream oil and gas industry. Structure I (sI) hydrate consisting of small 5^{12} cages and large $5^{12}6^2$ cages and Structure II (sII) hydrate consisting of small 5^{12} cages and large $5^{12}6^4$ cages are the two gas hydrate categories that can form in gas and oil fields (Chong et al. 2016, Jr 2003, Kelland 2014, Sloan 2007). Of the two hydrate forms, sII hydrates are most frequently observed in natural gas fields with mixtures of small hydrocarbon gases, whilst sI hydrates can be found in fields especially rich in methane gas. To guarantee the gas and oil products, together with produced water, being smoothly transported to their destination, many kinds of methods both physical and chemical, are used to prevent gas hydrates from forming. Among these, injecting low dosage hydrate inhibitors (LDHIs) can be an effective and economic method for some fields (Kelland 2006, Kelland 2018, Perrin et al. 2013). LDHIs can be split into two classes, kinetic hydrate inhibitors (KHIs) and anti-agglomerants (AAs). KHIs can delay the rate of nucleation and/or growth of gas hydrate crystals while AAs can prevent the already generated hydrate crystals from depositing on the pipe walls or agglomerating into large, pipeline-blocking masses.

Many water-soluble polymers are effective KHIs, such as, poly(N-vinylpyrrolidone)s (PVP), poly(N-vinylcaprolactam)s (PVCap), poly(N-isopropylmethacrylamide)s (PNIPMAM), polyester pyroglutamates, and hyperbranched poly(esteramide)s. Almost all of the commercial KHI products are based on these amide containing homopolymers or copolymers mentioned above (Kelland 2018, Magnusson et al. 2018). In addition, nearly all commercial KHIs are designed for sII-hydrate forming systems, so there is a need for high performing KHIs for fields where sI hydrate is

---

* Corresponding author.
E-mail address: qian.zhang@uis.no (Q. Zhang).

https://doi.org/10.1016/j.ces.2020.115632
0009-2509/© 2020 Elsevier Ltd. All rights reserved.

predominantly formed (Rithauddeen et al. 2014). It is known that KHIs at a certain dosage are not able to inhibit gas hydrate formation for the same amount of time and at the same subcooling for sI hydrate-forming gases as for a sII-forming gas (Abrahamsen and Kelland 2018). It is also known that a sII-forming gas can form some sI hydrates (Schicks et al. 2006, Uchida et al. 2004, Daraboina et al. 2011). Studies showed that varying cages including 5^{12}, $5^{12}6^2$, $5^{12}6^3$ and $5^{12}6^4$ have been identified from methane hydrate. The uncommon $5^{12}6^3$ cages act as a link for coexistence of sI and sII hydrate during the initial nucleation and growth phase (Walsh et al. 2009, Vatamanu and Kusalik 2010). Thus the situation is initially very dynamic in the first phases of hydrate formation and the KHI is acting to inhibit both and maybe other structures.

Similar to the amide group, the amine oxide group also has strong hydrophilicity as well as hydrogen-bond formation properties, which are usually considered as some of the necessities for KHIs with high performance. Therefore, amine oxide compounds have a high potential to be good KHIs. Research for using amine oxide compounds to solve gas hydrate formation problems was first reported as early as 1997 (Klug 2000). Using tetrahydrofuran (THF), which could form the same sII hydrates at atmospheric pressure as natural gas mixtures do at high-pressure. Klug et al. showed that amine oxides and their salts were very effective at preventing THF hydrate crystal growth. Tri-n-butylamine oxide (TBAO) showed particularly strong inhibitory effect on THF hydrate among all the tri-n-alkylamine oxides with alkyl chain groups varying from one to six carbon atoms (Kelland et al. 2012). In a later study, the n-butylated bis-amine oxides and tris-amine oxides were found to be better THF hydrate crystal inhibitors than the best monoamine oxide, TBAO (See Figure 1) (Kelland 2013b). Amine oxide derivatives of polyethyleneimine were also investigated as THF hydrate crystal growth inhibitors (Kelland and Mady 2016). Further studies showed that amine oxide derivatives of polyethyleneimine perform better than acylamide derivatives of polyethyleneimine, giving an interesting comparison of the two hydrophilic functional groups (Kelland and Mady 2016, Kelland et al. 2016).

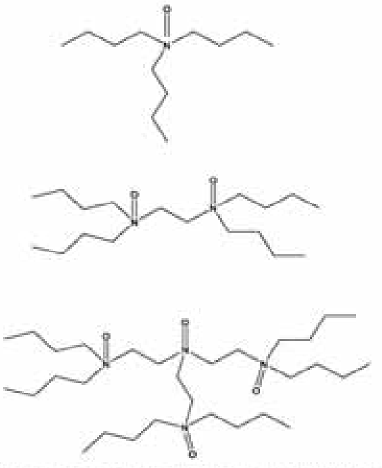

Fig. 1. Structures of tributylamine oxide (top), tetrabutyl-1, 2-ethanediamine bis-oxide (middle), and tris(ethylenedibutylamine oxide) amine oxide (bottom).

In addition, using a sII hydrate-forming synthetic natural gas (SNG) mixture, amine oxide compounds were also evaluated as natural gas hydrate KHIs. Studies show that TBAO and TPAO are poor natural gas hydrate KHIs when using alone, but they show very good synergistic KHI effect when combined with PVCap. The combination of TPAO and PVCap showed an especially strong KHI effect on sII gas hydrate formation (Kelland et al. 2012). Several kinds of n-butylated amine oxides of oligoethyleneamines and polyethyleneamines were shown to be very good KHIs on sII gas hydrates (See Figure 2 and Figure 3). These oligoethyleneamine n-butylated amine oxides included pentaethylenehexamine-butyl-amine oxide (PEHA-Bu-AO), tetraethylenepentamine-butyl-amine oxide (TEPA-Bu-AO), triethylene tetramine-butyl-amine oxide (TETA-Bu-AO), diethylenetriamine-butyl-amine oxide (DETA-Bu-AO), among which TEPA-Bu-AO performed the best on sII hydrate formation. TEPA-Bu-AO almost gave the same good inhibitory effect as low molecular weight HPEI-butyl-amine oxides (HPEI-Bu-AO) (Magnusson and Kelland 2015). Interestingly, HPEI-Bu-AOs gave better sII hydrate inhibition effect than the related LPEI derivatives, which was different from the performance ranking found for THF hydrate crystal growth inhibition. This may be related to a difference in the dominant kinetic hydrate inhibition mechanism on gas hydrates and THF hydrates for this class (Kelland et al. 2016).

The ability of oligo- and polyamine oxides to inhibit methane sI gas hydrates has been investigated. This is the first report of a gas hydrate study on sI gas hydrates for this class. Tetraethylenepentamine-alkyl-amine oxides and hyperbranched polyethyleneimine-alkyl-amine oxides were chosen, as both classes are easily accessible in two steps from commercial products. Compared to past studies on sII hydrates where n-butylated derivatives were almost exclusively used, more hydrophobic alkyl groups, such as, n-pentyl groups, isopentyl groups, isohexyl groups were incorporated. Although hyperbranched polyethyleneimine-n-pentyl-amine oxides with high molecular weight were reported to be water-insoluble, these new studies were kick-started by the discovery that low molecular weight hyperbranched polyethyleneimine-n-pentyl-amine oxides were water-soluble and therefore worthy of investigation (Kelland et al. 2016). Zwitterionic or cationic derivatives, hyperbranched polyethyleneimine-isopentyl-propylenesulfonate and hyperbranched polyethyleneimine-isopentyl quaternary ammonium salts were also synthesised and tested, to see if the amine oxide group or the size of the alkyl substituents is most critical for good KHI performance.

2. Materials and methods

2.1. Materials

All of the hyperbranched polyethyleneimines (HPEIs) used in this study were obtained from Nippon Shokubai Co., Ltd, Japan. They all have the same purity of 98% and include EPOMIN SP 003 (Mw = 300 g/mole), EPOMIN SP 006 (Mw = 600 g/mole), EPOMIN SP 012 (Mw = 1200 g/mole), and EPOMIN SP 200 (Mw = 10000 g/mole). Tetraethylenepentamine (TEPA) was purchased from Fluka, which is principally a mixture of 85% of linear TEPA with several branched or cyclic TEPA products and higher molecular weight products, the structures and percentages of which are not documented. In this study, we assumed 100% linear TEPA product when calculating Mw and mole ratio of reactants. Potassium carbonate (99.6%), 2-propanol (100.0%), THF (100.0%, stabilized with 0.025

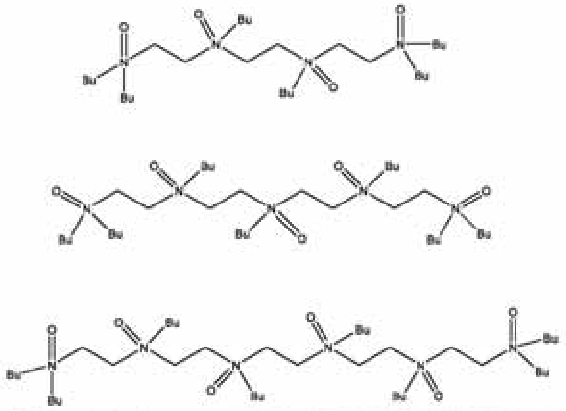

Fig. 2. Structure of the main components in TETA-Bu-AO (top), TEPA-Bu-AO (middle), and PEHA-Bu-AO (bottom).

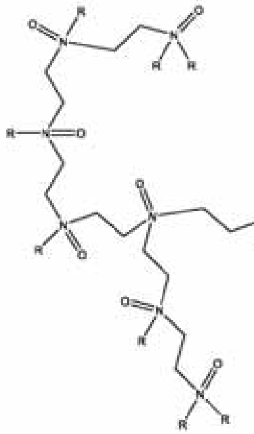

Fig. 3. Typical structure of the main component in a low molecular weight hyperbranched polyethyleneimine alkyl-amine oxide.

to 0.04% of BHT) and methyl iodide were purchased from VWR Chemicals. Ethylene glycol monoisobutyl ether (>98%), 1-bromo-4-methylpentane (>98%), and 1-bromopentane (>98%) were purchased from TCI Chemicals Europe. 1-bromobutane (≥98%), 1-bromo-3-methylbutane (≥98%), 1-iodopropane (≥98%), 1-iodoethane (≥98%), 1,3-propanesultone (98%), isobutyronitrile (≥98%), acetonitrile (≥99.9%), and hydrogen peroxide (30 wt% in water) were purchased from Merck. 2-butoxyethanol (99%) was purchased from Acros Organics. 1-iodohexane (98%, stabilized with copper) was purchased from Alfa Aesar. 1-bromo-3,3-dimethylbutane (98%) was purchased from Arctom Chemicals. Inhibex BIO-800 (36 wt% of N-vinylcaprolactam/ N-vinyl alcohol copolymer in 2-butoxyethanol) and Inhibex 101 (50 wt% of poly (N-vinylcaprolactam) in 2-butoxyethanol) were obtained from Ashland Chemical Co., US. Luvicap 55 W (53.8 wt% of N-vinylcapro lactam/N-vinylpyrrolidone copolymers in water) was obtained from BASF, Germany.

2.2. *Synthesis*

2.2.1. *Synthesis of amine oxides*

The procedure of synthesizing amine oxide compounds is the same as the previously reported procedure of making alkylated polyamine oxides (See Figure 4) (Kelland 2013a, Kelland and Mady 2016, Kelland et al. 2016). A mixture of an oligo- or polyamine (HPEI or TEPA), alkylating agent at 1 mol equivalent for each mole of N – H protons, potassium carbonate at 1.2 mol equivalent for each mole of N – H protons, and THF solvent were loaded in a round bottom flask and kept refluxed for a long enough time (1–3 days) to ensure the reaction was complete. After filtration and concentration under vacuum, the alkylated amine product was dissolved in 2-propanol (IPA) or 2-butoxyethanol (BGE). Then, hydrogen peroxide at 1.1 mol equivalent for each mole of nitrogen atoms was added at room temperature to obtain the target amine oxide product. 24 h later, the mixture was heated to 70 °C and kept for 2 h to destroy the excess hydrogen peroxide. Solutions of these amine oxide products in a mixture of water (residual from the hydrogen peroxide solution) and either IPA or BGE were used as such for the high pressure KHI performance tests. Organic solvent concentrations were kept to a level such that KHI tests at 2500 ppm polymer gave similar solvent concentration (ca. 5500–6000 ppm) in order to compare the performance ranking.

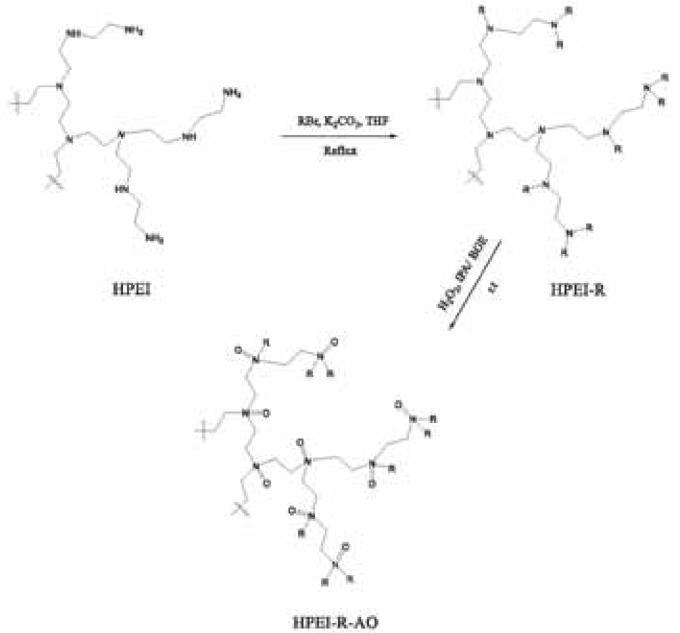

Fig. 4. Synthesis of hyperbranched polyethyleneimine-alkyl-amine-oxides.

2.2.2. *Synthesis of HPEI-isopentyl-propylenesulfonate.*

HPEI, 1-bromo-3-methylbutane at 1 mol equivalents for each mole of N – H protons, potassium carbonate at 1.2 mol equivalents for each mole of N – H protons, and THF solvent were loaded in a round bottom flask and kept refluxed for 72 h. After filtration and concentration under vacuum, the alkylated amine product was dissolved in acetonitrile. Then, 1, 3-propanesultone at 1.1 mol equivalents for each mole of nitrogen atoms was added and the mixture heated to 90 °C for 72 h. A solid product was obtained after concentration under vacuum. The sultone reacts completely with polyamines reported by Natus et al. (Natus and Goethals 1969)

2.2.3. *Synthesis of HPEI-isopentyl quaternary ammonium bromide*

HPEI, 1-bromo-3-methylbutane at 2.2 mol equivalents for each mole of N – H protons, potassium carbonate at 2.2 mol equivalents for each mole of N – H protons, and isobutyronitrile solvent were loaded in a round bottom flask and reacted at 75 °C for 72 h. After filtration and concentration under vacuum, the HPEI-isopentyl quaternary ammonium bromide was obtained and used for the later KHI tests without further purification. The synthesized products in this study are summarized in Table 1.

2.3. *Equipment and methods for KHI performance testing.*

High-pressure gas hydrate KHI tests were carried out in a rocker rig equipment manufactured by PSL Systemtechnik, Germany, which we have used in previous research (Kelland et al. 2013, Ree et al. 2017, Reyes et al. 2015, Zhang et al. 2018a). This equipment contains five parallel steel rocking cells, with a maximum effective volume of 40 mL for each cell. Thus five independent test results can normally be obtained in one day. Both the slow constant cooling method and the isothermal method were used to test KHI performance.

2.3.1. *Test procedure for the slow constant cooling method*

A steel ball for agitation and 20 mL of KHI in water solution was loaded into each cell. The air in the system was removed by a pump. Then, the system was purged with approximately 5 bar of pure methane gas. After releasing the purge gas, the system was vacuumed by the pump once again. When the temperature was stable at 20.5 °C, all the cells were pressurized to 110 bar with pure methane gas. With a maximum rocking angle of 40° and a rocking rate of 20 rocks/min, the system was cooled slowly and continuously at 1° C/h from 20.5 °C to 2 °C. After reaching 2 °C, the system was kept at this temperature for 1 h, and then it was heated

Table 1
Summary of the amine oxides and other products synthesized, the solvent carrier and their active polymer concentration.

Additive	Solvent	Concentration (wt. %)
TEPA-Et-AO	IPA/H_2O	29.4
TEPA-(n-Pro)-AO	IPA/H_2O	39.2
TEPA-(n-Bu)-AO	IPA/H_2O	38.7
TEPA-(iso-Pent)-AO	IPA/H_2O	30.3
TEPA-(n-Pent)-AO	IPA/H_2O	30.0
TEPA-(iso-Pent)-AO	BGE/ H_2O	27.3
HPEI-0.3 k-Et-AO	IPA/H_2O	27.8
HPEI-0.3 k-(n-Pro)-AO	IPA/H_2O	28.9
HPEI-0.3 k-(n-Bu)-AO	IPA/H_2O	30.6
HPEI-0.3 k-(iso-Pent)-AO	IPA/H_2O	31.7
HPEI-0.3 k-(n-Pent)-AO	IPA/H_2O	31.4
HPEI-0.3 k-(iso-Hex)-AO	IPA/H_2O	28.5
HPEI-0.3 k-(c-Hex)-AO	IPA/H_2O	25.1
HPEI-0.3 k-(n-Hex)-AO*	IPA/H_2O	42.4
HPEI-0.6 k-(iso-Pent)-AO	IPA/H_2O	31.0
HPEI-1.2 k-(iso-Pent)-AO	IPA/H_2O	31.0
HPEI-10 k-(iso-Pent)-AO	IPA/H_2O	32.1
HPEI-0.6 k-(n-Pent)-AO	IPA/H_2O	29.5
HPEI-1.2 k-(n-Pent)-AO	IPA/H_2O	30.7
HPEI-10 k-(n-Pent)-AO	IPA/H_2O	31.7
HPEI-1.2 k-(iso-Hex)-AO	IPA/H_2O	30.5
HPEI-0.3 k-(n-Bu)-AO	BGE/ H_2O	31.2
HPEI-0.3 k-(iso-Pent)-AO	BGE/ H_2O	31.3
HPEI-0.3 k-(n-Pent)-AO	BGE/ H_2O	30.6
HPEI-0.3 k-(iso-Hex)-AO	BGE/ H_2O	31.3
HPEI-0.3 k-(c-Hex)-AO	BGE/ H_2O	26.5
HPEI-0.3 k-(iso-Pent) quaternary ammonium Br		100%
HPEI-0.3 k-(iso-Pent)-propylenesulfonate		100%

* Water insoluble

quickly to 25 °C. At 110 bar the equilibrium temperature for pure methane gas hydrates is predicted to be 16 °C by Calsep's PVTSim containing cubic equation of state (EOS) (Abrahamsen and Kelland 2018, Zhang and Kelland 2018). But at 2 °C, and without any hydrate formation, the pressure drops to about 98 bar. This gives a subcooling of 13.3 °C at 2 °C and 98 bar by Calsep's PVTSim.

Typical temperature–time and pressure–time graphs using the slow constant cooling method can be seen in Fig. 5. The temperature graphs are overlapped. The point of the graphs in Fig. 5 is to show the reproducibility. For most KHI experiments, gas hydrates would be generated during the constant cooling period before the temperature reached 2 °C (i.e. 13.3 °C subcooling). However, if the KHI is very powerful, the gas hydrates may not form during this period. As a result, the slow constant cooling method will not be able to evaluate the very best KHIs. In this study, we found several KHIs that can prevent gas hydrates from forming even when the temperature was as low as 2 °C when using this method. This is the reason why we also used the isothermal method which will be described shortly.

Fig. 6 gives an example of how we analyze temperature–time and pressure–time graphs for each cell using the slow constant cooling method. The pressure drops a little when starting rocking, as some methane gas is dissolved in the aqueous fluid. The pressure then decreases linearly as the contents inside of each cell is cooled gradually. When the observable pressure first deviates from a straight line (Po), it means that some of the methane gas has become methane hydrates. The temperature corresponding to this pressure deviation is named the onset temperatures (To). The temperature corresponding to the steepest point of the pressure curve is called the rapid hydrate formation temperatures (Ta). The subcooling (ΔT) is then determined as the value of To minus Teq at pressure Po. As the formation of hydrates is an exothermic process, it is expected to see a temperature rise when hydrate forming. However, if the KHI is good at inhibiting macroscopic crystal growth and the cooling bath can conduct the heat away quickly, the temperature rise cannot be seen in the temperature graph.

2.3.2. Test procedure for the isothermal method

We were initially reluctant to carry out isothermal tests due to the stochastic nature of gas hydrate formation. Many years ago, we switched from this method to the slow constant cooling or stepwise ramping method as we found this gave less scattering in the data and more reliable estimates of the performance ranking. (The ranking was also the same as the isothermal tests). Nevertheless, we needed a method that could help differentiate the performance of the best amine oxide KHIs, preferably without varying the absolute pressure as this can affect KHI performance also (Kelland 2006, Kelland 2018, Magnusson et al. 2018, Perrin et al. 2013). We considered using the Crystal Growth Inhibition (CGI) test method developed by Total and Heriot Watt University but our first foray into this test method gave very variable data (Anderson et al. 2011, Mozaffar et al. 2016, Tohidi et al. 2015). (The CGI method involves making hydrates with the KHI present, then melting most but not all the hydrates, and then cooling again). Therefore, we used a standard isothermal method in this study. The filling of the cells with KHI fluid and 110 bar methane pressure at 20.5 °C was carried out the same as for the constant cooling method. With rocking angle of 40° at rocking rate of 20 rocks/min, the system was cooled quickly (10 °C / h) from 20.5 °C to 4 °C. After reaching 4 °C (ΔT = 11.3 °C), the system was kept at this temperature for a long enough time until gas hydrate was formed. We set the subcooling to be 11.3 °C for these tests to give delay times that were measurable in two days or less, a reasonably long time period but short enough to get sufficient carried experiments out.

Fig. 7(a) and (b) give examples how to analyze the temperature–time and pressure–time graphs for each cell using the isothermal KHI test method. The pressure decreases linearly as the gas inside of each cell is cooled quickly to 4 °C. After the temperature stabilizes at 4 °C, the pressure–time graph remains horizontal. Then, when the pressure deviates from a horizontal line, it means that some of the methane gas has been converted to methane hydrates. The time corresponding to this pressure deviation from when the system enters the hydrate forming region is called the gas hydrate induction time (t_i). (Actually, nucleation may have occurred at a microscopic level before t_i but could not be detected). The time from when the system enters the hydrate forming region until when the pressure trace first reaches the steepest point is called the gas hydrate rapid formation time (t_a). For some KHIs, it is difficult to find the t_i value, as we have tried to illustrate in Fig. 7(a) and (b). In Fig. 7(a), the first sign of pressure drop due to hydrate formation is relatively easy to determine, but in Fig. 7(b) the pressure drop is very slow for over a day, making an accurate determination of t_i more difficult.

3. Results and discussion

The results from the constant cooling tests are summarized in Table 2. Subcooling values are determined using the Teq value at Po. The average data were calculated from at least five results unless otherwise stated. Five tests was deemed sufficient to determine the best KHIs, as several products gave some test results with no hydrate formation down to the minimum test temperature of 2 °C. This is why we used the isothermal test method on the best products. The ΔT values for results with amine oxides in the

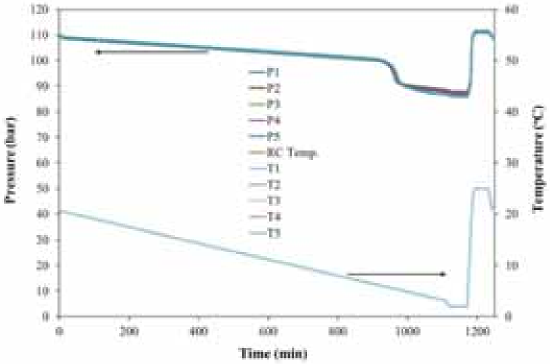

Fig. 5. Typical temperature–time and pressure–time graphs obtained from the slow constant cooling method. RC Temp. is the temperature of the water bath (The example shown is for TEPA-(n-Bu)-AO at concentration 2500 ppm).

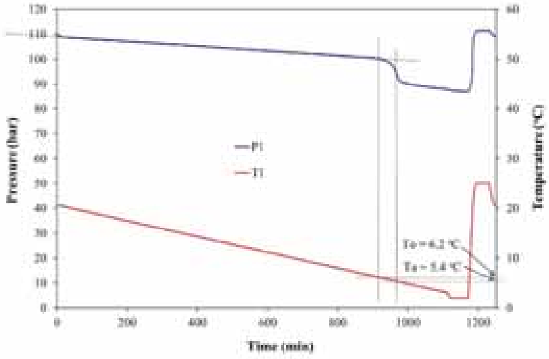

Fig. 6. Determination of To and Ta from the slow constant cooling method. (Example is for 2500 ppm of TEPA-(n-Bu)-AO).

TEPA-R-AO and HPEI-R-AO series are also summarized graphically in Fig. 8.

For the constant cooling tests, all solution with additives gave an improved KHI performance compared to pure water. The three commercial KHIs, Luvicap 55 W, Inhibex 101 and Inhibex BIO-800, gave good KHI performance on methane gas hydrates with average ΔT values of 10.0, 10.5 and 11.0 °C respectively.

Chronologically, we began our studies of the amine oxides of tetraethylenepentamine (TEPA-R-AO) and hyperbranched polyethylenimine (HPEI-R-AO) using n-butylated derivatives (R = Bu) as we had seen good performance in our studies on sII hydrates (Kelland and Mady 2016, Magnusson and Kelland 2015).

All of the polyamine oxides synthesised were either totally clear in solution at room temperature (ca. 20.5 °C) or slightly opaque. This enabled us to fill the rocking cells with all the test fluids at room temperature with no deposits formed. Those polymers that gave clear solutions at room temperature were heated to see if they had a cloud point. A few polymers gave some slight opaqueness to the solution on heating and none of them was observed to give any deposition up to 90 °C as 1 wt% solutions in deionized water.

In this study we discovered that substitution with larger alkyl groups than n-butyl could still give water-soluble amine oxides as long as the polymer molecular weight was kept low. For example the n-butylated amine oxide of HPEI with molecular weight of 10 000 g/mole had previously been shown to be water-insoluble at all temperatures at 2500 ppm. But in this study we found that lowering the HPEI molecular weight to 300–1200 g/mole could give

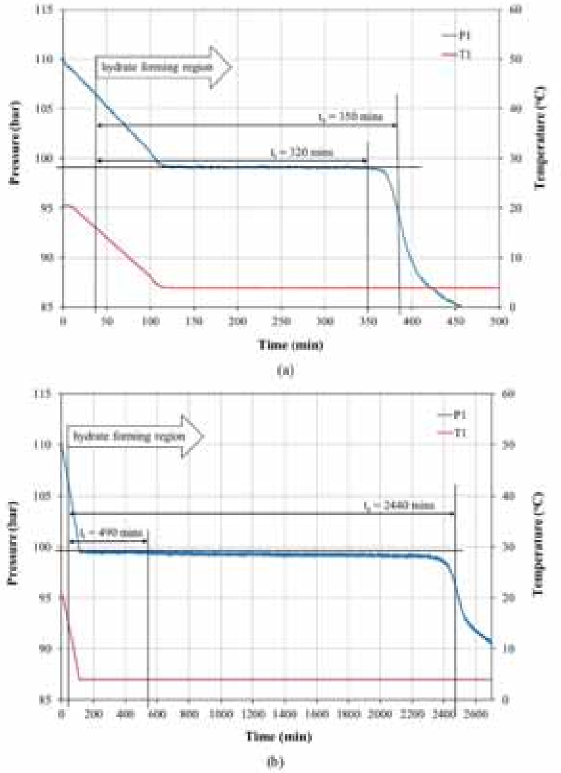

Fig. 7. Determination of t_i and t_a from the isothermal method: (a) 2500 ppm of HPEI-0.3 k-(iso-Pen)-AO and (b) 2500 ppm of HPEI-0.6 k-(iso-Pen)-AO.

water-soluble amine oxides even with C_{5-6} groups. The same solubility trend was found to be true for TEPA, which is a mixture of oligoamines with molecular weight average of approximately 220 g/mole.

As the results in Table 2 show, for the TEPA-R-AO series, we observed a trend in that increasing the size of the alkyl groups from ethyl to pentyl (n- or iso-pentyl) led to a clear improvement in the KHI performance, i.e. lower To and higher ΔT values. There is some precedence for pentyl groups giving improved performance over butyl groups in LDHIs. For example, Shell discovered that quaternary ammonium salts with pentyl groups were better hydrate growth inhibitors than the equivalent butylated salts (Klomp et al. 1995). Other more recent works have shown the same trend for amine oxide and quaternary ammonium salts (Klug 2000, Chua and Kelland 2012a, Magnusson and Kelland 2015, Kelland et al. 2012).

The same trend of increasing KHI performance with increasing size alkyl groups was also observed for the HPEI-R-AO series. Furthermore, the HPEI-R-AO series performed better than the equivalent TEPA-R-AO with the same size alkyl groups at the same concentration. For example, TEPA-(n-Bu)-AO gave an average To of 6.1 °C whereas HPEI-0.3 k-n-Bu-AO gave an average of 3.2 °C, both at 2500 ppm. Therefore, as we were looking to find the optimal polyamine oxide, we concentrated the rest of our investigation, including the isothermal studies, on the HPEI-R-AO series.

When the alkyl groups in HPEI-0.3 k-R-AO series contained 4 or more carbons, the measurement limitation occurs using the constant cooling method. This was due to the high performance of

Table 2
Summary of To and Ta values for KHIs at the active concentration of 1500 ppm and 2500 ppm in water and subcooling degree (ΔT) at To (For KHIs with To = 2 °C, the times at this temperature before hydrate onset are included).

Additive	Conc. (ppm)	To (°C)	ΔT at To (°C)	Ta (°C)	To − Ta (°C)
pure water		12.0 ± 0.6	3.6 ± 0.6	11.9 ± 0.6	0.1 ± 0.1
Luviscap 55 W	2500	5.4 ± 0.8	10.0 ± 0.8	4.6 ± 0.4	0.8 ± 0.4
Inhibex 101	2500	4.8 ± 0.8	10.5 ± 0.8	4.3 ± 0.6	0.6 ± 0.3
Inhibex BIO-800	2500	4.4 ± 0.3	11.0 ± 0.3	4.0 ± 0.2	0.4 ± 0.2
TEPA-Et-AO	2500	11.3 ± 0.3	4.3 ± 0.3	11.2 ± 0.3	0.1 ± 0.2
TEPA-(n-Pro)-AO	2500	8.5 ± 0.5	7.0 ± 0.5	8.2 ± 0.5	0.3 ± 0.1
TEPA-(n-Bu)-AO	2500	6.1 ± 0.3	9.4 ± 0.3	5.4 ± 0.2	0.7 ± 0.2
TEPA-(iso-Pen)-AO	2500	3.1 ± 0.2	12.2 ± 0.2	2.3 ± 0.4	0.8 ± 0.4
TEPA-(n-Pen)-AO	2500	4.2 ± 0.3	11.2 ± 0.3	4.0 ± 0.2	0.2 ± 0.1
HPEI-0.3 k-Et-AO	2500	10.7 ± 0.4	4.8 ± 0.4	10.6 ± 0.2	0.1 ± 0.1
HPEI-0.3 k-(n-Pro)-AO	2500	5.5 ± 0.4	9.9 ± 0.4	5.3 ± 0.4	0.2 ± 0.1
HPEI-0.3 k-(n-Bu)-AO	1500	5.5 ± 0.2	9.9 ± 0.2	5.3 ± 0.2	0.2 ± 0.1
	2500	3.2 ± 0.2	12.1 ± 0.2	3.1 ± 0.1	0.1 ± 0.1
HPEI-0.3 k-(iso-Pen)-AO	1500	3.3 ± 0.9	12.0 ± 0.9	3.1 ± 1.1	0.2 ± 0.8
	2500	2.0 ± 0.0 ^{a}	13.1 ± 0.0	2.0 ± 0.0	0 ± 0.0
HPEI-0.3 k-(n-Pen)-AO	1500	5.5 ± 0.2	9.8 ± 0.2	5.4 ± 0.2	0.1 ± 0.1
	2500	3.3 ± 0.1	12.0 ± 0.1	2.7 ± 0.5	0.6 ± 0.4
HPEI-0.3 k-(iso-Hex)-AO	1500	4.0 ± 0.6	11.1 ± 0.6	3.9 ± 0.6	0.1 ± 0.1
	2500^{b}	2.2 ± 0.2 ^{c}	13.1 ± 0.2 ^{c}	2.0 ± 0.0 ^{c}	0.2 ± 0.0 ^{c}
HPEI-0.3 k-(t-Hex)-AO	1500	4.1 ± 0.5	11.2 ± 0.5	4.0 ± 0.5	0.1 ± 0.1
	2500	2.0 ± 0.0 ^{d,e}	13.3 ± 0.0 ^{d}	2.0 ± 0.0 ^{d}	0 ± 0.0 ^{d}
HPEI-0.3 k-(iso-Pen)-quaternary ammonium bromide	2500^{b}	10.2 ± 0.1	5.3 ± 0.1	10.0 ± 0.1	0.2 ± 0.1
HPEI-0.3 k-(iso-Pen)-propylenesulfone	2500	8.8 ± 0.1	6.7 ± 0.1	6.9 ± 0.1	1.9 ± 0.2

[a] the times at 2 °C before hydrate onset for the five cells are 1143 ± 9 mins.
[b] not fully soluble in water.
[c] calculated from the two results obtained from 5 cells, no gas hydrate detected from the other three cells.
[d] calculated from the four results obtained from 5 cells, no gas hydrate detected from the other cell.
[e] the times at 2 °C before hydrate onset for the four cells with hydrate formation are 1151 ± 20 mins.

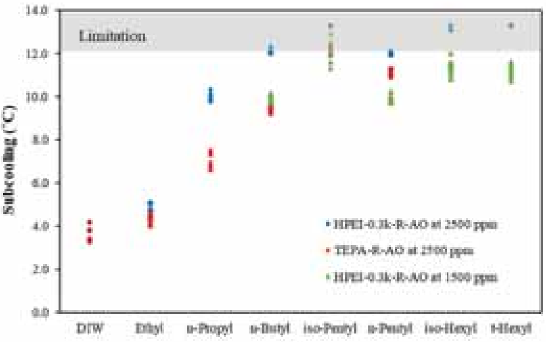

Fig. 6. ΔT values for amine oxides with different alkyl groups.

these polymers, and the fact that the lowest temperature using this method was 2 °C. However, the software also caused an unexpected and unprogrammed temperature drop at 3.1 °C (ΔT = 12.2 °C) of 1.1 °C down to 2 °C in 15 min (see Figs. 5 and 6), which could not be fixed by the supplier. This still means that To values obtained below 3.1 °C (i.e. ΔT ≥ 12.2 °C) can be compared between KHIs. For KHIs that gave first sign of pressure drop at 2 °C, we included the time at this temperature before this occurred.

Since several products in the HPEI-0.3 k-R-AO series fell in this category, we sought better ways to separate their ranking. As you will see later in this report, we ended up doing isothermal studies, but there are variations available within the same constant cooling test method. Thus, using this method, higher pressure was considered so that we could obtain greater subcoolings. However, some studies have shown that absolute pressure can affect KHI performance so we did not want to vary this parameter (Arjmandi et al. 2005, Kelland et al. 2008, Kelland et al. 2000, Peytavy et al. 2007).

A second method, which we deployed to avoid very low onset temperatures was to decrease the active polymer concentration to 1500 ppm. This was done for five HPEI-R-AO polymers with alkyl groups containing four or more carbon atoms. We observed that all polymers lost some KHI effect compared to tests at 2500 ppm, giving higher average To values as expected. However, the difference in To values was only sufficient to determine that the n-butylated and n-pentylated polymers performed a little worse than the other three polymers at a statistically significant level (>95%). The results at 1500 ppm also suggested that improvements on the butylated polymer could be made by lengthening the alkyl chain (iso-hexyl polymer) and/or splitting the end to form iso-alkyl or t-alkyl groups. The same conclusions were made from the results with the TEPA-R-AO series at 2500 ppm as shown in Table 2 or Fig. 8. The reason why the KHIs with long and branched alkyl groups have better KHI performance maybe because that these large hydrophobic groups can disturb the water structure on or around growing gas hydrate clusters, thus inhibiting the gas hydrate formation process (Kelland et al. 2015, Mady and Kelland 2018, Zhang et al. 2018a, Zhang et al. 2018b). We also tested two polymers that are not amine oxides. These are HPEI-0.3 k-(iso-Pen)-quaternary ammonium bromide and HPEI-0.3 k-(iso-Pen)-propylenesulfonate. These two polymers were derived from the same molecular weight HPEI core (0.3 k = 300 g/mole) and the same size iso-pentyl groups as the related HPEI-0.3 k-(iso-Pen)-AO, which contains amine oxide groups. The cationic (quaternary) and zwitterionic (quaternary sulfonate) polymers gave much higher To values and therefore worse KHI performance than the related amine oxide polymer. The only difference was some 2-propanol (IPA) solvent in the polyamine oxide tests but this solvent has been shown to have negligible synergistic effect on amine oxide products from a previous study (Kelland et al. 2012). Therefore, we attribute the better KHI performance of HPEI-0.3 k-(iso-Pen)-AO to the amine oxide groups and the strong hydrogen-bonding ability. This ability, together with the pendant alkyl groups, gives better interaction with either free water molecules or gas hydrates particle surfaces to prevent hydrate nuclei or crystal growth (Yagasaki et al. 2015, Yang and Tohidi 2011).

To further evaluate the KHI performance of the HPEI-R-AO series with alkyl groups of four or more carbon atoms, we carried out isothermal tests. The data are summarized in Table 3. The results of two commercial KHIs, Luvicap 55 W (a VP:VCap copolymer in water) and Inhibex BIO-800 (a VCap copolymer in butyl glycol ether) are also included for comparison. Each solution was tested five times to give the average data, but we repeated more times if the results were very scattered.

Table 3
Summary of induction time (t_i) and rapid hydrate formation time (t_a) values for KHIs at 2500 ppm active polymer in deionized water.

Additive	Synthesis solvent	t_i (min)	t_a (min)
Luvicap 55 W		87 ± 7	306 ± 4
Luvicap 55 W with added 5500 ppm BGE		88 ± 3	309 ± 6
Inhibex BIO800 in 5500 ppm BGE		93 ± 8	113 ± 8
TEPA-(iso-Pen)-AO	IPA	227 ± 8	237 ± 8
HPEI-0.3 k-(n-Bu)-AO	IPA	158 ± 28	172 ± 32
HPEI-0.3 k-(iso-Pen)-AO	IPA	300 ± 60	356 ± 54
HPEI-0.3 k-(n-Pen)-AO	IPA	380 ± 165	688 ± 322
HPEI-0.3 k-(iso-Hex)-AO [a]	IPA	807 ± 953	826 ± 954
HPEI-0.3 k-(t-Hex)-AO	IPA	730 ± 110	1026 ± 56
HPEI-0.6 k-(n-Pen)-AO	IPA	486 ± 156	2412 ± 572
HPEI-1.2 k-(n-Pen)-AO	IPA	120 ± 35	130 ± 35
HPEI-10 k-(n-Pen)-AO [a]	IPA	110 ± 12	121 ± 10
HPEI-0.6 k-(iso-Pen)-AO	IPA	518 ± 72	2406 ± 254
HPEI-1.2 k-(iso-Pen)-AO	IPA	864 ± 326	1630 ± 718
HPEI-10 k-(iso-Pen)-AO [a]	IPA	88 ± 3	93 ± 2
HPEI-1.2 k-(iso-Hex)-AO [a]	IPA	73 ± 3	76 ± 1
TEPA-(iso-Pen)-AO	BGE	238 ± 22	281 ± 29
HPEI-0.3 k-(n-Bu)-AO	BGE	109 ± 21	119 ± 21
HPEI-0.3 k-(iso-Pen)-AO	BGE	702 ± 349	878 ± 298
HPEI-0.3 k-(n-Pen)-AO	BGE	583 ± 548	1108 ± 1032
HPEI-0.3 k-(iso-Hex)-AO [a]	BGE	581 ± 350	598 ± 543
HPEI-0.3 k-(t-Hex)-AO	BGE	2976 ± 736	4876 ± 2606

[a] not fully soluble in water.

As the trend of the rapid hydrate formation time (t_a) is generally the same as that of the induction time (t_i), we focus on t_i in the follow text. For the amine oxides made in IPA solvent, Table 3 and Fig. 9 show that at the concentration of 2500 ppm, the average t_i values in the isothermal tests increases as you increase the carbons in the alkyl groups from 4 to 5 to 6. This is a statistically significant result from t-tests at the 95% confidence level. However, the average t_i values for the two pentylated HPEI-0.3 k-AO polymers (n- and iso-) were fairly similar and the ranking of them could not be differentiated. If we compare the results obtained from constant cooling test (see Table 2 and Fig. 9), they show that at the concentration of 1500 ppm, HPEI-0.3 k-(iso-Pen)-AO gave a better performance than HPEI-0.3 k-(n-Pen)-AO. This discrepancy between the two test methods may be due to testing at different concentrations. In addition, if we had chosen a different subcooling degree than 11.4 °C in the long-term isothermal tests it is possible we would had seen a clearer ranking difference between the pentylated amine oxides. For the hexylated derivatives, both HPEI-0.3 k-(iso-Hex)-AO and HPEI-0.3 k-(t-Hex)-AO clearly outperform HPEI-0.3 k-Pen-AO, but we could not differentiate between the performance of the two hexylated HPEI-0.3 k-AO polymers from statistical t-tests.

As the high flash point solvent BGE has been reported to be a very good synergist for several KHI polymers, we also made HPEI-0.3 k-R-AO in BGE. Results show that BGE gave optimum synergistic KHI effect on HPEI-0.3 k-(iso-Pen)-AO and HPEI-0.3 k-(t-Hex)-AO. This fits a theory we proposed earlier that better synergy may occur by having one product with a straight chain and the other with a branched alkyl (Zhang et al. 2018b). This theory may seem to break down when adding BGE to HPEI-0.3 k-(iso-Hex)-AO, as it did not improve the KHI performance. However, the solubility may be an issue here, as the HPEI-0.3 k-(iso-Hex)-AO made in BGE was not totally soluble in water at 2500 ppm.

The last sub-study using the isothermal test method was to investigate the effect of molecular weight on KHI polymer performance. Although they gave the best KHI performance, the branched hexylated polyamine oxide derivatives are very expensive to make and unlikely to have any commercial value. Therefore, we concentrated on the next best derivatives which were the pentylated polymers. Fig. 10 shows the induction time of HPEI-Pen-AO (n- or iso-) with molecular weights of 300, 600, 1200, and 10000 g/mole. These HPEI-Pen-AOs are made in IPA and the active KHI dosages of them in aqueous solution are 2500 ppm. Both HPEI-(n-Pen)-AO and HPEI-(iso-Pen)-AO with the 10000 g/mole molecular weight perform the poorest, as they are not fully soluble in water. They are also expected to be well over the molecular weight limitation for the optimal KHI performance. Normally, KHI polymers with the molecular weight of approximately 1000–3000 g/mole (ca. 8–20 monomer units) perform the best (Chua and Kelland 2012b, Kelland 2006, Magnusson and Kelland 2015). When the molecular weight increased from 300 to 1200 g/mole, an increasing trend in induction time can be seen on the HPEI-(iso-Pen)-AO series. However, for the HPEI-(n-Pen)-AO series, those polymers with the lowest molecular weight gave the longest induction time. The KHI performances of HPEI-0.3 k-(n-Pen)-AO and the HPEI-0.6 k-(n-Pen)-AO showed no statistical difference by the t-test method. At this time we have no explanation why the n-pentylated polyamine oxide with molecular weight 1200 g/mole did not perform as well as the iso-pentylated version. The cloud point of the two polymers are almost identical

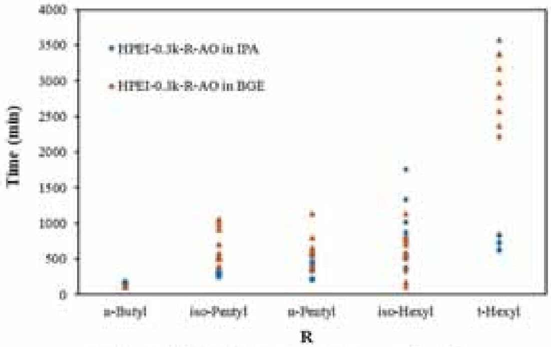

Fig. 9. t_i values for HPEI-0.3 k-R-AO with varying alkyl groups in IPA or BGE.

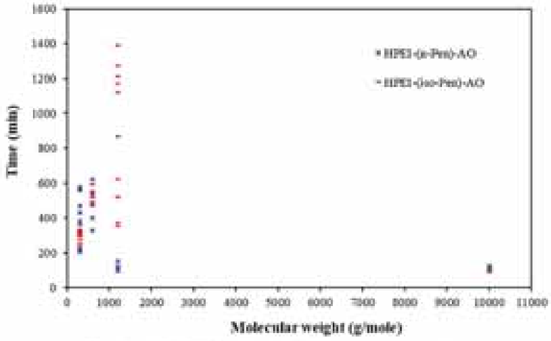

Fig. 10. t_i values for HPEI-Pen-AO made in IPA with varying molecular weights.

(19 °C and 18 °C respectively), which suggests that the degree of pentylation is similar.

Overall from our studies, it appears that branching on the ends of the alkyl chains is beneficial for polyamineoxide-based KHIs for sI-forming methane hydrate. This branching may have an iso-chain end, which resembles the size and shape of propane, and tert- chain end which resemble iso-butane (2-methylpropane). These alkyl chain ends are too large to enter either 5^{12} or $5^{12}6^2$ open cavities found in sI hydrates, but are the correct size to enter $5^{12}6^4$ open cavities of sII hydrate (or the $5^{12}6^8$ cavity of sH hydrate). Furthermore, it is known that methane hydrate can lead to the temporary formation of sII as the kinetic product as well as sI as the thermodynamic product. This comes from both laboratory and computer simulation studies (Lauricella et al. 2014, Ohno et al. 2009). Based on this knowledge, we speculate that these alkyl chain ends will enter or form $5^{12}6^4$ cavities around them, a process which inhibits the formation of the thermodynamically stable sI hydrate that does not contain this cage size.

4. Conclusion

Two series of polyamine oxides, TEPA-R-AO and HPEI-R-AO have been synthesized and investigated as sI gas hydrate KHIs in high-pressure rocking cells. TEPA-R-AO showed an increased KHI effect with increasing the number of carbons in the alkyl groups up to five carbon atoms. TEPA-(iso-Pen)-AO performed better than TEPA-(n-Pen)-AO. The HPEI-R-AO series generally gave better KHI performance than the TEPA-R-AO series. At a concentration of 2500 ppm, several polyamine oxides gave such good KHI efficacy that the minimum temperature limit of 2 °C was reached (13.3 °C subcooling at 98 bar).

To distinguish the ranking of these polymers, long-term isothermal experiments were deployed. The performance increased as the number of carbons in the alkyl groups was increased from 4 to 5 to 6 for HPEI-0.3 k-R-AO. The solvent BGE showed very good synergy with the polyamine oxides with branched alkyl groups, especially for those with *tert*-hexyl groups. With the synergistic effect of ca. 6000 ppm BGE, the average induction time of 2500 ppm HPEI-0.3 k-(t-hexyl)-AO improved from 730 to 2976 min. The effect of molecular weight on HPEI-Pen-AO was explored. The HPEI-(n-Pen)-AO with low molecular weights (300 g/mole and 600 g/mole) gave the most powerful KHI performance. For HPEI-(iso-Pen)-AO, a polymer molecular weight of 1200 g/mole gave the best KHI performance. End-chain branching of the alkyl groups appears to be useful for inhibition of sI hydrate formation. A possible reason for this based on stabilization of hydrate cages of the sI hydrate kinetic product was proposed.

In addition, HPEI-0.3 k-(iso-Pen)-quaternary ammonium and HPEI-0.3 k-(iso-Pen)-sultone were also synthesized and investigated as KHIs. Both of them gave significantly worse KHI performance than HPEI-0.3 k-(iso-Pen)-AO, the corresponding polyamine oxide of similar molecular weight. This underlines that the strongly hydrogen-bonding amine oxide group, and not just the correct size and shape alkyl group, is critical for good KHI performance.

CRediT authorship contribution statement

Qian Zhang: Data curation, Writing - original draft. **Malcolm A. Kelland:** Supervision.

Declaration of Competing Interest

The authors declare that they have no known competing financial interests or personal relationships that could have appeared to influence the work reported in this paper.

References

Zhang, Q., Kawatani, R., Ajiro, H., Kelland, M.A., 2018b. Optimizing the Kinetic Hydrate Inhibition Performance of N-Alkyl-N-vinylamide Copolymers. Energy Fuels 32, 4925–4931.

Zhang, Q., Kelland, M.A., 2018. Study of the Kinetic Hydrate Inhibitor Performance of Poly(N-vinylcaprolactam) and poly(N-isopropylmethacrylamide) with Varying End Caps. Energy Fuels 32, 9211–9219.

Paper VIII

Amine *N*-Oxide Kinetic Hydrate Inhibitor Polymers for High-Salinity Applications

Authors:

Qian Zhang*, Malcolm A. Kelland, Holger Frey, Jan Blankenburg, and Larissa Limmer

Published in Energy & Fuels 2020, 34 (5), 6298-6305.

This paper is not in Brage due to copyright.

Paper IX

Zwitterionic Poly (sulfobetaine methacrylate)s as Kinetic Hydrate Inhibitors

Authors:

Qian Zhang*, Malcolm A. Kelland, Evan M. Lewoczko, Caleb A. Bohannon, and Bin Zhao

Published in Chemical Engineering Science 2020, 229 (2021), 116031.

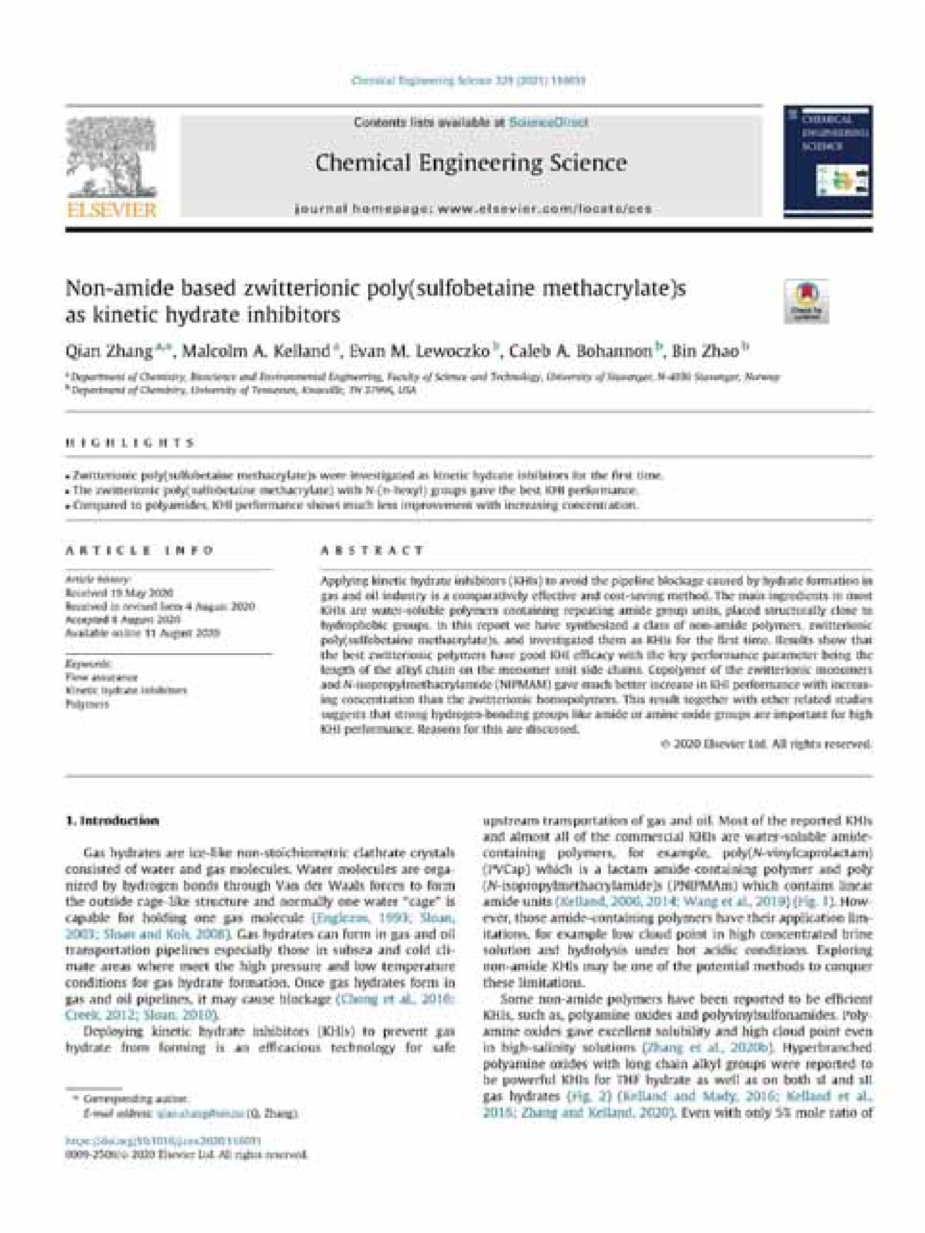

Chemical Engineering Science 229 (2021) 116031

Contents lists available at ScienceDirect

Chemical Engineering Science

journal homepage: www.elsevier.com/locate/ces

Non-amide based zwitterionic poly(sulfobetaine methacrylate)s as kinetic hydrate inhibitors

Qian Zhang[a,*], Malcolm A. Kelland[a], Evan M. Lewoczko[b], Caleb A. Bohannon[b], Bin Zhao[b]

[a] Department of Chemistry, Bioscience and Environmental Engineering, Faculty of Science and Technology, University of Stavanger, N-4036 Stavanger, Norway
[b] Department of Chemistry, University of Tennessee, Knoxville, TN 37996, USA

HIGHLIGHTS

- Zwitterionic poly(sulfobetaine methacrylate)s were investigated as kinetic hydrate inhibitors for the first time.
- The zwitterionic poly(sulfobetaine methacrylate) with N-(n-hexyl) groups gave the best KHI performance.
- Compared to polyamides, KHI performance shows much less improvement with increasing concentration.

ARTICLE INFO

Article history:
Received 19 May 2020
Received in revised form 4 August 2020
Accepted 8 August 2020
Available online 11 August 2020

Keywords:
Flow assurance
Kinetic hydrate inhibitors
Polymers

ABSTRACT

Applying kinetic hydrate inhibitors (KHIs) to avoid the pipeline blockage caused by hydrate formation in gas and oil industry is a comparatively effective and cost-saving method. The main ingredients in most KHIs are water-soluble polymers containing repeating amide group units, placed structurally close to hydrophobic groups. In this report we have synthesized a class of non-amide polymers, zwitterionic poly(sulfobetaine methacrylate)s, and investigated them as KHIs for the first time. Results show that the best zwitterionic polymers have good KHI efficacy with the key performance parameter being the length of the alkyl chain on the monomer unit side chains. Copolymer of the zwitterionic monomers and N-isopropylmethacrylamide (NIPMAM) gave much better increase in KHI performance with increasing concentration than the zwitterionic homopolymers. This result together with other related studies suggests that strong hydrogen-bonding groups like amide or amine oxide groups are important for high KHI performance. Reasons for this are discussed.

© 2020 Elsevier Ltd. All rights reserved.

1. Introduction

Gas hydrates are ice-like non-stoichiometric clathrate crystals consisted of water and gas molecules. Water molecules are organized by hydrogen bonds through Van der Waals forces to form the outside cage-like structure and normally one water "cage" is capable for holding one gas molecule (Englezos, 1993; Sloan, 2003; Sloan and Koh, 2008). Gas hydrates can form in gas and oil transportation pipelines especially those in subsea and cold climate areas where meet the high pressure and low temperature conditions for gas hydrate formation. Once gas hydrates form in gas and oil pipelines, it may cause blockage (Cheng et al., 2016; Creek, 2012; Sloan, 2010).

Deploying kinetic hydrate inhibitors (KHIs) to prevent gas hydrate from forming is an efficacious technology for safe upstream transportation of gas and oil. Most of the reported KHIs and almost all of the commercial KHIs are water-soluble amide-containing polymers, for example, poly(N-vinylcaprolactam) (PVCap) which is a lactam amide-containing polymer and poly(N-isopropylmethacrylamide)s (PNIPMAm) which contains linear amide units (Kelland, 2006, 2014; Wang et al., 2019) (Fig. 1). However, those amide-containing polymers have their application limitations, for example low cloud point in high concentrated brine solution and hydrolysis under hot acidic conditions. Exploring non-amide KHIs may be one of the potential methods to conquer these limitations.

Some non-amide polymers have been reported to be efficient KHIs, such as, polyamine oxides and polyvinylsulfonamides. Polyamine oxides gave excellent solubility and high cloud point even in high-salinity solutions (Zhang et al., 2020b). Hyperbranched polyamine oxides with long chain alkyl groups were reported to be powerful KHIs for THF hydrate as well as on both sI and sII gas hydrates (Fig. 2) (Kelland and Mady, 2016; Kelland et al., 2016; Zhang and Kelland, 2020). Even with only 5% mole ratio of

---

* Corresponding author.
E-mail address: qian.zhang@uis.no (Q. Zhang).

https://doi.org/10.1016/j.ces.2020.116031
0009-2509/© 2020 Elsevier Ltd. All rights reserved.

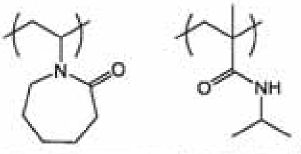

Fig. 1. Structures of the monomer units of *N*-vinylcaprolactam (left) and *N*-isopropylmethacrylamide (right).

N-n-propylvinylsulfonamide monomer units in the (*N*-n-propylvinylsulfonamide:*N*-vinyl-*N*-methyl acetamide) copolymer, this gave a KHI performance on a par with commercial PVCap (Zhang et al., 2020a) (Fig. 2). Thus, the excellent properties of these polymers led us to explore more non-amide based KHI polymer series.

A series of zwitterionic surfactants, such as 3-[*N*,*N*-dibutyl-*N*-(2-(3-carboxy-pentadecenoyloxy)propyl)]ammonio propanoate, have been reported to be efficient anti-agglomerants (AAs) (Kelland, 2006; Kelland et al., 2006). Alkyl zwitterions containing one to ten carbon atoms showed synergistic effect with amide-based KHI polymers (Colle et al., 2000). Tributylammoniumpropylsulfonate (TBAPS) gave slightly better crystal growth inhibition performance than commercial polyvinylpyrrolidone (PVP) on tetrahydrofuran (THF) hydrate (Storr et al., 2004). Zwitterionic poly(sulfobetaine methacrylate)s (PSBMAs) contain both sulfonate anion and amine cation in the pendent side chain of each repeat unit. The intriguing properties of zwitterionic PSBMAs, for example, superior hydrophilicity (Jiang and Cao, 2010; Mary et al., 2007; Shao and Jiang, 2015), antipolyelectrolyte effect (Laschewsky and Rosenhahn, 2018; Laschewsky, 2014), and ultralow biofouling property (Zhang et al., 2013), make them widely used in biomaterial, nanomedicine and healthcare applications (Blackman et al., 2019; Kao et al., 2017). Polyzwitterions were considered as poor KHIs as they are predominantly hydrophilic polymers (Kelland, 2011). However, the nitrogen atoms in zwitterionic PSBMAs provide covalent bonds for grafting hydrophobic alkyl groups that are considered to be the critical part of preventing gas hydrates from forming (Abrahamsen and Kelland, 2016; Ajiro et al., 2010; Zhang et al., 2020b). In addition, poly(2-acrylamido-1-alkanesulfonic acid, sodium salt)s that are structurally similar to zwitterionic PSBMAs have been reported as efficient KHIs, especially these with long alkyl side chains such as poly(2-acrylamido-1-hexanesulfonic acid, sodium salt) (Peiffer et al., 1999) (Fig. 3). Thus, *N*-alkylated zwitterionic PSBMAs have great potential to be efficient and environmentally-friendly KHIs. As part of a long-term project we have investigated non-amide classes of polymer to determine 1) If they can perform better than polyamides 2) If they have other advantages such as cost or better brine compatibility/cloud point 3) If they can help determine the KHI mechanism(s), which motivated this study.

We have synthesized a series of zwitterionic 3-((2-methacryloyloxyethyl)(methyl)(n-alkyl)ammonio)propane-1-sulfonate homopolymers with varying length of alkyl groups at the nitrogen atoms and these alkyl groups include n-butyl, n-pentyl and n-hexyl groups (Wang et al., 2018) (Fig. 3). We also synthesized zwitterionic 3-((2-methacryloyloxyethyl)(dipentyl)ammonio)propane-1-

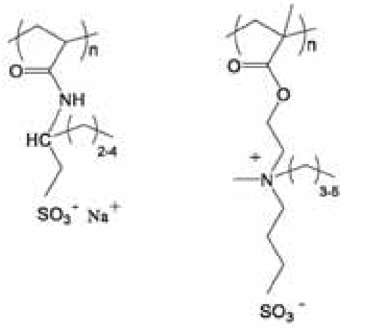

Fig. 3. Structures of poly(2-acrylamido-1-alkanesulfonic acid, sodium salt)s and zwitterionic poly(sulfobetaine methacrylate)s with varying N-alkyl side chains.

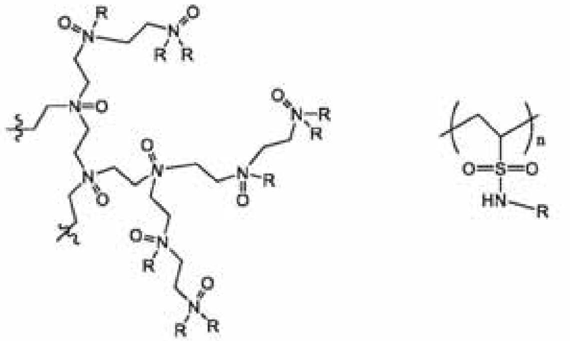

Fig. 2. Structures of hyperbranched polyamine oxide (right) and polyvinylsulfonamide (left). R = alkyl groups.

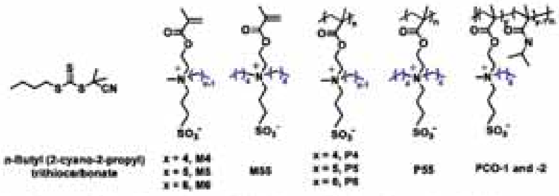

Scheme 1. Molecular structures of n-butyl (2-cyano-2-propyl) trithiocarbonate (the chain transfer agent), zwitterionic monomers, and polymers.

sulfonate homopolymer and copolymers from zwitterionic 3-((2-methacryloyloxyethyl)(methyl)(n-hexyl)ammonio)propane-1-sulfonate monomers and N-isopropylmethacrylamide (NIPMAM) monomers. We report here the KHI performance of these non-amide based zwitterionic homopolymers and copolymers for the first time.

2. Experimental section

2.1. Synthesis and characterization of zwitterionic polymers

The detailed information on the synthesis and characterization of the zwitterionic polymers is shown as a supplementary file. Scheme 1 shows the molecular structures of the zwitterionic monomers and polymers synthesized in this study.

2.2. Kinetic hydrate inhibition performance tests of zwitterionic polymers

The slow constant cooling (SCC) method was deployed to test the kinetic hydrate inhibition performance of the zwitterionic polymers. SCC tests were carried out in high-pressure rocker rig RC5, provided by PSL Systemtechnik, Germany. The SCC method and the high-pressure rocker rig have been reported in many previous studies (Abrahamsen and Kelland, 2016; Zhang et al., 2018a, 2018b). The testing process of the SCC method in the rocker rig equipment is as follows:

(1) 10.0 mL of solution with KHI polymer dissolved in it and a steel ball for agitation were loaded in each of the five steel cells.
(2) The air in the cells and the tubes of the system was removed by vacuuming, purging with synthetic nature gas (SNG) mixture (Table 1), and then vacuuming the second time.
(3) When the temperature of the cells was stabilized at 20.5 °C, the cells were pressurized to 76 bar by loading SNG mixture. The equilibrium temperature and pressure of this point were calculated by Calsep's PVTSim software using cubic equation of state (EOS), which consistent with the data measured from our rocker rig equipment (Chua and Kelland, 2012).
(4) After turning off the gas inlet-outlet valve of each cell, the cells were slowly cooled from 20.5 °C to 2 °C at a constant rate of 1 °C/h and meanwhile the cells were rocked for agitation of the solution in them. Theoretically, structure II (sII) hydrate can form as the most stable phase during the cooling period in this system, however structure I (sI) hydrate can potentially form if the temperature becomes low enough to enter the phase boundary of sI hydrate (Abrahamsen and Kelland, 2018).
(5) A local computer was used to collect the pressure and temperature data of each cell through sensors.

Table 1
Composition of synthetic nature gas mixture.

Component	mol %
methane	80.67
ethane	10.20
propane	4.90
CO_2	1.84
isobutane	1.53
n-butane	0.76
N_2	0.10

Fig. 4 shows typical graphs of pressure-time and temperature-time obtained from a SCC testing process of all five cells. The pressure dropped a little when the cells starting rocking as the SNG mixture is slightly soluble in water. With the temperature gradually cooling down, the pressure-time curves decreased linearly. When the temperature reached the gas hydrate onset temperature (T_o), the pressure deviated the decreasing line as some gas molecules were consumed to form gas hydrates (P_o). When the temperature reached the rapid hydrate formation temperatures (T_a), the pressure dropped the fastest due to the quick growth of gas hydrates involving a large number of gas consumption (P_a).

Fig. 5 shows how to analyze the pressure-time and temperature-time graphs obtained from one cell. Normally, a temperature rise is expected when gas hydrates form due to the exothermic reaction of gas hydrate formation. However, the temperature spike may not occur if the heat can be conducted away quickly enough to keep the temperature-time graph stable. Thus, for the RC5 equipment observing the pressure-time curve is the only way of getting the information of gas hydrate formation. From

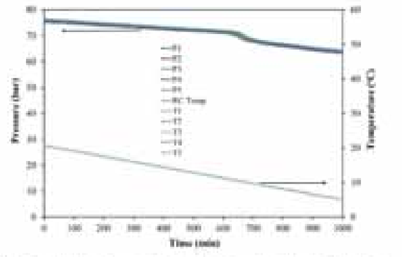

Fig. 4. Typical graphs of pressure-time and temperature-time obtained from all five cells. Example show with solution of P5-3 at 2500 ppm.

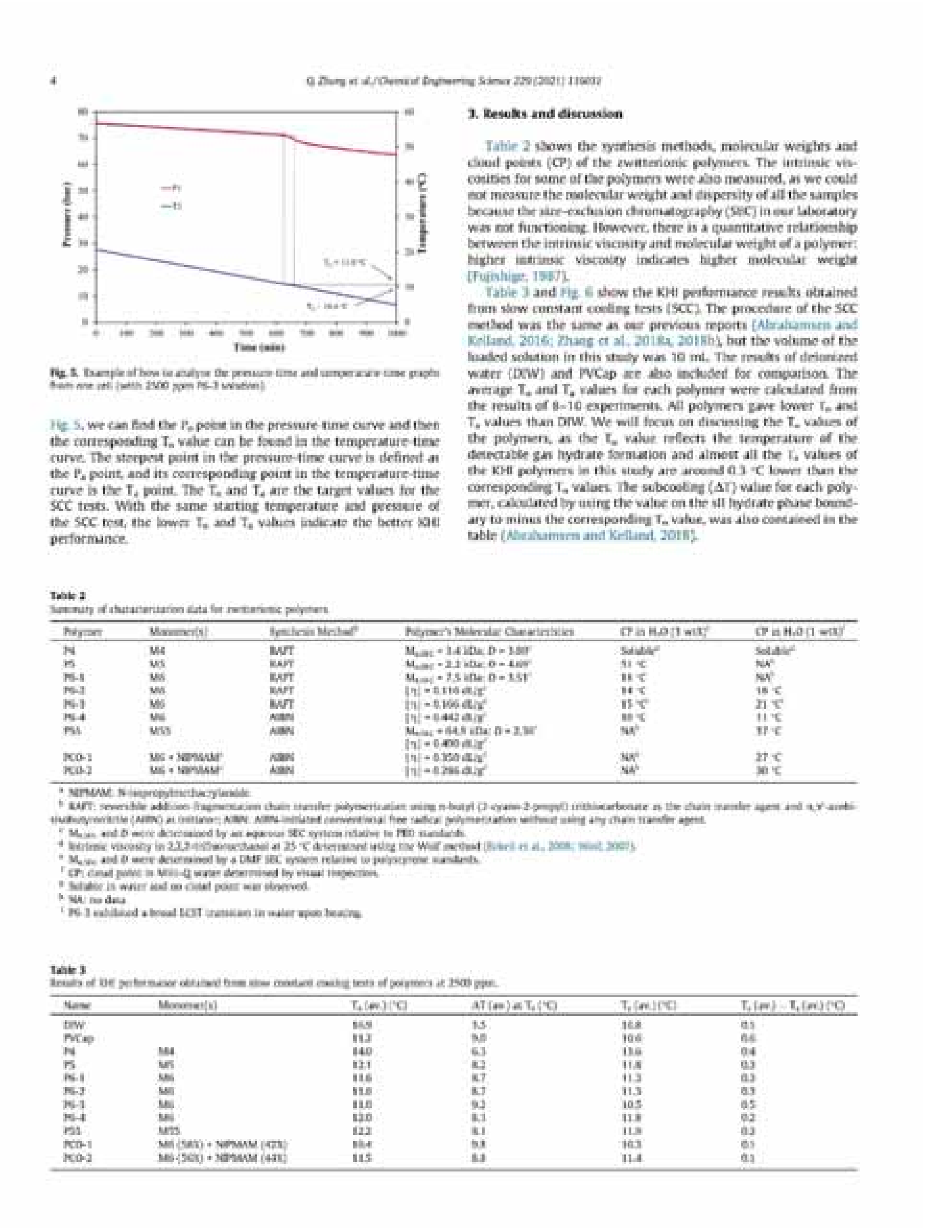

Pressure (bar)
Temperature (°C)
Time (min)
P1
T1
0
10
20
30
40
50
60
70
80
0
100
200
300
400
500
600
700
800
900
1000

Fig. 5. Example of how to analyze the pressure-time and temperature-time graphs from one cell (with 2500 ppm P6-3 solution).

Fig. 5, we can find the P_o point in the pressure-time curve and then the corresponding T_o value can be found in the temperature-time curve. The steepest point in the pressure-time curve is defined as the P_a point, and its corresponding point in the temperature-time curve is the T_a point. The T_o and T_a are the target values for the SCC tests. With the same starting temperature and pressure of the SCC test, the lower T_o and T_a values indicate the better KHI performance.

3. Results and discussion

Table 2 shows the synthesis methods, molecular weights and cloud points (CP) of the zwitterionic polymers. The intrinsic viscosities for some of the polymers were also measured, as we could not measure the molecular weight and dispersity of all the samples because the size-exclusion chromatography (SEC) in our laboratory was not functioning. However, there is a quantitative relationship between the intrinsic viscosity and molecular weight of a polymer: higher intrinsic viscosity indicates higher molecular weight (Fujishige, 1987).

Table 3 and Fig. 6 show the KHI performance results obtained from slow constant cooling tests (SCC). The procedure of the SCC method was the same as our previous reports (Abrahamsen and Kelland, 2016; Zhang et al., 2018a, 2018b), but the volume of the loaded solution in this study was 10 mL. The results of deionized water (DIW) and PVCap are also included for comparison. The average T_o and T_a values for each polymer were calculated from the results of 8–10 experiments. All polymers gave lower T_o and T_a values than DIW. We will focus on discussing the T_o values of the polymers, as the T_o value reflects the temperature of the detectable gas hydrate formation and almost all the T_a values of the KHI polymers in this study are around 0.3 °C lower than the corresponding T_o values. The subcooling (ΔT) value for each polymer, calculated by using the value on the sII hydrate phase boundary to minus the corresponding T_o value, was also contained in the table (Abrahamsen and Kelland, 2018).

Table 2
Summary of characterization data for zwitterionic polymers.

Polymer	Monomer(s)	Synthesis Method[b]	Polymer's Molecular Characteristics	CP in H_2O (5 wt%)[f]	CP in H_2O (1 wt%)[f]
P4	M4	RAFT	$M_{n(SEC)}$ = 1.4 kDa; Đ = 3.00[c]	Soluble[g]	Soluble[g]
P5	M5	RAFT	$M_{n(SEC)}$ = 2.2 kDa; Đ = 4.69[c]	51 °C	NA[h]
P6-1	M6	RAFT	$M_{n(SEC)}$ = 7.5 kDa; Đ = 3.51[c]	88 °C	NA[h]
P6-2	M6	RAFT	[η] = 0.116 dL/g[d]	84 °C	18 °C
P6-3	M6	RAFT	[η] = 0.166 dL/g[d]	85 °C[i]	21 °C
P6-4	M6	AIBN	[η] = 0.442 dL/g[d]	80 °C	11 °C
P55	M55	AIBN	$M_{n(SEC)}$ = 64.9 kDa; Đ = 2.30[e] [η] = 0.400 dL/g[d]	NA[h]	37 °C
PCO-1	M6 + NIPMAM[a]	AIBN	[η] = 0.350 dL/g[d]	NA[h]	27 °C
PCO-2	M6 + NIPMAM[a]	AIBN	[η] = 0.266 dL/g[d]	NA[h]	30 °C

[a] NIPMAM: N-isopropylmethacrylamide.
[b] RAFT: reversible addition-fragmentation chain transfer polymerization using n-butyl (2-cyano-2-propyl) trithiocarbonate as the chain transfer agent and α,α′-azobisisobutyronitrile (AIBN) as initiator; AIBN: AIBN-initiated conventional free radical polymerization without using any chain transfer agent.
[c] $M_{n(SEC)}$ and Đ were determined by an aqueous SEC system relative to PEO standards.
[d] Intrinsic viscosity in 2,2,2-trifluoroethanol at 25 °C determined using the Wolf method (Eckelt et al., 2008; Wolf, 2007).
[e] $M_{n(SEC)}$ and Đ were determined by a DMF SEC system relative to polystyrene standards.
[f] CP: cloud point in Milli-Q water determined by visual inspection.
[g] Soluble in water and no cloud point was observed.
[h] NA: no data.
[i] P6-3 exhibited a broad LCST transition in water upon heating.

Table 3
Results of KHI performance obtained from slow constant cooling tests of polymers at 2500 ppm.

Name	Monomer(s)	T_o (av.) (°C)	ΔT (av.) at T_o (°C)	T_a (av.) (°C)	T_o (av.) − T_a (av.) (°C)
DIW		16.9	3.5	16.8	0.1
PVCap		11.2	9.0	10.6	0.6
P4	M4	14.0	6.3	13.6	0.4
P5	M5	12.1	8.2	11.8	0.3
P6-1	M6	11.6	8.7	11.3	0.3
P6-2	M6	11.6	8.7	11.3	0.3
P6-3	M6	11.0	9.2	10.5	0.5
P6-4	M6	12.0	8.3	11.8	0.2
P55	M55	12.2	8.1	11.9	0.3
PCO-1	M6 (58%) + NIPMAM (42%)	10.4	9.8	10.3	0.1
PCO-2	M6 (56%) + NIPMAM (44%)	11.5	8.8	11.4	0.1

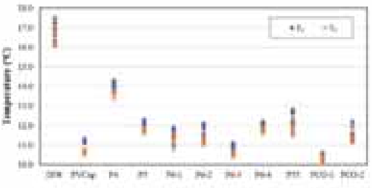

Fig. 6. T_o and T_a values obtained from slow constant cooling tests at 2500 ppm.

P4, P5, P6-1, P6-2 and P6-3 were synthesized through the reversible addition-fragmentation chain transfer polymerization (RAFT) with α,α′-azobisisobutyronitrile (AIBN) as initiator and n-butyl (2-cyano-2-propyl) trithiocarbonate as the chain transfer agent (CTA). P6-4, P55, PCO-1 and PCO-2 were synthesized through the AIBN-initiated conventional free radical polymerization without the addition of CTA.

At the concentration of 2500 ppm (or 0.25 wt%), P4 with N-butyl groups, P5 with N-pentyl groups and P6-1 with N-hexyl groups gave average T_o values (T_o (av.)) of 14.0, 12.1 and 11.6 °C respectively, indicating that the polymer with more hydrophobic side chains gave better KHI performance. The T_o values obtained for P6-1 are statistically significantly lower ($p < 0.05$ from t-test) than that of P5. The trend of the improved KHI performance of polymers with increasing hydrophobic side chains can be observed in other KHI polymer classes (Ajiro et al., 2010; Lin et al., 2017; Ree et al., 2019; Villano et al., 2009; Zhang and Kelland, 2020). However, the effect of n-hexyl groups is rarely observed as many of these KHI polymers with n-hexyl groups were water-insoluble. The reason why the polymer with more hydrophobic alkyl groups gave better KHI performance maybe due to an nucleation inhibition effect in which the hydrophobic groups in KHI polymers can work similarly as the hydrophobic small gas molecules that trigger the formation of clathrate water structures, resulting in a competition of the hydrophobic alkyl groups with the gas molecules that form gas hydrate nuclei. The more hydrophobic the alkyl group is, the more competitive will be. However, there appears to be an optimum maximum size to these hydrophobic groups. For example, past studies have shown that N-octylacrylamide copolymers were poor KHIs (Dirdal and Kelland, 2019). In addition, the clathrate water structures formed around the hydrophobic alkyl groups are restricted from growing to form supercritical-sized gas hydrate nuclei. Related to this, using molecular dynamic simulations, Custodio et al. reported that polygon water structures that predominately occur as pentagons were observed around the isopropyl groups of poly(N-isopropylacrylamide) (PNIPAM) near its lower critical solution temperature (LCST), and the predominated pentagon water structures were considered as clathrate-like behavior (Custodio et al., 2020).

The n-hexylated polymers P6-1, P6-2 and P6-3 were made using the same RAFT polymerization method and their cloud points (18, 14 and 15 °C respectively at 3 wt% in water) were similar. As expected, they gave fairly similar KHI performance with the T_o (av.) values being 11.6, 11.6 and 11.0 °C respectively, although the value for P6-3 was statistically lower ($p < 0.05$ from t-test) than P6-1 and P6-2. We did not have the molecular weight data of P6-2 and P6-3 due to long-term maintenance of the size exclusion chromatography (SEC) equipment, however the molecular weight of P6-3 was supposed to be somewhat larger than that of P6-2 according to the results of the intrinsic viscosity. Past studies showed that KHI polymers with comparatively low cloud point and low molecular weight usually gave better performance (Dirdal and Kelland, 2019; Kelland et al., 2015; Magnusson and Kelland, 2015; Yagasaki et al., 2018). Also, studies showed that among low molecular polymers there was an optimum molecular weight value for polymers to show excellent KHI performance, so this may be the reason why the performance increases for P6-3 (Farhadian et al., 2019; Zhang and Kelland, 2020).

The fourth n-hexylated polymer, P6-4 gave statistically significantly worse ($p < 0.05$ from t-test) KHI performance than P6-1, P6-2 and P6-3. This is probably because that the molecular weight of P6-4 from the intrinsic viscosity measurements clearly is larger than other polymers with n-hexyl groups. In addition, as the synthesis method of P6-4 was the AIBN-initiated conventional free radical polymerization without adding CTA, the end cap groups of the P6-4 polymer may be different from P6-1, P6-2 and P6-3, which can have an effect on its KHI performance. Reports showed that the existence of CTAs could add end cap functional groups to polymers during the polymerization procedure and the end cap functional groups have potential to affect the properties of the polymers (Ieong et al., 2011; Wan et al., 2019; Zhang and Kelland, 2018; Zhang et al., 2017).

Polymer P55 with n-dipentyl groups gave a T_o (av.) of 12.2 °C, which is almost the same KHI performance as P5. The reason why P55 did not give better KHI performance than P5 is probably a combination of two factors. The extra pentyl group in P55 increases the polymer hydrophobicity which in turn should improve the KHI performance of the polymer. However, this polymer has a significantly higher molecular weight than that of P5 which could reduce the performance. A lower molecular weight P55 was not available for testing.

The zwitterionic n-hexyl monomer, 3-([2-methacryloyloxyethyl](methyl)(n-hexyl)ammonio)propane-1-sulfonate (M6), was also copolymerized with the N-isopropylmethacrylamide (NIPMAM) monomer using the AIBN-initiated conventional free radical polymerization. This gave the copolymers PCO-1 and PCO-2. We did this because copolymerization with NIPMAM, a well-known monomer used in commercial KHI polymers, could be an efficient method to improve the performance of KHI polymers as well as raise the cloud point of NIPMAM polymer which is not suitable to inject into high temperature well fluids (Colle et al., 1999; Perrin et al., 2013; Zhang et al., 2018a). Compared to P6-4, the two copolymers PCO-1 and PCO-2 gave better KHI performance, which is probably an indication of the higher KHI activity of the NIPMAM monomer compared to M6. This is consistent with the results of a study in which a copolymer containing sodium 2-acrylamido-1-hexanesulfonate monomer units and NIPMAM monomer units in a molar ratio of 52:48 gave better KHI performance than the sodium 2-acrylamido-1-hexanesulfonate homopolymer (Peiffer et al., 1999).

We tested the KHI performance of the best homopolymer P6-3 and the best copolymer PCO-1 with concentrations varying from 1500 to 7500 ppm. Results in Table 4 and Fig. 7 show that P6-3 gave a small but statistically significant increasing KHI performance with increasing concentrations from 1500 to 2500 to 5000 ppm. However, when the concentration was increased from 5000 to 7500 ppm there was no improvement of the KHI performance of P6-3. To confirm this conclusion, we also tested P6-1 at different concentrations and the results showed that the same is true for P6-1. We assume that somehow, there is little increase in the number of hydrophobic groups available to perturb the water structure or prevent growth of hydrate particles. This could be because of clustering or even micellization of the zwitterionic polymers by polymer-polymer interactions between the hydrophobic groups with increasing aqueous concentration (Chevalier et al., 1992; Herrmann, 1966). In contrast, the NIPMAM copolymer PCO-1 gave increasing KHI performance when the con-

Table 4
The KHI performance of P6-1, P6-3 and PCO-1 at 1500, 2500, 5000 and 7500 ppm.

Entry at 1500 ppm	T_o (av.) (°C)	ΔT (av.) at T_o (°C)	T_a (av.) (°C)	T_o (av.) - T_a (av.) (°C)
P6-1	12.2	8.1	11.8	0.4
P6-3	11.8	8.5	11.5	0.3
PCO-1	12.0	8.3	11.9	0.1
Entry at 2500 ppm	**T_o (av.) (°C)**	**ΔT (av.) at T_o (°C)**	**T_a (av.) (°C)**	**T_o (av.) - T_a (av.) (°C)**
P6-1	11.6	8.7	11.3	0.3
P6-3	11.0	9.2	10.5	0.5
PCO-1	10.5	9.7	10.4	0.1
Entry at 5000 ppm	**T_o (av.) (°C)**	**ΔT (av.) at T_o (°C)**	**T_a (av.) (°C)**	**T_o (av.) - T_a (av.) (°C)**
P6-1	11.0	9.2	10.4	0.6
P6-3	10.2	10.0	9.6	0.6
PCO-1	8.9	11.3	8.7	0.2
Entry at 7500 ppm	**T_o (av.) (°C)**	**ΔT (av.) at T_o (°C)**	**T_a (av.) (°C)**	**T_o (av.) - T_a (av.) (°C)**
P6-1	11.0	9.2	10.4	0.6
P6-3	10.2	10.0	9.5	0.7
PCO-1	7.6	12.6	7.5	0.1

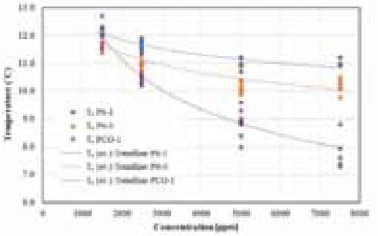

Fig. 7. To values of P6-1, P6-3 and PCO-1 at varying concentrations.

centration increased from 1500 to 2500 to 5000 to 7500 ppm. In addition, the degree of KHI performance improvement from low to high concentrations was greater than that of the zwitterionic homopolymers. This may be because the KHI performance of the amide-based NIPMAM monomer units more relies on the concentrations. They contain smaller iso-propyl hydrophobic side groups compared to the n-hexylated zwitterionic monomer, which will give weaker hydrophobic polymer-polymer interactions. The poor increase in performance at higher concentration for the P6 hompolymers may not just be an effect of the size of the hydrophobic groups. Past reports showed that the KHI performance of many non-amide KHI polymer series, such as cationic polymers, polyvinylsulfonamides and poly(alkyl ethylene phosphonate)s, does not improve as much with increasing concentration in the typical dosage window for field applications (0.1–1.0 wt% actives) as it does for amide-based KHI polymers (Lin et al., 2017; Nakarit et al., 2013; Zhang et al., 2020a). However, the amine oxide polymers showed a significant increase in performance with increasing concentration (Zhang et al., 2020b), and this maybe because amine oxides form strong hydrogen-bonds like amide groups. Therefore, we speculate that the effect on water molecules around the polymer from a strong hydrogen-bonding group is important, and not ionic dipole interactions which are observed with zwitterions and cationic groups. The strong hydrogen-bonding may lead to better water structuring (perturbation) than weak hydrogen-bonding groups or ionic groups, which will then have more effect on inhibiting hydrate nucleation formation.

4. Conclusions

A series of zwitterionic poly(sulfobetaine methacrylate)s with varying alkyl side chains were synthesized and investigated as kinetic gas hydrate inhibitors (KHIs) using synthetic natural gas mixture in high-pressure rocking cells for the first time. The KHI performance of these zwitterionic polymers increased with the length of the *N*-alkyl side groups increased from 4 to 5 to 6 carbon atoms. The zwitterionic poly(sulfobetaine methacrylate) with *N*-(n-hexyl) groups gave the best KHI performance. The copolymers containing zwitterionic 3-([2-methacryloyloxyethyl](methyl)(n-hexyl)ammonio)propane-1-sulfonate monomer units and *N*-isopropylmethacrylamide monomer units gave better KHI performance than the zwitterionic 3-([2-methacryloyloxyethyl](methyl)(n-hexyl)ammonio)propane-1-sulfonate homopolymers. The zwitterionic poly(sulfobetaine methacrylate)s homopolymers gave small improvement on KHI performance when increasing the concentration. In contrast, the improvement of the copolymers with the amide-containing NIPMAM monomer with increasing concentration was comparatively much greater. This may be due to clusters or micelles of the zwitterionic homopolymers forming at increasing concentrations. In addition, the strong hydrogen-bonding amide groups may lead to better water structuring (perturbation), resulting in more effect on inhibiting the formation of hydrate nucleation. This sheds light on why the best performing KHI polymers have strong hydrogen-bonding groups such as amide or amine oxide.

CRediT authorship contribution statement

Qian Zhang: Investigation, Data curation, Writing - original draft. **Malcolm A. Kelland:** Conceptualization, Supervision, Resources, Writing - review & editing. **Evan M. Lewoczko:** Data curation, Writing - original draft. **Caleb A. Bohannon:** Data curation, Writing - original draft. **Bin Zhao:** Supervision, Resources, Writing - review & editing.

Declaration of Competing Interest

The authors declare that they have no known competing financial interests or personal relationships that could have appeared to influence the work reported in this paper.

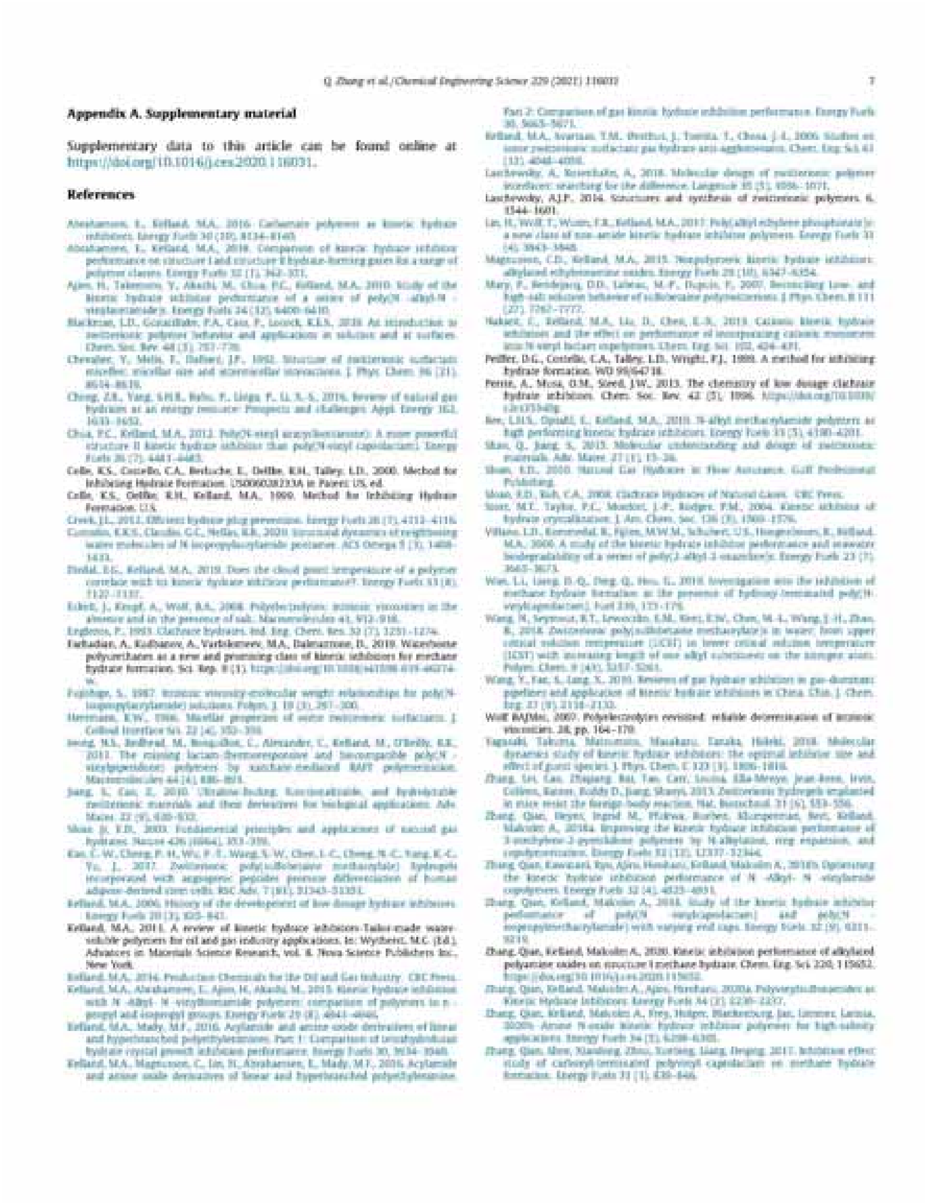

Appendix A. Supplementary material

Supplementary data to this article can be found online at https://doi.org/10.1016/j.ces.2020.116031.

References

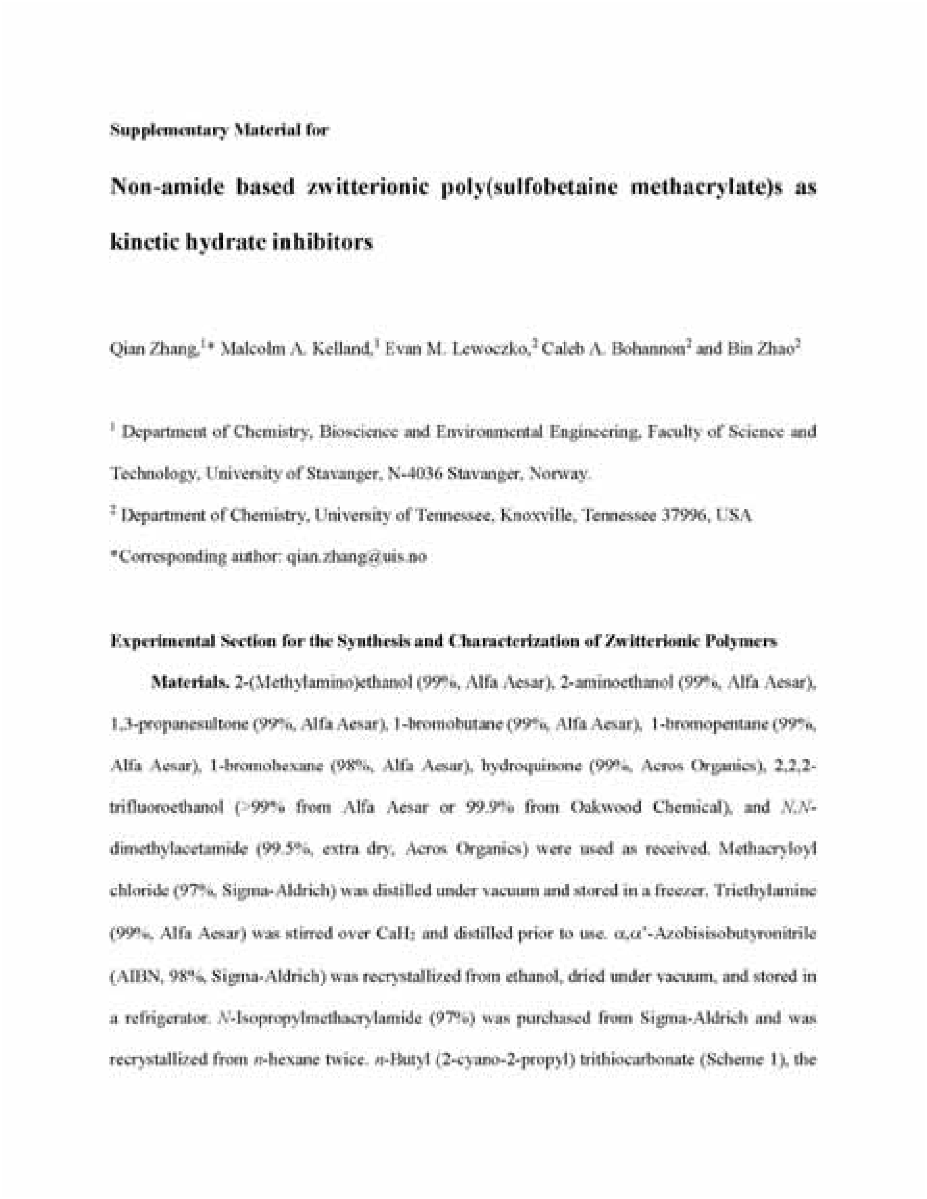

Supplementary Material for

Non-amide based zwitterionic poly(sulfobetaine methacrylate)s as kinetic hydrate inhibitors

Qian Zhang,[1]* Malcolm A. Kelland,[1] Evan M. Lewoczko,[2] Caleb A. Bohannon[2] and Bin Zhao[2]

[1] Department of Chemistry, Bioscience and Environmental Engineering, Faculty of Science and Technology, University of Stavanger, N-4036 Stavanger, Norway.

[2] Department of Chemistry, University of Tennessee, Knoxville, Tennessee 37996, USA

*Corresponding author: qian.zhang@uis.no

Experimental Section for the Synthesis and Characterization of Zwitterionic Polymers

Materials. 2-(Methylamino)ethanol (99%, Alfa Aesar), 2-aminoethanol (99%, Alfa Aesar), 1,3-propanesultone (99%, Alfa Aesar), 1-bromobutane (99%, Alfa Aesar), 1-bromopentane (99%, Alfa Aesar), 1-bromohexane (98%, Alfa Aesar), hydroquinone (99%, Acros Organics), 2,2,2-trifluoroethanol (>99% from Alfa Aesar or 99.9% from Oakwood Chemical), and *N,N*-dimethylacetamide (99.5%, extra dry, Acros Organics) were used as received. Methacryloyl chloride (97%, Sigma-Aldrich) was distilled under vacuum and stored in a freezer. Triethylamine (99%, Alfa Aesar) was stirred over CaH_2 and distilled prior to use. α,α'-Azobisisobutyronitrile (AIBN, 98%, Sigma-Aldrich) was recrystallized from ethanol, dried under vacuum, and stored in a refrigerator. *N*-Isopropylmethacrylamide (97%) was purchased from Sigma-Aldrich and was recrystallized from *n*-hexane twice. *n*-Butyl (2-cyano-2-propyl) trithiocarbonate (Scheme 1), the

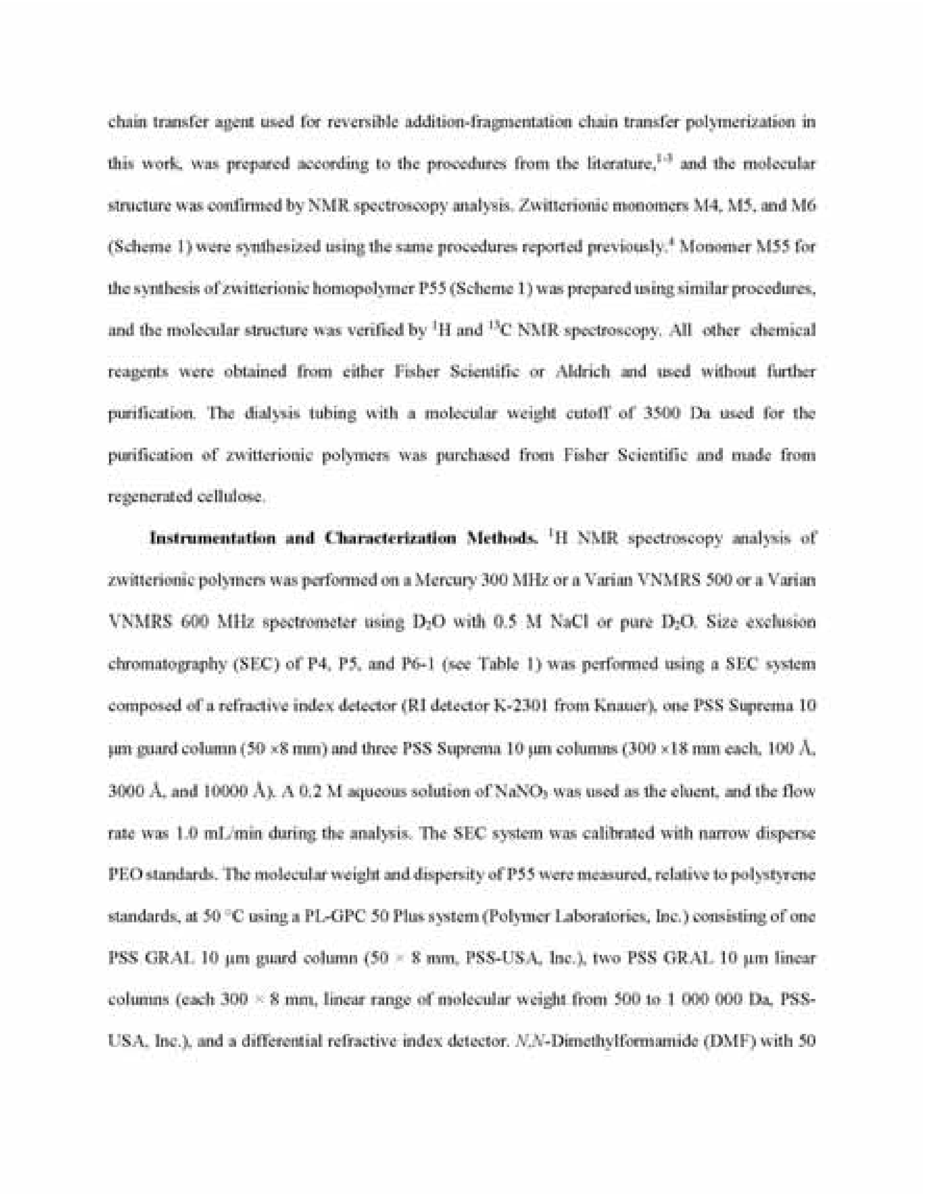

chain transfer agent used for reversible addition-fragmentation chain transfer polymerization in this work, was prepared according to the procedures from the literature,[1-3] and the molecular structure was confirmed by NMR spectroscopy analysis. Zwitterionic monomers M4, M5, and M6 (Scheme 1) were synthesized using the same procedures reported previously.[4] Monomer M55 for the synthesis of zwitterionic homopolymer P55 (Scheme 1) was prepared using similar procedures, and the molecular structure was verified by ^{1}H and ^{13}C NMR spectroscopy. All other chemical reagents were obtained from either Fisher Scientific or Aldrich and used without further purification. The dialysis tubing with a molecular weight cutoff of 3500 Da used for the purification of zwitterionic polymers was purchased from Fisher Scientific and made from regenerated cellulose.

Instrumentation and Characterization Methods. ^{1}H NMR spectroscopy analysis of zwitterionic polymers was performed on a Mercury 300 MHz or a Varian VNMRS 500 or a Varian VNMRS 600 MHz spectrometer using D_2O with 0.5 M NaCl or pure D_2O. Size exclusion chromatography (SEC) of P4, P5, and P6-1 (see Table 1) was performed using a SEC system composed of a refractive index detector (RI detector K-2301 from Knauer), one PSS Suprema 10 μm guard column (50 ×8 mm) and three PSS Suprema 10 μm columns (300 ×18 mm each, 100 Å, 3000 Å, and 10000 Å). A 0.2 M aqueous solution of $NaNO_3$ was used as the eluent, and the flow rate was 1.0 mL/min during the analysis. The SEC system was calibrated with narrow disperse PEO standards. The molecular weight and dispersity of P55 were measured, relative to polystyrene standards, at 50 °C using a PL-GPC 50 Plus system (Polymer Laboratories, Inc.) consisting of one PSS GRAL 10 μm guard column (50 × 8 mm, PSS-USA, Inc.), two PSS GRAL 10 μm linear columns (each 300 × 8 mm, linear range of molecular weight from 500 to 1 000 000 Da, PSS-USA, Inc.), and a differential refractive index detector. *N,N*-Dimethylformamide (DMF) with 50

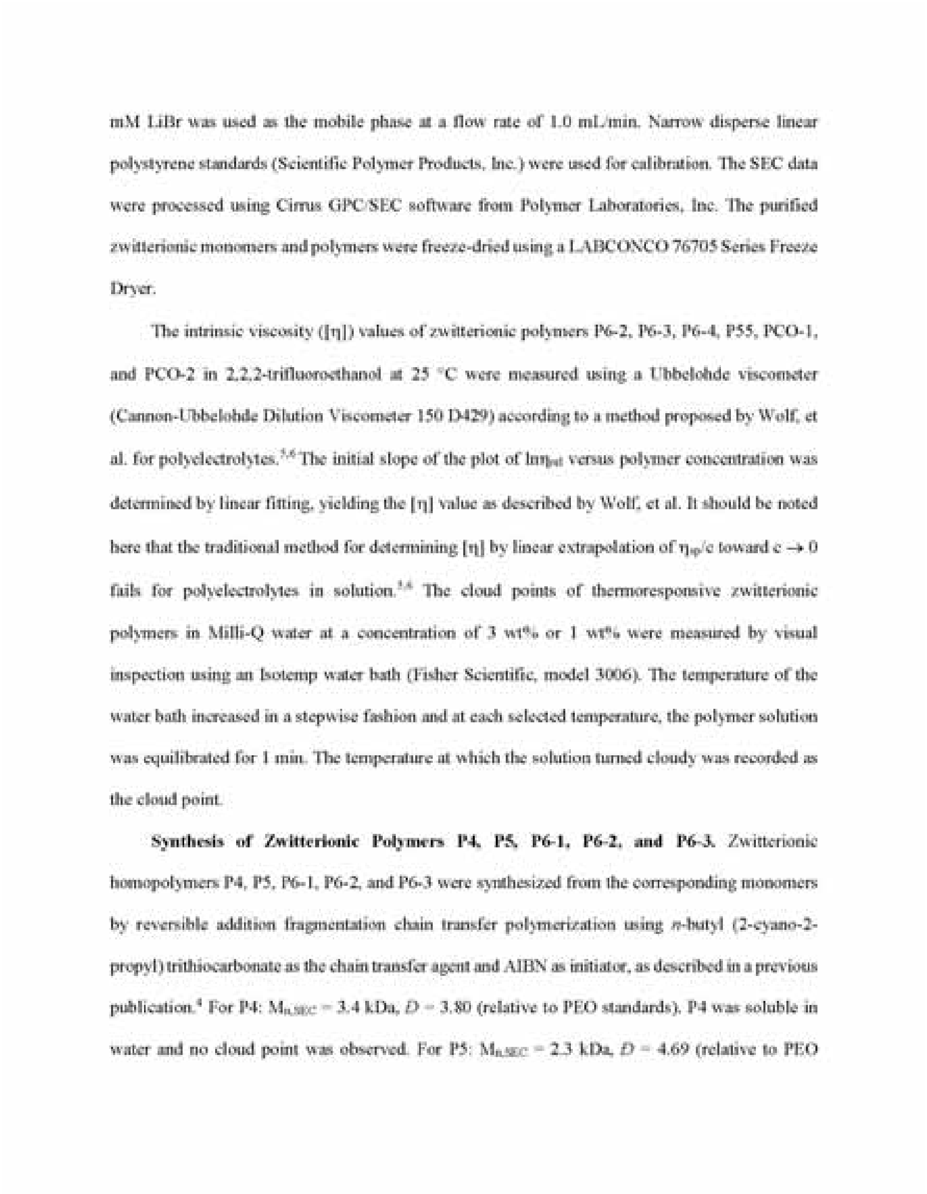

mM LiBr was used as the mobile phase at a flow rate of 1.0 mL/min. Narrow disperse linear polystyrene standards (Scientific Polymer Products, Inc.) were used for calibration. The SEC data were processed using Cirrus GPC/SEC software from Polymer Laboratories, Inc. The purified zwitterionic monomers and polymers were freeze-dried using a LABCONCO 76705 Series Freeze Dryer.

The intrinsic viscosity ([η]) values of zwitterionic polymers P6-2, P6-3, P6-4, P55, PCO-1, and PCO-2 in 2,2,2-trifluoroethanol at 25 °C were measured using a Ubbelohde viscometer (Cannon-Ubbelohde Dilution Viscometer 150 D429) according to a method proposed by Wolf, et al. for polyelectrolytes.[5,6] The initial slope of the plot of $\ln\eta_{rel}$ versus polymer concentration was determined by linear fitting, yielding the [η] value as described by Wolf, et al. It should be noted here that the traditional method for determining [η] by linear extrapolation of η_{sp}/c toward $c \to 0$ fails for polyelectrolytes in solution.[5,6] The cloud points of thermoresponsive zwitterionic polymers in Milli-Q water at a concentration of 3 wt% or 1 wt% were measured by visual inspection using an Isotemp water bath (Fisher Scientific, model 3006). The temperature of the water bath increased in a stepwise fashion and at each selected temperature, the polymer solution was equilibrated for 1 min. The temperature at which the solution turned cloudy was recorded as the cloud point.

Synthesis of Zwitterionic Polymers P4, P5, P6-1, P6-2, and P6-3. Zwitterionic homopolymers P4, P5, P6-1, P6-2, and P6-3 were synthesized from the corresponding monomers by reversible addition fragmentation chain transfer polymerization using *n*-butyl (2-cyano-2-propyl) trithiocarbonate as the chain transfer agent and AIBN as initiator, as described in a previous publication.[4] For P4: $M_{n,SEC} = 3.4$ kDa, $Đ = 3.80$ (relative to PEO standards). P4 was soluble in water and no cloud point was observed. For P5: $M_{n,SEC} = 2.3$ kDa, $Đ = 4.69$ (relative to PEO standards). The cloud point of P5 in water at a concentration of 3 wt% was about 51 °C. For P6-1: $M_{n,SEC}$ = 7.5 kDa, $Đ$ = 3.51 (relative to PEO standards). The cloud point of P6-1 in water at a concentration of 3 wt% was about 18 °C. The [η] of P6-2 in 2,2,2-trifluoroethanol at 25 °C was 0.116 dL/g. The cloud points of P6-2 in water at concentration of 3 wt% and 1 wt% were about 14 and 18 °C, respectively. The [η] of P6-3 in 2,2,2-trifluoroethanol at 25 °C was 0.166 dL/g. The cloud points of P6-3 in water at concentration of 3 wt% and 1 wt% were about 15 and 21 °C, respectively. Note that P6-3 exhibited a rather broad LCST transition in water upon heating, likely because of a broad molecular weight distribution. These characterization data are summarized in Table 1.

Synthesis of Zwitterionic Homopolymers P55 and P6-4 by Conventional Free Radical Polymerization Using AIBN as Initiator. 3-((2-(Methacryloyloxy)ethyl)-dipentylammonio)propane-1-sulfonate (M55, 0.603 g, 2.03 mmol), AIBN (7.1 mg, 0.043 mmol), 2,2,2-trifluoroethanol (2.039 g), and *N,N*-dimethylformamide (90.5 mg) were added to a 25 mL two-necked flask equipped with a magnetic stir bar. The mixture was degassed by freeze-pump-thaw and placed in a preheated oil bath with a temperature of 70 °C. After 17 h, the polymerization was stopped, and the polymer was purified by dialysis against MilliQ water using regenerated cellulose dialysis tubing (MWCO: 3500 Da). The purified polymer was concentrated and freeze dried to give a white powder (yield: 0.508 g, 84.2%). $M_{n,SEC}$ = 64.9 kDa and $Đ$ = 2.36 (relative to polystyrene standards using DMF with 50 mM LiBr as the mobile phase). The [η] of P55 in 2,2,2-trifluoroethanol at 25 °C was determined to be 0.490 dL/g. The cloud point of P55 in MilliQ water at 1 wt% was 37 °C. P6-4 was synthesized in a similar manner, and the [η] in 2,2,2-trifluoroethanol at 25 °C was determined to be 0.442 dL/g. The cloud points of P6-4 in water at concentration of 3 wt% and 1 wt% were about 10 and 11 °C, respectively (see Table 1).

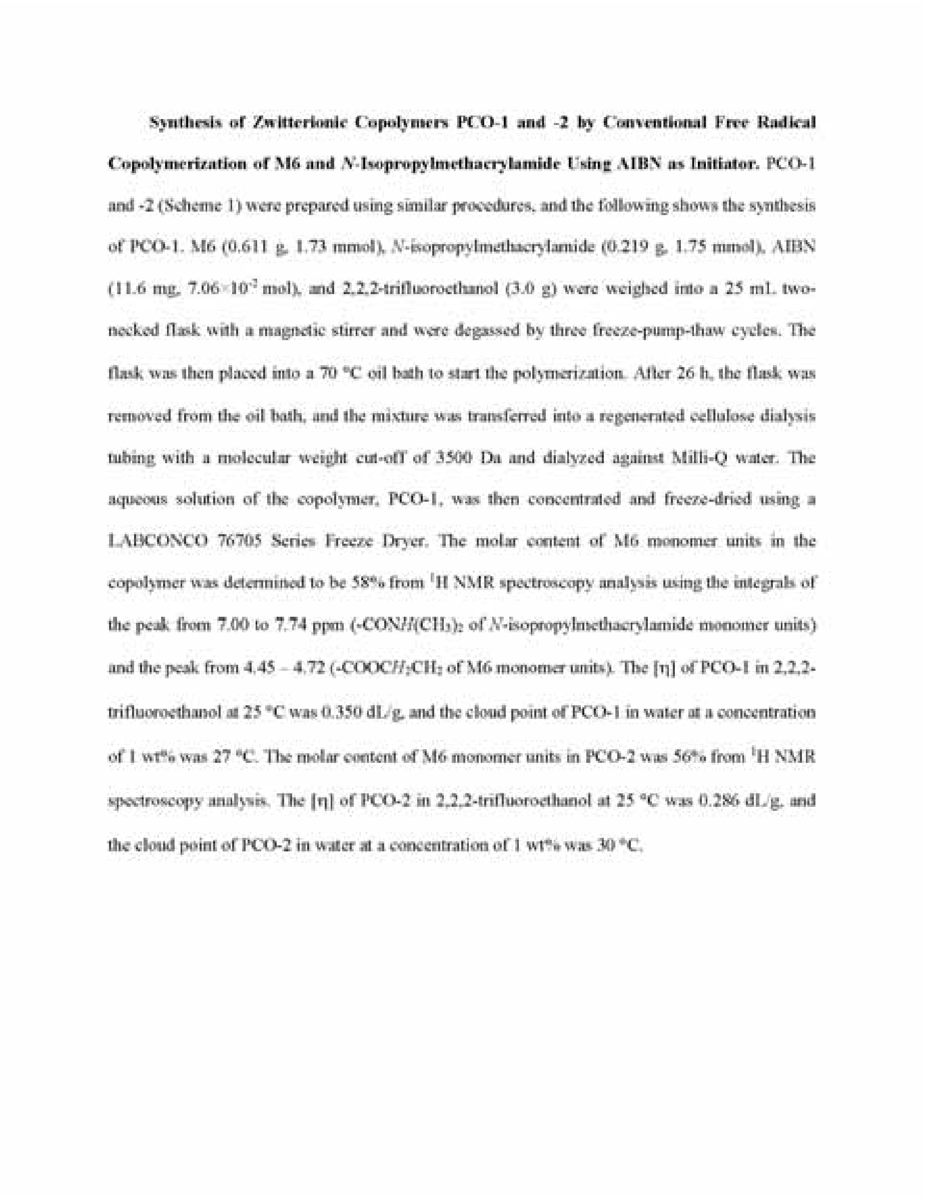

Synthesis of Zwitterionic Copolymers PCO-1 and -2 by Conventional Free Radical Copolymerization of M6 and *N*-Isopropylmethacrylamide Using AIBN as Initiator. PCO-1 and -2 (Scheme 1) were prepared using similar procedures, and the following shows the synthesis of PCO-1. M6 (0.611 g, 1.73 mmol), *N*-isopropylmethacrylamide (0.219 g, 1.75 mmol), AIBN (11.6 mg, 7.06×10^{-5} mol), and 2,2,2-trifluoroethanol (3.0 g) were weighed into a 25 mL two-necked flask with a magnetic stirrer and were degassed by three freeze-pump-thaw cycles. The flask was then placed into a 70 °C oil bath to start the polymerization. After 26 h, the flask was removed from the oil bath, and the mixture was transferred into a regenerated cellulose dialysis tubing with a molecular weight cut-off of 3500 Da and dialyzed against Milli-Q water. The aqueous solution of the copolymer, PCO-1, was then concentrated and freeze-dried using a LABCONCO 76705 Series Freeze Dryer. The molar content of M6 monomer units in the copolymer was determined to be 58% from ^{1}H NMR spectroscopy analysis using the integrals of the peak from 7.00 to 7.74 ppm ($-CON\mathit{H}(CH_3)_2$ of *N*-isopropylmethacrylamide monomer units) and the peak from 4.45 – 4.72 ($-COOC\mathit{H}_2CH_2$ of M6 monomer units). The [η] of PCO-1 in 2,2,2-trifluoroethanol at 25 °C was 0.350 dL/g, and the cloud point of PCO-1 in water at a concentration of 1 wt% was 27 °C. The molar content of M6 monomer units in PCO-2 was 56% from ^{1}H NMR spectroscopy analysis. The [η] of PCO-2 in 2,2,2-trifluoroethanol at 25 °C was 0.286 dL/g, and the cloud point of PCO-2 in water at a concentration of 1 wt% was 30 °C.

Table 1. Summary of Characterization Data for Zwitterionic Polymers

Polymer	Monomer(s)	Synthesis Method [b]	Polymer's Molecular Characteristics	CP in H_2O (3 wt%) [f]	CP in H_2O (1 wt%) [f]
P4	M4	RAFT	$M_{n,SEC}$ = 3.4 kDa; $Đ$ = 3.80 [c]	Soluble	Soluble
P5	M5	RAFT	$M_{n,SEC}$ = 2.3 kDa; $Đ$ = 4.69 [c]	51 °C	NA
P6-1	M6	RAFT	$M_{n,SEC}$ = 7.5 kDa; $Đ$ = 3.51 [c]	18 °C	NA
P6-2	M6	RAFT	$[\eta]$ = 0.116 dL/g [d]	14 °C	18 °C
P6-3	M6	RAFT	$[\eta]$ = 0.166 dL/g [d]	15 °C [g]	21 °C [g]
P6-4	M6	AIBN	$[\eta]$ = 0.442 dL/g [d]	10 °C	11 °C
P55	M55	AIBN	$M_{n,SEC}$ = 64.9 kDa; $Đ$ = 2.36 [e] $[\eta]$ = 0.490 dL/g [d]	NA	37 °C
PCO-1	M6 + NIPMAM [a]	AIBN	$[\eta]$ = 0.350 dL/g [d]	NA	27 °C
PCO-2	M6 + NIPMAM [a]	AIBN	$[\eta]$ = 0.286 dL/g [d]	NA	30 °C

[a] NIPMAM: *N*-isopropylmethacrylamide. [b] RAFT: reversible addition-fragmentation chain transfer polymerization; AIBN: α,α'-azobisisobutyronitrile (AIBN)-initiated conventional free radical polymerization. [c] $M_{n,SEC}$ and $Đ$ were determined by an aqueous SEC system relative to PEO standards. [d] Intrinsic viscosity in 2,2,2-trifluoroethanol at 25 °C determined using the Wolf method.[5,6] [e] $M_{n,SEC}$ and $Đ$ were determined by a DMF SEC system relative to polystyrene standards. [f] CP: cloud point in Milli-Q water determined by visual inspection. [g] P6-3 exhibited a broad LCST transition in water upon heating.

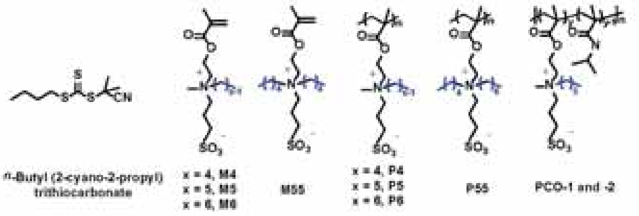

Scheme 1. Molecular Structures of *n*-Butyl (2-Cyano-2-propyl) Trithiocarbonate (the Chain Transfer Agent), Zwitterionic Monomers, and Polymers.

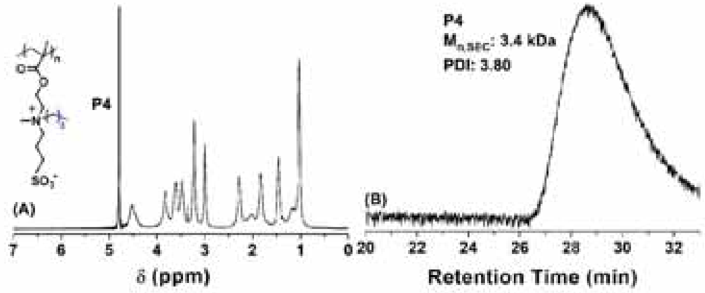

Figure 1. (A) ^{1}H NMR spectrum of P4 in D_2O and (B) SEC curve of P4 from an aqueous SEC system using a 0.2 M aqueous solution of $NaNO_3$ as eluent.

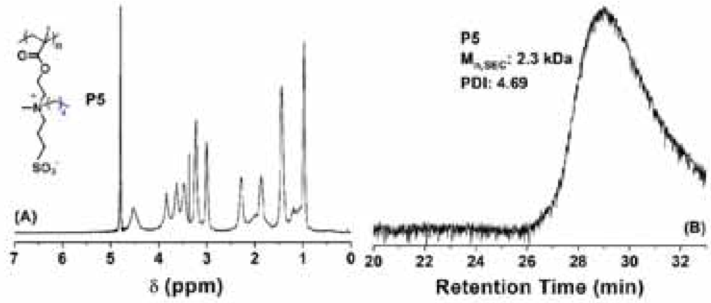

Figure 2. (A) ^{1}H NMR spectrum of P5 in D_2O and (B) SEC curve of P5 from an aqueous SEC system using a 0.2 M aqueous solution of $NaNO_3$ as eluent.

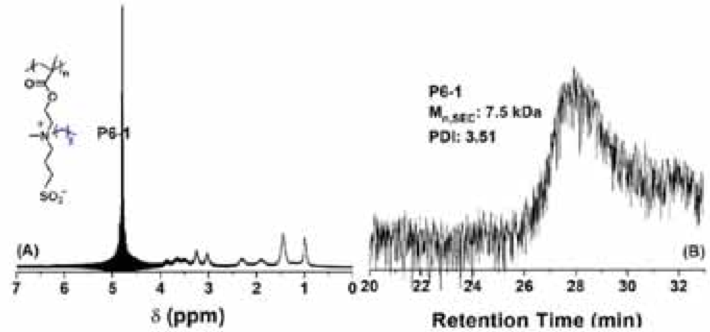

Figure 3. (A) ^{1}H NMR spectrum of P6-1 in D_2O and (B) SEC curve of P6-1 from an aqueous SEC system using a 0.2 M aqueous solution of $NaNO_3$ as eluent.

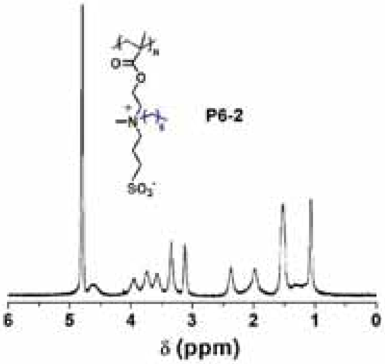

Figure 4. ^{1}H NMR spectrum of P6-2 in D_2O with 0.5 M NaCl.

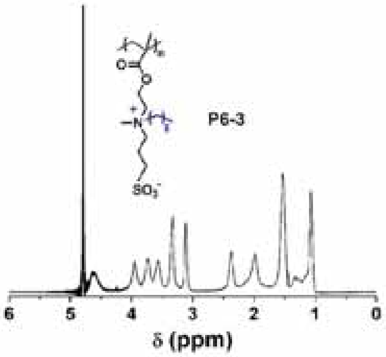

Figure 5. ^{1}H NMR spectrum of P6-3 in D_2O with 0.5 M NaCl.

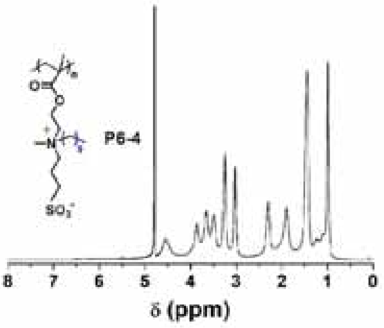

Figure 6. ^{1}H NMR spectrum of P6-4 in D_2O with 0.5 M NaCl.

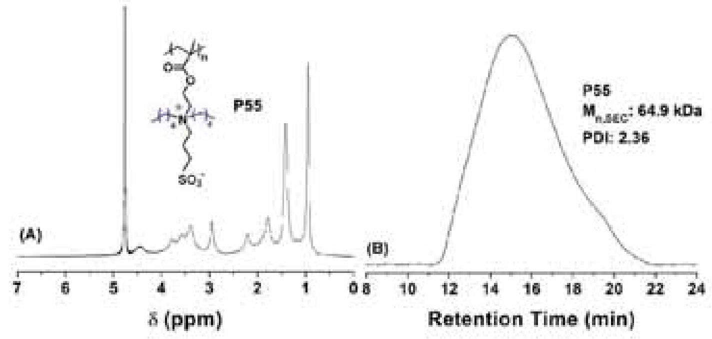

Figure 7. (A) ^{1}H NMR spectrum of P55 in D_2O and (B) SEC curve of P55 from an DMF SEC system using DMF with 50 mM LiBr as eluent.

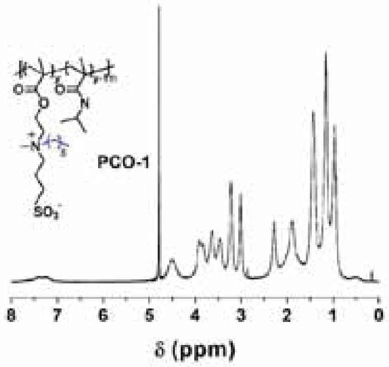

Figure 8. ^{1}H NMR spectrum of PCO-1 in D_2O.

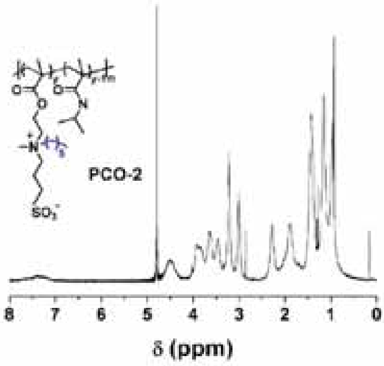

Figure 9. ^{1}H NMR spectrum of PCO-2 in D_2O.

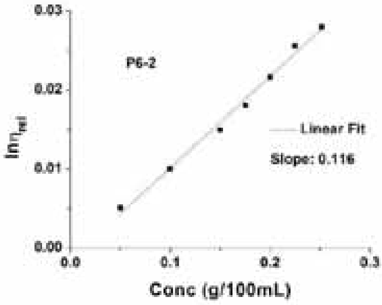

Figure 10. Plot of $\ln\eta_{rel}$ versus polymer concentration for P6-2. From the slope determined from linear fit, $[\eta] = 0.116$ dL/g.

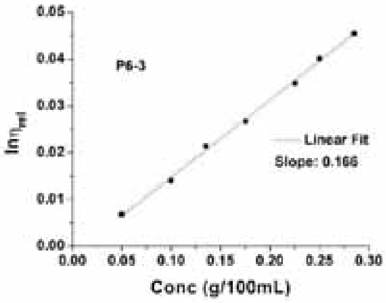

Figure 11. Plot of $\ln\eta_{rel}$ versus polymer concentration for P6-3. From the slope determined from linear fit, $[\eta] = 0.166$ dL/g.

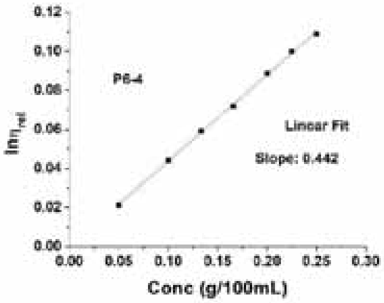

Figure 12. Plot of $\ln\eta_{rel}$ versus polymer concentration for P6-4. From the slope determined from linear fit, $[\eta] = 0.442$ dL/g.

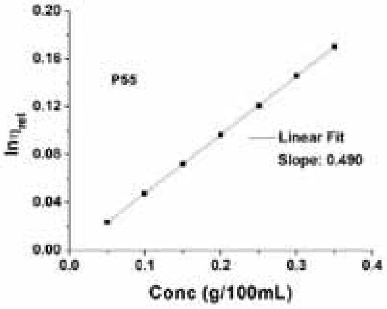

Figure 13. Plot of $\ln\eta_{rel}$ versus polymer concentration for P55. From the slope determined from linear fit, $[\eta] = 0.490$ dL/g.

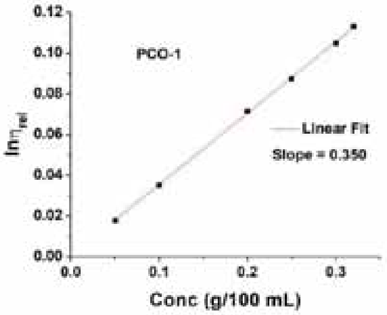

Figure 14. Plot of $\ln\eta_{rel}$ versus polymer concentration for PCO-1. $[\eta] = 0.350$ dL/g (the initial slope).

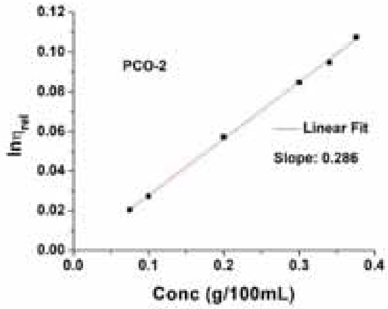

Figure 15. Plot of $\ln\eta_{rel}$ versus polymer concentration for PCO-2. From the slope determined from linear fit, $[\eta] = 0.286$ dL/g.

References:

1. Moad, G.; Chong, Y. K.; Postma, A.; Rizzardo, E.; Thang, S. H. Advances in RAFT Polymerization: the Synthesis of Polymers with Defined End-Groups. *Polymer* **2005**, *46*, 8458-8468.
2. Seymour, B. T.; Wright, R. A. E.; Parrott, A. C.; Gao, H. Y.; Martini, A.; Qu, J.; Dai, S.; Zhao, B. Poly(alkyl methacrylate) Brush-Grafted Silica Nanoparticles as Oil Lubricant Additives: Effects of Alkyl Pendant Groups on Oil Dispersibility, Stability, and Lubrication Property. *ACS Appl. Mater. Interfaces* **2017**, *9*, 25038–25048.
3. Fu, W. X.; Bai, W.; Jiang, S. S.; Seymour, B. T.; Zhao, B. UCST-Type Thermoresponsive Polymers in Synthetic Lubricating Oil Polyalphaolefin (PAO). *Macromolecules* **2018**, *51*, 1674–1680.
4. Wang, N.; Seymour, B. T.; Lewoczko, E. M.; Kent, E. W.; Chen, M.-L.; Wang, J.-H.; Zhao, B. Zwitterionic Poly(sulfobetaine methacrylate)s in Water: From Upper Critical Solution Temperature (UCST) to Lower Critical Solution Temperature (LCST) with Increasing Length of One Alkyl Substituent on the Nitrogen Atom. *Polym. Chem.* **2018**, *9*, 5257-5261.
5. Eckelt, J.; Knopf, A.; Wolf, B. A. Polyelectrolytes: Intrinsic Viscosities in the Absence and in the Presence of Salt. *Macromolecules* **2008**, *41*, 912-918.
6. Wolf, B. A. Polyelectrolytes Revisited: Reliable Determination of Intrinsic Viscosities. *Macromol. Rapid Commun.* **2007**, *28*, 164–170.

Paper X

High Cloud Point Polyvinylaminals as Non-amide Based Kinetic Gas Hydrate Inhibitors

Authors:

Malcolm A. Kelland*, Erik Gisle Dirdal, and Qian Zhang

Published in Energy & Fuels 2020, 34 (7), 8301-8307.

This paper is not in Brage due to copyright.